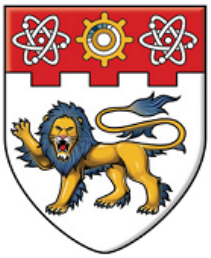

NANYANG TECHNOLOGICAL UNIVERSITY

MIXED METAL OXIDE ANODES FOR ELECTROCHEMICAL OXIDATION OF PHENOLIC POLLUTANTS

WU WEIYI

SCHOOL OF CIVIL AND ENVIRONMENTAL ENGINEERING

2016

MIXED METAL OXIDE ANODES FOR ELECTROCHEMICAL OXIDATION OF PHENOLIC POLLUTANTS

WU WEIYI

School of Civil and Environmental Engineering

A thesis submitted to the Nanyang Technological University
in fulfillment of the requirement for the degree of
Doctor of Philosophy

2016

ACKNOWLEGEMENTS

The completion of the thesis was made possible with the involvement of many people. First and foremost, I would like to express my heartfelt gratitude and appreciation to my supervisor, Associate Professor Lim Teik Thye. I have benefited a lot from his professional insights, invaluable advices, and great patience throughout the study. He has cared about his students in many aspects and always encouraged them to strive for excellence. I would also like to thank my co-supervisor, Dr. Huang Zhaohong from Singapore Institute of Manufacturing Technology (SIMTech, A*STAR). He is always willing to share with me his expertise in materials synthesis and process optimization and give me help whenever necessary.

Secondly, I would like to express my gratitude to Nanyang Environment and Water Research Institute (NEWRI), Environment Lab of School of Civil and Environmental Engineering, and Singapore Institute of Manufacturing Technology. The thesis cannot be done without their provision of experimental facilities.

Furthermore, I would like to thank my research group members for their support during my graduate study. Special thanks are given to Dr. Wang Penghua, Dr. Ronn Goei, Dr. Oh Wen Da, Mr. Hu Zhongting and Ms. Zhang Yiqing for their generous sharing of academic knowledge and technical skills. I would also like to thank all the lab staffs in Environment Lab, NEWRI and SIMTech who have provided me assistance throughout my study. They are Mrs. Lim-Tay Chew Wang, Mrs. Maria Chong Ai Shing, Ms. Pearlyn See Shen Yen, Mr. Tan Han Khiang, Mr. Ong Chee Yung, Ms. Elvy Riani Wanjaya, Dr. Han Yuan, Mr. Yeo Wee Kian Anthony, Dr. Zhou Qin and Mrs. Zhou Yujie.

I am always indebted to my family: my mom, Mrs. Wei Jiane, and my dad, Mr. Wu Fushan. Their unconditional love and firm support have given me strength, confidence and motivation in every step of this journey. I would like to give my very

special thanks to my wife, Ms. Wang Yuanyuan, for her encouragement and support in the past three years and much more.

Last but not least, I am most grateful to Nanyang Technological University for the offer of a PhD research scholarship. The financial support from NEWRI and CEE is gratefully acknowledged.

TABLE OF CONTENTS

SUMMARY

Mixed metal oxide (MMO) has been extensively used as the anode material for removal or alleviation of aqueous recalcitrant organics through electrochemical oxidation. Among the MMO anodes, antimony-doped tin dioxide (SnO_2-Sb) anode has been distinguished by its advantages of high oxygen evolution potential (OEP), easy preparation and cost effectiveness. However, its short service life has presented a main barrier for its large-scale applications. Therefore, the focus of this study was on (1) developing SnO_2-Sb anodes modified with microstructure deposit and polymer composites to obtain improved physical and chemical stability and enhanced electrocatalytic activity for oxidation of phenolic compounds, and (2) evaluating the potential of modified SnO_2-Sb anodes for practical application by comparative study with commercial boron-doped diamond (BDD) anode.

In the first phase of this study, novel SnO_2-Sb electrodes with polyetrafluoroethylene (PTFE) composite were fabricated by pulse electrodeposition. In this process, vertically aligned TiO_2 nanotubes (TiO_2-NTs) formed by anodization of Ti plate served as the substrate for SnO_2 eletrodeposition. Comparing with the conventional SnO_2-Sb electrode, TiO_2-NTs/SnO_2-Sb-PTFE electrodes have a higher oxygen evolution potential, improved surface hydrophobicity, superior hydroxyl radical ($HO^{\bullet}$) generation and enhanced electrocatalytic activity by incorporation of PTFE nanoparticles. The surfaces of the TiO_2-NTs/SnO_2-Sb-PTFE composite electrodes exhibit microspherical structure, which may provide more active sites for electrocatalytic reactions. More importantly, the electrodes exhibit a distinctive improvement of oxygen evolution potential (OEP) from 2.0 V (for SnO_2-Sb electrode) to 2.4 V (vs Ag/AgCl (3 M NaCl)). The electrocatalytic performance of TiO_2-NTs/SnO_2-Sb-PTFE compared with Ti/SnO_2-Sb(conventional) and TiO_2-NTs/SnO_2-Sb was investigated using phenol as model pollutant. The effects of initial solution

pH and types of supporting electrolyte on the performance efficiency were investigated. The anodic leaching of Sn ions was also studied under different conditions.

The second phase of the study was the development of a duplex-structured Sb-doped SnO_2 electrode modified by SnO_2-Sb-CNT composite (Ti/SnO_2-Sb/SnO_2-Sb-CNT) using pulse electrodeposition technique. SnO_2-Sb-CNT composite composed of 4 – 5 nm SnO_2-Sb particles was synthesized via co-precipitation prior to electrode preparation. Physicochemical and electrochemical characterization of Ti/SnO_2-Sb/SnO_2-Sb-CNT revealed that the novel duplex structured electrode had a larger electroactive surface area and lower charge transfer resistance than Ti/SnO_2-Sb prepared by thermochemical decomposition, due to its more compact and rough surface. It also improved the electrochemical stability of Ti/SnO_2-Sb/SnO_2-Sb-CNT with a service lifetime up to 86 h. The OEP of Ti/SnO_2-Sb/SnO_2-Sb-CNT was determined to be 2.2 V (vs Ag/AgCl (3 M NaCl)). Bulk electrolysis of bisphenol A (BPA) was conducted to evaluate the electrocatalytic performance of the electrodes at various current densities (10 – 40 mA cm^{-2}) and initial pH (3 – 11) of solution. Ti/SnO_2-Sb/SnO_2-Sb-CNT was able to adsorb more BPA molecules, which may contribute to its high current efficiency for electrochemical oxidation of BPA. A mechanism was proposed to illustrate the enhanced degradation of BPA by Ti/SnO_2-Sb/SnO_2-Sb-CNT via synergistic adsorption and electrochemical oxidation effect.

Finally, a comparative study was carried out on the electrocatalytic oxidation of BPA by the two types of modified SnO_2-Sb anodes and a commercial BDD anode. Although BDD was effective to remove BPA in Na_2SO_4 supporting electrolyte, its electrocatalytic performance was inhibited in NaCl supporting electrolyte due to the formation of organochlorine intermediates and polymer byproducts, resulting in a TOC removal rate of only 46.8%, much less than that achieved with Ti/SnO_2-Sb/SnO_2-Sb-CNT (64.2%) and TiO_2-NTs/SnO_2-Sb-PTFE (58.6%). Therefore, the

modified SnO_2-Sb anodes have the advantage of versatile electrocatalytic performance over BDD. The reaction pathways for BPA degradation were also proposed with the identification of four main aromatic intermediates and quantification of three aliphatic acid intermediates. Hydroxylation, oxidation and ring-opening reactions are involved in the reaction pathways.

Overall, the major contribution arising from this study is the fabrication of highly active SnO_2-Sb electrodes for electrocatalytic oxidation of aqueous phenolic pollutants. The findings also provide insights for the fabrication of other MMO anodes through modification of surface hydrophilicity and hydrophobicity, or incorporation of composites to obtain duplex structure. Especially, the modified SnO_2-Sb electrodes exhibit their flexibility for applications at various conditions through comparison with the outstanding commercial electrode, which show their practical significance for treating real water and industrial wastewater treatment.

LIST OF TABLES

LIST OF FIGURES

LIST OF ABBREVIATIONS

AAS	Atomic absorption spectroscopy
AFM	Atomic force microscopy
AOP	Advanced oxidation process
BDD	Boron-doped diamond
BPA	Bisphenol A
COD	Chemical oxygen demand
CA	Carbon aerogel
CNT	Carbon nanotube
CPE	Constant phase element
CTAB	Cetyltrimethylammonium
CV	Cyclic voltammetry
CVD	Chemical vapor deposition
DRS	Diffuse reflectance spectroscopy
DSA	Dimensionally stable anode
E_c	Specific energy consumption
EAOP	Electrochemical advanced oxidation process
EDS	Energy-dispersive X-ray spectroscopy
EF	Electro-Fenton
EIS	Electrochemical impedance spectroscopy
EO	Electrochemical oxidation
FESEM	Field emission scanning electron microscopy
FR	Fluorine resin
FTIR	Fourier-transform infrared spectroscopy
FTO	Fluorine doped tin oxide

HPLC	High performance liquid chromatography
IC	Ion chromatography
ICE	Instantaneous current efficiency
LC–MS/MS	Liquid chromatography tandem mass spectrometry
LSV	Linear sweep voltammetry
MCE	Mineralization current efficiency
MMO	Mixed metal oxide
NT	Nanotube
OEP	Oxygen evolution potential
OER	Oxygen evolution reaction
PCP	Pentachlorophenol
PED	Pulse electrodeposition
PEF	Photo electro-Fenton
PFCA	Perfluorocarboxylic acid
PFOA	Perfluorooctanoic acid
PVD	Physical vapor deposition
PTFE	Polytetrafluoroethylene
ROS	Reactive oxygen species
SCE	Standard calomel electrode
SEM	Scanning electron microscopy
SHE	Standard hydrogen electrode
TEM	Transmission electron microscopy
TOC	Total organic carbon
TGA	Thermogravimetric analysis
XAS	X-ray absorption spectroscopy
XPS	X-ray photoelectron spectroscopy
XRD	X-ray diffraction

LIST OF PUBLICATIONS

Parts of the findings presented in this thesis are presented in the following journal papers or manuscripts:

- **Wu W.**, Huang Z.H., Lim T.T.* (2014). Recent development of mixed metal oxide anodes for electrochemical oxidation of organic pollutants in water. Applied Catalysis A: General 480, 58-78.
- **Wu W.**, Huang Z.H., Lim T.T.* (2015). Enhanced electrochemical oxidation of phenol using hydrophobic TiO_2-NTs/SnO_2-Sb-PTFE electrode prepared by pulse electrodeposition. RSC Advances 5, 32245-32255.
- **Wu W.***, Huang Z.H., Lim T.T.* (2016). A comparative study on electrochemical oxidation of bisphenol A by boron-doped diamond anode and modified SnO_2-Sb anodes: influencing parameters and reaction pathways. Journal of Environmental Chemical Engineering 4, 2807-2815.
- **Wu W.***, Huang Z., Hu Z.T., He C, Lim T.T.* (2017). High performance duplex-structured SnO_2-Sb-CNT composite anode for bisphenol A removal. Separation and Purification Technology, accepted.
- Hu Z.T., Chen Z., Goei R., **Wu W.**, Lim T.T.* (2016). Magnetically recyclable Bi/Fe-based hierarchical nanostructures via self-assembly for environmental decontamination. Nanoscale 8, 12736-12746.

CHAPTER 1 INTRODUCTION

1.1 Background

Water scarcity has become an increasingly challenging issue facing the world, due to the population growth, rapid urbanization in developing countries, climate change and deteriorating water quality. Therefore, the need for water reclamation and reuse has been growing in order to overcome the above mentioned problems and meet the increasing demands of diverse water usage.

Nowadays, recalcitrant chemicals have been found to be continuously released into the natural and engineered water system. The presence of biorefractory or recalcitrant compounds could hinder the biological treatment of wastewater. Moreover, the restrictions and regulations have become stricter in the pursuit of sustainable development, and all of those have driven much research interest on the development of new and more effective water treatment technologies. An alternative technology to conventional treatment methods is advanced oxidation processes (AOPs). The principle of AOPs is based on the in situ generation of highly reactive transient species, mainly hydroxyl radical ($HO^{\bullet}$), which could oxidize or mineralize many refractory organics. Among them, electrochemical advanced oxidation process (EAOP) has received special interest, including electrochemical oxidation (EO), electro-Fenton process (EF) and photo electro-Fenton process (PEF) (Brillas et al. 2009). Electrochemical oxidation is able to degrade biorefractory organic pollutants completely and they can minimize the chemical input by employing electron as the clean reagent for reaction, which makes EO distinguished from other EAOPs. Due to its advantages, EO has been applied to oxidize or alleviate various types of recalcitrant organic pollutants including dyes, pesticides and herbicides, phenolic

compounds, personal care products, pharmaceuticals and antibiotics, steroid estrogens, plasticizers, perfluorinated chemicals, halogenated solvents, surfactants, chelating agents and microcystin toxins.

Among all the recalcitrant organic compounds, phenols and phenolic compounds are the most prevalent ones in some industrial wastewaters. They are hazardous and toxic compounds which may cause unpleasant taste and odor, and in Singapore they have been included in the list of prohibited organic compounds for discharging to the public sewer. The main sources of phenolic pollutants include oil refinery, textile, coal conversion, pharmaceutical, and petroleum and petrochemical industries. From the perspective of human health, phenols have to be properly handled or discharged, because of their suspected carcinogenic properties (Kim et al. 2002a). Traditional treatment methods for removing phenol such as active carbon adsorption, solvent extraction and chemical oxidation face the drawbacks of high cost and unwanted by-products production (Zhang et al. 2011a). Biological treatment is suitable for phenolic wastewater when the concentration is not exceeding 50 mg/L, beyond which there might be inhibitive to the process (Seker et al. 1997).

In recent years, many researchers are attempting to apply electrochemical oxidation for wastewater treatment, and the anode material is found to be critical for the process efficiency. Up to now, various types of electrodes including glassy carbon, Pt, PbO_2, IrO_2, RuO_2, SnO_2-Sb, graphite and BDD have been investigated for the electrochemical oxidation of organic pollutants. Some anodes favor the selective oxidation or conversion of the organics to various metabolites, while others can achieve complete degradation of organics to CO_2 and H_2O.

Among all the anodes investigated, mixed metal oxide (MMO) electrodes are of particular interests because of their satisfactory efficiency, easy preparation, and good physical and chemical stability under extreme conditions (Zhou et al. 2011b). On the other hand, comparing with other materials such as precious metal oxides and

BDD, MMO electrodes also have the advantage of being more cost-effective. Because of its versatility and cost-effectiveness, electrochemical oxidation using MMO anodes provides an efficient solution for degrading the recalcitrant and toxic organic compounds in the aquatic environment.

1.2 Knowledge gap and research motivation

As mentioned above, MMO anodes exhibit multiple advantages in their application for electrochemical oxidation. However, the success of MMO anodes for electrochemical oxidation of recalcitrant organics highly relies on the choice of MMO materials. Among MMO electrodes, Sb-doped SnO_2 anode has been demonstrated to have relatively high OEP and be superior for the oxidation of organic compounds (Adams et al. 2009, Grimm et al. 1998, Shao et al. 2014a). In addition, SnO_2-Sb anode is cost effective compared with other MMO anodes, making it more attractive for electrochemical oxidation process.

Pure SnO_2 is an n-type semiconductor with a band gap of 3.5 eV. Because of its considerably high resistivity at room temperature, direct use of SnO_2 as an electrode material is strongly restricted. Oxygen vacancy is the predominant atomic defect for SnO_2, and by reducing the concentration of oxygen vacancy the conductivity of SnO_2 can be improved. Doping of elements can greatly enhance the conductivity of SnO_2 electrode, and Sb is the most important dopant for SnO_2 electrodes because the higher valance of Sb^{5+} than Sn^{4+} and thus Sb could provide excessive electrons and function as electron donors.

Pollutants such as phenol and phenolic compounds can be readily oxidized at SnO_2-Sb anode comparing with Pt and other MMO anodes, favoring complete oxidation of pollutants to CO_2 and H_2O (Borras et al. 2007, Tran et al. 2009, Zhao et al. 2009). However, the short service life of SnO_2-Sb electrode resulting from the weak adhesion between Ti substrate and SnO_2 (Chen et al. 2005, Shao et al. 2014b,

Zanta et al. 2003, Zhang et al. 2014) or the formation of nonstoichiometry $SnO_{(2-x)}$ (CorreaLozano et al. 1997) has represented an insurmountable barrier to its commercial applications. Thus, it is important to overcome this problem by deliberatively designing the structure of SnO_2-Sb electrode and carefully selecting the suitable fabrication techniques.

Due to the nature of anode materials employed, the composition of wastewater and the range of operating parameters applied, the mechanisms involved in the electrocatalytic oxidation of recalcitrant organic compounds could be different by the generation of various oxidant species (Niu et al. 2013a, Souza et al. 2014). Besides, for a selected target pollutant, various intermediates are produced before complete mineralization is achieved (Chaplin 2014, Lin et al. 2013a, Radjenovic et al. 2011). Some of the intermediates may present as toxic byproducts, requiring them to be properly removed before the discharge of treated wastewaters. Therefore, the investigation of electrocatalytic performance of the anodes under various operating conditions with in-depth understanding of the reaction pathways has both scientific merits and practical significance.

1.3 Objectives and scopes of research

The research aimed to fabricate and characterize modified MMO anodes based on SnO_2-Sb for effective removal of recalcitrant phenolic compounds through electrochemical oxidation. At the later stage, the study also aimed to compare the performance and reaction mechanisms between modified MMO anodes and commercial BDD anode. The detailed scopes of the research are as follows:

1. Fabrication of hydrophobic SnO_2-Sb anode modified by PTFE composite and deposited on nanostructured TiO_2-NTs:

- To fabricate and characterize TiO_2-NTs/SnO_2-Sb-PTFE;
- To evaluate the electrocatalytic performance of TiO_2-NTs/SnO_2-Sb-PTFE

for phenol oxidation;

- To determine the optimized condition for TiO_2-NTs/SnO_2-Sb-PTFE fabrication;
- To investigate the influences of operating parameters on the process efficiency;
- To quantify the Sn leaching from the anodes;
- To investigate the advantages of TiO_2-NTs/SnO_2-Sb-PTFE over conventional Ti/SnO_2-Sb anode and the mechanisms involved.

2. Fabrication of duplex-structured Ti/SnO_2-Sb/SnO_2-Sb-CNT anode:

- To synthesize and characterize SnO_2-Sb-CNT composites;
- To fabricate Ti/SnO_2-Sb/SnO_2-Sb-CNT anodes by incorporation of SnO_2-Sb-CNT composites and to characterize the anodes;
- To determine the adsorption capacity of BPA by Ti/SnO_2-Sb/SnO_2-Sb-CNT;
- To evaluate the performance efficiency of Ti/SnO_2-Sb/SnO_2-Sb-CNT for synergistic adsorption and oxidation of BPA;
- To propose a mechanism for the process.

3. Comparison of the electrocatalytic oxidation of bisphenol A (BPA) by modified SnO_2-Sb anodes and BDD anode

- To compare the oxygen evolution potential of modified SnO_2-Sb anodes and BDD anode;
- To compare their electrocatalytic performance for BPA oxidation under various operating parameters;
- To investigate the influences of pH and type of supporting electrolyte on the performance efficiency;
- To determine the aliphatic byproducts and aromatic byproducts;
- To propose the reaction pathways for electrocatalytic oxidation of BPA;
- To sum up the benefits and drawbacks of modified SnO_2-Sb anodes

comparing to BDD anode.

1.4 Organization of thesis

This thesis comprises 6 chapters. Chapter 1 presents the background, gap of knowledge, motivation, objectives, scopes of the research and also organization of the thesis. Chapter 2 presents a critical review comprising the fundamentals of MMO anode materials, the syntheses and characterizations of MMO anodes, the modification of MMO anodes for improved electrocatalytic performance, the mechanisms of electrochemical oxidation by MMO anodes, and the operating parameters influencing the efficiency of electrochemical oxidation. Besides, the challenges and possible improvement of this technique are discussed. Chapter 3 describes the fabrication and characterization of hydrophobic TiO_2-NTs/SnO_2-Sb-PTFE anodes for electrochemical oxidation of phenol, and the comparison of their electrocatalytic efficiency with conventional Ti/SnO_2-Sb anode is provided. Chapter 4 describes the fabrication and characterization of Ti/SnO_2-Sb anode modified by SnO_2-Sb-CNT composite and the mechanism of its synergistic adsorption and electrochemical oxidation of BPA. Chapter 5 presents the comparative study on the electrochemical oxidation of BPA by commercial BDD anode and self-fabricated modified SnO_2-Sb anodes described in Chapter 3 and Chapter 4. Chapter 6 summarizes the important conclusions derived from the study as well as provides several recommendations for future study.

CHAPTER 2 LITERATURE REVIEW[1]

2.1 Introduction

Metal oxides represent one of the most important categories of solid catalysts which are widely used either as active phases or supports (Gawande et al. 2012). Because of their acid-base and redox properties, metal oxides have been extensively employed for heterogeneous catalysis. Among all kinds of metal oxide catalysts, those which contain more than one kind of metal cations are known as mixed metal oxides (MMOs). By mixing different metal oxides, new stable compounds can be formed, and some of them exhibit significant improvement in catalytic activity than their respective single-component metal oxides. This could be due to an increase in the surface area, an increase of active acidic or basic sites or a change in the chemical states of the metal ions. Some important applications of MMOs as heterogeneous catalyst include Al_2O_3 supported MMOs for $(CH_3)_2S_2$ degradation (Wang and Weng 1997), TiO_2-ZrO_2 for non-oxidative dehydrogenation of ethylcyclohexane (Wu et al. 1984), Mg-V-Al MMOs for oxidative dehydrogenation of propane (Blanco et al. 2008), $Fe_xCe_{1-x}O_2$ for N_2O degradation (Perez-Alonso et al. 2006), V-Sb-Nb MMOs for ammoxidation of propane (Guerrero-Perez et al. 2006), $LaNiO_3$ for ethanol reforming (Lin et al. 2013c) and RuO_2-IrO_2-SnO_2 for chloralkali process (Vazquez-Gomez et al. 2006).

Besides their applications as catalysts, MMOs have also been studied for a wide range of other purposes, i.e. semiconductors, sensors, photoconductive thin films, and electrode materials for lithium battery, fuel cell and environmental application

[1] This chapter is modified from the literature published in *Applied Catalysis A: General* in 2014 (vol. 480, pp. 58-78), of which the Ph.D. candidate is the first author.

(Arafat et al. 2012, Desilvestro and Haas 1990, Hua et al. 2012, Tucker 2010). Remarkable progress has been achieved in the research on MMO application as the anode material for electrochemical oxidation of recalcitrant pollutants in aqueous environment, since the treatment of water and wastewater has become a more challenging issue due to the ineffective degradation of those pollutants by conventional treatments which rely on biological process (Andreozzi et al. 2003, Li et al. 2013d). Several reviews have described the removal or alleviation of recalcitrant organic pollutants in water by electrochemical oxidation, with regard to the various MMO anodes employed and different mechanisms involved (Anglada et al. 2009, Martinez-Huitle and Andrade 2011, Martinez-Huitle and Ferro 2006, Panizza and Cerisola 2009). Typically, MMO anodes are prepared by depositing the MMO layer on inert substrates (titanium, carbon, stainless steel, etc.). Indeed, increasing efforts have been put forward to evaluating the ability of MMO anodes to remove or alleviate various types of recalcitrant organic pollutants including dyes, pesticides and herbicides, phenolic compounds, pharmaceuticals, antibiotics and hormones, plasticizers, perfluorinated chemicals, surfactants and derivatives, chelating agents and microcystin toxins.

Table 2.1 summarizes various types of recalcitrant organic pollutants which have been investigated for their electrochemical oxidation with different MMO anodes. The organic pollutants can be degraded by either direct oxidation or mediated oxidation with MMO anodes. In the mediated oxidation, the active chlorine generated from chlorides is the most commonly employed mediator. The active chlorine has the merit to treat landfill leachate (Tauchert et al. 2006, Turro et al. 2011) and reverse osmosis (RO) concentrate from water reclamation plants (Bagastyo et al. 2013, Bagastyo et al. 2011, Radjenovic et al. 2011, Zhou et al. 2011a), both of which have high salinity. In general, MMO anodes are effective to abate aqueous pollution caused by recalcitrant organics, even for those which have extraordinary strong C-F bond

(490 kJ. mol^{-1}) (Lin et al. 2012, Niu et al. 2012, Zhao et al. 2013, Zhuo et al. 2011). With appropriate MMO anodes and suitable operating condition for electrochemical oxidation, most recalcitrant organics can be completely removed, or alleviated to their acceptable levels suitable for subsequent biological treatment (Feng et al. 2013).

In this review, several aspects of MMO anodes are discussed, i.e. the classification of MMO anodes, their synthesis and characterization, and the surface modification of MMO anodes, with specific emphasis on the improvement of their catalytic activity to degrade aqueous organics pollutants by electrochemical oxidation. Several factors which have important effects on the process efficiency are also systematically discussed, including pH, temperature, current density and supporting electrolytes.

Overall, this review focuses on the following issues that arise:

- the extent to which the electrocatalytic activities of MMO anodes can be improved by specific surface modifications;
- the mechanisms that are responsible for the electrochemical degradation of organic pollutants at MMO anodes;
- the determination of electrogenerated reactive oxygen species (ROS) at MMO anodes that can be achieved by various qualitative and quantitative methods.

Table 2.1 Summary of various types of recalcitrant organic pollutants which can be degraded by MMO anodes

Compound		MMO anode type[a]	Current density ($mA.cm^{-2}$)	Removal efficiency[c]	Current efficiency	Service life (h)	Reference
Dyes and dye effluent	Acid Black 194	Ti/SnO_2-Sb/PbO_2-Pr	30	0.57-0.88 [COD]	0.014-0.024	-[d]	He et al. (2011)
	Acid Orange 7	Ti/SnO_2-Sb_2O_4	20	0.88 [TOC]	0.39	-	Ciriaco et al. (2011)
	Aniline	Ti/SnO_2-Sb	20	0.91 [COD]	0.20	-	Li et al. (2016)
		Ti/SnO_2-Sb/Pb_3O_4		0.86 [COD]	0.17		
		Ti/SnO_2-Sb/PbO_2		0.65 [COD]	0.14		
	C.I. Acid Red 73	Ti/SnO_2-Sb-CNT	25-100	0.78-0.96 [Color]	0.26-0.77	-	Xu et al. (2015a)
	Gold yellow X-GL	Ti/SnO_2-Sb_2O_3/PTFE-La-Ce-PbO_2	43-86	0.40-0.74 [COD]	-	-	Dai et al. (2013)
	Indigo carmine	Ti/IrO_2-SnO_2-Sb_2O_5	5-20	0.99 [COD]	-	-	Rodríguez et al. (2013)
	Industrial dye effluent	Ti/RuO_2/IrO_2	10-25	0.56-1 [COD]	-	-	Raghu et al. (2009)
	Industrial dye effluent	Ti/Ru-Ti-O	10-50	0.53-0.83 [COD]	0.47-0.89	-	Basha et al. (2012)
	Industrial dye effluent	SS/SnO_2-CeO_2	P[b]	0.49 [COD]	-	-	Zhang et al. (2010)
	Methyl orange	Ti/SnO_2-Sb/PbO_2-TiO_2	1	0.77 [Color]	-	158	Xu et al. (2013a)
	Methyl orange	Ti/PbO_2-Pr_2O_3	40	0.89 [COD]	0.17	750	Wang et al. (2012a)
	Methyl orange	Ti/TiO_2-NTs/SnO_2	30	0.59 [TOC]	-	-	Zhao et al. (2010b)
	Methyl orange	TiO_2-NTs/SnO_2-Sb	P	0.16-0.27 [Color]	-	116	Xu et al. (2011)
	Methyl orange	Ti/IrO_2-SnO_2-Sb_2O_5	P	0.98 [Color]	-	-	Chaiyont et al. (2013)
	Methyl orange	Ti/Ce-nanoTiO_2/Ce-PbO_2	50	0.97 [COD]	0.146	190	Xu et al. (2016)
	Orange II	Ti/SnO_2-Sb-Mn	10	0.46 [COD]	-	-	Yao et al. (2013)
	Reactive Black 8	Ti/RuO_2-IrO_2	31.7	0.32 [COD]	-	-	Wu et al. (2012)

Dyes and dye effluent *(continued)*	Reactive Blue 194	Ti/TiO_2-NTs/SnO_2-Sb/PbO_2	100-200	0.30-0.40 [TOC]	0.06-0.09	75	An et al. (2012)
	Reactive Blue 221	$Ti/IrO_2/TaO_2/RuO_2$	16.2	0.44 [COD]	0.04-0.065	-	Karuppiah and Raju (2009)
	Reactive Orange 4	Ti/SnO_2-Sb-Pt	125	0.9-0.95 [COD]	-	990	del Río et al. (2010)
	Reactive Red 120	Ti/IrO_2-RuO_2	15-50	0.32-0.43 [COD]	0.13	-	Panakoulias et al. (2010)
	Reactive Red 195	Ti/SnO_2-Sb/PbO_2	30	0.53-0.8 [TOC]	0.015-0.04	-	Song et al. (2010a)
	Reactive Red 198	$Ti/Ru_{0.3}Ti_{0.7}O_2$	5-89	0.40-0.80 [TOC]	-	-	Catanho et al. (2006)
	Selected disperse dyes	Ti/RhO_x-TiO_2	30	0.40 [Color]	0.1-0.2	-	Szpyrkowicz et al. (2005)
	Selected reactive dyes	Ti/SnO_2-Sb-Pt	125	0.99 [Color]			Sala et al. (2012)
	Selected reactive dyes	Ti/TiO_2-RuO_2-IrO_2	72.2	73.5 [COD]	-	-	Rajkumar and Kim (2006)
	Synthetic dye effluent	Ti/Ti-Pt-Ir-O	5-14	0.55-0.86 [COD]	0.045-0.314	-	Chatzisymeon et al. (2006)
Pesticides and herbicides	Atrazine	$Ti/Ru_xSn_{1-x}O_2$ ($0.1 \leq x \leq 0.3$)	10	0.21 [COD]	-	-	Malpass et al. (2010)
	Atrazine	$Ti/Ru_{0.3}Ti_{0.7}O_2$	10-120	0.04-0.46 [TOC]	-	-	Malpass et al. (2007)
	Carbaryl	$Ti/Ru_{0.3}Ti_{0.7}O_2$	40	0.58 [COD]	-	-	Malpass et al. (2013)
	Cyanuric acid	$Ti/Ru_{0.3}Ti_{0.7}O_2$	5-50	0.13-0.56 [TOC]	-	-	Malpass et al. (2009)
	Cypermethrin	Ti/SnO_2-Sb	40-80	0.44-0.76 [COD]	-	-	Bouya et al. (2012)
	Dichlorvos	Ti/SnO_2-Sb_2O_5	P	0.99 [COD]	-	-	Vargas et al. (2013)
	Methamidophos	Ti/SnO_2-Sb	20-30	0.40 [COD]	-	-	Martinez-Huitle et al. (2008)
	Glyphosate	$Ti/(RuO_2)_{0.7}(Ta_2O_5)_{0.3}$; $Ti/Ru_{0.3}X_{0.7}O_2$ (X = Ti, Sn or Pb); $Ti/Ir_{0.3}Sn_{0.7}O_2$	50	0.81-0.91 [COD]	0.20-0.40	-	Neto and De Andrade (2009)

Phenolic compounds	Benzoic acid	Ti/TiO_2-NTs/Sb-SnO_2	20	0.658 [COD]	0.261	45	Li et al. (2009)
	Phenol	Ti/SnO_2-Sb_2O_3/Nb_2O_5-PbO_2	0-50	0.72-0.84 [Phenol]	0.15-0.2		Yang et al. (2009)
	Phenol	Ti/SnO_2-Sb-Gd	20	0.74 [TOC]	-	-	Feng et al. (2008)
	Phenol	Ti/SnO_2-Sb_2O_3	10-50	0.17-1[TOC]	-	-	Zhu et al. (2008a)
	Phenol	Ti/SnO_2-Sb-Eu	20	0.90 [TOC]	-	-	Feng et al. (2010a)
	Cardanol	Ti/TiO_2-RuO_2	20-60	0.90-0.99 [TOC]	-	-	Santos et al. (2016)
		Ti/TiO_2-RuO_2-IrO_2		0.70-0.99 [TOC]			
	Phenol	Ti/SnO_2-Sb_2O_3/PbO_2	15	0.38-0.59 [COD]	0.20-0.45	8.4-29.5	Wang et al. (2009b)
		Ti/SnO_2-Sb_2O_3/MnO_2					
		Ti/SnO_2-Sb_2O_3/RuO_2-PbO_2					
	Phenol	Ti/SnO_2-Sb_2O_4-CNT	10	0.71 [COD]	-	4.3	Hu et al. (2010)
	Phenol	Ti/SnO_2-Sb_2O_5-RuO_2/α-PbO_2/β-PbO_2	10	0.94 [COD]	0.53	59	Zheng et al. (2011)
	Phenol	Ti/SnO_2-Sb-La	30	0.86 [COD];	0.406;	35.5;	Xu et al. (2012)
		Ti/SnO_2-Sb-Ru		0.82 [COD]	0.386	34	
	Phenol	Ti/TaO_x-IrO_x/BiO_x-TiO_2/BiO_x-TiO_2	P	-	0.6	-	Park et al. (2012)
	Phenol	Ti/TiO_2-BiO_x	14.7	0.60 [Phenol]	0.67	-	Park et al. (2009)
	Phenol	TiO_2-NTs/SnO_2-Sb-PTFE	20	0.94 [TOC]	0.116-0.178	51-103	Wu et al. (2015)
	Pentachlorophenol (PCP)	Ti/SnO_2-Sb	5-40	0.9-0.99 [PCP]	-	-	Niu et al. (2013a)
	4-chlorophenol	Ti/SnO_2-Sb/PbO_2-Er	20	0.81 [COD]	0.1-0.161	-	Kong et al. (2007)
	4-chlorophenol	Ti/SnO_2-Sb_2O_3/PbO_2-ZrO_2	200	0.96 [COD]	0.87	141	Yao et al. (2012)
	4-chlorophenol	Ti/IrO_2/RuO_2	39	0.9 [COD]	-	-	Wang and Wang (2008)

	4-chlorophenol	Ti/Sn-Sb-Ni-O	3.1	0.99 [TOC]	-	-	Wang et al. (2006)
	4-chloro-3-methyl phenol	Ti/SnO_2-Sb/PbO_2	1-30	-	0.065-0.2	175	Song et al. (2010b)
	2,4-dichlorophenol	Ti/SnO_2-Sb	2-40	0.928 [TOC]	-	-	Niu et al. (2013b)
Pharmaceuticals, antibiotics, hormones	Acetaminophen	Ti/TiO_2/RuO_2	24-180	0.90 [COD];	-	-	de Oliveira et al. (2011)
		Ti/Ta_2O_5/IrO_2		0.40 [COD]			
	Aspirin	Ti/PbO_2-La-Y	50	0.55 [COD]	0.18-0.52	-	Dai et al. (2016a)
	Cinnamic acid	Ti/PbO_2-Mo	5-40	0.14-0.51 [COD]	0.094-0.598	-	Dai et al. (2016b)
	Ciprofloxacin	Ti/SnO_2-Sb	10-40	0.86 [COD]	0.038-0.13	160	Wang et al. (2016)
	Ketoprofen	Ti/SnO_2-Sb	20	0.70 [TOC]	0.25	-	Fan et al. (2013)
	Metronidazole	Ti/SnO_2-Sb-Ce	4.8	0.10-0.31 [TOC]	-	-	Cheng et al. (2013a)
	Metronidazole	Ti/PbO_2-Co	10-70	0.22-0.56 [COD]	0.04-0.12	-	Dai et al. (2016c)
	Ofloxacin and Lincomycin	Ti/IrO_2/Ta_2O_5	20	0.30 [COD]	-	-	Carlesi Jara et al. (2007)
	Paracetamol	RVC/CuO/TiO_2/Al_2O_3	P	0.80-0.99 [TOC]	0.32-0.68	-	Valdez et al. (2012)
	Sulfamethoxazole	Ti/SnO_2-Sb/PbO_2-Ce	2-40	0.46-0.91 [TOC]	-	-	Lin et al. (2013b)
	Tetracycline	Ti/$Ru_{0.3}Ti_{0.7}O_2$	P	0.13-0.43 [COD]	-	-	Guoting et al. (2009)
	Various pharmaceuticals	Ti/Pt/SnO_2-Sb_2O_4	10-30	0.17-0.82 [COD]	0.45-0.88	-	Santos et al. (2013)
	17-α-ethylnylestradiol	Ti/SnO_2-Sb	10	0.99 [TOC]	0.075-0.2	-	Feng et al. (2010b)
Bisphenol-A	Bisphenol-A	Ti/SnO_2-Sb_2O_5/PbO_2	40	0.82 [COD]	-	-	Xue et al. (2011)
	Bisphenol-A	Ti/SnO_2-Sb	10-50	0.90 [TOC]	-	-	Cui et al. (2009b)

	Bisphenol-A	Ti/TiO_2-RuO_2	6.5-30	0.09 [COD]	-	-	Pereira et al. (2012)
Plasticizers	Di(2-ethylhexyl) phthalate (DEHP)	Ti/IrO_2-RuO_2	7.7	0.8 [DEHP]	-	-	Espinoza et al. (2016)
	Diethyl phthalate	Ti/IrO_2/RuO_2	39	0.40 [COD]	-	-	Wang et al. (2010a)
	Diethyl phthalate	Ti/SnO_2-Sb	20-40	-	0.001-0.026		Vazquez-Gomez et al. (2012)
Nitrophenol	2-nitrophenol	Ti/PbO_2-Ce	20	0.91 [COD]	0.383	895	Liu et al. (2011)
	4-nitrophenol	Ti/SnO_2-Sb_2O_5	50	0.94 [COD]	-	-	Liu et al. (2012a)
	4-nitrophenol	Ti/TiO_2-NTs/SnO_2-Sb	20	0.91 [TOC]	-	-	Chai et al. (2011)
	4-nitrophenol	Ti/CeO_2-RuO_2-SnO_2	20	0.86 [COD]	0.336	340	Liu et al. (2012b)
	4-nitrophenol	Ti/SnO_2-Sb_2O_5-IrO_2	P	0.75 [TOC]	0.468		Chu et al. (2012)

[a]MMO anode type - SS, stainless steel; FR - fluorine resin; RVC - reticulated vitreous carbon; CA - carbon aerogel; RDE - rotating disk electrode; CNT - carbon nanotubes;

[b]P-Operated at potentiostatic mode;

[c]Removal efficiency: determined by COD, TOC, Color and pollutant concentration;

[d]Data not reported.

2.2 Metal oxide systems of MMO anodes

2.2.1 Bulk mixed metal oxide anode

Bulk mixed metal oxide anodes represent one kind of MMO anodes of which the anode surface layers comprise completely mixed metal oxides. Methods including thermochemical decomposition (Feng et al. 2010a), electrodepostion (Hu et al. 2010), chemical vapor deposition (CVD) (Gelfond et al. 2010) and physical vapor deposition (PVD) (Lee et al. 2012) have been employed to produce the bulk mixed metal oxide layer. For each preparation, the employed precursor solution contains a mixture of metal precursors. Thus, different metal oxides can be deposited on the substrate concurrently and homogenously. The mixed metal oxides can be binary, ternary or quaternary system and so on in accordance with the number of metal cations involved. Fig. 2.1a shows a conceptual diagram of the surface composition in a binary metal oxide anode system. In a bulk mixed metal oxide system, the MMO layer with completely mixed MMO components provides active sites for electrocatalytic reactions. For the application of removing or alleviating organic compounds in wastewater, some of the important MMO anodes based on the bulk mixed metal oxide system include Sn-Sb binary MMO anodes, Ir-Ru binary MMO anodes, Ir-Ta binary MMO anodes, Ti-Ru binary MMO anodes, Ti-Bi binary MMO anodes, Ir-Ru-Sn ternary MMO anodes, Ce-Ru-Sn ternary MMO anodes and Ru-Ir-Sn-Ti quaternary MMO anodes.

Normally parameters such as roughness or porosity factors are used to describe the surface of solid electrodes. However, it is important to gain some insights into the distribution of the surface sites and internal sites since the anode surface is of much concern, and major reactions take place in the MMO anode surface if it is not permeable. One way to determine the ratio of internal region to total surface region is by calculating the morphology factor (φ_{morph}) (Da Silva et al. 2001, Malpass et al.

2006). The morphology factor is analogues to the porosity factors proposed by Trasatti and coworkers (1990, 1995, 1997). It can be considered as a measure of the ratio of the internal and total surface areas, and can be estimated using Eqn (2,1):

$$\varphi_{morph} = \frac{C_{d,i}}{C_d} \tag{2.1}$$

where $C_{d,i}$ and C_d are the internal and total differential capacitances of the mixed oxides region respectively, and they represent the corresponding surface areas. The values of φ_{morph} range from 0 to 1. In general, φ_{morph} close to 0 indicates small or negligible contribution of the internal sites to the overall differential capacitance, and the value approaching 1 indicates a large internal region of the electrode.

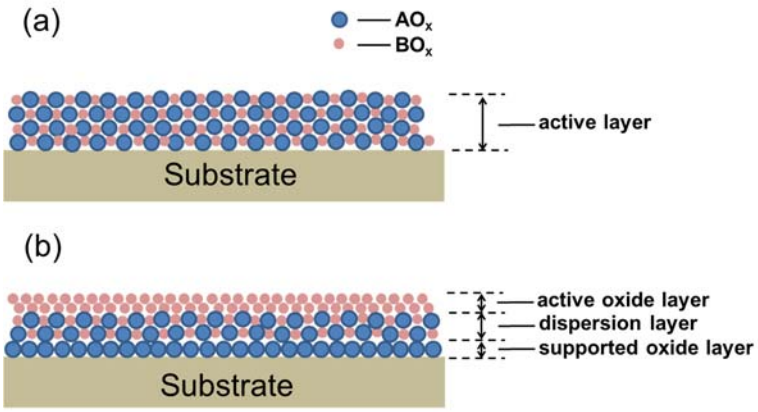

Fig. 2.1 Conceptual diagram and surface oxides structures of (a) binary bulk mixed metal oxide anode and (b) supported metal oxide anode.

2.2.2 Supported metal oxide anode

It is always desired for MMO anodes to have improved electrocatalytic performance or prolonged service life by mixing the metal oxides in the surface layer, as what has been discussed for the bulk MMO system. However, sometimes such twin goals can be realized by depositing one active metal oxide film on the other metal oxide support (Wang et al. 2007b). Such kind of metal oxide anodes are known

as supported metal oxide anodes. It has been demonstrated that spontaneous dispersion of one crystalline metal oxide over the other metal oxide may take place by surface spreading above the Tammann temperature (T_{TAM}=1/2 T_{MP}, where T_{MP} is the melting point of metal oxide) (Chen et al. 1996, Haber et al. 1995), or at a reduced temperature (240 – 400 ^{o}C) (Deng 2008). Thus, a dispersion layer comprising a mixture of different metal oxides will be formed. For those supported metal oxide anodes which require a calcination process for their fabrication, the calcination temperatures usually range from 400 ^{o}C to 700 ^{o}C, which are high enough for the occurrence of spontaneous dispersion and formation of MMOs layer. In addition, when the active oxide layer is prepared using facile methods like electrodepostion, such dispersion effect was also confirmed by XRD (An et al. 2011). For the purpose of this review, the supported metal oxide anodes are discussed as MMO anodes.

The layered structure of active oxide layer, dispersion layer and supported oxide layer in supported metal oxide anode is illustrated in Fig. 2.1b. Although the supported oxide layer does not directly participate in the surface reactions including organic compounds oxidation, oxygen evolution or oxidizing reagents generalization, it can enhance the performance of the MMO anode by: (1) increasing the electrocatalytic activity of the surface layer (An et al. 2012, Zanta et al. 2003), (2) enhancing the mechanical and chemical stability of the surface, and thus prolonging the service life (Zheng et al. 2011), (3) improving the electrode conductivity (Kong et al. 2012) and (4) increasing the surface area and hence the reaction rates (Zhao et al. 2009). Some supported metal oxides which are widely employed include single metal oxides of α-PbO_2, RuO_2, IrO_2, Al_2O_3, TiO_2 nanotubes (TiO_2-NTs), and binary MMOs of Ir-Ru-O, Ir-Ta-O and Sn-Sb-O.

2.3 Synthesis of MMO anodes

Various synthesis methods have been attempted to fabricate MMO anodes.

These methods fall into two main groups, i.e. chemical methods (e.g. thermochemical decomposition, electrodeposition, anodization, sol-gel method, spin coating, CVD), and physical methods (e.g. magnetron sputtering, PVD). When introducing the different metal oxide components to a bulk MMO anode or supported metal oxide anode, various synthesis strategies can be applied. For example, either thermochemical degradation or electrodeposition can be employed as the only synthesis technique when introducing the homogeneous MMO film onto a bulk MMO anode (Chaiyont et al. 2013, Chellammal et al. 2012) or supported metal oxide anode (An et al. 2011). However, in more common cases with supported metal oxide anodes, the metal oxide films are prepared layer by layer by different synthesis techniques, including thermochemical degradation of the support layer and electrodeposition of the active layer (Niu et al. 2012). Such attempts result in good anti-corrosion property of the inner layer and electrocatalytic active outer layer. Recent approaches for the synthesis of various MMO anodes, and their corresponding physicochemical characteristics and performances are presented in Table 2.2.

Indeed, the stability of MMO anodes is critical for their industrial application, in which the cost-effectiveness of process has to be considered. In laboratory-scale studies, the stability of MMO anodes can be accessed by accelerated life test. At specific temperature, the accelerated life tests are carried out in a three electrode cell under galvanostatic conditions at 100 – 1000 $mA.cm^{-2}$ in highly concentrated H_2SO_4 solutions, and the service life is defined as the duration from beginning of the test to the time at which the cell potential reaches a given value (Chen et al. 2005, CorreaLozano et al. 1997, Hu et al. 2011). However, there is a lack of consistency in the test conditions in previous studies, which makes it difficult to compare the service life of MMO anodes. To avoid the “disguised service life”, accelerated life test must be rigorously conducted with a good protocol of quality control, and the experimental conditions have to be well defined.

Table 2.2 MMO anodes: synthesis techniques, physicochemical characteristics and performances

Synthesis techniques	Anodes	Physicochemical characteristics and performance	Reference
Thermochemical decomposition			
Dip-coating and bake	Ti/SnO_2-Sb/Ce	SEM showed "mud-crack" surface morphology; XRD rutile phase of SnO_2 was observed by XRD. Limited conversion of oxidation byproducts to CO_2 was found.	Cheng et al. (2013b)
	Ti/SnO_2-Sb-Eu (SnO_2-Sb inner layer prepared by thermal decomposition)	Rutile type SnO_2 increased with pyrolysis temperatures in the range of 550–750 ℃. Eu^{3+} (95 pm) replaced the Sn^{4+} with smaller ionic radii (71 pm), resulted in lattice expansion. Best phenol removal efficiency (96.4%) was achieved when the pyrolysis temperature was 750 ℃.	Feng et al. (2010a)
	Ti/CeO_2-RuO_2-SnO_2	The crystal size decreased by incorporation of Ce, which in turn increased the specific surface area of anode.	Liu et al. (2012b)
	SS/CeO_2-SnO_2	"Cracked-mud" morphology was distinct. The size of 'mud' islands of SnO_2-CeO_2 coating was smaller than that of SnO_2 film.	Zhang et al. (2010)
	Ti/IrO_2-SnO_2-Sb_2O_5	The surface morphology was "crack-mud" type.	Tian et al. (2007)
	Ti/$(Ru_{1-x}Ti_x)O_2$	XPS showed a charge transfer from the RuO_2 to the TiO_2, resulted in enhanced oxygen evolution reaction.	Näslund et al. (2013)
	Ti/BiO_x-TiO_2	Heavy doping level of Bi enabled the electrode both photoelectron-catalytic and electrocatalytic activites.	Park et al. (2012)
	TiO_2-NTs/SnO_2-Sb (TiO_2-NTs prepared by anodization)	Electron transfer resistance of TiO_2-NTs/SnO_2-Sb (0.59 kΩ) was much less than Ti/SnO_2-Sb (3.85 kΩ). Lattice parameters of TiO_2-NTs/SnO_2 were also smaller.	Li et al. (2009)
Spray pyrolysis	Ti/SnO_2-Sb_2O_5	Small uniform particles were predominant, and the film was polycrystalline with a tetragonal structure.	Yao (2011)
	Ti/IrO_2/SnO_2–Sb_2O_5	The electrode surface is low rugosity/porosity compared with Ti/IrO_2. IrO_2 interlayer strongly increases the electrode service life. 95% TOC elimination of p-CP can be acheavied.	Zanta et al. (2003)

Synthesis techniques	Anodes	Physicochemical characteristics and performance	Reference
Sol-gel	Ti/IrO_2-SnO_2-Sb_2O_5	SEM showed uniformly distributed rough surface. Effective removal of methyl orange dye was acheived.	Chaiyont et al. (2013)
	Ti/SnO_2-Sb-La; Ti/SnO_2-Sb-Ru	XRD studies evidenced the tetragonal rutile structure of RuO_2; no diffraction peak of La, Ru or Sb was found. Ti/SnO_2-Sb-La showed lowest impedance and best electrocatalytic activity.	Xu et al. (2012)
	Ti/SnO_2-RuO_2-IrO_2; Ti/Ta_2O_5-IrO_2; Ti/RhO_2-IrO_2	SEM showed a heterogeneous cracked morphology for Ti/Ta_2O_5-IrO_2 and rough coating with a grain-like appearance for Ti/RhO_2-IrO_2. More than 90% phenol can be removed.	Makgae et al. (2008)
Electrodeposition			
Continious electrodeposition	TiO_2-NTs/SnO_2-Sb (TiO_2-NTs prepared by anodization)	XRD showed rutile phase of SnO_2 and no diffraction peak of Sb. Enhanced phenol degradation activity was obtained by TiO_2-NTs substrate.	Wang et al. (2013b)
	TiO_2-NTs/SnO_2-Sb/PbO_2 (TiO_2-NTs prepared by anodization)	"Flower-like" surface is observed by SEM; XRD studies confirmed β-PbO_2 on the surface. Phenols can be completely degraded, and the electrocatalytic activity debased as the morphology became more compact.	An et al. (2012)
	Ti/SnO_2-Sb_2O_3/MnO_2 (SnO_2-Sb_2O_3 prepared by sol-gel)	Compact and homogeneous MnO_2 layer was produced.	Lin et al. (2012)
	Ti/SnO_2-Sb/Ce-PbO_2 (SnO_2-Sb_2O_3 prepared by thermal decomposition)	Porous nanocrystalline PbO_2 film was found. The anode showed better performances for perfluorooctanoic acid (PFOA) degradation.	Niu et al. (2012)
	Ti/TiO_2/PbO_2 (TiO_2 prepared by anodization)	The surface of the anodized titanium electrodes is not homogeneous; electrodeposition of PbO_2 occurred selectively on the (0001) grains.	Devilliers and Mahé (2010)
	Ti/SnO_2-Sb_2O_5-RuO_2/ α-PbO_2/β-PbO_2 (SnO_2-Sb_2O_5-RuO_2 prepared by thermal decomposition)	The prevailing crystal structure was β-PbO_2 in the surface; α-PbO_2 layer had a cauliflower structure with average size 4 μm, and β-PbO_2 had angular crystals with average size 6 μm. An increase in lifetime was obtained.	Zheng et al. (2011)
	Ti/SnO_2-Sb_2O_3/ Nb_2O_5-PbO_2 (SnO_2-Sb_2O_5 prepared by thermal decomposition)	Orthorhombic α-PbO_2 and tetragonal β-PbO_2 are found; improvement in electrical conductivity and hydrophilicity was obtained by doping Nb.	Yang et al. (2009)

Synthesis techniques	Anodes	Physicochemical characteristics and performance	Reference
Electrodeposition (continued)	TiO_2-NTs/PbO_2 (TiO_2-NTs prepared by anodization)	SEM showed PbO_2 grew around TiO_2-NTs	Li et al. (2013c)
Pulse electrodeposition	Ti/SnO_2-Sb_2O_4-CNT	SEM revealed granular surface structure. Prolonged life time and better COD removal was achieved compared with dip coating.	(Hu et al. (2010), Hu et al. (2011))
	Ti/TiO_2-NTs/SnO_2-Sb (TiO_2-NTs prepared by anodization)	The electrode had high OEP (2.4 V vs SCE), high electrocatalytic activity with 97.4% TOC removal for fluorobenzene. Compared with sol-gel made SnO_2, higher crystallinity, higher order degree of atomic lattice, and less oxygen vacancies were achieved.	Wu et al. (2011)
CVD	Ti/IrO_2/SnO_2	XRD confirmed existence of high purity Ir protective layer; SEM observed dense, homogeneous surface with high roughness.	Klamklang et al. (2009)
	Ti/IrO_x/SnO_2	The SnO_2 films were slightly textured either in the (110) or (200) direction. (110) preferential orientation is favored at high deposition temperatures and high metal salt concentration.	Duverneuil et al. (2002)
PVD	Si/$Ir_xRu_{1-x}O_2$	Highly single crystalline $Ir_xRu_{1-x}O_2$ nanowires were formed. E_g phonon mode from pure RuO_2 nanowire linearly blue shifted with incorporating Ir contents.	Lee et al. (2012)
Magnetron sputtering	Glass/ZnO_2-SnO_2	The Sn $3d_{5/2}$ peak can be resolved into two parts located at 486.7 and 486.0 eV, which corresponded to Sn^{4+} and Sn^{2+}.	Wang et al. (2011)

Among all the chemical methods, thermochemical decomposition, or pyrolysis, is the most widely applied method for the fabrication of SnO_2-based MMO anodes or Ir- and Ru-based MMO anodes. The main advantage of this synthesis method is its easy operation. In a typical thermochemical decomposition procedure, the metal salts, of which metal chlorides are most frequently used, are directly dissolved in the alcohol solvent. The alcohol solvent includes isopropanol, ethanol, butanol or their mixtures. In order to avoid the hydrolysis of the metal salts, it is necessary to introduce acidity to the precursor solution by adding hydrochloric acid. It is worth noting that the calcination temperature plays a critical role in the electrocatalytic

performance of MMO anodes. As reported by Domashevskaya et al (2013), when preparing SnO_2 anodes, a calcination temperature less than 450 ^oC would lead to the incomplete oxidation of tin precursor, resulting in the formation of SnO_x ($1<x<2$) nanolayer and a reduced band gap. Feng et al (2010a) described Eu doped Ti/SnO_2-Sb electrodes fabricated at various temperatures ranging from 450 to 850 ^oC, and observed well developed SnO_2 crystal and better electrocatalytic performance for phenol degradation when the anode calcination temperature is 750 ^oC. However, high calcination temperature may not extend the service life of MMO anodes (Watts et al. 2008). In view of above mentioning reasons, the most popularly used calcination temperature for SnO_2 is among 500 to 550 ^oC to ensure both the high electrocatalytic activity and anode stability. One of the main drawbacks of thermochemical degradation is the tendency to form cracks due to the high internal pressure of surface layer, and the cracks may lead to the poor stability.

Sol-gel method has been developed to produce the SnO_2 based MMO electrodes to overcome the drawbacks of direct thermochemical decomposition. First proposed by Pechini (1967), the sol-gel method can achieve colloidal precursor solution by dissolving the citric acid into a mixture of ethylene glycol and ethanol. After that the desired molar ratio of metal salt precursors are added and the solution is treated with ultrasonication for several hours, followed by the dip coating procedure. Modification of Pechini method has been made by Canevari et al (2011) to use organic metal compound $(C4H11)_2Sn(OCOCH_3)_2$ as precursor, and grafting Sb(V) into the SnO_2 surface.

Electrodepositon can be regarded as a facile method for the preparation of MMO anodes, and it has particularly extensive application for the preparation of PbO_2-based MMO anodes. For electrodeposited PbO_2, depositing conditions including pH, depositing current, Pb source and depositing temperature can have significant influence on the surface morphology, adhesion property and crystal forms of the

resulting PbO_2 (Li et al. 2011). For SnO_2- based MMO anodes, preparation by electrodeposition gives rise to regularly dispersed surface morphology compared to the thermochemical decomposition method, as illustrated in Fig. 2.2. In order to improve the anti-corrosion property of MMO anodes, single layer or multi interlayers may be applied to the substrate before electrodeposition of the outer layer, which is rather typical in the supported metal oxide system.

CVD appears to be the least attempted chemical method for preparing MMO anodes, due to its high operation cost and the difficulty in introducing several metal precursors in the furnace. Physical methods employed to fabricate MMO anodes include magnetron sputtering and PVD. The main difference between physical methods and chemical methods is the metal precursors used. Both magnetron sputtering and PVD directly employ metal oxides rather than metal salts as their precursors, and it is reported that physical methods contribute to better crystalline formation (Lee et al. 2012). But so far, few reports have been found about electrochemical oxidation of organic compounds with MMO anodes which were prepared by physical methods.

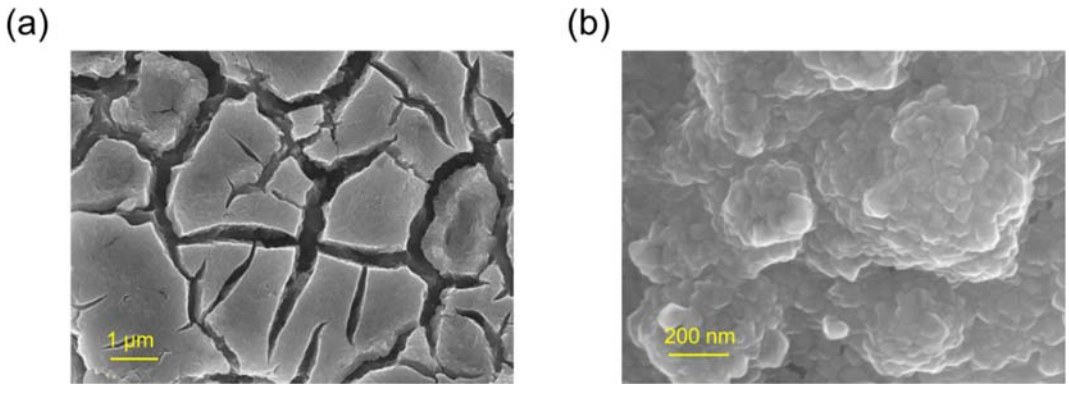

Fig. 2.2 SEM of TiO_2/SnO_2-Sb electrodes prepared by the authors by (a) thermal decomposition and (b) electrodeposition.

2.4 Surface modification of MMO anodes

2.4.1 Deposits with nano- and microstructure

MMO anodes with nanostructured deposits have drawn a lot of interest in the recent years. For their application in electrochemical oxidation/degradation of organic compounds, the main goal of nanostructured MMO anodes is to increase the surface area, and hence the reaction rates.

Many papers report the anodic oxidation of Ti substrate to get vertically aligned TiO_2 nanotubes (TiO_2-NTs). They can serve as the tubular template wherein metal oxides are implanted aiming to have improved loading capacity of Ti substrate. The mean pore diameters of the TiO_2-NTs range between 100 and 220 nm, according to the different anodization condition. PbO_2 is reported to be directly deposited into the TiO_2-NTs by pulse electrodeposition (Tan et al. 2011) and photoelectrodeposition (Pan et al. 2012). However the SEM images of the resulting anode showed the blocking of TiO_2-NTs by PbO_2, resulting in a limited increase of active surface area. Li et al. (2013c) fabricated a novel TiO_2-NTs/PbO_2 structure by introducing an electrochemical reduction step and modifying parameters of pulse electrodeposition, and finally the crystalline structured β-PbO_2 nanoparticles were successfully deposited without blocking the TiO_2-NTs. The real atomic percentage of Pb of the anode surface was found to be 11.75%, and such novel structure can effectively degrade phenol with 96.6% removal efficiency and 88.7% COD removal at current density of 30 mA cm^{-2} in NaCl electrolyte. Similar approaches have also been adopted to deposit SnO_2 on TiO_2-NTs by thermal decomposition (Chen et al. 2014, Li et al. 2009), pulse electrodepostion (Wu et al. 2011), hydrothermal method (Meng et al. 2013) and electrodeposition (Chen et al. 2010, Wang et al. 2013b). Fig. 2.3a illustrates the fabrication of TiO_2-NTs with enhanced conductivity by electrochemical reduction of the bottom TiO_2-NTs and subsequent Cu deposition (Macak et al. 2007).

After SnO_2-Sb deposition, the anode could have a distinctively high oxygen evolution potential (OEP) of 2.4 V vs SCE. The mass loading of Ti/TiO_2-NTs/SnO_2 is 1.4 times higher than that of Ti/SnO_2, and mineralization current efficiency and first-order kinetic constant for BA degradation were also 1 and 3.5 times greater (Zhao et al. 2009). Moreover, the Ti/TiO_2-NTs/SnO_2 can also serve as the support for PbO_2 deposition (An et al. 2012) to enhance its chemical and physical resistance.

The other approach is through self-assembly of surfactants in the precursor solutions of metal oxides to form micelles, and mesoporous MMOs layers can be formed by simply removing the surfactant templates (Pan et al. 2007, Wang et al. 2009a). Fig. 2.3b shows the mesoporous SnO_2-Sb anode fabricated by evaporation induced self-assembly (EISA) using pluronic F127 (Fan et al. 2013). In addition, F127 could reduce the surface energy of SnO_2 growth, which inhibited the aggregation of SnO_2. In other studies, Zhao and coworkers (2011, 2012b) first reported the assembling of 2D macroporous SnO_2 to 1D TiO_2-NTs by using liquid crystal soft template prepared by self-assembly block copolymer (styrene phenol polyoxyethylene ether, or SPPE). The SnO_2 layer is about 100 nm in thickness with 2D nanoscale pore structure in horizontal direction (diameters of macroporous pores 150-400 nm). The fabricated mesoporous SnO_2/TiO_2-NTs showed both excellent photo-catalytic and electrocatalytic oxidation performances for removing 4-nitrophenol and reducing its toxicity. In general, their study presents concept and new insight to develop photoelectric functional materials for degradation of toxic organic pollutants with high concentration.

Recently, carbon aerogel (CA) has attracted considerable attention as novel porous substrate for MMO anodes, due to their three-dimensional network structure, good electrical conductivity and high surface area (Wang et al. 2012b, Wu et al. 2010, Zhao et al. 2013). Fig. 2.4a illustrates the preparation process of a novel SnO_2-Sb/CA electrode. After CA fabrication, SnO_2-Sb was deposited on CA by thermochemical

decomposition. However, calcination temperature is critical due to the reducibility of CA, which would reduce SnO_2 to metallic Sn at high heat treatment (>700 ^oC) (Wu et al. 2010). The optimal calcination temperature is 600 ^oC at which well dispersed SnO_2-Sb nanoparticles were achieved (Fig. 2.4b). In electrochemical oxidation of PFOA, SnO_2-Sb/CA showed much better performance than SnO_2-Sb/Ti by improving the TOC removal from 17% to 86% as well as doubling the HO• generation (Zhao et al. 2013).

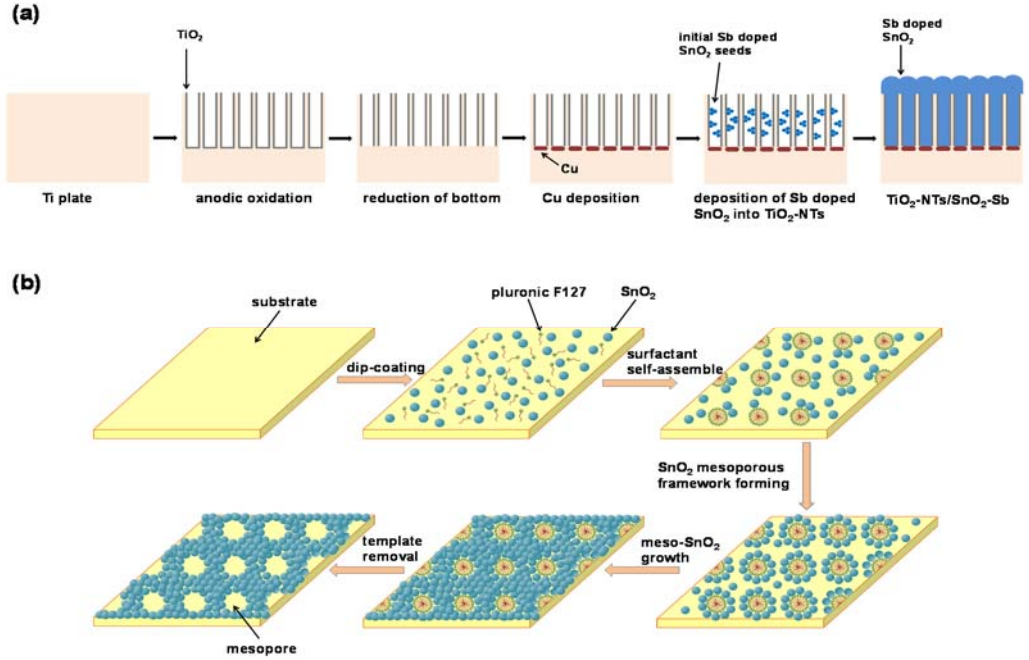

Fig. 2.3 Schematic illustration of (a) the formation process of TiO_2-NTs/SnO_2-Sb electrodes (modified from Chen et al. (2010)) (b) growth of mesoporous SnO_2 electrode by EISA method (modified from Fan et al. (2013)).

It should be noticed that the above mentioned MMO anodes are based on supported metal oxide system. Hence, no complete mixture of TiO_2 and other metal oxide was achieved in the anode surface. However, the advantages of a high surface area have driven research efforts to modifying bulk MMO anodes. Frolova et al. (2012) reported a nanostructured Pt/SnO_2-SbO_x-RuO_2 via reversed micelles assisted by adding surfactant (cetyltrimethylammonium bromide, or CTAB). The ternary MMO

have tetragonal rutile-like structure (P4/mnm), with a specific surface area of ~100 $m^2.g^{-1}$. Lee et al. (2012) described deposition of highly single crystalline $Ir_xRu_{1-x}O_2$ nanowires on Si(001) wafer by PVD of IrO_2 and RuO_2 mixtures at 700 °C and under atmospheric pressure.

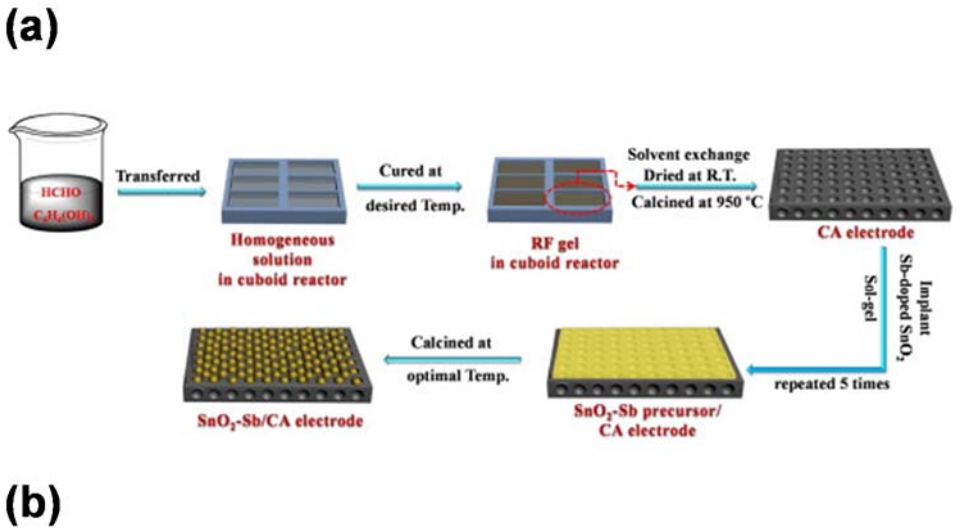

Fig. 2.4 (a) Schematic illustration for fabrication novel SnO_2-Sb/CA electrode; and (b) SEM images of SnO_2-Sb/CA electrodes calcined at 600 ºC (Zhao et al. 2013).

2.4.2 Doped MMO anodes

For the past 15 years, many attempts have been put forward to develop doped MMO electrodes in order to obtain improved characteristics (e.g. electrocatalytic activity, photoelectrocatalytic activity, corrosion resistance and conductivity) or desired properties (e.g. hydrophilic-hydrophobic properties). The doped components,

or dopants, can be simply introduced to MMO anodes by including dopant ions into the precursor solution or electrodeposition bath, or by more complicated methods (e.g. grafting). It is not surprising that the performances of the anodes are greatly enhanced after doping. However, it is worth noting that the extent of property improvement by certain dopant is really dependent on anode materials. Moreover, the level of dopants and doping conditions can result in obviously different effects on the physicochemical property and oxidation performance of MMO anode (Datta et al. 2013, Liu et al. 2011).

For each preparation, it is important to identify whether the ions are incorporated into the metal oxide lattice or whether the anode surface film is a mixture of different metal oxides. Kong et al. (2007) used XRD to investigate PbO_2 films doped with four rare earth metal elements (La, Ce, Er and Gd) of the same concentration (2.5 g L^{-1}). Well defined diffraction peaks of rare earth oxides La_2O_3, CeO_2 and Er_2O_3 were found in La-PbO_2, Ce-PbO_2 and Er-PbO_2 layers, suggesting the crystal structures of corresponding rare earth oxides present in the surface film. In the case of Gd-PbO_2 layer, doping did not disturb the crystal structures of β-PbO_2 but there was evidence of alternation of main crystal plane from β(101) to β(301). When introducing the dopants to the surface MMO layer, the synthesis methods employed can also influence the surface crystal phases, which was reported by Wang et al. (2012a). In their study of preparing Ti/PbO_2-Pr_2O_3 by cyclic voltammetry (CV) and co-electrodeposition, XRD peaks of Pr_2O_3 were only found for the electrode prepared by the former method.

Nevertheless, it is worth noting that the oxidation states of dopants may be uncertain, even though they are usually assumed to be at their highest oxidation state. He et al. (2011) reported in the Ti/SnO_2-Sb/PbO_2-Pr anode, Pr existed in the form of Pr_6O_{11} which can be regarded as complex compound with four PrO_2 and one Pr_2O_3. The ionic radius of Pr^{4+} (90 pm) is close to that of Pb^{4+} (84 pm), which influences the

nucleation and crystal growth of PbO_2. While Pr^{3+} has a larger ionic radius (101 pm) and leads to the expansion of surface particles. Another typical example of coexistence of different oxidation states is Sb doped Ti/SnO_2 electrode. In an earlier study by Terrier et al. (1995), the lower oxidation state Sb^{3+} was found to overtake the higher oxidation state Sb^{5+} in Sb $3d_{3/2}$ XPS peak when the Sb doping level was increased. Indeed, more studies about the effect of dopants oxidation states on the MMO anodes electrocatalytic activity are needed.

Some of the dopants used and their corresponding improvements to different types of MMO anodes are summarized in Table 2.3. Among them, fluoride ions are non-metallic dopants that have been widely used to improve the conductivity of SnO_2 or improve the adhesion and stability of PbO_2 (Li et al. 2011). In Ti/PbO_2-Co-F MMO anode, the fluoride ions are found to inhibit the incorporation of Co into the surface film (Andrade et al. 2008). Li et al. (2013a) described an Ti/Ni-Sb-SnO_2 anode with fluorine doped tin oxide (FTO) interlayer, and the service life time of the modified MMO anode was improved by a factor of 6. Bi(III)-doped MMO anodes are very practical for catalyzing the oxidation of organic compounds. In addition, Bi(III) has the great potential to introduce photoelectrocatalytic property when they are doped with photocatalyst TiO_2 (Park et al. 2012). Ce(IV)-doped MMO anode is another commonly used MMO anodes for oxidations, and such reactions involve the oxidation of pharmaceuticals (Cheng et al. 2013b, Lin et al. 2013b), nitrophenol (Liu et al. 2011, Liu et al. 2012b) and perfluorinated chemicals (Niu et al. 2012). Co(II)-doped PbO_2 improved the performance efficiency for metronidazole degradation but excessive doping may lead eventually to the formation of unwanted composite oxide (Dai et al. 2016c). Other rare earth elements, such as La, Mo, Ru, Zr, Eu, Pr, Er are also reported as dopants for SnO_2 and PbO_2 electrodes, with the function of enhancing the electrocatalytic activity for organic oxidation or improving the electrochemical stability of the electrodes (Table 2.3).

Table 2.3 Doped MMO anodes and proposed roles of the dopants

Dopant	Active anode material	Purpose	References
Sb(V)	SnO_2	Improve the conductivity;	Terrier et al. (1995)
F(-I)	SnO_2	Prolong the electrode service life; catalyzes organic degradation	Li et al. (2013a) Cid et al. (2013) Armijo et al. (2010)
F(-I)	PbO_2	Catalyzes organic degradation; improves chemical and electrochemical stability	Wang et al. (2010b) Andrade et al. (2008)
F(-I)	IrO_2	Catalyzes O_2 evolution	Kadakia et al. (2013)
Bi(III)	SnO_2	Catalyzes organic degradation	Zhuo et al. (2011)
Bi(III)	PbO_2	Catalyzes organic oxidation	Liu et al. (2009b) Borras et al. (2003)
Bi(III)	TiO_2	Enhance photoelectrocatalytic acitivity	Park et al. (2012)
Ce(IV)	PbO_2	Improves stability; catalyzes •OH generation and catalyzes organic degradation	Liu et al. (2011) Li et al. (2013b) Al et al. (2005) Lin et al. (2013b)
La(III)	SnO_2	Catalyzes organic oxidation	Xu et al. (2012)
Mo(IV)	PbO_2	Catalyzes organic oxidation	Dai et al. (2016b)
Ru(IV)	PbO_2	Catalyzes organic oxidation	Xu et al. (2012)
Zr(II)	PbO_2	Decrease grain size of electrode and improve life span	Yao et al. (2012)
Co(II)	PbO_2	Catalyzes organic degradation	Kim et al. (2005) Andrade et al. (2008) Dai et al. (2016c)
Eu(III)	SnO_2	Catalyzes TOC removal	Feng et al. (2010a)
Pr(IV)	PbO_2	Catalyzes organic degradation and improves electrode stability	He et al. (2011) Wang et al. (2012a)
Er(III)	PbO_2	Catalyzes organic degradation	Kong et al. (2007)

Several papers report quantitative comparisons of the properties of doped and undoped MMO anodes. Xu et al (2012) compared the cyclic voltammetry curves of undoped Ti/SnO_2-Sb electrode with Ti/SnO_2-Sb-La and Ti/SnO_2-Sb-Ru electrodes in 0.1M KCl solution containing 5 mM $K_4[Fe(CN)_6]$ solution. The peak currents of doped Ti/SnO_2-Sb electrodes are greatly improved from 0.37 $mA.cm^{-2}$ to 0.52

$mA.cm^{-2}$ and 0.60 $mA.cm^{-2}$, suggesting higher voltammetric charge which is attributed to an increase of the active surface area. Liu et al. (Liu et al. 2011) investigated the impedance and electrocatalytic efficiency of undoped Ti/PbO_2 and Ti/PbO_2-Ce electrodes with different Ce doping levels (0.7–14 mM Ce in electrodeposition bath), and 3.5 mM was found to be the optimal doping level since the lowest charge-transfer resistance and highest chemical oxidation demand (COD) removal of 2-nitrophenol was obtained. Nevertheless, if Ce is doped at a high level, the Ti/PbO_2-Ce electrode even experiences retrogress in electrocatalytic activity comparing with Ti/PbO_2. Indeed, it is of research interest to determine the optimal doping level of the dopants in MMO anodes.

2.4.3 Polymer composites

Polymers are another type of material employed to introduce or enhance specific properties of MMO anodes. Polypyrrole and PbO_2 were co-electrodeposited on Ti/SnO_2/PbO_2 substrate, and the modified electrode had hydrophobic surface, which exhibited a remarkable enhancement in oxidizing hydrophobic organic compounds due to the strong hydrophobic interaction between the electrode surface and organic substrates (Hwang and Lee 1996). Zhou and coworkers (2005a, 2005b, 2004, 2002) described a novel PbO_2 electrode with electrodeposited polytetrafluoroethylene (PTFE) layer, and it is found to have a good resistance to corrosion and excellent electrocatalytic activity to degrade nitrophenol. The good performance of PTFE-deposited PbO_2 anode for organics oxidation was also reported by Tong et al. (2008) and Hong et al. (2011). The PTFE modified MMO anodes are reported to be able to exhibit complete electrochemical oxidation of some organic pollutants (Dai et al. 2013, Zhao et al. 2010a). It is worth mentioning that the Ti/TiO_2-NTs/PbO_2-PTFE even showed a higher removal efficiency (98.8%) for 2,4-dichlorophenoxyacetic acid than boron doped diamond (BDD) anode (79.3%) and less energy consumption.

Ti/TiO_2-NTs/PbO_2-FR had super hydrophobic surface and it was believed that more absorbed $HO^{\bullet}$ is released from the anode surface to become free $HO^{\bullet}$, which could participate in organic oxidation rather than oxygen evolution. In general, MMO anodes with deposited polymer composites are desired to have hydrophobic property and they are promising material for environmental application of electrochemical oxidation.

2.5 Characterization of MMO anodes

The crystal studies of metal-based catalysts, as well as quantitative comparison of their reaction rates were significantly conducted in the 1970s by the introduction of several characterization techniques. However, the catalysis science of MMO experienced a much slower development than other metal-based catalysts due to the reasons: (1) the complexity of MMO catalysts (e.g. possible existence of different oxidation states, coexisting bulk and surface phases, various surface termination functionalities) and (2) the requirement of new spectroscopic techniques to determine such structural details (Wachs 2005). To date, various characterization methods have been employed to examine the physiochemical, electrochemical and crystallochemical properties of MMO anodes. These widely applied techniques include: X-Ray diffraction (XRD), Raman spectroscopy, X-Ray adsorption spectroscopy (XAS), thermogravimetric analysis (TGA), scanning electron microscopy and transmission electron microscopy (SEM and TEM), energy-dispersive X-ray spectroscopy (EDS), linear sweep voltammetry (LSV), cyclic voltammetry (CV), scanning electrochemical microscopy (SECM), electrochemical impedance spectroscopy (EIS), UV-Vis diffuse reflectance spectroscopy (DRS), X-Ray photoelectron spectroscopy (XPS), atomic force microscopy (AFM) and Fourier-transform infrared (FTIR) spectroscopy. The characterization techniques for MMO anodes and the corresponding characteristics reported are summarized in Table 2.4.

Table 2.4 Characterization techniques for MMO anodes

Characterization techniques	Characteristics studied	Findings
XRD	Crystal structure analysis	γ-Al_2O_3:18.5°, 37.3°, 42.6°, 46.3°, 67.0°; SnO_2(110): 22.6°; SnO_2(101): 33.9°; SnO_2(211): 51.8° (Chen et al. 2012a).
XAS	Local coordination or electronic structure analysis	A small amount of Ti atoms are incorporated into crystalline RuO_2 and occupy Ru sites in octahedral RuO_6 (Chen et al. 2013).
TGA	Evaporation of solvent and decomposition points of metal precursors	Evaporation of free water molecules and solvent: 0-200 ℃; decomposition of metal chlorides: 200-400 ℃; stable coating layer: 400 ℃ and above (Makgae et al. 2005).
SEM/EDS	Surface morphology and elemental compositions	Uniformly distributed particles of IrO_2-SnO_2-Sb_2O_5 (1-5 μm in height) give rise to an thickness of coating layer about 2 μm) in Ti/ IrO_2-SnO_2-Sb_2O_5 electrode (Chaiyont et al. 2013).
TEM	Size of dopants particles	Pt nanoparticles are well dispersed in the support surface of TiO_2-RuO_2 and in the particle size of 4-8 nm (Lo et al. 2013).
LSV	Onset potential of OER	TiO_2-NTs/SnO_2 prepared by electrodeposition has higher OEP than that of TiO_2-NTs/SnO_2 prepared by thermal decomposition.
CV	Electroactive surface area of MMO anodes	The total voltammetric charge and outer voltammertic charge of Ti/SnO_2-Sb-TiN anode are 4.5 and 3.6 times those for Ti/SnO_2-Sb anode (Duan et al. 2014).
SECM	Electrocatalytic activity of MMO anodes	Electrocatalytic OER activity of the mixed $(Ru_{0.76}:Ti_{0.24})O_2$ coating is 13% higher compared to the RuO_2 coating (Näslund et al. 2013).

EIS	Electrochemical systems analysis	Charge transfer resistance: Ti/SnO_2-Sb_2O_5 (492.70 $\Omega.cm^{-2}$) > Ti/SnO_2-Sb_2O_5-IrO_2 (8.94 $\Omega.cm^{-2}$) > Ti/SnO_2–Sb_2O_5-RuO_2 (4.44 $\Omega.cm^{-2}$) (Adams et al. 2009).
Raman	Stoichiometry and crystalline quality analysis of MMO	E_g mode of pure RuO_2 linearly blue shifts with incorporating Ir amounts in $Ir_xRu_{1-x}O_2$ mixed oxide systems (Lee et al. 2012).
UV-Vis DRS	Valance state analysis of metallic elements in precursor solution	One less intense band of Ru(III) (341 nm) is found when mixed Ru(IV) and Sn(II) using aqueous HCl as solvent (Coteiro et al. 2006).
XPS	Elemental surface chemistry analysis	Mn: Mn(IV) is verified by Mn $2p_{3/2}$ and Mn $2p_{1/2}$ at 642.2 eV and 653.8 eV; Sn: Sn(IV) is verified by Sn $3d_{5/2}$ and Sn $3d_{3/2}$ at 486.7 eV and 495.3 eV (Chen et al. 2012a).
AFM	High-resolution surface image of MMO coating layer	The roughness of Ti/TiO_2-RuO_2-IrO_2 increases by increasing the amount of IrO_2 in the coating layer (Yousefpour and shokuhy 2012).
FTIR	Analysis of organic deposits on MMO anodes	Organic species do not exist in the TiO_2-AgO film after annealing at 500 ^oC (Mohammadi and Fray 2011).

XRD can provide structural information of the MMO anodes surface films by examining the crystal phases. Since the metal oxides can be mixed or laid in different manners, the XRD patterns of MMO anodes comparing with single-component metal oxide may be influenced in different ways. In most supported metal oxide systems, the surface layer acts as the electrocatalytic active layer and its XRD pattern is not influenced by the property of the inner layer, indicating an identical surface crystal structure (Zheng et al. 2011). However, in a mixed metal oxide system, the mixture of metal oxides in the surface may influence the XRD pattern in the forms of (1) appearance of additional diffraction peaks (Kong et al. 2007) as a result of new crystal

phase formation and (2) visible difference on the half-width and intensity of diffraction peaks (Cui et al. 2009a, Feng et al. 2008), due to the expansion of metal oxide lattice through incorporation of other elements. However, it should be pointed out that sometimes the introduction of dopants into MMO films does not cause any noticeable changes in the XRD patterns (Wang et al. 2013b, Xu et al. 2012, Zhang et al. 2010). In such cases, the presence of dopants with small doping level is usually verified by other techniques including XPS, XAS and Raman Spectroscopy.

XPS is employed to determine the quantitative atomic composition, and also the oxidation states of surface elements. This property makes it particularly useful to study the doped MMO anodes. In MMO anodes, the binding energy peaks of O1s include two parts: the main peak with lower binding energy value (~530 eV) is attributed to the lattice oxygen, while the peak with high binding energy value (531–532eV) is believed to be the adsorbed oxygen. The O 1s peak was found to be lower in Gd doped Ti/SnO_2-Sb anode than that of sample lacking Gd, suggesting more lattice oxygen present in Gd doped Ti/SnO_2-Sb (Feng et al. 2008). Its higher lattice oxygen content increased the activity of the adsorbed hydroxyl radicals, hence improved the anode performance. However, it should be noticed that the XPS spectra of Sb $3d_{5/2}$ and O 1s are overlapped, so it is necessary to fit the XPS spectra into three peaks to identify the presence of Sb. For MMO anodes, dopants are usually in their highest oxidation states, but there are exceptions if the MMO anodes are calcined at low temperatures or the dopants are at high doping level. Cui et al. (2009a) described rare earth elements doped with Ti/SnO_2-Sb anodes, which was prepared by thermal decomposition with the presence of both Ce^{3+} and Ce^{4+}, and the presence of Ce^{3+} might have negative effect on the electrocatalytic activity of Ti/SnO_2-Sb due to the increased oxygen vacancies. However, in Ce doped Ti/SnO_2-Sb and Ti/PbO_2 electrodes where Ce presents in the form of highest oxidation states, improved electrocatalytic activity for organic oxidation was observed (Kong et al. 2007, Li et

al. 2013b, Liu et al. 2011).

EIS is a technique for the characterization of electrochemical systems. Electrochemical impedance is usually measured by applying a small AC amplitude sinusoidal potential to the system and measuring the response current. The response current will be a sine wave at the same frequency but its phase shifted. Therefore by varying the frequency of signal, the impedance of the system can be determined as a function of frequency. Typically for electrochemistry characterization, a frequency range of 100 kHz to several milli Hertz is used. EIS has been used to study the system resistance and deactivation mechanism of MMO anodes. For example, Lassali et al (2000) found that the oxidation of Ti substrate, which resulted in poorly doped TiO_2, lead to the deactivation of $Ti/Ir_{0.3}Ti_{(0.7-x)}Sn_xO_2$ anodes by analyzing their system equivalent circuit of EIS under accelerated conditions. Adams et al (2009) corroborated chronopotentiometry (CP) and EIS findings and observed the lowest charge-transfer resistance for oxygen evolution in Ti/SnO_2-Sb_2O_5-RuO_2 electrode, comparing with Ti/SnO_2-Sb_2O_5-IrO_2, Ti/SnO_2-Sb_2O_5-PtO_x and Ti/SnO_2-Sb_2O_5 electrodes. In another study, the Ti/SnO_2-Sb_2O_5 electrode without interlayer showed an increase in charge-transfer resistance of oxide/solution interface faradaic process from 28 to 3200 Ω cm^{-2} after 45 min life time test, however this number only increased from 26 to 35 Ω cm^{-2} after 60 min life time test when FTO interlayer is applied (Li et al. 2013a).

Different from those characterization techniques which focus on the surfaces characteristics of MMO anodes, TGA gives an insight into the physical and chemical changes of the precursor solutions during pyrolysis. Makgae et al (2005) conducted TGA in a flow of air (100 – 700 ^oC) at the rate of 10 ^oC/min for their coating containing hydrated $SnCl_2$, $RuCl_3$ and $IrCl_3$ precursors separately and a mixture of them, after evaporation at 100 ^oC. For the precursors containing single metal chloride, initial mass losses took place between 0 and 200 ^oC, followed by sharp mass losses

at 400 ^{o}C. They were attributed to the evaporation of solvent and decomposition of chloride ions respectively. A thermal curve obtained for the three mixed metal chlorides showed a similar behavioral pattern to that of single metal chloride, indicating that polymerization occurred between the three mixed metals. However, a previous study by Kim et al (2002b) reported higher temperature (600 ^{o}C) for sufficient conversion of $IrCl_3$ to IrO_2, and the conclusion was also supported by the corresponding XRD analysis.

2.6 Active and non-active MMO anodes

During electrochemical oxidation of organic pollutants at high potentials, secondary reactions (e.g. oxygen evolution reaction or OER) will take place inevitably and decrease the current efficiency for the desired reactions. Furthermore, the nature of anode material, including the adsorptive ability and electrocatalytic activity, plays an essential role in both the selectivity and efficiency of the process by influencing the rate-limiting steps (Martinez-Huitle et al. 2008, Martinez-Huitle et al. 2004a). In order to interpret the observations, a comprehensive model has been described by Comnimellis et al. (1994), including the anodic oxidation of organics and simultaneous oxygen evolution. Based on the different oxidation pathways proposed by the model, the anodes can be divided into two classes: active anode and non-active anode. Active anodes present low oxygen evolution potential (OEP), and only partial oxidation of organics can be achieved by the chemisorbed $HO^{\bullet}$ in the anode surface. In contrast, non-active anodes present high OEP and the physisorbed $HO^{\bullet}$ gives complete oxidation to the organic compounds. As an extension of Comnimellis's work, Scialdone developed a theoretical model involving both direct anodic oxidation and mediated oxidation routes by means of physisorbed and chemisorbed $HO^{\bullet}$ (Scialdone 2009), and by means of active chlorine species (Scialdone et al. 2009b). In the theoretical model, several assumptions were defined

and relationships between instantaneous current efficiency (ICE) and operating parameters were presented with regard to mass transfer control, oxidation control and mixed kinetic regimes. The theoretical predictions matched well with experimental observations for electrochemical oxidation of carboxylic acids at IrO_2-Ta_2O_5 anode (Scialdone et al. 2011, Scialdone et al. 2009a).

In order to comprehend the performances of various MMO anodes, OEP (in H_2SO_4 or Na_2SO_4) of some commonly investigated MMO anode materials are given in Table 2.5. All the values are calculated compared to the standard hydrogen electrode (SHE). In general, MMO anodes which contain IrO_2 and RuO_2 especially in bulk MMO have low values of OEP. It indicates that only partial oxidation of pollutants can be achieved. However, those IrO_2 and RuO_2 based MMO anodes, i.e. dimensionally stable anodes (DSAs), have received wide application in wastewater treatment because of their good resistance to corrosion. One way to improve the electrochemical oxidation efficiency of these anodes is by applying low current densities, at which OER is not favored.

Table 2.5 Oxygen evolution potential of various MMO anodes

Anode	Oxygen evolution potential (V) vs SHE	Condition	Reference
TiO_2-NTs/SnO_2	1.84-2.19	0.5 M H_2SO_4	Chen et al. (2010)
Ti/SnO_2-Sb	2.05	0.1 M Na_2SO_4	Xu et al. (2013b)
Ti/SnO_2-Sb_2O_3-Nb_2O_5/PbO_2	2.04	0.05 M Na_2SO_4	Yang et al. (2009)
TiO_2-NTs/SnO_2	1.80	0.1 M Na_2SO_4	Zhao et al. (2009)
TiO_2-NTs/Sb-SnO_2/PbO_2	1.74	0.5 M Na_2SO_4	An et al. (2012)
Ti/SnO_2-Sb_2O_5/PbO_2	1.74	0.1 M Na_2SO_4	Xue et al. (2011)
Ti/IrO_2-Ta_2O_5	1.53	0.5 M H_2SO_4	Zhou et al. (2011a)
Ti/IrO_2-SnO_2-Sb_2O_5	1.52	0.05 M Na_2SO_4	Chaiyont et al. (2013)
Ti/IrO_2-RuO_2	1.50	0.5 M H_2SO_4	Zhou et al. (2011a)
Ti/RuO_2-IrO_2-SnO_2-TiO_2	1.44	0.5 M Na_2SO_4	Chellammal et al. (2012)

In contrast, SnO_2- and PbO_2-based MMO anodes show high OEP, and they are ideal electrodes for complete oxidation of organics in wastewater treatment. Chen et al. (2010) reported that the TiO_2-NTs/SnO_2 electrode prepared by electrodeposition has higher OEP than that of TiO_2-NTs/SnO_2 prepared by thermochemical decomposition, which is desirable for electrochemical oxidation of organics. PbO_2 is another typical material with high OEP, but the presence of interlayers like RuO_2-TiO_2 and IrO_2-Ta_2O_5 will decrease the OEP, resulting from the richer crystalline orientations of PbO_2 when it was deposited on interlayers (Kong et al. 2012).

Although SnO_2- and PbO_2-based MMO anodes are attractive for electrochemical oxidation of recalcitrant organics, their industrial application may be restricted by their specific features. For SnO_2-based MMO anodes, the main problem is their short service life, which is attributed to the formation of a certain degree of nonstoichiometry $SnO_{(2-x)}$ during OER (CorreaLozano et al. 1997). This modification of the anode gives rise to the internal stress of the oxidized layer, and finally its detachment from the electrode. The service life of SnO_2-based MMO anodes can be improved by increasing the electrode mass loading (CorreaLozano et al. 1997), applying isomorphous interlayer (Chen et al. 2010), modifying the conditions of thermochemical decomposition (Carlesi Jara et al. 2011) or doping with platinum (del Río et al. 2010). However, the value of service life still remains low for practical application. While for PbO_2-based MMO anodes, the main issue is the release of toxic Pb ions into treated water. Pb ions were found to be released at ppm levels (5 to 15 mg L^{-1}) during electrochemical oxidation of phenol with Ti/IrO_2-Ta_2O_5/PbO_2 electrodes. Nevertheless, the values were significantly influenced by the electrodeposition conditions of PbO_2 (Tahar and Savall 1999). Reductive dissolution of PbO_2 in acidic solution in the presence of Br^- (Lin and Valentine 2010), I^- (Lin et al. 2008) or natural organic materials (NOMs) (Dryer and Korshin 2007, Lin and Valentine 2008, Shi and Stone 2009) also gives rise to the release of soluble Pb (II)

into solutions. Besides Pb (II) ions, soluble Pb (IV) can be also present in solution and act as a strong oxidant during electrochemical oxidation of organics (Bock and MacDougall 1999). The above-mentioned factors have restricted the application of PbO_2 as anodic material in wastewater treatment, where the Pb contamination of the treated water must be avoided.

2.7 Direct and mediated anodic oxidation of organics

The electrochemical oxidation of organic pollutants can take place in two ways. The pollutants can be oxidized at the anode surface by direct electron transfer or by physisorbed or chemisorbed $HO^{\bullet}$ generated from OER, and this process is called direct anodic oxidation. Or, the pollutants can be degraded by mediated anodic oxidation, which takes place in the bulk solution by oxidizing reagents electrogenerated at the anode surface. Fig. 2.5 shows the schematic illustration of the direct and mediated anodic oxidation mechanisms. Both of the two oxidation mechanisms have been studied using MMO anodes.

The studies investing phenolic compounds degradation have shown that aromatic ring intermediate compounds were produced, including catechol, hydroquinone and benzoquinone. Benzoquinone was subsequently oxidized to aliphatic carboxylic acids resulting from aromatic ring cleavage, including maleic acid, malonic acid, formic acid and acetic acid (Li et al. 2009, Niu et al. 2013a, Song et al. 2010b). Fig. 2.6a shows the degradation pathway of phenol on MMO anodes (Makgae et al. 2008). Compared with other anodes, MMO anodes have the merit of fully alleviating the intermediates of phenolic compounds oxidation. Otherwise they will accumulate and form polymeric compounds (Cui et al. 2009b, Li et al. 2005).

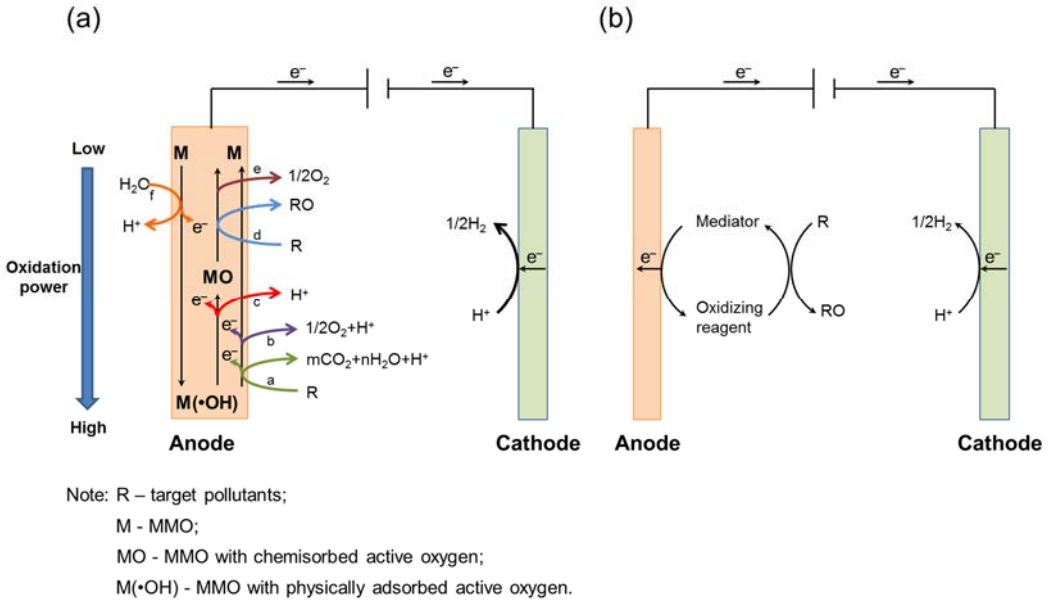

Fig. 2.5 Mechanistic schemes for (a) direct and (b) mediated electrolytic treatment of pollutants.

In other studies, several groups have reported electrochemical treatment of perfluorinated chemicals including perfluorocarboxylic acid (PFCA) and perfluorooctanoic acid (PFOA) at MMO anodes (Lin et al. 2012, Lin et al. 2013a, Ma et al. 2015, Niu et al. 2012, Zhuo et al. 2011). The mechanistic investigation of PFOA degradation (Fig. 2.6b) has shown that the whole process was initialized by direct electron transfer at anode surface, and followed by two different reaction pathways: (1) perfluoroheptyl radical $F\text{-}(CF_2)_{6\text{-}n}\text{-}CF_2$ combined with $HO^{\bullet}$ to produce thermally unstable alcohol $F\text{-}(CF_2)_{7\text{-}n}\text{-}OH$, and (2) perfluoroheptyl radical $F\text{-}(CF_2)_{6\text{-}n}\text{-}CF_2$ reacted with oxygen to produce perfluoroheptylperoxy radical $F\text{-}(CF_2)_{7\text{-}n}\text{-}OO\bullet$, and then combined with another perfluoroheptylperoxy radical to form perfluoroalkoxy radical $F\text{-}(CF_2)_{7\text{-}n}\text{-}O\bullet$. Intermediates of the two degradation pathways later underwent CF_2 unzipping cycle steps, and PFOA can be finally decomposed to CO_2 and HF by repeating the cycle steps.

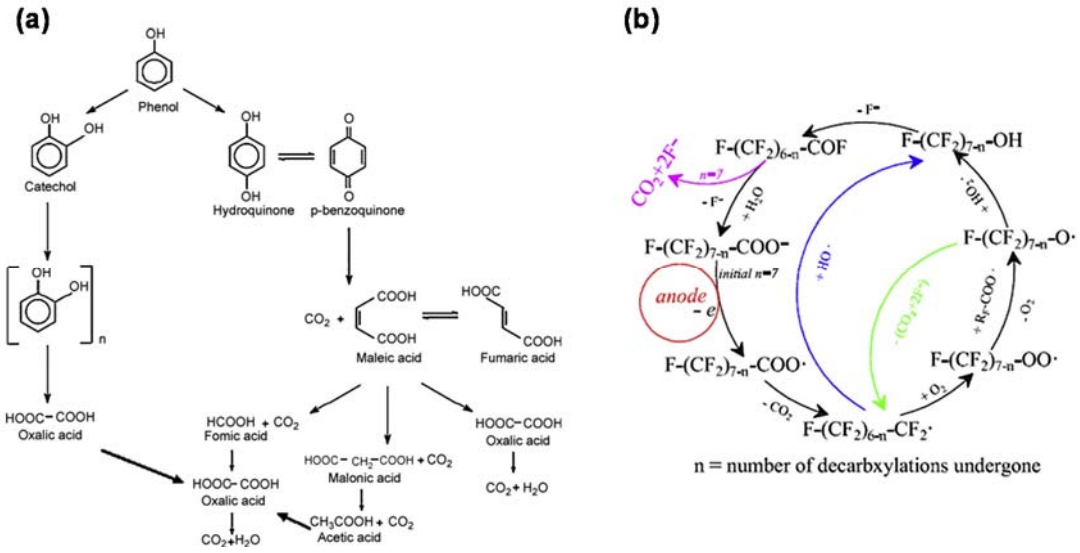

Fig. 2.6 (a) Schematic diagram of the electrochemical degradation mechanism of PFOA (Lin et al. 2012); and (b) reaction pathway for the phenol electrocatalytic oxidation on MMO anodes (Makgae et al. 2008).

Direct anodic oxidation is attractive because it does not need chemical additives which may cause secondary pollution. However, efficient oxidation of organic compounds can only be achieved with non-active MMO anodes which employed SnO_2 or PbO_2 as the active layer, and this phenomenon is observed by many comparative studies (Lin et al. 2012, Pelegrino et al. 2002, Radjenovic et al. 2011). Mao et al. (2008) investigated the oxidation of azo dye at Ti/SnO_2-Sb and Ti/SnO_2-Sb/PbO_2 MMO anodes, and the former electrode showed better electrocatalytic activity than the latter. However, no noticeable differences between SnO_2-Sb and PbO_2 electrode is reported in treating landfill leachate (Cossu et al. 1998). The main problem during direct anodic oxidation is the deactivation of the anode surface, due to the formation of polymer on the anode surface (Li et al. 2005). The extent of deactivation depends on the adsorption properties of anode surface and the nature and concentration of the target organics (Panizza and Cerisola 2009). In practical application, sometimes strong anodic current are required intermittently to oxidize the polymer in the anode.

For the electrochemical oxidation of pollutants through the mediated oxidation at

MMO anodes, the electrochemically generated oxidizing reagents include ozone, chlorine, peroxide, hypochlorite, peroxodisulfate, and Fenton's reagent (Juttner et al. 2000). Among these, active chlorine generated from chlorides is probably the most commonly produced mediators, due to their effective activity and ubiquitous presence in wastewaters at elevated concentration compared to other species. The active chlorine usually presents in the form of Cl_2, HClO and ClO^-, with the following reactions:

$$Cl_2 + 2e^- \leftrightarrows 2Cl^-, \qquad E^0 = 1.36\ V \tag{2.2}$$

$$2HClO + 2H^+ + 2e^- \leftrightarrows Cl_2 + 2H_2O, \qquad E^0 = 1.63\ V \tag{2.3}$$

$$ClO^- + H_2O + 2e^- \leftrightarrows Cl^- + 2OH^-, \qquad E^0 = 0.90\ V \tag{2.4}$$

The oxidizing power of the active chlorine is dependent on solution pH, which makes the mediated oxidation more effective in acidic condition (Szpyrkowicz et al. 2000). In most cases, the organic pollutants can be eliminated at the suitable chloride concentration (Martinez-Huitle and Ferro 2006). However, the variation of active chlorine species is strongly influenced by electrolysis conditions such as time, temperature and electrode material (Neodo et al. 2012). Metallic mediators have also found their application in mediated oxidation at MMO anodes. In this case, stable, low-valence metal ions are oxidized to reactive, high-valence mediators. Some of the important redox couples of metallic mediators include Ag(I)/Ag(II) , Co(II)/Co(III), Fe(II)/Fe(III) and Ce(III)/Ce(IV) (Chen et al. 2012b, Chu et al. 2012, Farmer et al. 1992, Raju et al. 2010). However, employing metallic mediators may have a risk of introducing high toxicity in the effluent and an addition step to recover the metallic species is required before discharging the effluents (Martinez-Huitle and Ferro 2006).

2.8 Determination of reactive oxygen species

The determination of reactive oxygen species (ROS), mainly generated from OER in the anode, has become an important approach to understand the mechanism of

oxidation of organic pollutants at MMO anodes. Among the ROS, $HO^{\bullet}$, H_2O_2, $O_2^{\bullet-}$ and $HO_2^{\bullet}$ (hydroperoxyl radical) are of special research interest because of their strong oxidative abilities, especially in acidic solution (Wardman 1989).The rate of ROS formation provides a mechanistic parameter to investigate the feasibility of these oxidative species generated by anodic oxidation, and hence the catalytic activity of the anode material can be evaluated. However, the above mentioned ROS are highly reactive and unstable in solution, with considerably short life span. In addition, in high pH condition they will convert to the anion forms, which exhibit much lower oxidative abilities:

$$HO^{\bullet} + OH^{-} \leftrightarrows O^{\bullet-} + H_2O, \qquad pK_b = 2.1 \tag{2.5}$$

$$H_2O_2 + OH^{-} \leftrightarrows HO_2^{-} + H_2O, \qquad pK_b = 2.4 \tag{2.6}$$

$$HO_2^{\bullet} + OH^{-} \leftrightarrows O_2^{\bullet-} + H_2O, \qquad pK_b = 9.2 \tag{2.7}$$

Since the ROS in solution are difficult to be determined by direct measurements, reagents known as chemical probes or ROS scavengers have been employed to react with them and form stable products. These products can be qualitatively or quantitatively analyzed by various techniques. Table 2.6 summarized the various reported analysis techniques and corresponding scavengers for detection of electrogenerated ROS in some studies. Moreover, those ROS scavengers were also added to the bulk solutions as effective quenchers of selective ROS, since it is interesting to investigate the role of individual ROS in organics removal by advanced oxidation processed (AOPs) by inhibiting their aquatic presence (Wang and Lim 2011). However, to the best of authors' knowledge, related study has not been reported for electrochemical oxidation at MMO anodes.

Table 2.6 Analysis techniques employing ROS scavengers for the determination of electrogenerated ROS

ROS type	Analysis techniques	ROS scavengers	Determination accuracy	Remark	Reference
$HO^{\bullet}$	ESR	5,5-dimethyl-1-pyrroline-N-oxide (DMPO)	Quantitative	DMPO-$HO^{\bullet}$ was generated with hyperfine constants $\alpha_N = \alpha_H = 14.0$ G and g-value =2.0065.	(Cheng et al. (2003), Wang and Wang (2008), Yu et al. (2006))
	HPLC	benzoic acid; dimethyl sulfoxide (DMSO); salicylic acid	Quantitative	$HO^{\bullet}$ scavengers reacted with $HO^{\bullet}$ and the concentration of final products are analyzed by HPLC.	(Fan et al. (2013), Gao et al. (2009), Tai et al. (2004), Wu et al. (2007))
	UV-vis	p-nitrosodimethylaniline (RNO)	Quantitative	RNO was bleached by $HO^{\bullet}$, with maximum absorbance at 440 nm and 350 nm reported.	(Feng et al. (2003), Martinez-Huitle et al. (2004b))
	PL	terephthalic acid	Qualitative	Highly fluorescent product was generated with corresponding PL signal at 425 nm.	(Ishibashi et al. (2000a), 2000b), Yu et al. (2013))
	Fluorescence	aminophenyl fluorescamine	Quantitative	Excitation and emission wavelengths were set to 490 nm and 520 nm respectively.	Cohn et al. (2008)
$HO_2^{\bullet}$/ $O_2^{\bullet-}$	ESR	5,5-dimethyl-1-pyrroline-N-oxide (DMPO)	Quantitative	DMPO-$O_2^{\bullet-}$ and nitroxide-like radicals were generated, with hyperfine constants $\alpha_N = 14.1$ G, $\alpha_H^{\beta} = 10.8$ G and $\alpha_H^{\gamma} = 1.4$ G for DMPO-$O_2^{\bullet-}$ and $\alpha_N = 1.4$ G for nitroxide-like radical.	Diaz-Uribe et al. (2010)
	Fluorescence	luminol	Quantitative	3-aminophthalate of excited state was generated and emitted light at wavelength 425 nm.	Nosaka et al. (2002)
	HPLC	hydroethidine	Quantitative	2-hydroxyethidium was generated and its concentration was analyzed by HPLC.	Georgiou et al. (2008)
H_2O_2	UV-vis	2,9-dimethyl-1,10-phenanthroline (DMP)	Quantitative	Maximum absorbance wavelength obtained at 454 nm.	Kosaka et al. (1998)

Comparing with Pt and Ti anodes, the HO• production on Ti/RuO_2-TiO_2 anode is much larger (Feng et al. 2003). One way to increase the HO• production is by surface modification. The HO• production on mesoporous SnO_2-Sb (61.7 μmol.L^{-1}) is twice that of the conventional one (30.3 μmol.L^{-1}). Moreover, the yield of HO• on SnO_2-RuO_2 was found to be significantly enhanced by doping with Ce, which could act as active centers on Ce-Ru-SnO_2 and increase the active sites (Liu et al. 2012b). More water molecules were adsorbed and discharge to generate HO•. Furthermore, by coupling with ultrasonic irradiation, the concentration of HO• could have a maximum 54% increase, leading the TOC removal from 33% to 86% (Zhao et al. 2013).

2.9 Factors influencing electrochemical oxidation efficiency

There are several operating variables that can influence the electrochemical oxidation of organic pollutants by MMO anodes, as outlined and discussed in the following review.

2.9.1 pH

Solution pH is an important factor for electrochemical oxidation of organic pollutants using MMO anodes. The effect of pH on anodic oxidation has been well reported in literature. The findings are diverse and sometimes even contradictory, depending on the types of target pollutants, types of supporting electrolytes and types of MMO anodes. In general, many published literature report that the removal efficiency of organic pollutants by electrochemical oxidation tends to increase in the lower pH range, with a few exemptions. Such trend can be explained from the viewpoint of thermodynamics, taking into account that the oxidative power of solution oxidative species varies with pH. In the direct anodic oxidation where inert supporting electrolytes are employed, the first reaction is the HO• generation from the oxidation of water molecules:

$$H_2O \rightarrow HO^{\bullet} + H^+ + e^- \quad (2.8)$$

In standard condition (T = 298 K, [HO•] = 1 M), the redox potential for $HO^{\bullet}_{aq}/H_2O$ couple at pH = 0 is 2.59 V. According to Nernst relationship, the redox potential for $HO^{\bullet}_{aq}/H_2O$ couple at different pH can be given by:

$$E^o(HO^{\bullet}_{aq}/H_2O) = 2.59 - 0.059\ pH \quad (2.9)$$

Thus, a value of 2.18 V for $E^o(HO^{\bullet}_{aq}/H_2O)$ at pH = 7 and 1.77 V for E^o(HO $HO^{\bullet}_{aq}/OH^-$) at pH = 14 can be obtained. The pK_a of HO• is 11.9, which results in $E^o(^{\bullet}O^-_{aq}/OH^-)$ = 1.64 V at pH = 14 (Koppenol and Liebman 1984). Since the HO• exhibits higher oxidative potential in the lower pH range, it is not surprising that better removal efficiency for organic pollutants is achieved. Moreover, the OER caused by HO• radicals or water oxidation is inhibited at the acidic condition (Eqn 7 and 8):

$$2\ HO^{\bullet} \rightarrow O_2 + 2H^+ + 2e^- \quad (2.10)$$

$$2H_2O \rightarrow 2O_2 + 4H^+ + 4e^- \quad (2.11)$$

Thus, the oxidation of organic pollutant is favored at acidic pH range. For electrochemical oxidation of real wastewater which contains various anions, acidic condition also reduces the concentration of HCO_3^- and CO_3^{2-} which are strong HO• scavengers (Li et al. 2001, Turro et al. 2011).

Many studies have reported the influence of pH on mediated anodic oxidation of organics in chlorine solution with MMO anodes. In most cases, the degradation of organic pollutants is attained by anodically generated active chlorine species at suitable pH ranges (Asaithambi et al. 2012, Lin et al. 2012, Scialdone et al. 2009a, Wang et al. 2007a, Xu et al. 2013b). The solution pH can affect the form of active chlorine species and their oxidation potentials (Panizza and Cerisola 2004). However, chlorine molecule ($E^o(Cl_2/Cl^-)$ = 1.36 V) only exists in neutral or acidic solution. When the proton and chloride concentrations are not high enough, chlorine molecule will dissolve in the water by disproportionation to form hypochlorous acid and

chloride:

$$Cl_2 + H_2O \rightarrow HClO + Cl^- + H^+ \quad (2.12)$$

$$HClO \rightarrow ClO^- + H^+ \quad (2.13)$$

The pK_a of hypochlorous acid is 7.54. In the lower pH range, the dominant form of active chlorine is hypochlorous acid ($E^o(HClO/Cl_2)$ = 1.63 V or $E^o(HClO/Cl^-)$ = 1.48 V), which has considerably higher oxidation potential than hypochlorite ($E^o(ClO^-/Cl^-)$ = 0.89 V) in alkaline media. Thus, the organic pollutants are removed more efficiently in acidic media. However, when treating paper mill wastewater using Ti/Co/SnO_2-Sb_2O_5 anode, much better COD removal and decolorization rate was obtained at pH =11 than pH = 3 (Wang et al. 2007a).

In addition, pH may influence the process efficiency through electromigration mass transfer. It is reported that the solubility or ionization degree of cationic dyes can be improved at lower pH condition (Shiraishi et al. 2008), which could enhances the dispersion of dye and decreases the resistance to mass transfer. In other study, the degradation of PFOA by Ti/SnO_2-Sb-based MMO anodes was found to be more favorable in acidic solution (Lin et al. 2012). However, under strongly acidic condition (pH = 3), the removal efficiency of PFOA by the anodes decreased again because of the weak dissociation ability of PFOA at low pH, which limited the electromigration mass transfer. Similar result was observed in pentachlorophenol (PCP) degradation by Ti/SnO_2-Sb anode. The anion form of PCP at higher pH can be much more easily adsorbed on the anode surface, resulting in the enhanced PCP degradation at pH =11. Nevertheless, some organic compounds may experience polymerization at higher pH, including dye (Samet et al. 2006) and phenol (Tahar et al. 2009, Tahar and Savall 2009). The polymer films have low permeability and show strong adhesion to the MMO anodes, which lead to the anode fouling problems. Though in most cases acidic condition favors the organic pollutants degradation by MMO anodes, the decrease of electrode service life and leaching of toxic metal ions

in acidic media should also be taken into consider in practical application of wastewater treatment.

Several reasons may give rise to the discrepancies on the reported pH influences on electrochemical oxidation of organic pollutants by MMO anodes. One important reason is that the solution pH is not constant throughout the electrochemical oxidation process, since OER in the anode and hydrogen evolution reaction (HER) in the cathode involve drastic hydrogen ions generation and consumption. However, their influences on solution pH are difficult to determine. In other study, Rajkumar et al. (Rajkumar et al. 2005) investigated the electrochemical oxidation of phenol at initial pH from 3 to 10 using Ti/TiO_2-RuO_2-IrO_2 anode, and they found the final pH always in the range 8 – 8.5. The authors explained such observation from the viewpoint of bicarbonate buffering effect. In addition, some literature did not report clearly whether the pH was initial or final pH, and whether solution pH was maintained during the electrochemical oxidation process

2.9.2 Temperature

A change in temperature will change both the reaction rates of organic degradation in bulk and capacity of $HO^{\bullet}$ adsorption in the MMO anode surface. The effect of temperature on the anodic oxidation of organic compounds has been investigated with respect to different MMO anodes. Some published literature report increased organics removal with solution temperature. For example, the first-order kinetic rate constant (k) of lignin oxidation by Ti/TiO_2-NTs/PbO_2 electrode was found to increase from 0.0018 min^{-1} at 20 ^oC to 0.0043 min^{-1} at 60 ^oC (Pan et al. 2012). In other study, the rate was even 2.7–fold higher at 65 ^oC than at 23 ^oC for electrochemical oxidation of 4-chorophenol with quaternary Ti/Sn-Sb-Mn-Pt-O anode (Meaney and Omanovic 2007). By plotting ln k vs 1/T through Arrhenius equation, the activation energy (E_a) can be derived:

$$\ln k = -E_a/RT + \ln A \quad (2.14)$$

where A refers to the frequency factor which is a constant, and R refers to the universal gas constant.

Many studies found the influence of temperature on removal rates of target pollutants was in good accordance with this equation (Borras et al. 2007, Pan et al. 2012, Tolba et al. 2010). E_a can be regarded as the energy barrier for electrochemical oxidation reaction to occur, which provides a thermodynamic view of the electrocatalytic activity of MMO anodes. For example, the E_a of lignin oxidation by Ti/TiO_2-NTs/PbO_2 anode (16 kJ mol^{-1}) was slightly smaller than that by Ti/RuO_2-IrO_2 (20 kJ mol^{-1}), indicating better electrocatalytic activity of Ti/TiO_2-NTs/PbO_2 which lowered the energy barrier.

However, several studies reported that the electrochemical oxidation of target organic pollutants remained unaffected by change of temperature. Examples are electrochemical oxidation of maleic acid at Ti/IrO_2-Ta_2O_5 anode (Scialdone et al. 2011) and p-methoxyphenol at Ti/SnO_2-Sb anode (Borras et al. 2007). Both of the organics have strong C=C bond (614 kJ mol^{-1}). It was unclear whether this strong bond gave rise to the temperature-independent electrochemical oxidation process.

In mediated oxidation process, it is generally acknowledged that the increase of temperature favors the electrogeneration of oxidative reagents like active chlorine, peroxodisulfate and ROS, thus improve the process efficiency (Canizares et al. 2006). However, a contradictory observation was made by Neodo et al. (Neodo et al. 2012), who investigated the electrolysis of dilute chloride solutions at Ti/RuO_2-SnO_2 and found that the detected concentration of active chlorine species was reduced when increasing the temperature from 10 ºC to 65 ºC. The observation may result from the drastic active chlorine consumption reactions at high temperature. Indeed, more studies are needed to illustrate the mechanism of temperature influence on both mediated anodic oxidation and mediated oxidation at MMO anodes.

Considering the additional cost that operation at high temperature may bring, electrochemical oxidation of organic pollutants is usually conducted at ambient temperature. Nevertheless, there is also argument that high temperature is on applicable scale for electrochemical oxidation at MMO anodes. Since electrochemical oxidation is an exothermic process and heat can also be generated by the solution resistance, high operating temperatures may be maintained without much additional cost. In addition, there is study confirmed that MMO anodes are more stable at high temperature than other anodes like BDD, meanwhile they exhibit more significant improvement in the pollutants removal efficiency with increasing temperature (Scialdone et al. 2011). All of these reasons make it attractive for operation at appropriate high temperature.

2.9.3 Current density

Current density is considered as an important operating parameter for electrochemical oxidation of organics at MMO anodes, for the purpose of both mechanistic study and cost-effectiveness analysis. In electrochemical oxidation, the capability of electron transfer and generation of oxidizing agents ($HO^{\bullet}$, $HO_2^{\bullet}$, ozone or active chlorine) rely on the applied current density (Niu et al. 2013a). Perez et al. (2010) found that the generation of ClO_3^- and free chlorine were significantly enhanced by increasing the current density from 50 mA cm^{-2} to 100 mA cm^{-2}. Rapid oxidation was also confirmed by Neodo et al. (Neodo et al. 2012), and such effect was far more distinctive on Ti/RuO_2-SnO_2 anode than Pt anode. Although high current densities favor the electrochemical oxidation of many pollutants, obvious enhancement of the energy efficiency is observed when the applied current densities are at a low level.

In industrial application, high current density is seldom employed for the electrochemical oxidation of organics due to (1) the enhancement of removal rate by

increasing current density is relatively low when it is already at a high level, (2) side reaction such as OER consumed the $HO^{\bullet}$ and competes with the electrochemical oxidation of contaminants (Comninellis 1994, Marselli et al. 2003) and (3) extra energy are consumed since the temperature of the solution is significantly increase at high current density. From the process kinetic point of view, the oxidation of pollutants may be mass transfer limiting reaction when the current density is high, and a better COD removal can be achieved by simply increasing the flow rate of supporting electrolyte (Rodríguez et al. 2013, Scialdone et al. 2009b).

Regarding MMO anodes, the choice of upper limit of applied current density should be more discreet compared with other anodes such as BDD and Pt. The crystalline structures and chemical states of MMO compounds in the surface layer are likely to change irreversibly under high current density, resulting in anode deactivation. Besides, semi-empirical study also reported that the optimal current densities were far from the diffusion-limiting current density (Jara and Fino 2010).

2.9.4 Supporting electrolyte

Various types of supporting electrolyte have been employed for electrochemical oxidation of organic pollutants at MMO anodes, with the primary goal of increasing the solution conductivity. Intense research interest has been devoted to investigating the influence of types and concentrations of supporting electrolytes on the electrochemical oxidation of organic pollutants. In general, supporting electrolytes were prepared by salts including neutral salts ($NaClO_4$, Na_2SO_4, NaCl and $NaNO_3$) and reducing salts ($NaSO_3$ and $NaNO_2$) (Niu et al. 2013a). Among them, $NaClO_4$ and $NaNO_3$ are highly stable compounds which can avoid producing any oxidizing species liable to react with organic compounds (Malpass et al. 2007, Turro et al. 2011), making them suitable for studying direct anodic oxidation at the MMO anodes. Many studies have shown the superiority of NaCl over Na_2SO_4 and other electrolytes,

especially for the treatment of solutions containing dyestuff (Awad and Galwa 2005, Rajkumar et al. 2007, Sakalis et al. 2005). However, the addition of chloride ions enhanced mainly the decolorization efficiency but not the TOC reduction (An et al. 2012), indicating more effective attack to the chromophoric groups of the dyestuff molecule by active chlorine. Promotion factor (*f*) was proposed by Zhou et al. (Zhou et al. 2011b) to assess the role of mediated oxidation by presence of additional NaCl, which can be given by:

$$f = K_{obs2}/K_{obs1} - 1 \quad (2.15)$$

where K_{obs2} and K_{obs1} are the apparent rate constant for pseudo first order reactions with and without NaCl. In their study, *f* can be as large as 73.3 for electrochemical oxidation of methyl orange at RuO_2- based MMO anode.

Compared with BDD anode and non-active MMO anodes, electrochemical oxidation by active anodes have a greater influence by the presence of Cl^-, due to their inefficiency to produce $HO^{\bullet}$ radicals (Bagastyo et al. 2013). The main drawback of employing NaCl as supporting electrolyte is its possible formation of organochlorine compounds (RCl), which can be present as persistent compounds and even more toxic than their parent compounds. However, studies have shown that RCl could be quickly consumed before the end of electrolysis (Comninellis and Nerini 1995).

2.10 Conclusions

MMO anodes, prepared by depositing MMO layer on inert substrates, provide technical merit in treating wastewaters containing recalcitrant organic pollutants by electrochemical oxidation. Compared with single-component mixed metal oxide anode, they exhibit better electrocatalytic activity resulting from the increase of active sites and a change in the oxidation states of the metal ions. Intense research efforts have been devoted to the surface modification of MMO anodes, aiming to increase

the surface area or introducing expected properties to the MMO layer. Such approaches include nano- and microstructure deposits, element doping and polymer composites. In addition, electrochemical oxidation at MMO anodes has the advantage of coupling direct and mediated oxidation processes, making it an attractive technique for treating various types of polluted water. In general, MMOs exhibit better process efficiency of electrochemical oxidation in acidic media and at high temperature, but the optimal operating conditions on application scale still remain arguable.

As yet the links between the surface structure of MMO anodes and their electrocatalytic performance is still not clearly established in literature, as well as the role of ROS in pollutants removal or alleviation. Hence, more such information is required by careful characterization with state-of-art analysis techniques. In addition, MMO anodes have several drawbacks such as limited life span and toxic cation leaching in strong acidic solution, which may limit scale-up of them for electrochemical oxidation of organic pollutants.

CHAPTER 3 ENHANCED ELECTROCHEMICAL OXIDATION OF PHENOL USING A HYDROPHOBIC TiO_2-NTs/SnO_2-Sb-PTFE ELECTRODE[2]

3.1 Introduction

Various attempts have been made to improve the physical and chemical stability as well as the electrocatalytic performance of SnO_2-Sb electrodes. One approach is to develop doped SnO_2-Sb electrodes by including some noble or transition metal ions (Bi, Ir, Fe, Ni, Eu, La, Ce, Ru or Gd, etc.) into the precursor solutions or electrodeposition bath (Chu et al. 2013, Feng et al. 2010a, Feng et al. 2008, He and Mho 2004, Li et al. 2013a, Lin et al. 2013a, Lin et al. 2013b, Liu et al. 2012b, Zhang et al. 2011b, Zhuo et al. 2011). By introducing dopants, improvement of the electrocatalytic performances of SnO_2-Sb electrodes would be obtained. However, there are still some remarkable limitations of this approach. For example, the introduction of Ce into SnO_2-Sb electrode did not lead to higher removal of pollutant although the service lifetime was enhanced (Zhang et al. 2011b). The incorporation of Eu reduced the grain sizes of SnO_2-Sb but the increase of oxygen vacancies of SnO_2 was undesirable for its electrocatalytic performance (Feng et al. 2010a). Moreover, the introduction of Ir led to a lower OEP (Chu et al. 2013). Therefore, it is important to develop highly stable SnO_2-Sb electrode without sacrificing its electrocatalytic activity.

Recently, SnO_2-Sb electrodes with nanostructured and microstructured design have drawn much interest. One of the most important approaches is by employing

[2] This chapter is modified from the literature published in *RSC Advances* in 2015 (vol.5, pp 32245-32255), of which the Ph.D. candidate is the first author.

highly ordered substrate (Chen et al. 2010, Wang et al. 2013b, Zhao et al. 2009). Highly ordered vertically aligned TiO_2 nanotubes (TiO_2-NTs) can be prepared by anodization of Ti substrates, with mean pore diameters ranging from 100 to 220 nm. With the property of large surface area, TiO_2-NTs can serve as tubular template wherein SnO_2-Sb are implanted aiming to obtain improved loading capacity of Ti substrate (Han et al. 2014). TiO_2-NTs/SnO_2-Sb prepared by pulse electrodeposition has been verified to have distinctive oxygen evolution potential of about 2.4 V vs SCE and show a remarkably better electrocatalytic activity compared with the SnO_2-Sb electrode prepared by sol-gel method (Wu et al. 2011). Meanwhile, polymers are attractive materials to introduce specific properties of metal oxide anodes. Polypyrrole and polyetrafluoroethylene (PTFE) composites have been used to introduce the hydrophobicity of PbO_2 electrode, and to obtained improved OEP and electrocatalytic activity (Hwang and Lee 1996, Zhao et al. 2010a). In other work, TiN composite has also been incorporated on SnO_2-Sb electrode for improved electrocatalytic activity (Duan et al. 2014).

This chapter presents a type of novel TiO_2-NTs/SnO_2-Sb-PTFE composite electrodes fabricated by pulse electrodeposition to obtain the larger specific surface area and hydrophobic electrode surface. The surface morphology, crystalline structure and electrochemical properties of the novel electrodes were investigated. The capability of $HO^{\bullet}$ generation on the electrodes were also evaluated. Phenol was selected as the model pollutant to investigate the performance of the as-prepared electrodes. The effects of pH and supporting electrolytes (Na_2SO_4 and NaCl) on the process efficiency were investigated, with a proposed mechanism presented to depict the electrochemical oxidation processes in different electrolytes. Sn ions leaching of TiO_2-NTs/SnO_2-Sb-PTFE was also studied under different conditions of electrochemical oxidation to evaluate its feasibility for environmental application.

3.2 Experimental

3.2.1 Chemicals and materials

All the chemicals were of analytical grade and used without further purification. $SnCl_2.2H_2O$, $SbCl_3$, Na_2SO_4, NaCl, NaF, NH_4Cl, PTFE, glycerol, dimethyl sulfoxide (DMSO), 2,4-dintrophenylhydrazine and (3-aminopropyl)trimethoxysilane were obtained from Sigma-Aldrich. Merck's absolute acetone, NaOH pellet, HCl and phenol were used in the experiments. PTFE was in the form of emulsion with 60 wt% dispersion in water. Pure titanium plates (99.9%) with a thickness of 0.5 mm were purchased from Qixin Company (Baoji, China).

3.2.2 TiO_2-NTs preparation

Pure titanium plates (60mm × 20mm) were polished by mechanical polisher with 120, 320, 800 and 1200 grid sand papers in sequence. Then they were washed in acetone and Milli Q water with ultrasonic assistance for 15 min, respectively. After that the titanium plates were immersed in 18% hydrochloric acid at 85 ^oC for 20 min to remove titanium oxide. In order to fabricate TiO_2-NTs substrate, the clean Ti plate was anodized in a two-electrode cell (1 cm distance) at room temperature, in which the clean Ti acted as anode and another titanium plate with same dimension as the cathode. The electrolyte is an aqueous solution containing a mixture of glycerol and Milli Q water (1.3:1 v/v), NaF (0.5 wt%) and Na_2SO_4 (0.2 M). Anodization experiments were carried out at a voltage of 30 V for 240 min with continuous magnetic stirring. Finally, the prepared substrates were annealed at 500 ^oC for 90 min at both a heating and cooling rate of 1 $^oC\ min^{-1}$ to get vertically aligned TiO_2-NTs.

3.2.3 TiO_2-NTs/SnO_2-Sb-PTFE preparation

TiO_2-NTs/SnO_2-Sb-PTFE were prepared by pulse electrodeposition in a two-

electrode cell (1 cm distance) using potentiostat (PGSTAT302N, Autolab) at 40 °C. Fig. 3.1 shows the schematic diagram for electrode design and preparation. Prior to pulse electrodeposition, TiO_2-NTs were pretreated by reduction in 1 M NH_4Cl at a potential of −1.5 V vs Ag/AgCl (3 M NaCl) at 40 °C, aiming to improve the conductivity of TiO_2-NTs substrate. Then the TiO_2-NTs were vertically immersed into the electrolyte which was consisted of 0.1 M $SnCl_2.2H_2O$, 0.02 M $SbCl_3$ and a certain concentration of hydrochloric acid, and they were degased in an ultrasonic bath for 10 min to remove the trapped air in the TiO_2-NTs. The impregnation of NTs with electrolyte is expected to favor the initial growth of SnO_2-Sb on the internal walls of the NTs. The nominal area of the electrode surface is 10 cm^2.

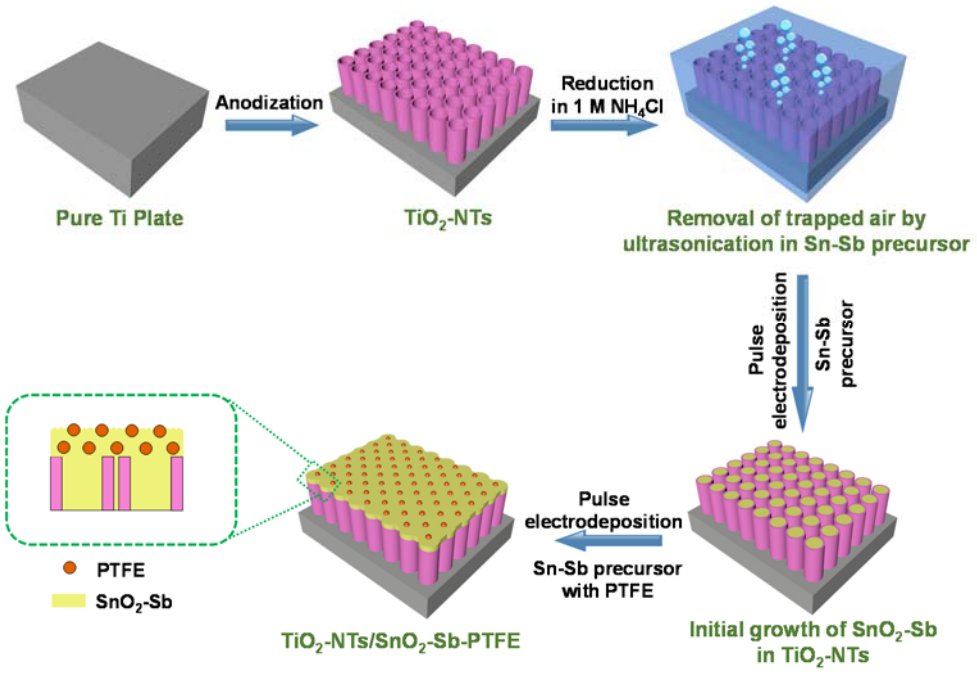

Fig. 3.1 Schematic illustration of TiO_2-NTs/SnO_2-Sb-PTFE electrode preparation.

The initial deposition of SnO_2-Sb was conducted in the above electrolyte. A pulse current with an anodic pulse (5 mA cm^{-2}, 50 ms), a cathodic pulse (−5 mA cm^{-2}, 5 ms) and a relaxation time (0 mA cm^{-2}, 1 s) was applied at 40 °C for 15 min. After that, the electrode was put into electrolytes consisted of 0.1 M $SnCl_2.2H_2O$, 0.02 M $SbCl_3$, a certain concentration of hydrochloric acid and plural PTFE dispersions (0,

1.5, 4.5 and 13.5 mL L^{-1}) using the same pulse electrodeposition method for 2 h. A 0.05 wt % (3-aminopropyl)trimethoxysilane solution was added in the electrolyte to lower the surface tension. The resulting electrodes were marked as TiO_2-NTs/SnO_2-Sb, TiO_2-NTS/SnO_2-Sb-PTFE(1.5), TiO_2-NTS/SnO_2-Sb-PTFE(4.5) and TiO_2-NTS/SnO_2-Sb-PTFE(13.5) with respect to the different concentrations of PTFE in the electrodeposition baths.

The conventional Ti/SnO_2-Sb electrode having the same nominal surface area was prepared by thermochemical decomposition according to the literature (Montilla et al. 2004).

3.2.4 Bulk electrolysis experiments

Bulk electrochemical oxidation of phenol was carried out in a 200 ml single-compartment electrochemical cell at room temperature for 6 h under continuous stirring, and the schematic of the setup is illustrated in Fig. 3.2. The Conventional Ti/SnO_2-Sb electrode prepared by thermochemical decomposition, TiO_2-NTs/SnO_2-Sb and TiO_2-NTS/SnO_2-Sb-PTFE electrodes prepared by pulse electrodeposition were employed as the anodes, and a titanium plate with the same area served as the cathode. The distance between the two electrodes was 1 cm. The influencing factors that were investigated including the types of supporting electrolytes (Na_2SO_4 and NaCl) and the initial solution pH (pH = 3, 7 and 11). Either 0.05 M Na_2SO_4 or 0.1 M NaCl were used as the supporting electrolytes for synthetic wastewater solution containing 5 mM phenol. Initial pH of solutions were adjusted by adding drops of 1 M HCl, 0.5 M H_2SO_4 or 1M NaOH solutions. The current density was set as 20 mA cm^{-2}, and the samples were drawn for analysis with 1 h time interval. The accelerated life tests were conducted by anodic polarization at current density of 100 mA cm^{-2} in 0.1 M H_2SO_4 at room temperature to evaluate the service lifetime of the electrodes. The accelerated life in hours was determined by the time when the cell potential

increased 5 V from the initial value (Montilla et al. 2004).

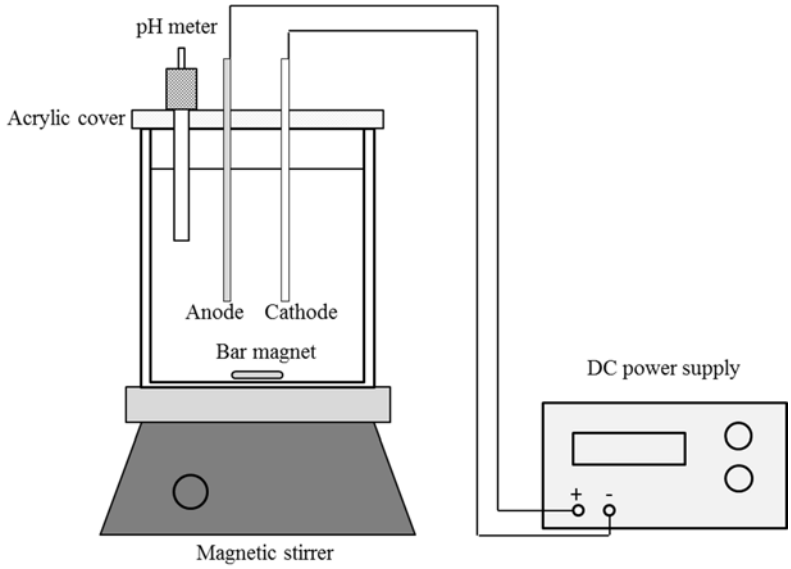

Fig. 3.2 Schematic diagram of the single-compartment electrochemical cell.

The electrocatalytic performance of the electrodes were evaluated by measurement of total organic carbon (TOC) and specific ultra-violet absorbance at wavelength of 254 nm ($SUVA_{254}$). $SUVA_{254}$ is defined as the UV absorbance at wavelength of 254 nm normalized by dissolved organic carbon (DOC) concentration, which is equivalent to the determined TOC since the solutions were crystal clear. The TOC of the samples were measured by a TOC analyzer (TOC-L/CPH, Shimadzu). The UV absorbance of the samples at wavelength of 254 nm were determined by a UV-Vis spectrophotometer (UV 9000, Metash). $HO^{\bullet}$ was quantitatively determined by high-performance liquid chromatography (HPLC, Perkin Elmer Series 200) with DMSO trapping according to literature (Tai et al. 2004). The organic acid intermediates of phenol oxidation were qualitatively determined by ion chromatography (IC, Thermo Scientific Dionex ICS-2100). Atomic absorption spectroscopy (AAS, Perkin Elmer AAnalyst 100) was used to analyze the leached Sn ions in the solutions after 6 h bulk electrolysis.

The completely electrochemical oxidation of phenol can be expressed as:

$$C_6H_6O + 11H_2O \rightarrow 6CO_2 + 28H^+ + 28e^- \quad (3.1)$$

At given time t, the mineralization current efficiency (MCE) of the electrochemical oxidation process can be calculated by the following equation (Liu et al. 2009a):

$$\text{MCE}\,(\%) = \frac{100.\Delta[\text{TOC}]_{\text{exp}}}{\Delta[\text{TOC}]_{\text{theory}}} \tag{3.2}$$

where $\Delta[\text{TOC}]_{\text{exp}}$ and $\Delta[\text{TOC}]_{\text{theory}}$ (mg dm^{-3}) are the experimental TOC change and theoretical TOC change at given time t, respectively. The value of $\Delta(\text{TOC})_{\text{theory}}$ can be calculated by:

$$\Delta[\text{TOC}]_{\text{theory}} = \frac{1000.n_c\text{ItM}}{n_e\text{FV}} \tag{3.3}$$

where n_c is the number of organic carbon, I is the applied current (A), t is the electrolysis time (s), M is the molar mass of carbon (M = 12 g mol^{-1}), n_e is the number of electron transfers, F is the Faraday constant (96485 C mol^{-1}) and V is the volume of solution (dm^3). For phenol oxidation, n_C and n_e are 6 and 28 respectively.

The specific energy consumption (E_c, kWh kgTOC^{-1}) can be calculated as follows:

$$E_C = \frac{1000.E_{\text{cell}}\text{It}}{\Delta[\text{TOC}]_{\text{exp}}\text{V}} \tag{3.4}$$

where E_{cell} is the average cell potential (V), I is the applied current (A), t is the electrolysis time (h), $\Delta[\text{TOC}]_{\text{exp}}$ is the experimental TOC change (mg dm^{-3}) and V is the volume of solution (dm^3).

3.2.5 Analytical techniques

The surface morphology and element composition of the electrodes were characterized using field emission scanning electron microscopy (FESEM, JEOL-7660F) and energy-dispersive X-ray spectroscopy (EDS, Oxford Xmax80 LN2 Free). The crystal structure of the fabricated electrodes were characterized by X-ray diffraction (XRD, Bruker D8 Advance) with Cu-Ka (λ=1.5418 Å) operating at 40 kV and 40 mA, with corresponding 2θ range of 10-80°. The contact angle of water on

the electrode surface was determined by a contact angle meter (DSA100) with 5 μL water droplet added. Electrochemical properties of the electrodes were investigated in a conventional three-electrode system using electrochemical workstation (PGSTAT 302N, Autolab). Pt served as the counter electrode and Ag/AgCl (3 M NaCl) served as the reference electrode, and the electrolyte was 0.5 M Na_2SO_4. Cyclic voltammetry (CV) was performed to determine the OEP of the electrode with the scan range of 0.3-3.0 V and scan rate of 50 mV s^{-1}. Anodic polarization experiments were studied using chronoamporometric method at a potential of 1.4 V and 3.0 V vs Ag/AgCl (3 M NaCl) respectively for 10 s with/without 5 mM phenol. Electrochemical impedance spectroscopy (EIS) was carried out at 1.0 V. The frequency ranges from 100 kHz to 5 mHz with an amplitude of 10 mV, and equivalent circuit simulation was applied to determine the values of electrochemical parameters.

3.3 Results and discussions

3.3.1 Characteristics of TiO_2-NTS/SnO_2-Sb-PTFE

3.3.1.1 Surface structure and wetting property

The surface morphology of the TiO_2-NTs substrate and the fabricated electrodes is examined by FESEM. As can be seen in Fig. 3.3a, highly ordered TiO_2-NTs were uniformly grown on Ti plate with an average pore diameter of 100 nm, and the thickness of the wall ranges from 10 to 20 nm. The surface of the conventional SnO_2-Sb electrodes shows “mud-cracked” structure (Fig. 3.3b), which is a typical structure in MMO anodes prepared by thermochemical decomposition. The crack is undesirable because it would give rise to the weak adhesion between SnO_2 and Ti substrate. In addition, such cracks may lead to the permeation of electrolyte into the Ti substrate, and finally the formation of a passivating layer between SnO_2-Sb and Ti substrate. It was also confirmed by the accelerated life test that the conventional Ti/SnO_2-Sb electrode has a lowest service lifetime of only 6.4 h (Table 3.1). In Fig.

3.3c, improvement of the surface morphology is observed in TiO_2-NTs/SnO_2-Sb fabricated by pulse electrodeposition. The SnO_2-Sb nanoparticles show microspherical shape with diameters ranging from 100 to 200 nm, and no crack is observed on the electrode surface comparing with the conventional Ti/SnO_2-Sb. The service lifetime of TiO_2-NTs/SnO_2-Sb was also improved up to 28 h, which is 4.3 times that of the conventional Ti/SnO_2-Sb. After the incorporation of PTFE nano particles, a layer of PTFE can be observed on the surfaces of all the three electrodes with different PTFE loadings (Fig. 3.3d-f). Compared with TiO_2-NTs/SnO_2-Sb without PTFE, the electrode surfaces with PTFE loading become rough in morphology. Such morphology leads to increased specific surface area which can provide more active sites for the electrocatalytic oxidation reactions to take place. It is also notable that a reduced SnO_2-Sb particle grain size is observed at TiO_2-NTs/SnO_2-Sb-PTFE(4.5), indicating grain refining effect for SnO_2-Sb deposition. The accelerated service lifetime of TiO_2-NTs/SnO_2-Sb-PTFE(4.5) and TiO_2-NTs/SnO_2-Sb-PTFE(13.5) were further improved up to 98h and 103 h, corresponding to 15.3 and 16 times that of the conventional SnO_2-Sb, respectively.

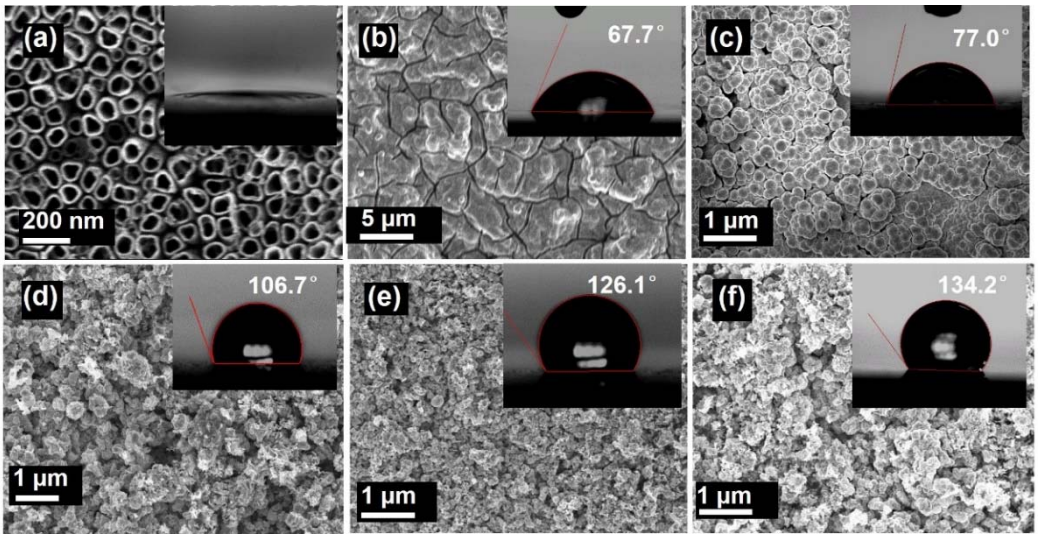

Fig. 3.3 FESEM images and contact angles (inset) of (a) TiO_2-NTs, (b) conventional TiO_2 /SnO_2-Sb, (c) TiO_2-NTs/SnO_2-Sb, (d) TiO_2-NTs/SnO_2-Sb-PTFE(1.5), (e) TiO_2-NTs/SnO_2-Sb-PTFE(4.5) and (f) TiO_2-NTs/SnO_2-Sb-PTFE(13.5).

Table 3.1 Parameters of the Ti/SnO_2-Sb(conventional), TiO_2-NTs/SnO_2-Sb and TiO_2-NTs/SnO_2-Sb-PTFE electrodes

Electrode	OEP (V vs Ag/AgCl)	Service lifetime (h)	Current density without phenol[a] (mA cm^{-2})	Current density with phenol[e] (mA cm^{-2})	ΔCurrent density (mA cm^{-2})	Contact angle (°)
Conventional Ti/SnO_2-Sb	2.0	6.4	8.32	10.54	2.22	67.7
TiO_2-NTs/SnO_2-Sb	2.1	28	8.47	11.60	3.13	77.0
TiO_2-NTs/SnO_2-Sb-PTFE(1.5)	2.2	51	10.29	14.71	4.42	106.7
TiO_2-NTs/SnO_2-Sb-PTFE(4.5)	2.4	98	10.21	16.55	6.34	126.1
TiO_2-NTs/SnO_2-Sb-PTFE(13.5)	2.4	103	9.36	12.41	3.05	134.2

[e]Current densities were measured at the potential of 3.0 V vs Ag/AgCl (3 M NaCl).

The elements Ti, Sn, Sb, F, C and O were detected by EDS on TiO_2-NTs/SnO_2-Sb-PTFE electrodes. Fig. 3.4 shows the uniform distribution of elements Sn, Sb, F and C on TiO_2-NTs/SnO_2-Sb-PTFE(4.5) by elemental mapping. The atomic percentages of the elements are investigated and listed in Table 3.2. There is still a small portion of Ti detected on the electrode surfaces. However, more amount of Ti was detected on the conventional Ti/SnO_2-Sb (1.15%), which is possibly due to the cracks of the electrode leading to the exposure of Ti substrate. Sb/Sn ratios of TiO_2-NTs/SnO_2-Sb-PTFE electrodes are around 4%, while the value is 2.6% on the conventional Ti/SnO_2-Sb. It should be noted that when the PTFE loading in the electrodepositon bath increases 3 times from 4.5 ml L^{-1} to 13.5 ml L^{-1}, the real atomic percentage of F in the electrode surface only increases by a factor of 1.8 (from 0.58% to 1.08%). It indicates that PTFE loading of TiO_2-NTs/SnO_2-Sb-PTFE(13.5) has reached a saturation level and further increase of PTFE in the electrodepositon bath would not result in higher PTFE content in the electrode surface.

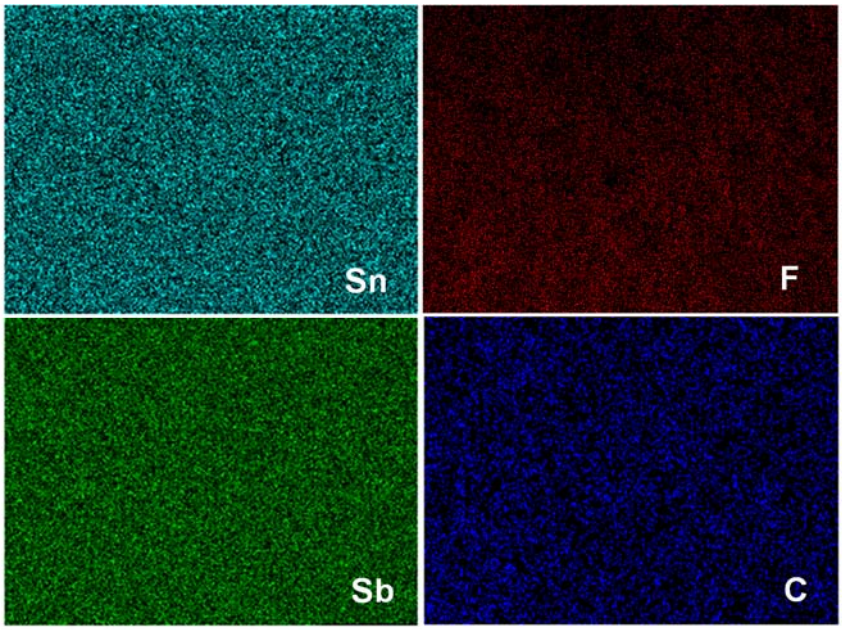

Fig. 3.4 Elemental mappings of Sn, Sb, F and C on the surface of TiO_2-NTs/SnO_2-Sb-PTFE(4.5).

Table 3.2 Elemental compositions of Ti/SnO_2-Sb(conventional), TiO_2-NTs/SnO_2-Sb and TiO_2-NTs/SnO_2-Sb-PTFE electrode surfaces

Electrode	Elemental composition (Atomic%)					
	Ti	Sn	Sb	C	F	O
Conventional Ti/SnO_2-Sb	1.15	32.3	0.84	-	-	66.7
TiO_2-NTs/SnO_2-Sb	0.76	32.1	1.33	-	-	65.8
TiO_2-NTs/SnO_2-Sb-PTFE(1.5)	0.61	33.3	1.28	0.12	0.22	64.5
TiO_2-NTs/SnO_2-Sb-PTFE(4.5)	0.52	32.3	1.41	0.30	0.58	64.9
TiO_2-NTs/SnO_2-Sb-PTFE(13.5)	0.48	32.4	1.22	0.57	1.08	64.3

The contact angle of TiO_2-NTs (Fig. 3.3a) is very low (below 10°) and shows its super hydrophilic property. Both the conventional Ti/SnO_2-Sb and TiO_2-NTs/SnO_2-Sb have hydrophilic surface (contact angles 67.7° and 77° respectively). For TiO_2-NTs/SnO_2-Sb-PTFE, because of the strong hydrophobicity of PTFE, its surface wetting property prominently changes and the contact angles are 106.7°, 126.7° and 134.2° respectively with the increasing PTFE loading.

Fig. 3.5 compares the XRD patterns of various electrodes. TiO_2 is indexed to anatase phase with diffraction peaks at 2θ = 25.6°, 38.1° and 48.3°. The diffraction peaks at 2θ = 26.8°, 34.1° and 52.0° are indexed to the (110), (101) and (211) planes of SnO_2. No obvious peaks of Sb are detected due to the incorporation of Sb into the SnO_2 crystals. The intensities of (101) and (211) peaks for SnO_2 of conventional Ti/SnO_2-Sb and TiO_2-NTs/SnO_2-Sb are similar. However, the intensity of (110) peak is much stronger in the conventional TiO_2-NTs/SnO_2-Sb, indicating a preferred orientation of SnO_2 along (110) direction. The diffraction peak at 2θ = 18.2° suggests that PTFE has been successfully incorporated in the electrode surface coating. The higher PTFE loading, the stronger the peak intensity.

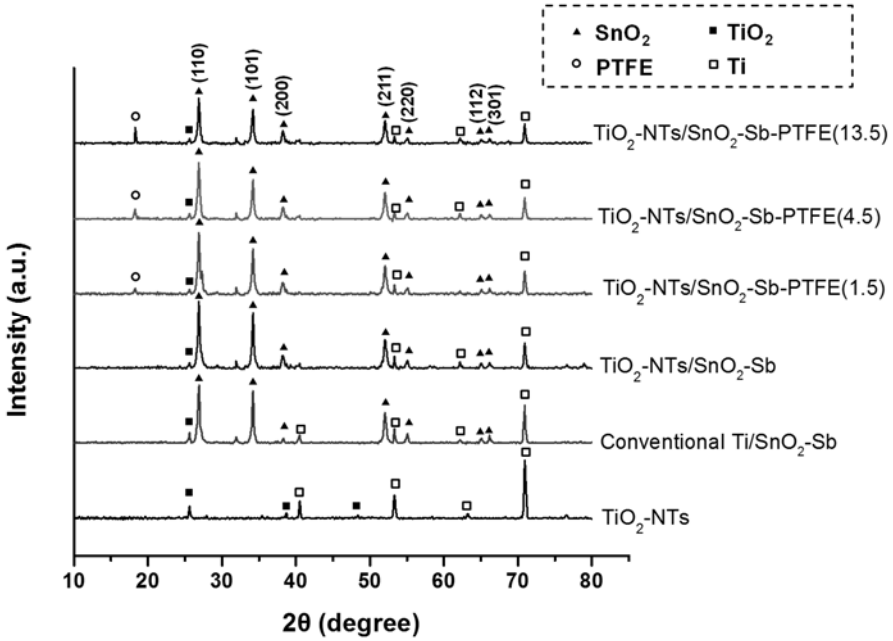

Fig. 3.5 XRD patterns of the electrodes.

3.3.1.2 Electrochemical properties

In environmental application of anodes, OEP is an important indicator of electrocatalytic activities for organics oxidation. Fig. 3.6 shows the CV curves of the conventional Ti/SnO_2-Sb, TiO_2-NTs/SnO_2-Sb and TiO_2-NTs/SnO_2-Sb-PTFE

electrodes in 0.5 M Na_2SO_4, and the corresponding values of OEP are given in Table 3.1. The conventional Ti/SnO_2-Sb has a lowest OEP of 2.0 V, and the value increases slightly to 2.1 V in TiO_2-NTs/SnO_2-Sb fabricated by pulse electrodeposition. However, after introducing PTFE the OEP of the anodes are further increased, with the highest OEP of 2.4 V observed in TiO_2-NTs/SnO_2-Sb-PTFE(4.5) and TiO_2-NTs/SnO_2-Sb-PTFE(13.5). First, the enhancement of OEP is attributed to the change of surface wetting property from hydrophilic to hydrophobic, which inhibits the surface adsorption of hydrophilic $HO^{\bullet}$. Second, PTFE hinders the movement of $HO^{\bullet}$ into the electrode interior. Thus, the oxygen evolution reaction (OER) is inhibited (Zhao et al. 2010a).

The anodic polarization of the electrodes was studied at a constant potential of 1.4 V and 3.0 V vs Ag/AgCl (3 M NaCl) to investigate their electrocatalytic activities towards phenol. At 1.4 V which is below the OEP, no background current was observed either in the presence or absence of phenol, suggesting phenol cannot be oxidized at this potential. When the potential was set as 3.0 V, the current densities of the five electrodes ranged from 8.32 mA cm^{-2} to 10.29 mA cm^{-2} in 0.5 M Na_2SO_4 (Table 3.1). However, after the addition of 5 mM phenol, there were drastic increases of the current densities. The increment of current density of TiO_2-NTs/SnO_2-Sb-PTFE(4.5) (6.34 mA cm^{-2}) was significantly greater than that of conventional Ti/SnO_2-Sb (2.22 mA cm^{-2}) and TiO_2-NTs/SnO_2-Sb (3.13 mA cm^{-2}), revealing its superior electrocatalytic activity towards phenol. Nevertheless, the value was much smaller in TiO_2-NTs/SnO_2-Sb-PTFE(13.5) (3.05 mA cm^{-2}) compared with TiO_2-NTs/SnO_2-Sb-PTFE(4.5). Such phenomenon is attributed to their differences of surface morphology. The particle size of SnO_2-Sb on TiO_2-NTs/SnO_2-Sb-PTFE(4.5) is much smaller, indicating more active sites for the oxidation of phenol to take place, so that the electrocatalytic activity is improved.

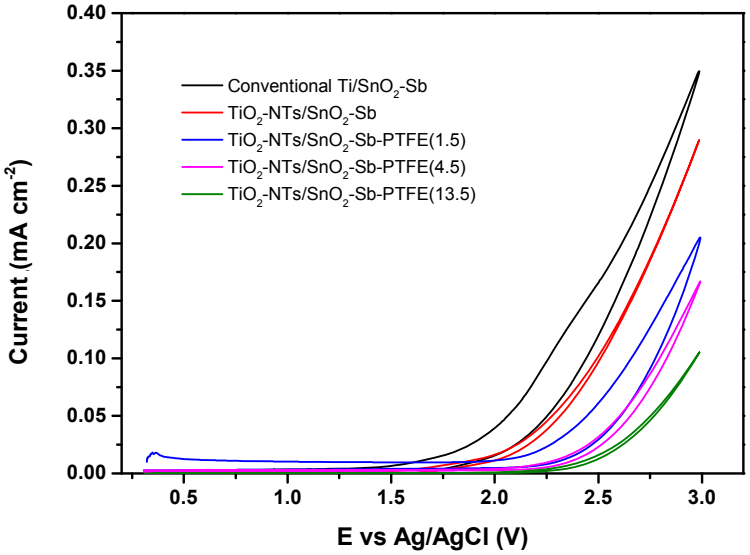

Fig. 3.6 Cyclic voltammetric curves of the electrodes in 0.5 M Na_2SO_4 with potential range of 0.3 – 3.0 V vs Ag/AgCl (3 M NaCl) and scan rate of 50 mV s^{-1}.

EIS studies were carried out to further investigate the electrochemical impedance of the novel electrodes. Fig. 3.7a shows the Nyquist plots of the electrodes. As shown in the figure, well developed semicircle patterns are observed, which suggested that mass diffusion control is negligible (Liu et al. 2012b). TiO_2-NTs substrate is non-conductive with an electrochemical impedance larger than 20000 Ω. After partial reduction of TiO_2-NTs substrate and pulse electrodeposition of SnO_2-Sb, the electrochemical impedance decreased significantly. Equivalent circuit module $R_s(R_{ct}Q)$ was employed to better interpret the EIS results (Fig. 3.7b). The simulation values of the electrochemical parameters are given in Table 3.3. In this circuit model, R_s represents the uncompensated ohmic resistance between the working electrode and referrence electrode, R_{ct} is the charge transfer resistance, and Q is the constant phase element (CPE) of double layer. The values of n are all in the range of 0.75 – 1 representing the performance of the electrodes are close to pure capacitors. Comparing with the conventional Ti/SnO_2-Sb, R_s of TiO_2-NTs/SnO_2-Sb decreases by the employment of TiO_2-NTs substrate, suggesting better conductivity. Slight increases of R_s are observed at TiO_2-NTs/SnO_2-Sb-PTFE electrodes. This is probably due to the property of PTFE which is non-conductive. Despite the slight increases of

R_s, it should be noted that the charge transfer resistances decrease significantly at TiO_2-NTs/SnO_2-Sb-PTFE electrodes. TiO_2-NTs/SnO_2-Sb-PTFE(4.5) has a lowest R_{ct} of only 54.13 Ω cm^{-2}, which is only 38% and 53% that of conventional Ti/SnO_2-Sb and TiO_2-NTs/SnO_2-Sb by pulse electrodeposition. Lower R_{ct} results in the faster electron transfer on electrode surface, indicating an improvement of electrocatalytic activity by incorporation of PTFE nanoparticles. Meanwhile, the R_s of TiO_2-NTs/SnO_2-Sb-PTFE(4.5) (5.30 Ω cm^{-2}) is also smaller than that of the conventional Ti/SnO_2-Sb (5.89Ω cm^{-2}). Thus, TiO_2-NTs/SnO_2-Sb-PTFE(4.5) is expected to exhibit much better electrocatalytic activity. Moreover, the TiO_2-NTs/SnO_2-Sb-PTFE electrodes showed higher capacitance, which can result from electrochemically active surface area of the coatings (Da Silva et al. 2002).

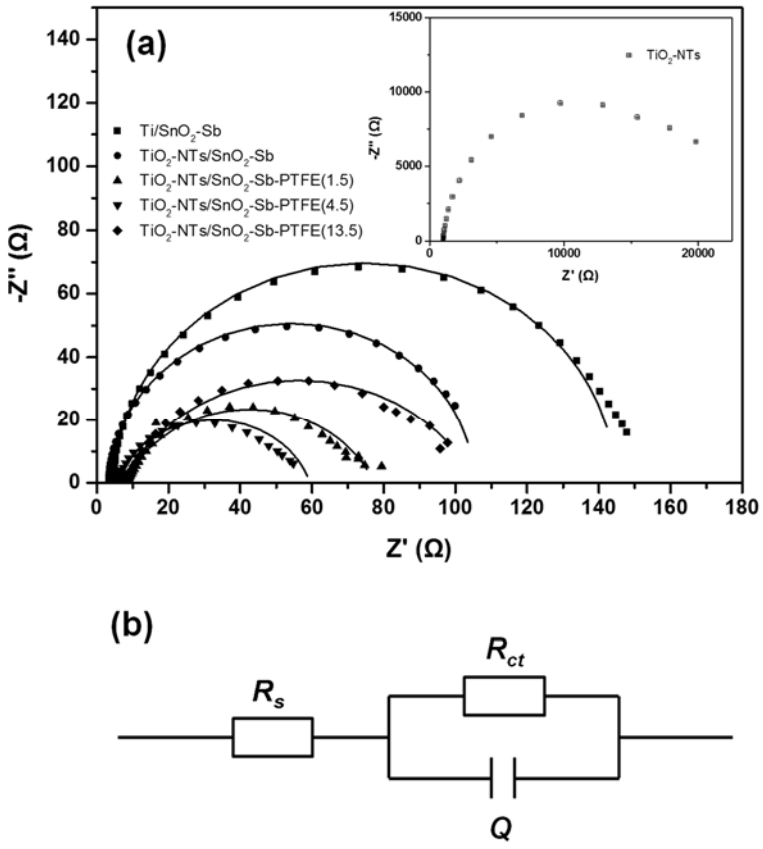

Fig. 3.7 (a) Nyquist plots of the electrodes and simulation curves of the EIS results (inset is the Nyquist plot of TiO_2-NTs) and (b) equivalent circuit model $R_s(R_{ct}Q)$.

Table 3.3 EIS simulating parameters of Ti/SnO_2-Sb(conventional), TiO_2-NTs/SnO_2-Sb and TiO_2-NTs/SnO_2-Sb-PTFE electrodes

Electrodes	R_s (error%) (Ω cm^{-2})	R_{ct} (error%) (Ω cm^{-2})	n	CPE (error%) (mF cm^{-2})
Conventional Ti/SnO_2-Sb	5.89 (0.48)	139.57 (0.74)	0.923	0.54 (0.59)
TiO_2-NTs/SnO_2-Sb	4.32 (1.26)	101.45 (0.633)	0.941	0.52 (1.12)
TiO_2-NTs/SnO_2-Sb-PTFE(1.5)	7.71 (3.41)	69.64 (6.44)	0.757	1.96 (16.47)
TiO_2-NTs/SnO_2-Sb-PTFE(4.5)	5.30 (2.31)	54.13 (3.77)	0.814	1.04 (11.90)
TiO_2-NTs/SnO_2-Sb-PTFE(13.5)	6.97 (2.32)	98.62 (5.49)	0.746	2.14 (9.74)

3.3.2 Electrochemical oxidation of phenol

3.3.2.1 Influence of PTFE loadings

Fig. 3.8 shows the removal of TOC during electrochemical oxidation of phenol in 0.05 M Na_2SO_4. When using the conventional Ti/SnO_2-Sb, the removal of TOC of phenol is only 69% after 6 h electrochemical oxidation at pH 7. An improvement of TOC removal (73%) is observed at TiO_2-NTs/SnO_2-Sb fabricated by pulse electrodeposition. As mentioned above, such enhancement is probably attributed to the reduced electrochemical impedance and the improved surface morphology of the 3-dimensional TiO_2-NTs. Moreover, the TOC removal efficiency was greatly enhanced in TiO_2-NTs/SnO_2-Sb-PTFE electrodes (up to 93%), indicating the improved electrocatalytic activity of phenol oxidation by incorporation of PTFE in the electrode surfaces. The enhancement of TOC removal can be attributed to several reasons. First, the high OEP of TiO_2-NTs/SnO_2-Sb-PTFE favors the $HO^{\bullet}$ generation. Second, the surfaces of TiO_2-NTs/SnO_2-Sb-PTFE electrodes are hydrophobic, so that the $HO^{\bullet}$ generated would be released as free $HO^{\bullet}$ rather than combining together for oxygen evolution. Hence, the removal efficiency is enhanced. The above results were verified by the $HO^{\bullet}$ concentration in solution (Fig. 3.9). The TiO_2-NTs/SnO_2-Sb-

PTFE electrodes showed superior ability of HO• generation (up to 36 μM) than Ti/SnO_2-Sb(conventional) (26 μM) and TiO_2-NTs/SnO_2-Sb (28 μM) after 240 min bulk electrolysis. The best TOC removal was obtained in TiO_2-NTs/SnO_2-Sb-PTFE(4.5) which has the highest HO• generation (Fig. 3.8b). In addition, the TiO_2-NTs/SnO_2-Sb-PTFE(4.5) has notably smaller SnO_2-Sb particles, which also give more active sites for phenol degradation.

The $SUVA_{254}$ degradation of the 5 electrodes is represented in the inset of Fig. 3.8. $SUVA_{254}$ is strongly correlated with the aromatic extent of pollutants. The higher the $SUVA_{254}$, the higher degree of aromaticity of the dissolved organic compounds (Weishaar et al. 2003). Increase of $SUVA_{254}$ in the first hour using Ti/SnO_2-Sb(conventional), TiO_2-NTs/SnO_2-Sb and TiO_2-NTs/SnO_2-Sb-PTFE(13.5) as anodes shows that the cleavage reaction of aromatic ring is not favored despite the TOC decreases. The main aromatic intermediates of phenol involves catechol, hydroquinone and benzoquinone (Makgae et al. 2008). When using TiO_2-NTs/SnO_2-Sb-PTFE(4.5) and TiO_2-NTs/SnO_2-Sb-PTFE(1.5) as anodes, the $SUVA_{254}$ decreased readily during the 6 h electrochemical oxidation, indicating phenol and aromatic intermediates undergo ring cleavage reactions. IC measurements showed that they were subsequently oxidized to aliphatic acids including maleic acid, oxalic acid, acetic acid and formic acid. Finally, they can be completely degraded to CO_2 and H_2O. The final $SUVA_{254}$ after 6 h electrochemical oxidation is 0.098 $SUVA_{254,0}$ on TiO_2-NTs/SnO_2-Sb-PTFE(4.5), which is only 29% and 46% that of Ti/SnO_2-Sb(conventional) and TiO_2-NTs/SnO_2-Sb. This result suggests that TiO_2-NTs/SnO_2-Sb-PTFE(4.5) has the merit of fully alleviating the aromatic intermediates into mineral acids, which are biodegradable and environmentally more benign.

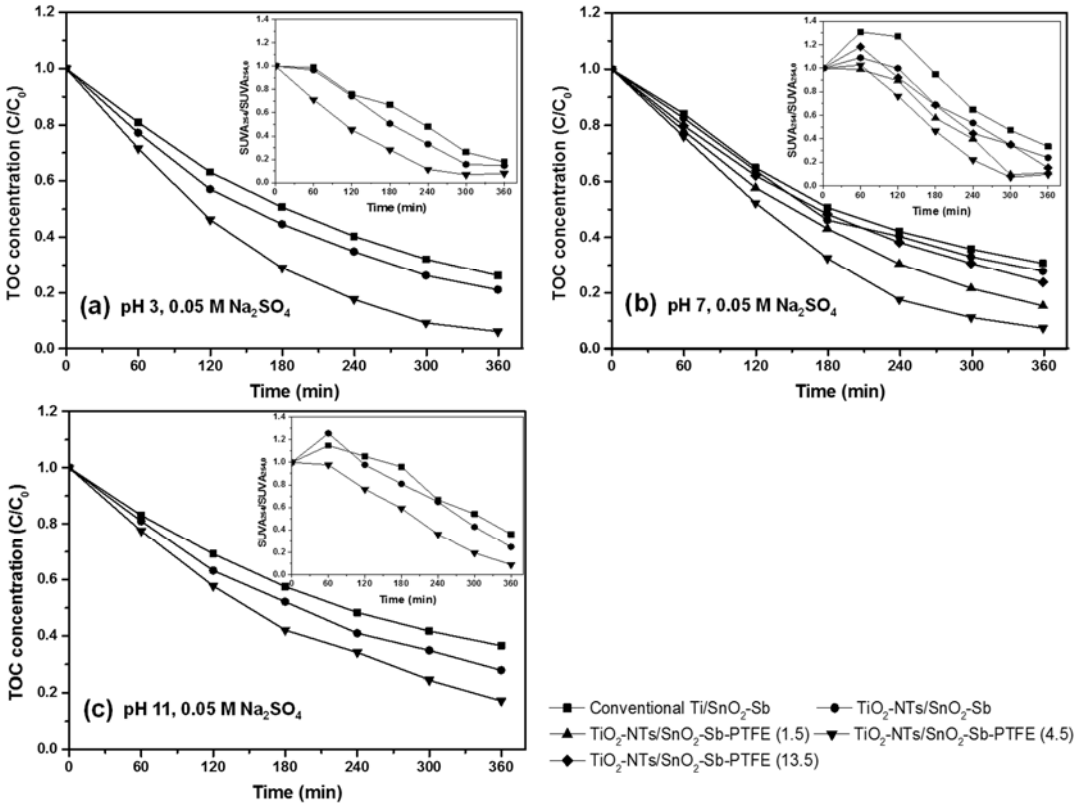

Fig. 3.8 TOC concentration and $SUVA_{254}$ as a function of time during phenol degradation at: (a) pH 3; (b) pH 7; (c) pH 11.

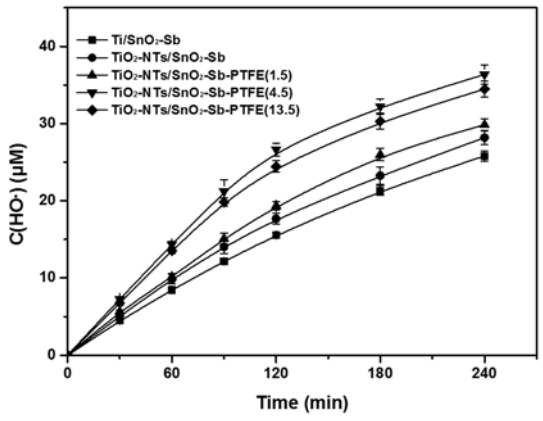

Fig. 3.9 Concentration evolution of hydroxyl radicals on the electrodes in 0.05 M Na_2SO_4.

Fig. 3.10a shows the MCE of different electrodes. The highest MCE was obtained on TiO_2-NTs/SnO_2-Sb-PTFE(4.5) (17.8 % at 1 h and 11.6 % at 6 h). Therefore, TiO_2-NTs/SnO_2-Sb-PTFE(4.5) exhibits the highest efficiency for phenol oxidation.

Besides, TiO_2-NTs/SnO_2-Sb-PTFE(4.5) has the lowest E_c among the 5 electrodes (Fig. 3.10b). The E_c of TiO_2-NTs/SnO_2-Sb-PTFE(4.5) to reach 60% TOC removal is 49 kWh $kgTOC^{-1}$, which is only 0.68 time that of Ti/SnO_2-Sb(conventional) and 0.78 time that of TiO_2-NTs/SnO_2-Sb. On the basis of above analysis, TiO_2-NTs/SnO_2-Sb-PTFE(4.5) appears to be the most optimal electrode with the most TOC removal and $SUVA_{254}$ decrease, highest MCE and lowest energy consumption.

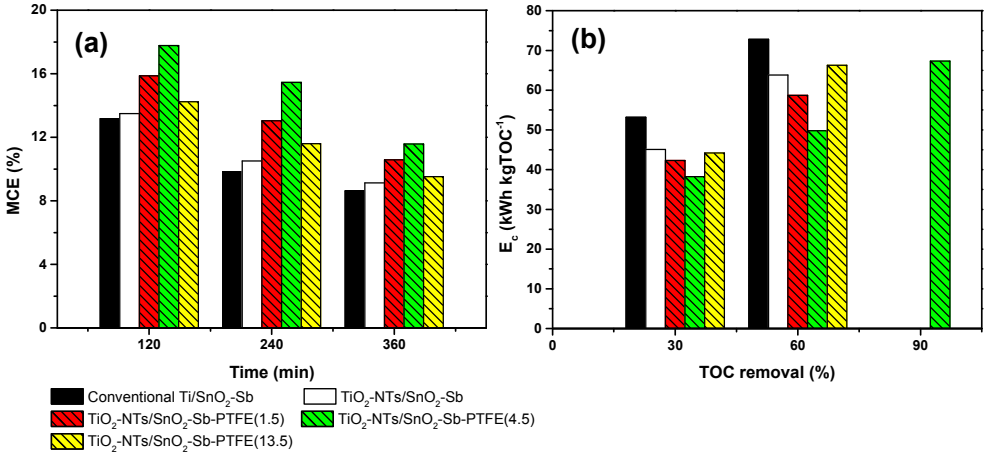

Fig. 3.10 (a) MCE changes with time and (b) specific energy consumption with TOC removal rate at pH 7 in 0.05 M Na_2SO_4.

3.3.2.2 Influence of pH

The effect of pH on phenol oxidation by the different electrodes was investigated in 0.05 M Na_2SO_4. Fig. 3.8 shows that all of the 3 electrodes achieve better TOC removals in acidic solutions than that in neutral and basic solutions. The TOC removals at pH 3 are 74%, 79% and 94% respectively using Ti/SnO_2-Sb, TiO_2-NTs/SnO_2-Sb and TiO_2-NTs/SnO_2-Sb-PTFE(4.5) as anodes. The $SUVA_{254}$ also decreases more rapidly, indicating a faster ring cleavage of the aromatic intermediates. On the contrary, TOC removals are not favorable at pH 11.

The ionization of phenol is strongly related to solution pH. Phenol has an acid dissociation constant (pK_a) of 9.95. When pH < pK_a, the non-ionized phenol presents as the dominant species, and when pH > pK_a, phenol will be ionized and the dominant

species is the phenoxide anion. At initial solution pH of 11, phenol could exist as phenoxide anion which is negatively charged, so they may be attracted toward the positively charged anode. However, the electrocatalytic performance of Ti/SnO_2-Sb, TiO_2-NTs/SnO_2-Sb and TiO_2-NTs/SnO_2-Sb-PTFE(4.5) electrodes for phenol degradation still decreases despite of this phenomenon. The results can be explained from the viewpoint of thermodynamics, because the oxidative power of $HO^{\bullet}$ varies with pH. $HO^{\bullet}$ radicals are generated from the oxidation of water:

$$H_2O \rightarrow HO^{\bullet} + H^+ + e^- \quad (3.5)$$

Given that the redox potential of $HO^{\bullet}_{aq}/H_2O$ is 2.59 V at pH 0 at the standard condition, the relationship between solution pH and redox potential of $HO^{\bullet}_{aq}/H_2O$ can be calculated by Nernst equation:

$$E^o(HO^{\bullet}_{aq}/H_2O) = 2.59 - 0.059\ pH \quad (3.6)$$

Thus, the values of $E^o(HO^{\bullet}_{aq}/H_2O)$ are 2.41, 2.18 and 1.94 at pH 3, 7 and 11. Therefore, higher TOC removal can be achieved in low pH range. However, in the basic solution with pH 11, the decrease of TOC removal is at a greater extent using TiO_2-NTs/SnO_2-Sb-PTFE(4.5) (82%) as anode than those using conventional Ti/SnO_2-Sb (64%) and TiO_2-NTs/SnO_2-Sb (73%). This is probably because the electrocatalytic oxidation of phenol with TiO_2-NTs/SnO_2-Sb-PTFE(4.5) relies more on $HO^{\bullet}$ generation. Hence, the phenol oxidation is greatly influenced when the oxidative power of $HO^{\bullet}$ reduces in the basic solution.

3.3.2.3 Influence of supporting electrolytes

The types of supporting electrolytes may influence the types of oxidative species generated, and hence the process efficiency of electrochemical oxidation. Fig. 3.11 shows the TOC removals and the corresponding $SUVA_{254}$ of phenol using different anodes in 0.05 M Na_2SO_4 and 0.1 M NaCl at pH 7. TOC removals in the presence of 0.1 M NaCl are slightly higher than those in the presence of 0.05 M Na_2SO_4 with Ti/SnO_2-Sb(conventional) and TiO_2-NTs/SnO_2-Sb. However, a decrease of TOC

removal efficiency is observed with TiO_2-NTs/SnO_2-Sb-PTFE(4.5). The active chlorine will be generated in the presence of Cl^- through the following reactions (Cheng and Kelsall 2007):

$$2Cl^- \rightarrow Cl_2 + e^- \quad (3.7)$$

$$Cl_2 + H_2O \rightarrow HClO + H^+ + Cl^- \quad (3.8)$$

$$HClO \rightarrow ClO^- + H^+ \quad (3.9)$$

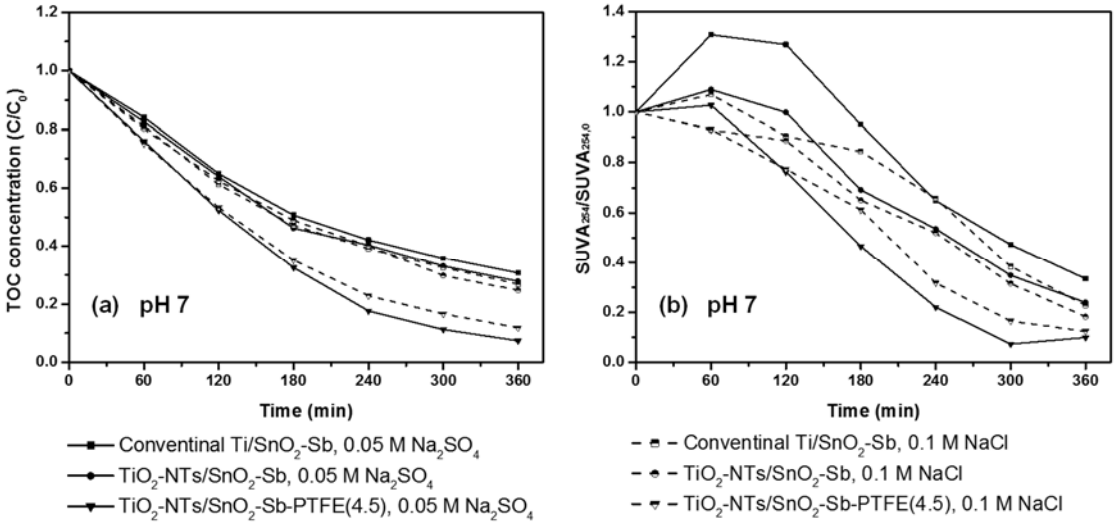

Fig. 3.11 (a) TOC concentration and (b) $SUVA_{254}$ as a function of time during phenol degradation at pH 7

Fig. 3.12 shows the schematic illustration of electrochemical oxidation of phenol using TiO_2-NTs/SnO_2-Sb-PTFE(4.5) and conventional Ti/SnO_2-Sb as anodes in 0.05 M Na_2SO_4 and 0.1 M NaCl. In 0.1 M NaCl, the presence of active chlorine is pH dependent and the main active chlorine species for phenol oxidation are Cl_2 ($pH \leq 3$), HClO ($3 < pH < 8$) and ClO^- ($pH \geq 8$) (Cheng and Kelsall 2007). Although the oxidative power of Cl_2 (1.36 V), HClO (1.63 V) and ClO^- (0.90 V) are lower than that of $HO^\bullet$ (2.59 V), their massive production and longer lifetime over $HO^\bullet$ make them degrade phenol more effectively. However, for TiO_2-NTs/SnO_2-Sb-PTFE(4.5) which has superior generation of free $HO^\bullet$ due to its hydrophobic surface, the TOC removal is inhibited by the following competing reactions (Grebel et al. 2010):

$$Cl^- + HO^\bullet \rightarrow Cl^\bullet + OH^- \quad (3.10)$$

$$Cl_2 + HO^{\bullet} \rightarrow HClO + Cl^{-} \quad (3.11)$$

The Cl^{-} and Cl_2 played the role of $HO^{\bullet}$ scavengers so that TOC removal by free $HO^{\bullet}$ is not favorable. Therefore, the TOC removal efficiency decreases in 0.1 M NaCl. All of the 3 electrodes obtain faster $SUVA_{254}$ decrease in the presence of NaCl in the first 2 h (Fig. 3.11). This is because active chlorine tends to react with electron rich moieties such as of aromatic intermediates (Scialdone et al. 2009b), hence, the aromatic rings open more easily. However, after 2 h the decrease of $SUVA_{254}$ of phenol with TiO_2-NTs/SnO_2-Sb-PTFE(4.5) is slower in 0.1 M NaCl than that in 0.05 M Na_2SO_4, indicating the inhibition of phenol degradation by less amount of $HO^{\bullet}$.

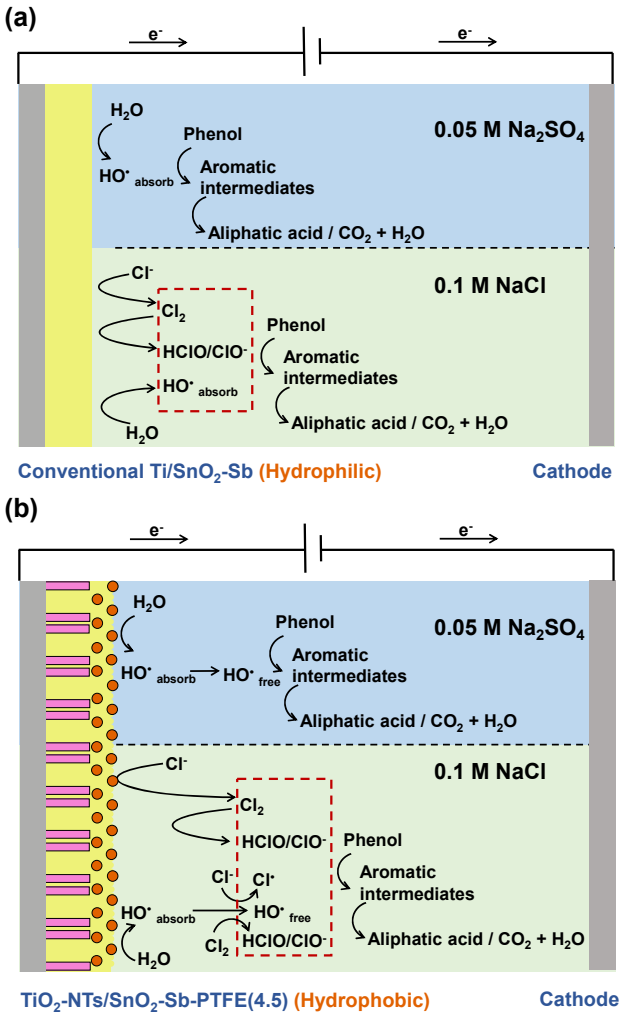

Fig. 3.12 Schematic illustration of electrochemical oxidation of phenol in 0.05 M Na_2SO_4 and 0.1 M NaCl using (a) conventional Ti/SnO_2-Sb and (b) TiO_2-NTs/SnO_2-Sb-PTFE(4.5).

3.3.3 Leaching of Sn ions

In industrial application using SnO_2 electrodes for removing organic compounds, the leaching of Sn ions has become an issue of concern which may cause the secondary pollution. Fig. 3.13a shows the concentration of Sn ions released from the electrodes after 6 h electrochemical oxidation at different initial solution pH in 0.05 M Na_2SO_4. Sn concentrations detected at Ti/SnO_2-Sb(conventional) were larger than those of TiO_2-NTs/SnO_2-Sb and TiO_2-NTs/SnO_2-Sb-PTFE electrodes at all solution pH. At pH 3, Sn dissolved concentration was 1.1×10^{-4} M using the conventional Ti/SnO_2-Sb as anode, while those released from TiO_2-NTs/SnO_2-Sb-PTFE electrodes were 7.1×10^{-5} M to 8.0×10^{-5} M. With the increase of initial solution pH from 3 to 7, Sn leaching further decreased but not significantly. However, at initial solution pH 11, only trace amount of Sn ions was detected with the lowest value of 3.6×10^{-6} M at TiO_2-NTs/SnO_2-Sb-PTFE(13.5). The concentration of the leached Sn ions was greatly influenced by the final solution pH. During OER at anodes, the simultaneously generation of H^+ gives rise to a dramatic decrease of solution pH. The high OEP of TiO_2-NTs/SnO_2-Sb-PTFE electrodes could inhibit the OER, thus less H^+ is generated and Sn leaching is not favorable. Final solution pH was low at initial solution pH 3 and 7. However, the final solution pH was near neutral at initial solution pH 11, where the dissolution of Sn ions is inhibited. On the other hand, PTFE could also present a barrier for SnO_2 and electrolytes to contact, which inhibits the anodic dissolution of SnO_2.

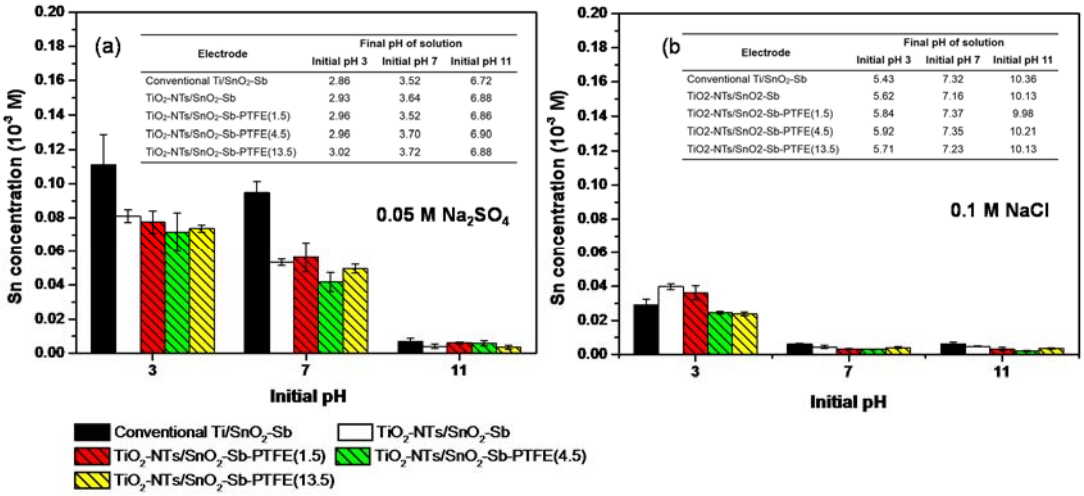

Fig. 3.13 Leached Sn ions concentration (± S.D) after 6 h electrochemical oxidation in (a) 0.05 M Na_2SO_4 and (b) 0.1 M NaCl (insets are the final pH of solutions after 6 h electrochemical oxidation).

The Sn ions leaching can be further inhibited using 0.1 M NaCl as supporting electrolyte (Fig. 3.12b). Cl_2 can be generated at anode surface without H^+ generation, but the solution H^+ is consumed at the cathode to form H_2. Thus, there is an increase of solution pH after 6 h of electrochemical oxidation. Therefore, Sn ions are not likely to be leached out. Lowest Sn ions concentration was detected to be only 2×10^{-6} M at basic solution with initial pH 11 using TiO_2-NTs/SnO_2-Sb-PTFE(4.5). In general, the TiO_2-NTs/SnO_2-Sb-PTFE can effectively inhibit the leaching of Sn ions through the presence of PTFE layer.

3.4 Conclusions

TiO_2-NTs/SnO_2-Sb-PTFE composite electrode with highly hydrophobic surface, high oxygen evolution potential (2.4 V vs Ag/AgCl (3 M NaCl)), small electrochemical resistance and good stability was successfully prepared by pulse electrodeposition method. The TiO_2-NTs/SnO_2-Sb-PTFE exhibited remarkably better electrocatalytic performance for phenol degradation than the conventional Ti/SnO_2-Sb prepared by thermochemical decomposition and TiO_2-NTs/SnO_2-Sb without PTFE. The TOC removal and $SUVA_{254}$ degradation of phenol confirmed 4.5 mL L^{-1}

to be the optimal PTFE loading for TiO_2-NTs/SnO_2-Sb-PTFE electrodes. The pH and types of supporting electrolytes (Na_2SO_4 and NaCl) had more significant influence on phenol oxidation efficiency with TiO_2-NTs/SnO_2-Sb-PTFE(4.5) electrode, which had the superior ability of $HO^{\bullet}$ generation because of its hydrophobic surface. The TiO_2-NTs/SnO_2-Sb-PTFE also showed leaching-resistant for the leaching of Sn ion, making it have the environmental merit for the degradation of recalcitrant organic pollutants in aquatic systems.

CHAPTER 4 HIGH PERFORMANCE DUPLEX-STRUCTURED SnO_2 ANODE MODIFIED BY SnO_2-Sb-CNT COMPOSITE FOR BISPHENOL A REMOVAL: ELECTROCHEMICAL OXIDATION ENHANCED BY ADSORPTION

4.1 Introduction

Chapter 3 describes a hydrophobic TiO_2-NTs/SnO_2-Sb-PTFE anode which can effectively removal aqueous phenol by electrochemical oxidation due to the effective release of free $HO^{\bullet}$ from anode surface into solution. Among the phenolic compounds, bisphenol A (BPA) serves as an important chemical in polymer industry and has been widely used as a monomer for the production of epoxy resins and polycarbonate resins. However, it is also known as an endocrine disrupter which has been found in natural environment and treated effluents due to its extensive usage (Oehlmann et al. 2009). The exposure of BPA may affect the human health by its estrogenic activity even in very low concentration levels (Erler and Novak 2010, Joseph et al. 2011), therefore it has to be properly dealt with.

Recently, carbon nanotubes (CNTs) modified SnO_2-Sb catalysts have attracted much research interests. The unique properties of CNTs including high specific surface area, high chemical stability and good electrical properties have made it a promising support for metal catalyst. Several works reported the synthesis of SnO_2-Sb-CNT composites for various applications including electrocatalytic oxidation (Li et al. 2012a, Li et al. 2015a, Wang et al. 2013a), supercapacitor (Vinoth et al. 2016), lithium ion battery (Li et al. 2015b, Xu et al. 2015b), gas sensor (Liu et al. 2015,

Mendoza et al. 2014) and electrochemical filter (Gao and Vecitis 2011). Moreover, a few works have reported the CNT-modified SnO_2-Sb electrodes for electrocatalytic purposes (Hu et al. 2010, Hu et al. 2011, Zhang et al. 2014). Zhang et al. fabricated a Ti/SnO_2-Sb-CNT electrode which had improved OEP, prolonged service life and enhanced electrocatalytic efficiency compared to Ti/SnO_2-Sb (Zhang et al. 2014). Comparing to CNT-modified SnO_2-Sb electrode, a modification of SnO_2-Sb electrode by SnO_2-Sb-CNT composite may have the advantage of stronger bonding between CNT and SnO_2-Sb as well as a larger surface loading by the SnO_2-Sb of the composite. However, the modification of SnO_2 electrode by SnO_2-Sb-CNT composite has not been reported. Furthermore, CNTs has been verified to be effective adsorbent for various organic pollutants (Lin and Xing 2008, Ren et al. 2011), having the potential to improve the electrocatalytic performance for organic pollutants removal by synergistic adsorption and electrochemical oxidation.

This chapter presents the development of SnO_2-Sb electrodes modified by a layer of SnO_2-Sb-CNT composites coating using pulse electrodeposition technique to obtain duplex structure. SnO_2-Sb-CNT composites were incorporated into the electrode surface through SnO_2 growth between SnO_2-Sb-CNT composites and electrode substrate, which could be verified by the improved surface loading of modified electrodes. The electrodes are denoted as Ti/SnO_2-Sb/SnO_2-Sb and Ti/SnO_2-Sb/SnO_2-Sb-CNT(n) (n = 0.2, 0.4, 0.8) by controlling the CNTs loading of the SnO_2-Sb-CNT composites. The surface morphology, crystalline structure and electrochemical properties of the duplex-structured Ti/SnO_2-Sb/SnO_2-Sb-CNT electrodes were investigated. The electrocatalytic performance of the modified electrodes were evaluated through 1-h adsorption followed by subsequent 6-h electrochemical oxidation of synthetic BPA wastewater. The capabilities of hydroxyl radical ($HO^{\bullet}$) generation capabilities of the anodes were evaluated to give an insight into their improved performance efficiency. The influences of water matrix species

containing humic acid (HA) and alginate on BPA degradation were also investigated. Finally, we proposed a mechanism to depict the enhancement of BPA oxidation by the modified electrodes coupling the electrochemical oxidation and adsorption processes.

4.2 Experimental

4.2.1 Chemicals and materials

All chemicals in the experiments were of analytical grade and used without further purification. Sigma-Aldrich's bisphenol-A, humic acid and sodium alginate were used. Multiwall carbon nanotubes (CNTs) were purchased from Nanotech Port Co. (Shenzhen, China). Pure acetonitrile (LC grade) were obtained from Merck. The other chemicals and materials used are the same as described in Section 3.2.1. All the solutions used in the experiments were prepared with Milli-Q water (18.2 MΩ cm).

4.2.2 Synthesis of SnO_2-Sb-CNT composites

The SnO_2-Sb-CNT composites were fabricated by co-precipitation method followed by calcination. Prior to the experiments, raw CNTs were pretreated to remove impurities and introduce oxygen-containing functional groups onto the surface of the CNTs following the steps described in literature (He et al. 2015). In a typical synthesis procedure, 0.05 M $SnCl_2.2H_2O$, 0.0025 M $SbCl_3$ and CNTs (0, 0.2, 0.4 and 0.8 g L^{-1}) were dissolved in HCl solution of pH 1. Then the solutions were mixed under ultrasonic assistance for 10 min followed by magnetic stirring for 6 h, in order to get homogenous dispersion of CNTs in the solutions. After that, 0.25 M NaOH solution was added dropwise into the solutions under magnetic stirring until its pH approached 7. Precipitation containing a mixture of metal hydroxides coated on CNTs was formed after these steps. Then the precipitation was separated from solution by centrifuge and then rinsed with Milli-Q water. This procedure was

repeated for 3 times to remove the Cl^- ions in the solution, before it was dried in the air at 60 ^oC for 6 h and annealed at 300 ^oC for 1 h. Finally, the composites were continuously grinded by ball milling technique using Al_2O_3 balls to obtain smaller particles with uniform size before their further use. The as-prepared composites were abbreviated as SnO_2-Sb (without CNTs addition) and SnO_2-Sb-CNT(n) (n = 0.2, 0.4 and 0.8) respectively according to the amount of CNTs added into the precursor solutions.

4.2.3 Fabrication of Ti/SnO_2-Sb/SnO_2-Sb-CNT electrodes

Pure titanium plates (60 mm x 20 mm) were pretreated to remove the impurities on the surface by the same method described in Section 3.2.2. After that, the clean titanium plates were conserved in pure isopropanol before use.

Fig. 4.1 shows the schematic diagram for preparation of SnO_2-Sb-CNT composites and duplex-structured Ti/SnO_2-Sb/SnO_2-Sb-CNT electrodes. In general, there are two steps involved in the fabrication of duplex-structured Ti/SnO_2-Sb/SnO_2-Sb-CNT electrode. First, a SnO_2-Sb interlayer was introduced on the titanium substrate by thermochemical decomposition. Afterwards, the outer layer was prepared by pulse electrodeposition in a two-electrode (1-cm distance) electrodeposition bath containing 0.1 M $SnCl_2.2H_2O$, 0.02 M $SbCl_3$, 0.1 M hydrochloric acid, 0.05 wt% (3-aminopropyl)trimethoxysilane and 2 g L^{-2} as-prepared SnO_2-Sb or SnO_2-Sb-CNT composites in well-mixed suspension. A pulse current with an anodic pulse (5 mA cm^{-2}, 50 ms), a cathodic pulse (5 mA cm^{-2}, 5 ms) and a relaxation time (0 mA cm^{-2}, 1s) was applied at 40^oC for 2 h. The pulse electrodeposition experiments were carried out under continuous magnetic stirring at 800 rpm. Finally, the electrodes were annealed in the muffle furnace at 400 ^oC for 1 h at both a heating and a cooling rate of 1 ^oC min^{-1}. The surface loading amount (in g m^{-2}) of the electrode was calculated by measuring the weight difference of pristine Ti substrates and as-prepared

electrodes. The nominal area of the electrode surface is 8 cm^2. For comparison, Ti/SnO_2-Sb electrode of the same nominal surface area was prepared by thermochemical decomposition technique according to the literature (Montilla et al. 2004).

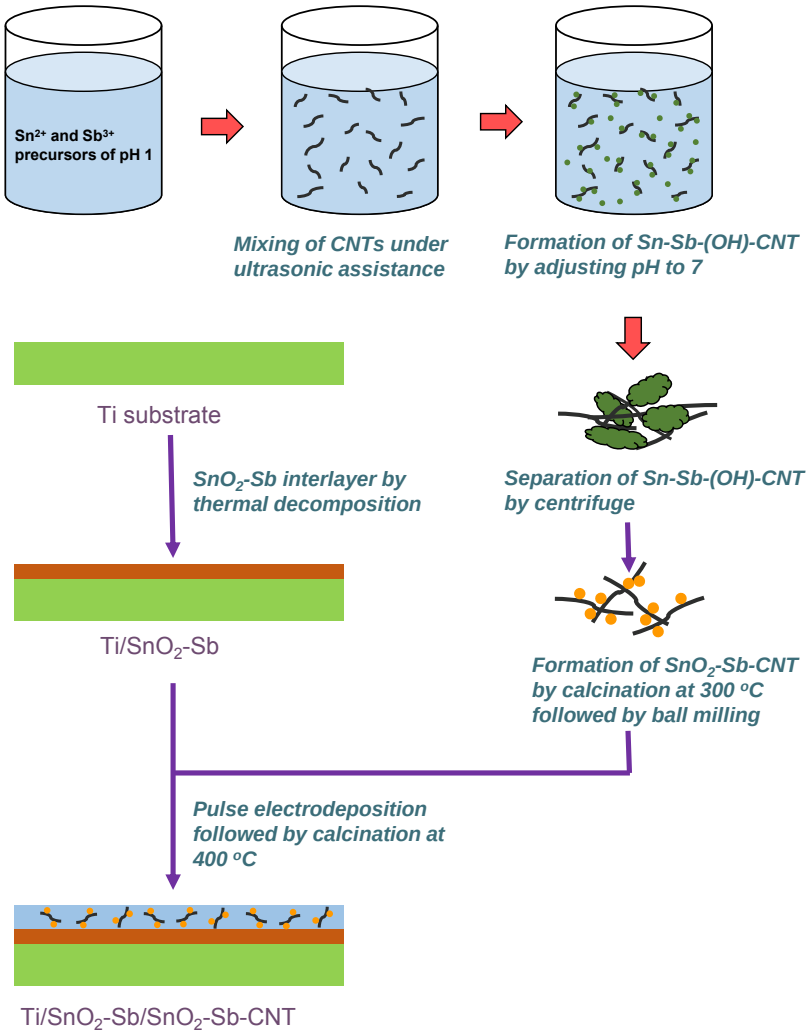

Fig. 4.1 Schematic illustration of Sn-Sb-O-CNT composite and Ti/SnO_2-Sb/SnO_2-Sb-CNT electrode preparation.

4.2.4 Performance evaluation

The performance of the as-prepared electrodes was studied by bulk electrolysis of BPA. Synthetic wastewater containing 100 mg L^{-1} BPA and 0.05 M Na_2SO_4 was added into a 200 mL single-compartment cell under continuous stirring. The as-

prepared electrodes were used as anodes, with a titanium plate of the same nominal area serving as cathode. There was 1-cm space between the anode and cathode. Prior to the 6-h bulk electrolysis experiments, the anodes were immersed into the synthetic wastewater under 1-h magnetic stirring to reach adsorption equilibrium. Influencing parameters were investigated by varying the initial solution pH (3, 7 and 11) and applied current density (10, 20 and 40 mA cm^{-2}). Solution pH was adjusted by adding 0.5 M H_2SO_4 and 1 M NaOH dropwise. The aliquot solutions were drawn for analysis at 1-h time interval. The accelerated life tests were carried out by anodic polarization of the electrodes in 0.1 M H_2SO_4 at a current density of 100 mA cm^{-2} at room temperature, and the value of service lifetime was defined as the time duration when the cell potential increased 5 V from the initial value (Montilla et al. 2004).

BPA concentrations were determined by HPLC equipped with a UV-Vis spectrophotometer at 220 nm wavelength and a C18 column (Hypersil Gold). The mobile phase used was acetonitrile/water (40/60, v/v) at a flow rate of 1 ml L^{-1}. TOC determination employed the same equipment described in Section 3.2.4. $HO^{\bullet}$ was also quantitatively determined by high-performance liquid chromatography with DMSO as trapping reagent according to literature (Tai et al. 2004). The mineralization current efficiency (MCE) was also calculated to evaluate the process efficiency according to the equations described in Section 3.2.4, while n_C and n_e are 15 and 72 respectively for BPA oxidation.

4.2.5 Analytical techniques

FESEM, EDS, XRD was employed to characterize the surface morphologies and elemental composition of SnO_2-Sb-CNT composites and duplex-structured Ti/SnO_2-Sb/SnO_2-Sb-CNT electrodes using the same equipment described in Section 3.2.5. The SnO_2-Sb-CNT composites were further characterized by transmission electron microscopy (TEM, JEOL JEM-2010). X-ray photoelectron spectroscopy (XPS, Axis

Supra) was employed to analyze the chemical states of the elements of the electrodes. Brunauer-Emmet-Teller (BET) analysis (Quantachrome Autosorb) were conducted to analyze the specific surface area ($S_{B\text{-}E\text{-}T}$) of the composites through N_2 adsorpsion/desorption method. Electrochemical properties of the electrodes were investigated using a potentiostat (PGSTAT 302N, Autolab) equipped with a three-electrode cell with Pt serving as the counter electrode and Ag/AgCl (3 M NaCl) serving as the reference electrode. Linear sweep voltammetry (LSV) was conducted to determine the oxygen evolution potential with the scan range of 0.3 V– 3.0 V and a scan rate of 50 mV s^{-1} in 0.5 M Na_2SO_4. CV was employed to evaluate the voltammetric charges of the electrodes in 0.5 M H_2SO_4 with potential range of 0.3V – 0.8 V and scan rates of 10 mV s^{-1} – 100 mV s^{-1} (Chen et al. 2010). EIS was conducted in 5 mM $K_3[Fe(CN)_6]/K_4[Fe(CN)_6]$ at a background voltage of 0 V with frequency ranges from 100 kHz to 10 mHz and amplitude of 10 mV.

4.3 Results and discussions

4.3.1 Characteristics of composites and electrodes

4.3.1.1 Physical characterization

Fig. 4.2 compares the TEM images of SnO_2-Sb-CNT composites. Both SnO_2-Sb particles and CNTs are well identified through TEM. The SnO_2-Sb is formed as spherical particles with an average diameter of 4 – 5 nm with all of the composites. CNTs can be easily distinguished from SnO_2-Sb particles according to their shape and lighter color. However, the distribution of SnO_2-Sb particles on CNTs surfaces seems to be greatly influenced by the CNTs loading amount during co-precipitation. The SnO_2-Sb particles tend to form agglomeration in SnO_2-Sb-CNT(0.2) and SnO_2-Sb-CNT(0.4), and only a small part of SnO_2-Sb particles are located on CNTs outer walls (Fig 4.2a and 4.2b). Nevertheless, more uniform attachment of SnO_2-Sb particles was found in SnO_2-Sb-CNT(0.8) (Fig. 4.2c). Distinct lattice arrays of SnO_2

are observed at a higher resolution with a lattice distance of 0.33 nm (Fig. 4.2d), corresponding to the SnO_2(110) facet.

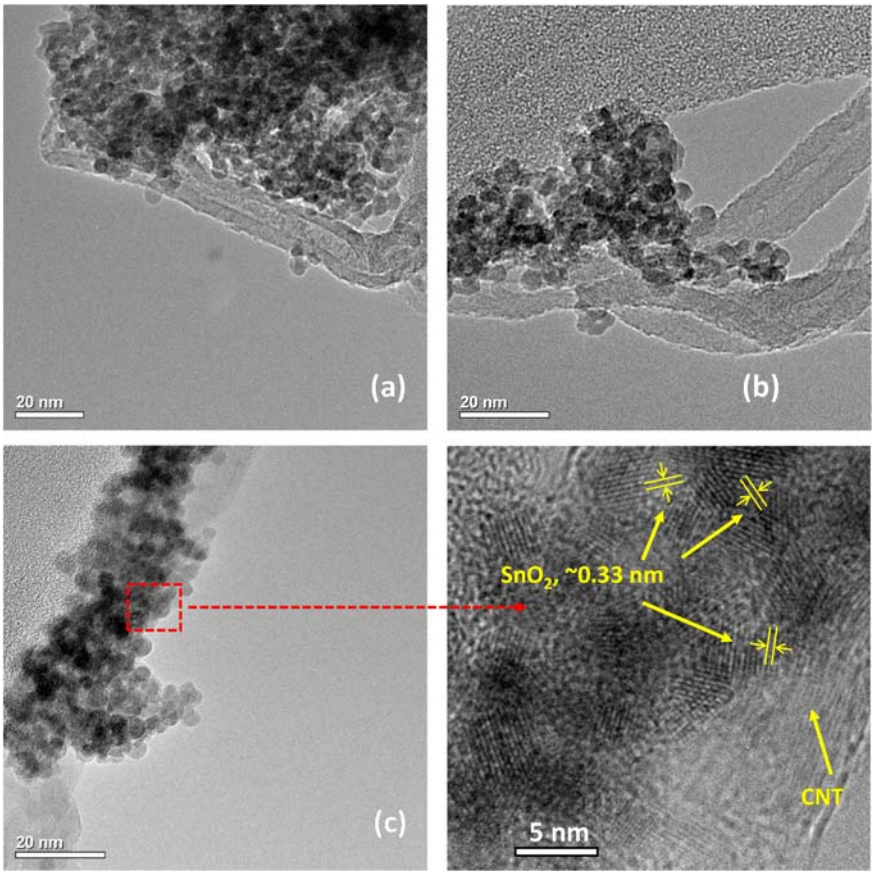

Fig. 4.2 TEM images of (a) SnO_2-Sb-CNT(0.2), (b) SnO_2-Sb-CNT(0.4) and (c) SnO_2-Sb-CNT(0.8) composites.

Fig. 4.3a-c shows the FESEM images of SnO_2-Sb-CNT composites. SnO_2 agglomeration was observed in SnO_2-Sb-CNT(0.2) and SnO_2-Sb-CNT(0.4), which is in accordance with the TEM observations. The higher CNTs loading amount in SnO_2-Sb-CNT(0.8) could provide more sites for SnO_2-Sb to attach, resulting in stronger bonding and more uniform SnO_2-Sb distribution on CNTs walls. BET analysis gives a further insight into the physical properties of the composites. The specific surface areas of the SnO_2-Sb-CNT composites were characterized to range from 101.6 to 132.6 $m^2\ g^{-1}$, which prominently larger than that of SnO_2-Sb (89.8 $m^2\ g^{-1}$) (Table 4.1). The improved specific surface area of SnO_2-Sb-CNT is attributed to the

incorporation of CNTs, which has a high specific surface area of 180.8 m^2 g^{-1}.

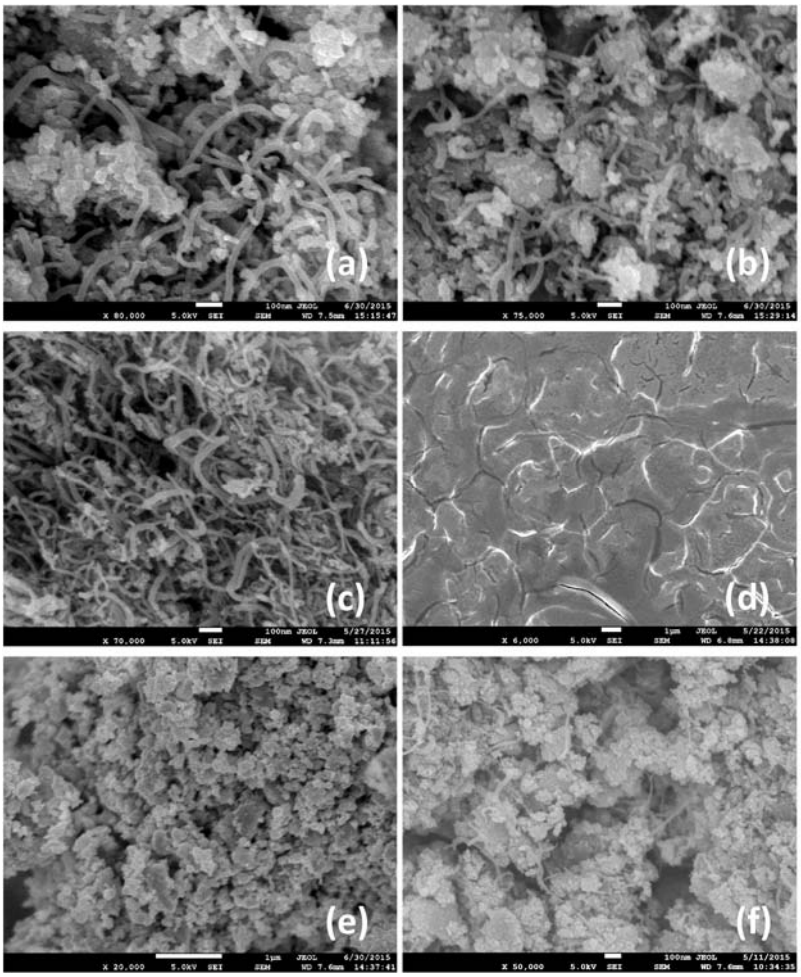

Fig. 4.3 FESEM images of (a) SnO_2-Sb-CNT(0.2), (b) SnO_2-Sb-CNT(0.4), (c) SnO_2-Sb-CNT(0.8), (d) Ti/SnO_2-Sb, (e) Ti/SnO_2-Sb/SnO_2-Sb and (f) Ti/SnO_2-Sb/SnO_2-Sb-CNT(0.8) electrodes.

It can be seen that the surface of Ti/SnO_2-Sb fabricated by thermochemical decomposition shows “mud-cracked” structure (Fig. 4.3d). Such cracks may have a negative effect on the adhesion between substrate and electrode surface caused by the permeation of electrolyte into the Ti substrate. Improvement of surface morphology is observed with the modified electrodes. Both Ti/SnO_2-Sb/SnO_2-Sb and Ti/SnO_2-Sb/SnO_2-Sb-CNT show a rough surface with microspherical SnO_2-Sb particles (Fig. 3e and Fig. 3f), which could increase the specific surface area of the modified electrodes and provide more active sites for electrocatalytic reactions. The presence

of CNTs indicates that SnO_2-Sb-CNT composite has been successfully incorporated in the surface of modified electrode.

Table 4.1 Specific surface areas and BPA adsorption capacities of CNTs, SnO_2-Sb and SnO_2-Sb-CNTs composites

Composite	$S_{B\text{-}E\text{-}T}$ (m^2 g^{-1})	Adsorption capacity (mg g^{-1})
CNTs	180.8	62.3 ± 2.2
SnO_2-Sb	89.8	19.2 ± 0.7
SnO_2-Sb-CNT(0.2)	101.6	25.7 ± 1.9
SnO_2-Sb-CNT(0.4)	110.5	43.7 ± 2.2
SnO_2-Sb-CNT(0.8)	132.6	53.6 ± 1.8

EDS was employed to determine the elemental composition of the electrode surfaces. Elements of Ti, Sn, Sb, O and C were detected on duplex-structured Ti/SnO_2-Sb/SnO_2-Sb-CNT, and their corresponding atomic percentages are listed in Table 4.2. Negligible Ti component was detected on the electrode surfaces, which is possibly due to their non-crack surface morphologies. The SnO_2-Sb-CNT composites have been successfully incorporated in the electrode surfaces with atomic percentage of C ranging from 2.08% to 14.82%. However, it is interesting that the atomic percentage of C of the duplex-structured Ti/SnO_2-Sb/SnO_2-Sb-CNT electrodes does not increase in proportion to the CNTs loading of SnO_2-Sb-CNT composites. It could be probably related to the amount of surface loading of the electrodes. As can be seen in Table 4.3, Ti/SnO_2-Sb/SnO_2-Sb-CNT(0.8) has a larger surface loading (64.3 g m^{-2}) than that of Ti/SnO_2-Sb/SnO_2-Sb-CNT(0.4) (52.6 g m^{-2}), so that atomic percentage of C increased by a factor greater than 2. The Sb/Sn ratio was calculated and listed in Table 4.2. Sb/Sn is 3.07% at Ti/SnO_2-Sb, while at Ti/SnO_2-Sb/SnO_2-Sb and Ti/SnO_2-Sb/SnO_2-Sb-CNT the values are in the range of 4.37 – 5.37%, which are close to the theoretical value of Sb/Sn ratio (5%) of SnO_2-Sb and SnO_2-Sb-CNT composites.

Table 4.2 Elemental compositions of the electrode surfaces

Electrode	Elemental composition (atomic %)					
	Ti	Sn	Sb	C	O	Sb/Sn
Ti/SnO_2-Sb	1.18	32.30	0.99	-	65.62	0.0307
Ti/SnO_2-Sb/SnO_2-Sb	0.14	33.40	1.46	-	64.99	0.0437
Ti/SnO_2-Sb/SnO_2-Sb-CNT(0.2)	-	32.66	1.55	2.08	64.01	0.0475
Ti/SnO_2-Sb/SnO_2-Sb-CNT(0.4)	-	31.05	1.59	5.94	61.84	0.0512
Ti/SnO_2-Sb/SnO_2-Sb-CNT(0.8)	-	29.38	1.58	14.82	54.49	0.0537

Table 4.3 Parameters of the electrodes

Electrode	OEP (V vs. Ag/AgCl)	Service lifetime (h)	Surface loading (g m^2)
Ti/SnO_2-Sb	2.0	6.4	18.9 ± 3.2
Ti/SnO_2-Sb/SnO_2-Sb	2.0	42	38.1 ± 3.2
Ti/SnO_2-Sb/SnO_2-Sb-CNT(0.2)	2.1	60	44.0 ± 2.6
Ti/SnO_2-Sb/SnO_2-Sb-CNT(0.4)	2.2	63	52.6 ± 3.3
Ti/SnO_2-Sb/SnO_2-Sb-CNT(0.8)	2.2	86	64.3 ± 4.6

4.3.1.2 Physicochemical characterization

Fig. 4.4 compares the XRD patterns of Ti/SnO_2-Sb, Ti/SnO_2-Sb/SnO_2-Sb and Ti/SnO_2-Sb/SnO_2-Sb-CNT electrodes. Polycrystalline SnO_2 is observed in all of the electrodes with diffraction peaks at 2θ = 26.8, 34.1°, 38.2°, 52.1°, 55.1°, 65.0° and 66.2°. The sharp peak at 71° and several small peaks are indexed to Ti and TiO_2 in Ti/SnO_2-Sb. However, no such peaks are shown in Ti/SnO_2-Sb/SnO_2-Sb and Ti/SnO_2-Sb/SnO_2-Sb-CNT, which confirmed that the electrode surfaces are covered with SnO_2 layer without cracks. This is in accordance with the EDS observation. Duplex-structured Ti/SnO_2-Sb/SnO_2-Sb-CNT has a stronger peak at 2θ = 26.8 than other electrodes, demonstrating a preferred orientation of SnO_2 along (110) direction.

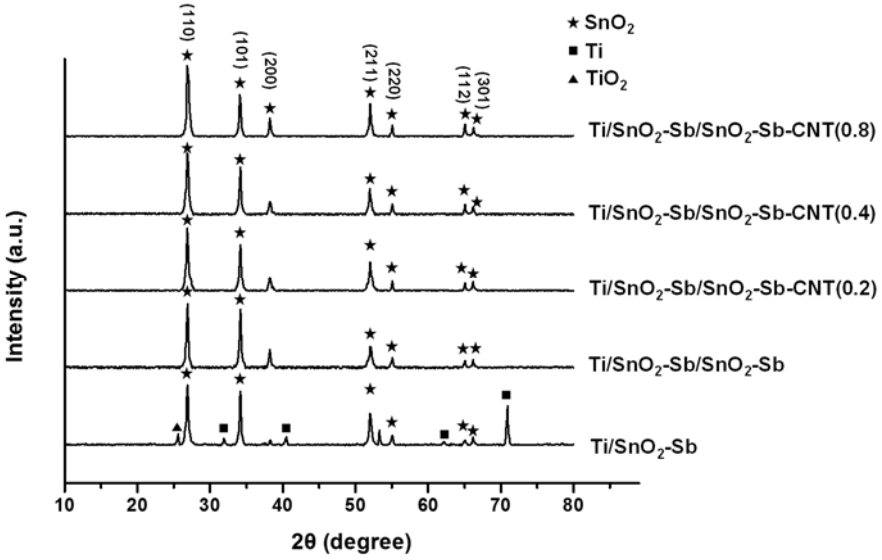

Fig. 4.4 XRD patterns of the electrodes.

The existence of Sn^{4+}, Sb^{5+} and C on Ti/SnO_2-Sb/SnO_2-Sb-CNT surface is confirmed by XPS (Fig. 4.5). Fig. 4.5a shows the XPS spectra of Ti/SnO_2-Sb/SnO_2-Sb-CNT(0.8) with distinguished peaks. It should be noted that the XPS spectra of O 1s and Sb $3d_{5/2}$ are overlapped due to their similar binding energy. More detailed information could be obtained by fitting the overlapped spectra in to three peaks, including Sb $3d_{5/2}$ spectra and two O 1s spectra (Fig. 4.5b – d). Table 4.4 summarizes the binding energy of C 1s, Sn $3d_{5/2}$, Sb $3d_{5/2}$ and deconvoluted values of O 1s and Sb $3d_{5/2}$ peaks. No shift of Sn $3d_{5/2}$ binding energy is observed, indicating that the electronic structure of SnO_2 is not influenced by Sb dopant (Yang et al. 2012). The fitted O 1s spectra with lower binding energy (530.85 – 530.95 eV) is indexed to the oxygen that is incorporated to the SnO_2 lattice, namely lattice oxygen (O_{lat}). On the contrary, the fitted O 1s spectra with higher binding energy (532.02 – 532.34 eV) is assigned to the absorbed oxygen species (O_{ab}) such as hydroxide or organic oxygen. The percentage of O_{lat} and O_{ab} was calculated by their peak areas of XPS spectra. As shown in Table 4.4, Ti/SnO_2-Sb has a highest O_{lat}% of 75.22%, however, it is decreased by incorporation of SnO_2-Sb-CNT composites (69.95% for Ti/SnO_2-

Sb/SnO_2-Sb-CNT(0.2) and 66.11% for Ti/SnO_2-Sb/SnO_2-Sb-CNT(0.4)). A discrepancy of O_{lat}% is observed in Ti/SnO_2-Sb/SnO_2-Sb-CNT(0.8), which has a O_{lat}% of 74.37%. The chemical states of oxygen could influence the hydroxyl radical ($HO^{\bullet}$) generation on the electrode surface, thus the electrochemical performance of SnO_2-based electrodes. The O_{lat} originated from SnO_2 lattice is likely to increase the activity of absorbed $HO^{\bullet}$ (Feng et al. 2008). On the other hand, O_{ab} has higher activity than O_{lat} and participates in the redox reactions of electrode-electrolyte surface, so that it plays an important role for the generation of reactive oxygen species such as $HO^{\bullet}$ (Xu et al. 2012, Yang et al. 2012). Since O_{lat} and O_{ab} could have a positive effect on the electrocatalytic activity of duplex-structured Ti/SnO_2-Sb/SnO_2-Sb-CNT in different aspects, other characterization techniques should be employed to evaluate the electrocatalytic activity of the modified electrodes.

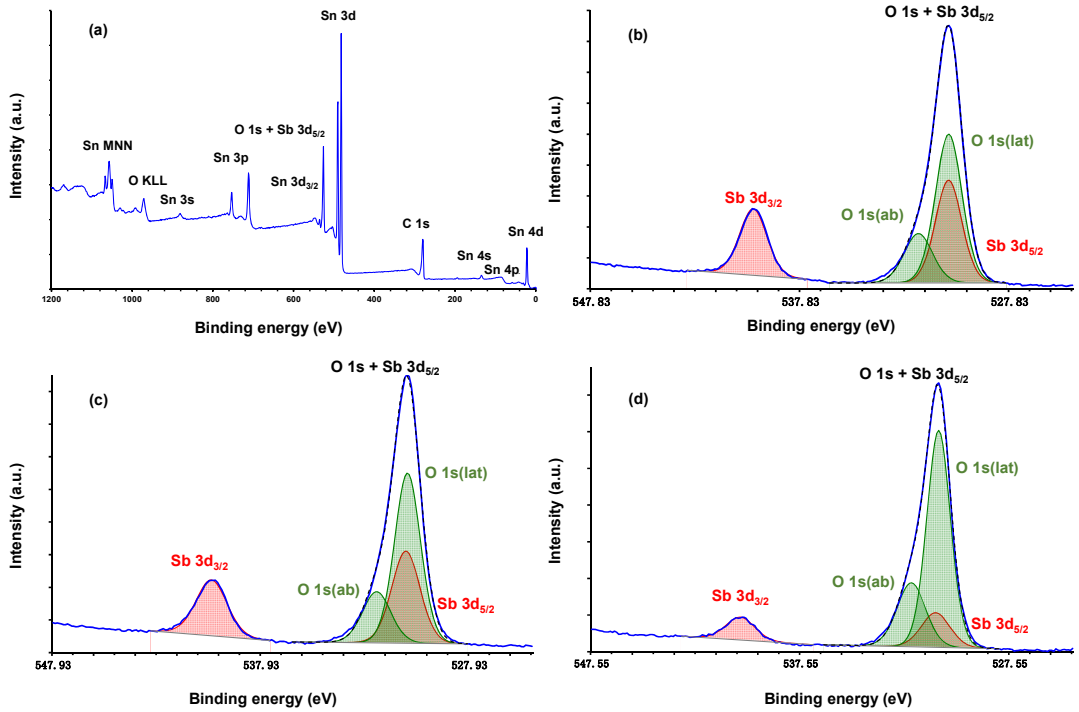

Fig. 4.5 Survey XPS spectra of (a) Ti/SnO_2-Sb/SnO_2-Sb(0.8); O 1s and Sb 3d region of (b) Ti/SnO_2-Sb, (c) Ti/SnO_2-Sb/SnO_2-Sb and (d) Ti/SnO_2-Sb/SnO_2-Sb-CNT(0.8).

Table 4.4 XPS analysis on the surfaces of the electrodes

Electrode	Binding energy (eV)					O_{lat}%	O_{ab}%
	C 1s	Sn $3d_{5/2}$	Sb $3d_{5/2}$	O 1s(ad)	O 1s(lat)		
Ti/SnO_2-Sb	285.06	486.97	530.85	532.34	530.85	75.22	24.78
Ti/SnO_2-Sb/SnO_2-Sb	285.01	487.07	531.09	532.26	530.95	73.72	26.28
Ti/SnO_2-Sb/SnO_2-Sb-CNT(0.2)	285.00	486.93	530.99	532.26	530.95	69.95	30.05
Ti/SnO_2-Sb/SnO_2-Sb-CNT(0.4)	284.02	486.97	531.05	532.28	530.85	66.11	33.88
Ti/SnO_2-Sb/SnO_2-Sb-CNT(0.8)	284.07	486.99	530.88	532.02	530.87	74.37	25.63

4.3.2 Electrochemical characterization

4.3.2.1 Linear sweep voltammetry

The LSV experiments were carried out to examine the oxygen evolution potential (OEP) of the electrodes (Fig. 4.6), and the corresponding values are given in Table 4.3. Both Ti/SnO_2-Sb and duplex-structured Ti/SnO_2-Sb/SnO_2-Sb have a similar OEP of 2.0 V, but a difference in the slopes of LSV curves is observed. However, enhancement of OEP was obtained in Ti/SnO_2-Sb/SnO_2-Sb-CNT (2.1 V – 2.2 V) after incorporation of CNTs. Higher OEP indicates that the oxygen evolution reaction is inhibited, which is a competing reaction for organics oxidation. It suggests that he interaction of $HO^{\bullet}$ and Ti/SnO_2-Sb/SnO_2-Sb-CNT electrode surface is weak, contributing to the high reactivity of $HO^{\bullet}$ for oxidation of organic compounds (Kapalka et al. 2008). Therefore, duplex-structured Ti/SnO_2-Sb/SnO_2-Sb-CNT electrodes are expected to exhibit better electrocatalytic performance than those without CNTs incorporation.

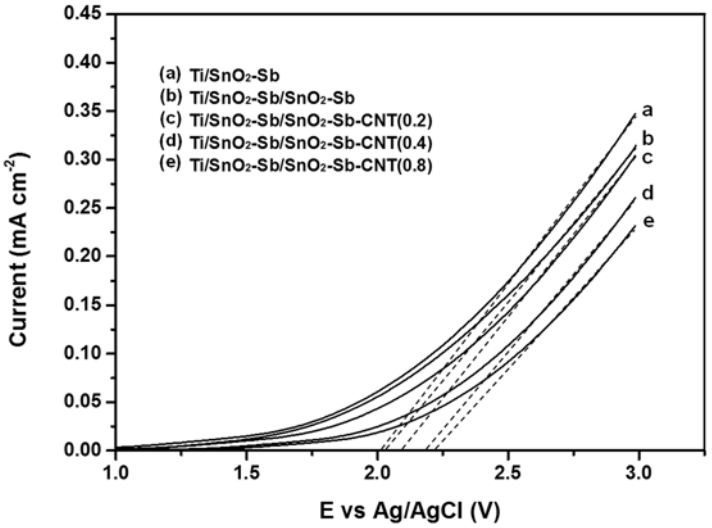

Fig. 4.6 Linear sweep voltammetric curves of the electrodes in 0.5 M Na_2SO_4 at a scan rate of 50 mV s^{-1}.

4.3.2.2 Voltammetric charge analysis

The voltammetric charge (q^*) analysis was conducted to evaluate the electroactive surface of the electrodes. Electroactive surface area is related to the number of active sites for charge transfer when the electrochemical reaction occurs. Therefore, electroactive surface area could reflect the electrocatalytic activity of electrodes for organic oxidation. A larger q^* indicates a larger electroactive surface area and thus higher electrocatalytic activity. The electrochemical activity of the electrodes was evaluated by the following equation (Ardizzone et al. 1990):

$$(q^*)^{-1} = (q_T^*)^{-1} + k_1 v^{1/2} \quad (4.1)$$

where q_T^* is the total voltammetric charge, k_1 is the slope of linear fitting and v is the scan rate. Fig. 4.7 shows the relationship of $(q^*)^{-1}$ versus square root of the scan rate (v). When the v approaches 0, solution is fully accessible to the inner electroactive sites so that the corresponding q^* tends to be the total voltammetric charge (q_T^*), which is the theoretical amount of electrochemical active sites of the electrode surface. Thus, q_T^* could be determined by extrapolating the linear plots to $v^{1/2} = 0$. Conversely, when the v approaches infinity, the access of solution to the inner electroactive sites

is inhibited so that the corresponding q^* indicates the outer voltammetric charge (q_o^*). Hence, q_o^* could be determined by extrapolating the linear fit of q^* to $v^{-1/2} = 0$ in the following equation:

$$q^* = q_o^* + k_2 v^{-1/2} \quad (4.2)$$

where k_2 is the slope of linear fitting. Fig. 4.7b shows that there is some deviation from the linear fit at high scan rate range, which could result from the uncompensated ohmic drop that decreases q^*. The inner voltammetric charge (q_i^*) could also be calculated by the following equation:

$$q_i^* = q_T^* - q_o^* \quad (4.3)$$

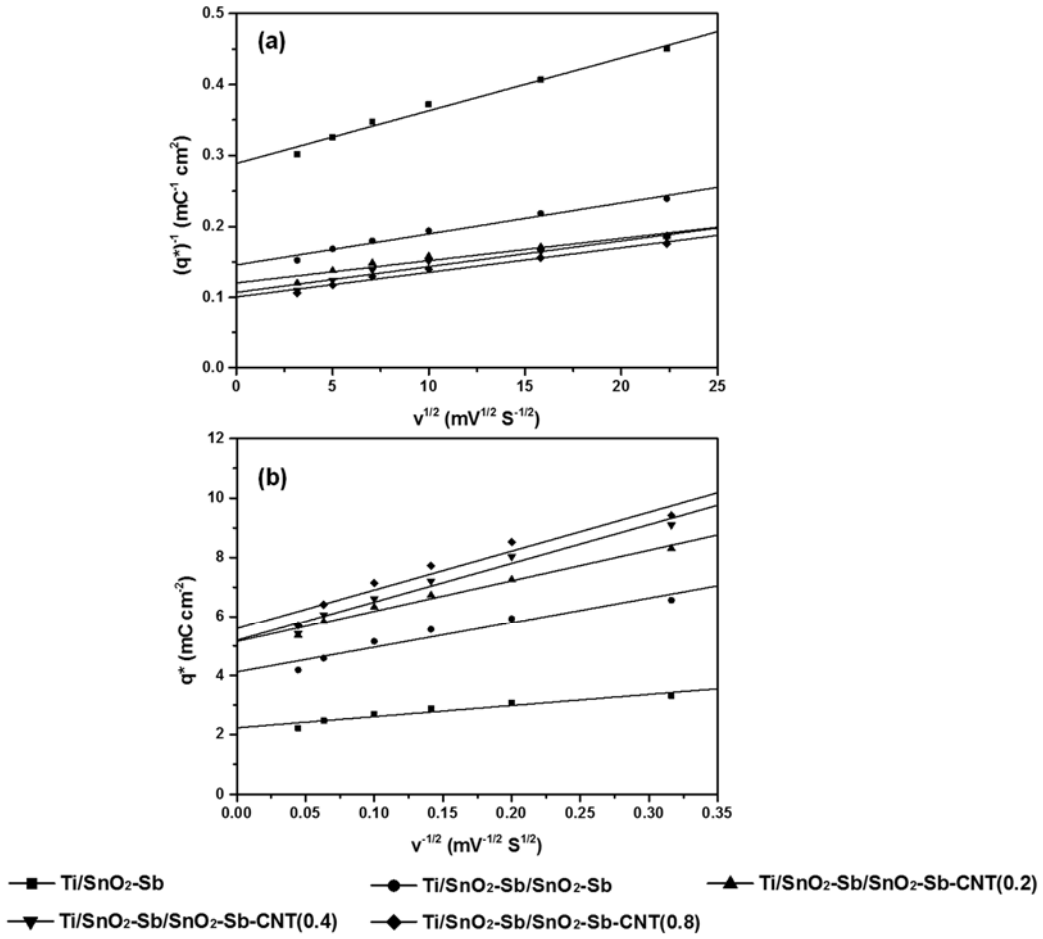

Fig. 4.7 (a) Extrapolation of the total charge (q_T^*) for the electrodes from the representation of $(q^*)^{-1}$ versus $v^{1/2}$ and (b) extrapolation of outer charge q_0^* for the electrodes from the representation of q* versus $v^{-1/2}$.

The calculated q_T^*, q_o^* and q_i^* of the electrodes are listed in Table 4.5. The q_T^* of Ti/SnO_2-Sb was 3.47 mC cm^{-2}. However, q_T^* is significantly improved by incorporation of SnO_2-Sb-CNT composites (8.29 – 9.92 mC cm^{-2}), which is due to a larger electroactive surface area of duplex-structured Ti/SnO_2-Sb/SnO_2-Sb-CNT. This is in agreement with the FESEM observation. The electrochemical porosity was also evaluated by the ratio of inner-to-total voltammetric charge (q_i^*/q_T^*). The higher electrochemical porosity of Ti/SnO_2-Sb/SnO_2-Sb-CNT meant the electrolyte is more difficult to diffuse through the inner part of the electrode at high scan rate, which is due to the compact surface of Ti/SnO_2-Sb/SnO_2-Sb-CNT. Since duplex-structured Ti/SnO_2-Sb/SnO_2-Sb-CNT(0.8) has both the largest q_o^* and q_T^*, it is expected to have more active sites for electrochemical oxidation reactions.

Table 4.5 Total, outer and inner charges and electrochemical porosity of the electrodes

Electrodes	q_T^* (mC cm^{-2})	q_0^* (mC cm^{-2})	q_i^* (mC cm^{-2})	q_i^*/q_T^*
Ti/SnO_2-Sb	3.47	2.23	1.24	0.357
Ti/SnO_2-Sb/SnO_2-Sb-CNT	6.86	4.12	2.76	0.402
Ti/SnO_2-Sb/SnO_2-Sb-CNT(0.2)	8.29	5.15	3.14	0.379
Ti/SnO_2-Sb/SnO_2-Sb-CNT(0.4)	9.32	5.19	4.13	0.443
Ti/SnO_2-Sb/SnO_2-Sb-CNT(0.8)	9.92	5.59	4.33	0.436

4.3.2.3 Electrochemical impedance spectroscopy

Electrochemical impedance spectroscopy (EIS) was employed to reflect the influence of SnO_2-Sb-CNT composites on the charge transfer resistance of the electrodes. Fig. 4.8 shows the Bode modulus, Bode phase and Nyquist plots of the electrodes. As can be seen in Fig. 4.8c, the Nyquist plots of Ti/SnO_2-Sb/SnO_2-Sb and Ti/SnO_2-Sb/SnO_2-Sb-CNT electrodes consist of two parts: semicircle pattern at high frequency range and a straight line at low frequency range, which indicates that the

charge transfer reaction and diffusion of the surface-electrolyte interface, respectively. However, Nyquist plot of Ti/SnO_2-Sb shows a pattern of only semicircle with significantly larger radius, demonstrating that the charge transfer resistance of Ti/SnO_2-Sb is high and the diffusion of surface-electrolyte interface is negligible. The Bode plots and Nyquist plots of Ti/SnO_2-Sb/SnO_2-Sb and Ti/SnO_2-Sb/SnO_2-Sb-CNT electrodes can be well fitted by $R_s[CPE_{dl}(R_{ct}CPE_0)]$ model. In this model, R_{ct}, R_s, CPE_{dl} and CPE_0 represent the charge transfer resistance of surface-electrolyte interface, uncompensated ohmic resistance between working electrode and reference electrode, constant phase element of double layer and constant phase element between the electrode surface and substrate. The fitted values of the components are listed in Table 4.6. Lowest R_{ct} of 16.72 Ω cm^{-2} is obtained with Ti/SnO_2-Sb/SnO_2-Sb-CNT(0.8), which is 64% that of Ti/SnO_2-Sb/SnO_2-Sb. It indicates faster electron transfer on the electrode surface of Ti/SnO_2-Sb/SnO_2-Sb-CNT(0.8). In addition, the calculated value of CPE_{dl} also increases with the CNT loading of SnO_2-Sb-CNT composite. The CPE_{dl} value of Ti/SnO_2-Sb/SnO_2-Sb-CNT(0.8) is almost two times that of Ti/SnO_2-Sb/SnO_2-Sb, which is in accordance with the larger electroactive surface area of Ti/SnO_2-Sb/SnO_2-Sb-CNT(0.8). Besides, the values of n for CPE_{dl} also increase with CNT loading, indicating that the performance of the electrodes are more close to capacitors other than resistors in the surface-electrolyte interface. In general, duplex-structured Ti/SnO_2-Sb/SnO_2-Sb-CNT(0.8) should have improved electrocatalytic performance due to its smaller electrochemical impedance.

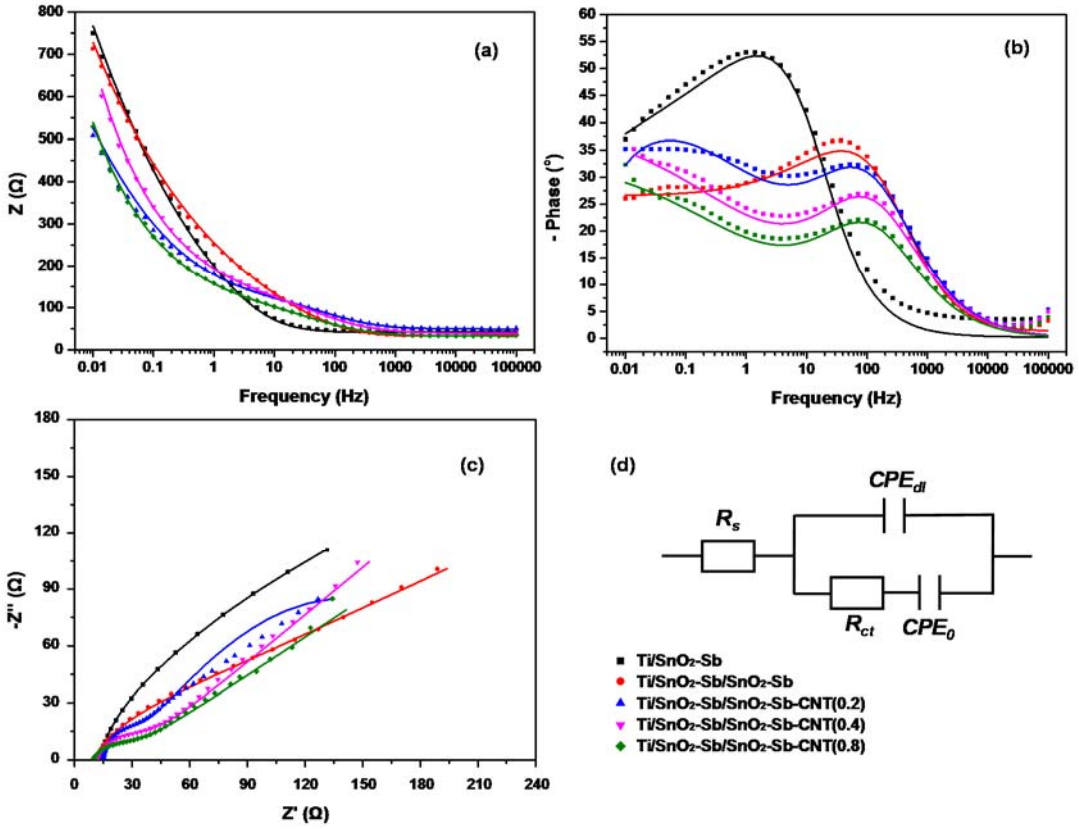

Fig. 4.8 (a) Bode modulus plot, (b) Bode phase plot and (c) Nyquist plot of the electrodes and (d) equivalent circuit model employed for data simulation (simulated plots are provided as solid lines).

Table 4.6 EIS simulating parameters of Ti/SnO_2-Sb/SnO_2-Sb and Ti/SnO_2-Sb/SnO_2-Sb-CNT electrodes using R[Q(RQ)] equivalent circuit model

Electrodes	**R_s (error%)** (Ω cm^{-2})	**R_{ct} (error%)** (Ω cm^{-2})	**CPE_{dl} (error%)** (mF cm^{-2})	**n_1**	**CPE_0 (error%)** (mF cm^{-2})	**n_2**
Ti/SnO_2-Sb/SnO_2-Sb	13.21 (3.83)	26.13 (27.97)	1.21 (0.78)	0.453	0.05 (12.11)	0.831
Ti/SnO_2-Sb/SnO_2-Sb-CNT(0.2)	15.53 (2.18)	19.05 (11.34)	1.68 (9.16)	0.659	0.31 (3.46)	0.412
Ti/SnO_2-Sb/SnO_2-Sb-CNT(0.4)	12.43 (5.07)	25.31 (5.73)	1.95 (0.98)	0.711	0.71 (10.58)	0.347
Ti/SnO_2-Sb/SnO_2-Sb-CNT(0.8)	9.69 (0.86)	16.72 (8.64)	2.34 (14.49)	0.722	0.62 (2.61)	0.380

4.3.2.4 Electrochemical stability

From the practical application viewpoint, it is important to gain some insights into the electrochemical stability of electrodes, since the electrode with a long service life and good resistance to corrosion could have economic attractiveness. The electrochemical stability of the electrodes were evaluated by accelerated life test. Table 4.3 summarizes the service lifetime of Ti/SnO_2-Sb and modified electrodes. The service lifetime of Ti/SnO_2-Sb is 6.4 h, and after incorporation of pulse electrodeposited SnO_2-Sb, it could be prolonged by a factor of 6.5 times to 42 h. Moreover, further improvement of service lifetime is obtained with Ti/SnO_2-Sb/SnO_2-Sb-CNT electrodes. Ti/SnO_2-Sb/SnO_2-Sb-CNT(0.8) has a highest service lifetime of 86 h, corresponding to 13.4 times that of Ti/SnO_2-Sb. These results demonstrates that Ti/SnO_2-Sb/SnO_2-Sb-CNT electrodes prepared by pulse electrodeposition exhibit prominently improved electrochemical stability compared to Ti/SnO_2-Sb by thermochemical decomposition. This could be due to several reasons. First, the compact electrode surface of duplex-structured Ti/SnO_2-Sb/SnO_2-Sb-CNT could inhibit the permeation of electrolyte into electrode inner part, so that less corrosion occurred and the conductivity was less influenced. Second, SnO_2-Sb-CNT composites significantly enhance the surface loading of the electrodes from 18.9 g m^2 to 64.3 g m^2, which gives extra durability against corrosive reactions. Third, due to the large specific surface areas of SnO_2-Sb-CNT composites, their incorporation into Ti/SnO_2-Sb/SnO_2-Sb-CNT electrodes could reduce the actual current densities on the electrode surfaces. This could also be reflected by the larger electroactive area of Ti/SnO_2-Sb/SnO_2-Sb-CNT. Therefore, the service lifetime Ti/SnO_2-Sb/SnO_2-Sb-CNT is further improved.

4.3.3 Performance evaluation

4.3.3.1 Adsorption of BPA

The adsorption of BPA by Ti/SnO_2-Sb and the modified electrodes was first investigated in the synthetic BPA wastewater of pH 7, prior to the application of current (Fig.8). After 1-h adsorption, decreases of BPA concentration equivalent to 1.6% - 4.9% of the initial amount were observed with Ti/SnO_2-Sb/SnO_2-Sb and Ti/SnO_2-Sb/SnO_2-Sb-CNT electrodes (Fig. 8a), demonstrating that the modified electrodes could adsorb BPA. However, Ti/SnO_2-Sb shows negligible BPA adsorption. Such effects are related to the SnO_2-Sb and SnO_2-Sb-CNT composites in the outer layers of the modified electrodes. To verify this point, the adsorption capacities of BPA by the as-prepared composites were also evaluated and summarized in Table S1. Pristine CNTs have a BPA adsorption capacity of 62.3 mg g^{-1} for the synthetic wastewater of pH 7. Both SnO_2-Sb and SnO_2-Sb-CNT composites could adsorb BPA, but their adsorption capacities were greatly influenced by the CNTs loading amount. A higher CNTs loading amount leads to larger BPA adsorption capacity up to 53.6 mg g^{-1} with SnO_2-Sb-CNT(0.8), which is 2.8 times that of SnO_2-Sb (19.2 mg g^{-1}) and 2.1 times that of SnO_2-Sb-CNT(0.2). The result was in accordance with the most prominent BPA adsorption by Ti/SnO_2-Sb/SnO_2-Sb-CNT(0.8), which may have the potential to improve the mass transfer of BPA molecules from bulk solution to anode surface and therefore to enhance the performance efficiency.

4.3.3.2 BPA degradation and TOC removal

Both BPA concentration and TOC of the synthetic wastewater of pH 7 were determined to evaluate the performance efficiency of the electrodes during 6-h electrochemical oxidation at a current density of 20 mA cm^{-2} (Fig. 4.9a and 4.9b). A BPA degradation rate of 79% was achieved using Ti/SnO_2-Sb as anode after 6-h bulk electrolysis. However, improved degradation of BPA was obtained with the modified

electrodes in ascending order: Ti/SnO_2-Sb/SnO_2-Sb (85%) < Ti/SnO_2-Sb/SnO_2-Sb-CNT(0.2) (88%) < Ti/SnO_2-Sb/SnO_2-Sb-CNT(0.2) (90%) < Ti/SnO_2-Sb/SnO_2-Sb-CNT(0.2) (97%). Fig. 4.9b shows that only 58% TOC removal was obtained using Ti/SnO_2-Sb as anodes after 6-h bulk electrolysis. An improvement of TOC removal (68%) was observed in Ti/SnO_2-Sb/SnO_2-Sb, which could be attributed to the larger surface loading and electroactive surface area by pulse electrodeposition technique. Nevertheless, the TOC removal performance was further enhanced up to 80% by modifying with SnO_2-Sb-CNT composites, indicating a higher electrocatalytic activity for BPA oxidation. Comparing to the rate of BPA degradation, that of TOC removal is much smaller, demonstrating that BPA was converted to other organic compounds before it was fully oxidized to CO_2 and H_2O. The values of MCE for BPA oxidation are also shown in Fig. 8c. The highest MCE was obtained on Ti/SnO_2-Sb/SnO_2-Sb-CNT(0.8), which is 1.41 times that of Ti/SnO_2-Sb for 2-h operation (25.1 % vs 17.8 %) and 1.37 times for 6-h operation (14.6% vs 10.6%).

There are several reasons for the improved performance of Ti/SnO_2-Sb/SnO_2-Sb-CNT. First, the larger electroactive surface area of Ti/SnO_2-Sb/SnO_2-Sb-CNT provides more active sites for electrochemical oxidation reactions. Second, the high OEP of Ti/SnO_2-Sb/SnO_2-Sb-CNT benefits the generation of $HO^{\bullet}$ radical. It is well known that SnO_2-based electrodes are classified as typical “non-active” electrode, which could provide active sites for physisorbed $HO^{\bullet}$. Hence, $HO^{\bullet}$ plays an important role in oxidation of organic compounds by SnO_2 electrodes and could significantly influence the performance efficiency. The evaluation of $HO^{\bullet}$ generation ability of the electrodes by DMSO trapping shows that the best $HO^{\bullet}$ evolution in solutions (28.3 μM) was obtained in duplex structured Ti/SnO_2-Sb/SnO_2-Sb-CNT(0.8), which also exhibited the best TOC removal efficiency.

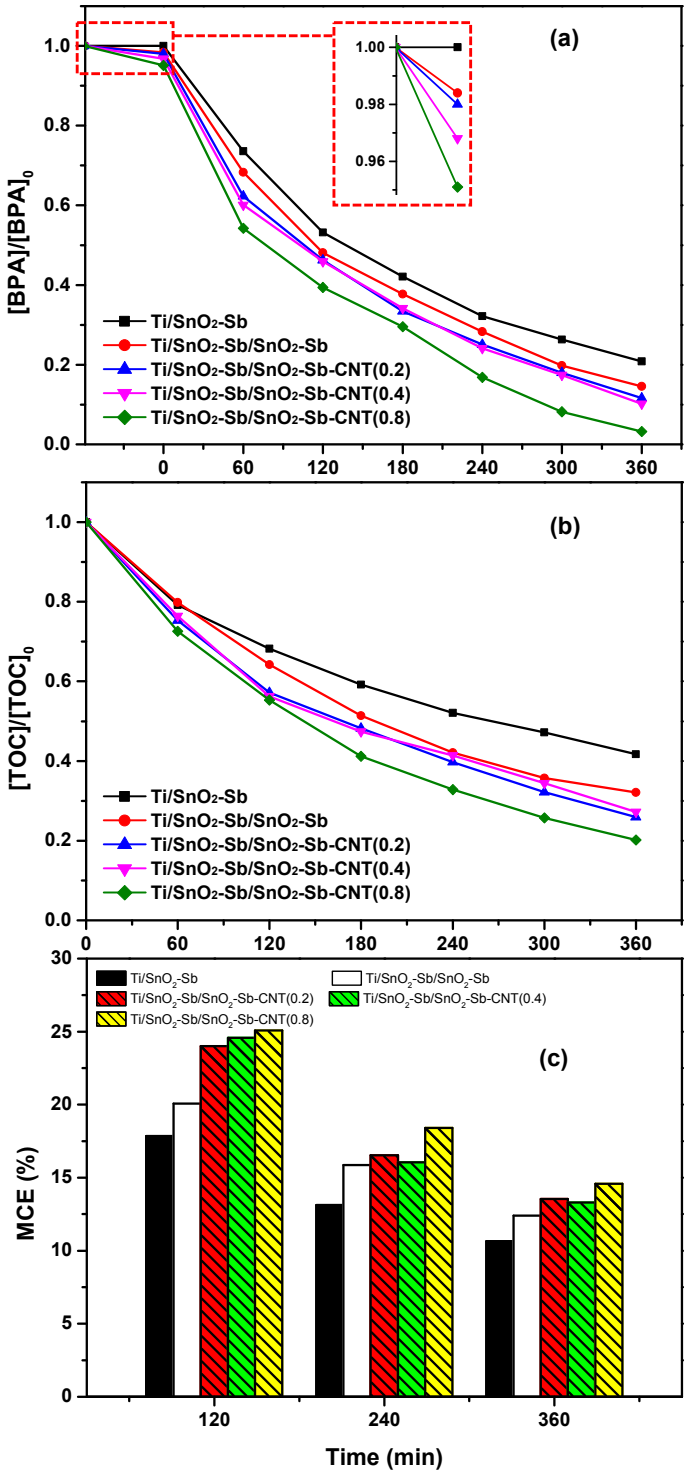

Fig. 4.9 Performance of (a) BPA degradation, (b) TOC removal and (c) mineralization current efficiency of the electrodes at pH 7 in 0.05 M Na_2SO_4.

Both BPA degradation and TOC removal results demonstrate that the electrocatalytic performance can be improved by incorporation of SnO_2-Sb-CNT

composite using pulse electrodeposition, comparing to Ti/SnO_2-Sb by thermochemical decomposition. Such improvement is related to the more electroactive surface of Ti/SnO_2-Sb/SnO_2-Sb-CNT as well as its capability for BPA adsorption. Fig. 4.10 proposes a mechanism to depict the electrochemical oxidation of BPA enhanced by adsorption. The oxidation process starts with the generation of physisorbed $HO^{\bullet}$ on the electrode surface by water splitting when there is potential applied:

$$SnO_2 + H_2O \rightarrow SnO_2(HO^{\bullet}) + H^+ + e^- \quad (4.4)$$

Some of the physisorbed $HO^{\bullet}$ are released into the solution to form aqueous $HO^{\bullet}$. The $HO^{\bullet}$ is quite unstable species of short lifespan. They can either combine together for oxygen evolution reaction (OER) or react with organic compound to generate intermediates or CO_2. Since OER is the main compete reaction for BPA oxidation, it is important to obtain effective utilization of $HO^{\bullet}$ for BPA degradation. From the viewpoint of mass transfer, the adsorption of BPA on Ti/SnO_2-Sb/SnO_2-Sb-CNT surface supplies more chance for physisorbed $HO^{\bullet}$ to attack adsorbed BPA molecules, thus the $HO^{\bullet}$ utilization efficiency is improved. Moreover, CNT itself is an active anode material for organic oxidation, and the adsorbed BPA could be oxidized by direct electron transfer on the CNT surface. The other advantage is that through adsorption of BPA, there will be a BPA molecule-rich diffuse layer near the electrode-electrolyte interface, which improves the efficiency of aqueous $HO^{\bullet}$ consumption by BPA near the electrode surface. Therefore, the electrocatalytic activity of duplex Ti/SnO_2-Sb/SnO_2-Sb-CNT electrode could be improved by adsorption of BPA onto the anode surface.

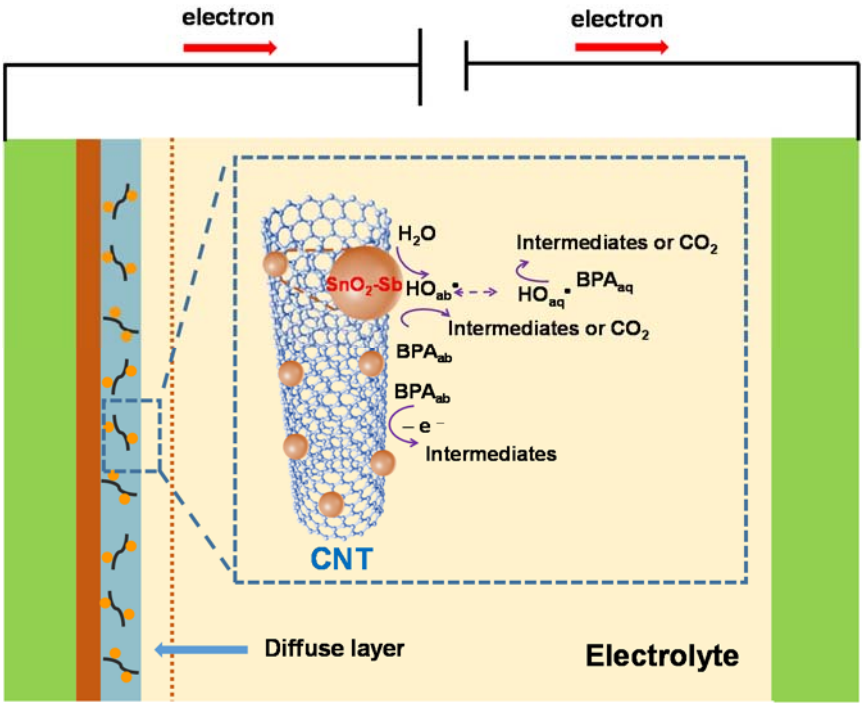

Fig. 4.10 Proposed mechanism for synergistic adsorption and electrochemical oxidation of BPA.

4.3.3.3 Influence of operating parameters

Ti/SnO_2-Sb/SnO_2-Sb-CNT(0.8) stands out as the most optimal electrode with highest pollutants removal rate, largest current efficiency and best capability for BPA adsorption. Thus, it was selected for comparison with Ti/SnO_2-Sb and Ti/SnO_2-Sb/SnO_2-Sb under various current densities and initial pH for performance evaluation. The TOC removal and BPA degradation results are well fitted with pseudo-first-order rate constants. The decrease of BPA after 1-h adsorption, apparent rate constants (k) for TOC removal and BPA degradation, MCE and final pH of synthetic wastewater are summarized in Table 4.7. It is obvious that both TOC removal and BPA degradation are enhanced at high current density. However, the current efficiency is inevitably compromised. When the current density increased from 20 mA cm^{-2} to 40 mA cm^{-2}, there was a prominent increase in $k_{[TOC]}$ of Ti/SnO_2-Sb/SnO_2-Sb-CNT(0.8) comparing to Ti/SnO_2-Sb and Ti/SnO_2-Sb/SnO_2-Sb, indicating the improved

electrocatalytic activity by incorporation of CNTs. At applied current density of 10 mA cm^{-2}, the highest MCE (23.6%) was obtained with Ti/SnO_2-Sb/SnO_2-Sb-CNT(0.8).

The solution pH may influence the electrocatalytic performance of the electrodes in several aspects. First, the ionization of BPA is strongly related to solution pH. BPA has an acid dissociation constant (pK_a) ranging from 9.6 to 10.2 (Staples et al. 1998). When pH < pK_a, the non-ionized BPA presents as the dominant species, and when pH > pK_a, BPA will be ionized and the dominant species are bisphenolate anions. At pH 11, the negatively charged bisphenolate anions may be attracted toward the positively charged anode by electric potential. However, the electrocatalytic performance of the electrodes for BPA degradation still decreases despite of this phenomenon. It is not surprising since the oxidative potential of aqueous $HO^{\bullet}$ is directly affected by the solution pH, which could be calculated by the Nernst equation (Wardman 1989):

$$E^o(HO_{aq}^{\bullet}/H_2O) = 2.59 - 0.059\ pH \quad (4.5)$$

The values of $E^o(HO_{aq}^{\bullet}/H_2O)$ are 2.41, 2.18 and 1.94 at pH 3, 7 and 11 respectively. Thus, the $HO^{\bullet}$ generated by the electrode shows lower oxidative power in synthetic wastewater of pH 11, leading to decreased BPA degradation and TOC removal rates. However, comparing to Ti/SnO_2-Sb and Ti/SnO_2-Sb/SnO_2-Sb, duplex-structured Ti/SnO_2-Sb/SnO_2-Sb-CNT(0.8) shows remarkably stable performance at initial solution pH of 3 and 7. This is probably due to the fact that BPA is adsorbed on the electrode surface of duplex-structured Ti/SnO_2-Sb/SnO_2-Sb-CNT(0.8), so that the absorbed $HO^{\bullet}$ ($HO_{ab}^{\bullet}$) generated on the electrode surface plays a more important role for BPA oxidation than Ti/SnO_2-Sb. Because the oxidative potential of $HO_{ab}^{\bullet}$ is less influenced by solution pH compared to the aqueous $HO^{\bullet}$ ($HO_{aq}^{\bullet}$), the electrocatalytic activity of Ti/SnO_2-Sb/SnO_2-Sb-CNT(0.8) could remain stable at high pH range.

On the other hand, initial solution pH could also influence the adsorption capacity

of BPA by Ti/SnO_2-Sb/SnO_2-Sb-CNT(0.8). As can be seen in Table 4.7, there was a dramatic decrease of BPA adsorption by Ti/SnO_2-Sb/SnO_2-Sb-CNT(0.8) at pH 11 (1.3% of initial BPA) than those at pH 3 (5.5% of initial BPA) and 7 (4.9% of initial BPA). Therefore, Ti/SnO_2-Sb/SnO_2-Sb-CNT(0.8) has a lower electrocatalytic activity for BPA degradation at pH 11 due to the lower BPA adsorption on the electrode surface. On the basis of above analysis, duplex-structured Ti/SnO_2-Sb/SnO_2-Sb-CNT(0.8) has the benefit for application at high current density and acidic to neutral pH range without severe decrease of the performance efficiency.

4.3.3.4 Influence of water matrix species

Fig. 4.11 shows the effect of humic acid (HA) and sodium alginate on BPA degradation by Ti/SnO_2-Sb/SnO_2-Sb-CNT(0.8). HA and alginate exist as two common components of natural organic matter (NOM) in aqueous phase (Tong et al. 2011). In the presence of 10 mg L^{-1} HA, the adsorption of BPA by Ti/SnO_2-Sb/SnO_2-Sb-CNT(0.8) was significantly decreased from 4.9% to 1.8% of the initial BPA, indicating that HA could act as a effectively competitive compound for BPA adsorption. As a consequence, the BPA degradation rate was decreased from 97% to 86%. However, the presence of sodium alginate did not show notable effect on the adsorption of BPA by Ti/SnO_2-Sb/SnO_2-Sb-CNT(0.8) (4.9% vs 4.2%), as well as the performance efficiency of BPA degradation (97% vs 93%). Therefore, the electrochemical oxidation of BPA by Ti/SnO_2-Sb/SnO_2-Sb-CNT(0.8) is strongly related to the adsorption of BPA by the electrode surface.

Table 4.7 The first order rate constant for TOC removal, the first order rate constant for BPA degradation, specific energy consumption and mineralization current efficiency of electrodes under various conditions

Electrode	Conditions	Adsorption of BPA (%)	BPA degradation (%)	$k_{[BPA]}$ (1×10^{-3} min^{-1})	R_1^2	TOC removal (%)	$k_{[TOC]}$ (1×10^{-3} min^{-1})	R_2^2	MCE (%)	Final solution pH
Ti/SnO_2-Sb	j=10 $mA.cm^{-2}$; pH=7	-	64.8	2.9	0.991	42.2	1.5	0.995	15.42	3.23
	j=20 $mA.cm^{-2}$; pH=3	-	78.8	4.2	0.978	62.3	2.8	0.983	11.38	3.06
	j=20 $mA.cm^{-2}$; pH=7	-	79.2	4.4	0.985	58.3	2.5	0.979	10.65	3.98
	j=20 $mA.cm^{-2}$; pH=11	-	75.2	3.8	0.996	55.8	2.3	0.992	10.19	6.82
	j=40 $mA.cm^{-2}$; pH=7	-	96.9	9.8	0.992	74.5	3.8	0.985	6.81	3.96
Ti/SnO_2-Sb/SnO_2-Sb	j=10 $mA.cm^{-2}$; pH=7	1.8	70.4	3.3	0.981	48.7	1.8	0.992	17.79	3.28
	j=20 $mA.cm^{-2}$; pH=3	1.5	87.4	5.6	0.969	71.5	3.5	0.979	13.06	3.14
	j=20 $mA.cm^{-2}$; pH=7	1.6	85.4	5.5	0.988	67.9	3.1	0.991	12.41	5.01
	j=20 $mA.cm^{-2}$; pH=11	0.8	79.5	4.3	0.982	65.2	2.9	0.988	11.91	6.88
	j=40 $mA.cm^{-2}$; pH=7	1.6	98.2	11.0	0.969	80.6	4.6	0.976	7.36	4.06
Ti/SnO_2-Sb/SnO_2-Sb-CNT(0.2)	j=20 $mA.cm^{-2}$; pH=7	2.0	88.4	5.9	0.991	74.1	3.6	0.995	13.54	4.68
Ti/SnO_2-Sb/SnO_2-Sb-CNT(0.4)	j=20 $mA.cm^{-2}$; pH=7	3.2	89.8	6.4	0.982	72.8	3.6	0.987	13.30	4.82
Ti/SnO_2-Sb/SnO_2-Sb-CNT(0.8)	j=10 $mA.cm^{-2}$; pH=7	5.1	80.2	4.6	0.982	64.6	2.9	0.991	23.60	3.97
	j=20 $mA.cm^{-2}$; pH=3	5.5	95.9	8.9	0.973	80.8	4.5	0.988	14.76	3.12
	j=20 $mA.cm^{-2}$; pH=7	4.9	96.8	9.8	0.979	79.8	4.4	0.975	14.58	5.04
	j=20 $mA.cm^{-2}$; pH=11	1.3	87.7	5.7	0.994	73.2	3.8	0.996	13.37	7.18
	j=40 $mA.cm^{-2}$; pH=7	4.9	100	15.4	0.976	95.3	8.4	0.989	9.14	4.28

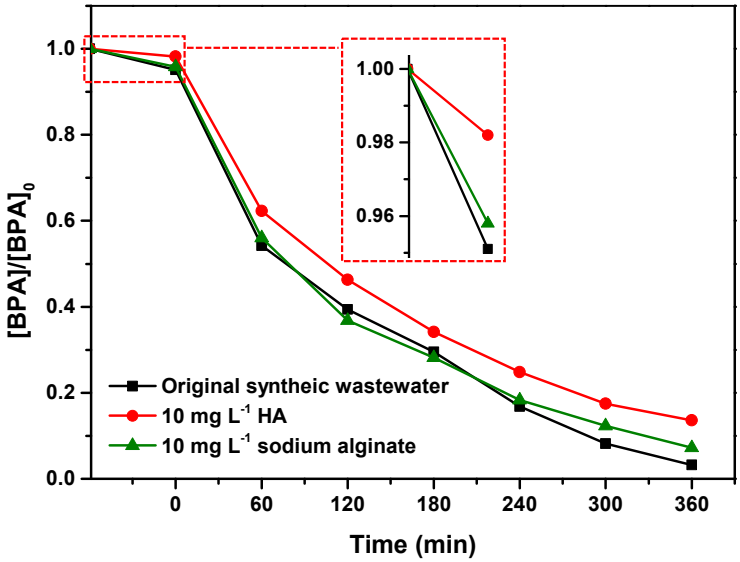

Fig. 4. 11 Performance of BPA degradation in the presence of HA and sodium alginate at pH 7 in 0.05 M Na_2SO_4.

4.4 Conclusions

Highly active duplex-structured SnO_2 electrode modified by SnO_2-Sb-CNT composite (Ti/SnO_2-Sb/SnO_2-Sb-CNT) was successfully prepared by pulse electrodeposition. It exhibits good adsorption capacity for BPA, high oxygen evolution potential (2.2 V vs Ag/AgCl (3 M NaCl)), large electroactive surface area and good electrochemical stability. The duplex-structured Ti/SnO_2-Sb/SnO_2-Sb-CNT shows synergistic adsorption and electrochemical oxidation effect for BPA degradation, which prominently improves the performance efficiency compared with Ti/SnO_2-Sb fabricated by thermochemical decomposition. Moreover, the electrocatalytic performance of duplex-structured Ti/SnO_2-Sb/SnO_2-Sb-CNT(0.8) was stable over a wide range of current density and under acidic to neutral pH condition, making it economically attractive for practical applications in degradation of aqueous recalcitrant organic pollutants. However, the adsorption of BPA by Ti/SnO_2-Sb/SnO_2-Sb-CNT could be inhibited by other organic matter such as HA, leading to a decreased performance efficiency for electrochemical oxidation of BPA.

CHAPTER 5 ELECTROCHEMICAL OXIDATION OF BISPHENOL A BY BORON-DOPED DIAMOND AND MODIFIED SnO_2-Sb ANODES: INFLUENCING PARAMETERS AND REACTION PATHWAYS[3]

5.1 Introduction

Chapter 3 and Chapter 4 describe two types of modified SnO_2-Sb anodes, i.e. TiO_2-NTs/SnO_2-Sb-PTFE and Ti/SnO_2-Sb/SnO_2-Sb-CNT. Both of the two electrodes exhibit improved electrocatalytic performances for oxidation of phenolic compounds comparing with Ti/SnO_2-Sb fabricated by thermochemical decomposition. However, the mechanisms involved are different. For TiO_2-NTs/SnO_2-Sb-PTFE, the enhancement on the release of free $HO^{\bullet}$ by the hydrophobic surface plays an important role in the improved electrocatalytic activity of the electrode. For Ti/SnO_2-Sb/SnO_2-Sb-CNT, it enables synergistic adsorption and electrochemical oxidation of BPA and thus the electrocatalytic performance is improved.

In recent years, boron doped diamond (BDD) has been verified to be a very attractive anode material for removal of organic pollutants through direct anodic oxidation due to its notably high OEP (Alfaro et al. 2006, Zhu et al. 2008b). Moreover, BDD has the advantage of high physical and electrochemical stability compared with other electrodes (Kraft 2007, Panizza and Cerisola 2009, Yu et al. 2014), which is an important factor for its successful commercialization. Commercial BDD anodes have been reported for the total removal of various phenolic compounds, such as phenol

[3] This chapter is modified from the literature published in *Journal of Environmental Chemical Engineering* in 2016 (vol.4, pp 2087-2015), of which the Ph.D. candidate is the first author.

(Sun et al. 2012), 4-nitrophenol (Rabaaoui et al. 2013), 4-chlorophenol (Rodrigo et al. 2001) and bisphenol A (Murugananthan et al. 2008, Pereira et al. 2012). However, the expensive cost on the fabrication of BDD material has presented a main barrier for its scale-up or extensive applications. Thus, from the viewpoint of practical application, a comparative study of the modified SnO_2-Sb anodes fabricated in this study with the commercial BDD anode would be meaningful to provide some insights into their electrocatalytic performance and as potential alternative anodes for practical applications.

The byproducts of BPA during the treatment process may also exhibit high endocrine-disrupting effect (Hu et al. 2002). Therefore, it is important to achieve completely mineralization of BPA to final products such as CO_2 and water or to environmentally benign products such as aliphatic organic acids (Yang et al. 2016). To date, various techniques have been employed for the removal of aqueous BPA such as biological treatment (Nguyen et al. 2013), adsorption (Tsai et al. 2006), wet oxidation (Lua et al. 2015) and AOPs (Oh et al. 2014, Wang and Lim 2011). In recent years, electrochemical oxidation has emerged as a promising method for the removal or alleviation of aqueous BPA contaminants (Xue et al. 2011, Zhao et al. 2014). However, anode material is crucial to the success of this application (Cui et al. 2009b).

This chapter presents a comparative study on the electrochemical oxidation of BPA by the modified SnO_2 anodes described in Chapter 3 and Chapter 4 and the commercial BDD anode. The surface morphology, OEP and ability in $HO^{\bullet}$ generation of the three anodes were compared. The influences of operating parameters such as initial solution pH and the type of supporting electrolyte on the electrocatalytic performance of the three electrodes were investigated. The intermediate byproducts of BPA oxidation with the different anodes were also determined to elucidate the reaction pathways.

5.2 Experimental

5.2.1 Chemicals and materials

All of the chemicals were of analytical grade and used without further purification. Acetonitrile (LC–MS grade) was obtained from Merck. Nb/BDD anode with a coating thickness of 5 μm and boron concentration of 2500 ppm was purchased from NeoCoat Co., Switzerland. All other chemicals and materials are described in Section 3.2.1 and Section 4.2.1.

5.2.2 Bulk electrolysis of bisphenol A

The 6-h bulk electrolysis experiments of BPA were conducted in the same single-compartment electrochemical cell described in Section 3.2.4. BDD, TiO_2-NTs/SnO_2-Sb-PTFE and Ti/SnO_2-Sb/SnO_2-Sb-CNT were employed as the anodes. Synthetic wastewater containing 100 mg L^{-1} BPA was prepared in 0.05 M Na_2SO_4 supporting electrolyte. The influence of pH on the electrocatalytic performance was investigated by adjusting the initial solution pH to 3, 7 and 11 using 0.5 M H_2SO_4 or 1M NaOH. The current applied is 0.16 A and the nominal area of the electrodes is 8 cm^2. The influence of the type of supporting electrolyte on electrocatalytic performance was also investigated by comparing the electrochemical oxidation of BPA in 0.1 M NaCl and 0.05 M Na_2SO_4 at pH 7.

The aliquot solutions were drawn for analysis at 1-h interval. The elctrocatalytic performances of the electrodes were evaluated by determining the TOC and BPA concentration of the samples. TOC determination employed the same equipment described in Section 3.2.4. BPA concentrations were determined by HPLC equipped with a UV-Vis spectrophotometer at 220 nm wavelength and a C18 column (Hypersil Gold). The mobile phase used was acetonitrile/water (40/60, v/v) at a flow rate of 1 ml L^{-1}. Mineralization byproducts of formic acid, acetic acid, oxalic acid and sulfate

ion, chloride ion and chlorate ion were quantified through IC. Other byproducts were verified by liquid chromatography tandem mass spectrometry (LC–MS/MS, Agilent 6460 Triple Quadrupole LC/MS System) equipped with a C18 column (ID = 2.1 mm, length = 100 mm and particle size = 5 μm, Shim-pack Shimadzu) in negative ionization mode. The mobile phase started with 30/70 (v/v) acetonitrile/water and was increased linearly to 90/10 (v/v) in 8 min, kept for 4 min, then decreased linearly to 30/70 (v/v) in 1 min, and finally kept for 5 min. The flow rate was set as 0.2 mL min^{-1}.The sheath gas and drying gas temperature were kept at 350 ^{o}C and 225 ^{o}C respectively. Other parameters including nozzle voltage (0 V positive; 1500 V negative), fragmentor voltage (135 V), capillary voltage (4000 V positive; 3600 V negative) and delta electron multiplier voltage (200 V) were set.

5.2.3 Electrode characterization techniques

LSV was employed to determine the OEP of the electrodes using the same method described in Section 4.2.6. The chlorine evolution potential of the electrodes was also examined through LSV in 3 M NaCl electrolyte with a scan range of 0 V– 2.0 V, meanwhile other conditions were kept the same. FESEM images of the electrodes were also taken.

5.3 Results and discussions

5.3.1 Characterization of the anodes

5.3.1.1 Surface morphology

Fig. 5.1 compares the FESEM images of TiO_2-NTs/SnO_2-Sb-PTFE, Ti/SnO_2-Sb/SnO_2-Sb-CNT and BDD electrodes. The surface morphologies of TiO_2-NTs/SnO_2-Sb-PTFE and Ti/SnO_2-Sb/SnO_2-Sb-CNT have been discussed in Section 3.3.1 and Section 4.3.1, respectively. They both have rough surfaces with microshperical SnO_2 particles (Fig. 5.1a and Fig. 5.1b), resulting in the larger specific

surface area of the electrodes. Therefore, it could provide more active sites for electrocatalytic reactions, contributing to their improved electrocatalytic activity than conventional Ti/SnO_2-Sb fabricated by thermal chemical decomposition. In contrary, BDD electrode exhibits a rather different surface morphology with well-arranged crystals of different grain sizes. No cracks or voids could be observed on BDD electrode surface, leading to its good anti-corrosion property.

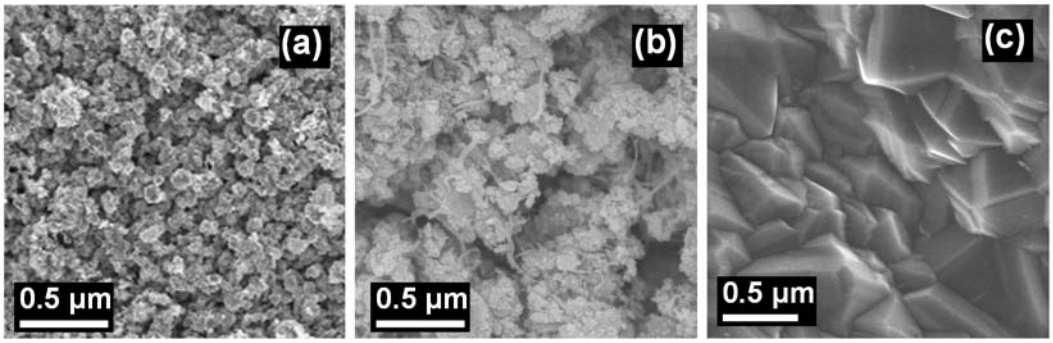

Fig. 5.1 FESEM images of (a) TiO_2-NTs/SnO_2-Sb-PTFE, (b) Ti/SnO_2-Sb/SnO_2-Sb-CNT and (c) BDD anodes.

5.3.1.2 Linear sweep voltammetry

OEP is an important indicator of anode materials in the application for electrocatalytic oxidation of recalcitrant organic compounds. Since the oxygen evolution reaction is a main competitive reaction for the degradation of organics by $HO^{\bullet}$, anodes with high OEP are expected to obtain better utilization efficiency of $HO^{\bullet}$ for organic oxidation. LSV experiments were conducted in 0.5 M Na_2SO_4 to determine the OEP of TiO_2-NTs/SnO_2-Sb-PTFE, Ti/SnO_2-Sb/SnO_2-Sb-CNT and BDD anodes (Fig. 5.2). The highest OEP was obtained with BDD anode (2.5 V vs Ag/AgCl (3 M NaCl)). However, the TiO_2-NTs/SnO_2-Sb-PTFE anode has an OEP (2.4 V vs Ag/AgCl (3 M NaCl)) close to that of BDD. This is due to its hydrophobic surface which hinders the recombination of hydrophilic $HO^{\bullet}$, as has been discussed in Section 3.3.1.2. Ti/SnO_2-Sb/SnO_2-Sb-CNT has a smallest OEP of 2.2V (vs Ag/AgCl (3 M NaCl)), but still higher than that of conventional Ti/SnO_2-Sb (2.0 V

vs Ag/AgCl (3 M NaCl)).

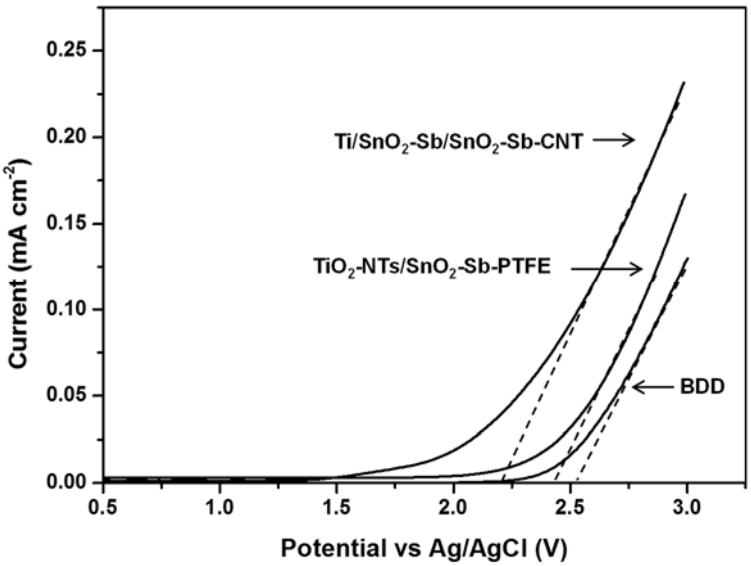

Fig. 5.2 Linear sweep voltammetric curves of TiO_2-NTs/SnO_2-Sb-PTFE, Ti/SnO_2-Sb/SnO_2-Sb-CNT and BDD anodes in 0.5 M Na_2SO_4 at a scan rate of 50 mV s^{-1}.

5.3.2 Bulk electrolysis of BPA

5.3.2.1 Influence of anode materials

Fig. 5.3 shows the time course of BPA degradation and TOC removal using TiO_2-NTs/SnO_2-Sb-PTFE, Ti/SnO_2-Sb/SnO_2-Sb-CNT and BDD anodes at different solution pH (3, 7 and 11) in 0.05 M Na_2SO_4. It is obvious that the type of anode material has a remarkable influence on their electrocatalytic performances of BPA oxidation. In general, BDD anode shows the best electrocatalytic activity for BPA oxidation at various pH, which is probably due to its high OEP. TiO_2-NTs/SnO_2-Sb-PTFE and Ti/SnO_2-Sb/SnO_2-Sb-CNT show similar performance for BPA degradation. All of the three electrodes could achieve very high BPA degradation rate (> 95%) in pH 3 and pH 7 solutions. However, a greater difference in TOC removal rates of the three anodes was observed. The superior TOC removal by BDD anode indicates that more BPA molecules are completely mineralized to CO_2 and H_2O, demonstrating its higher electrocatalytic activity.

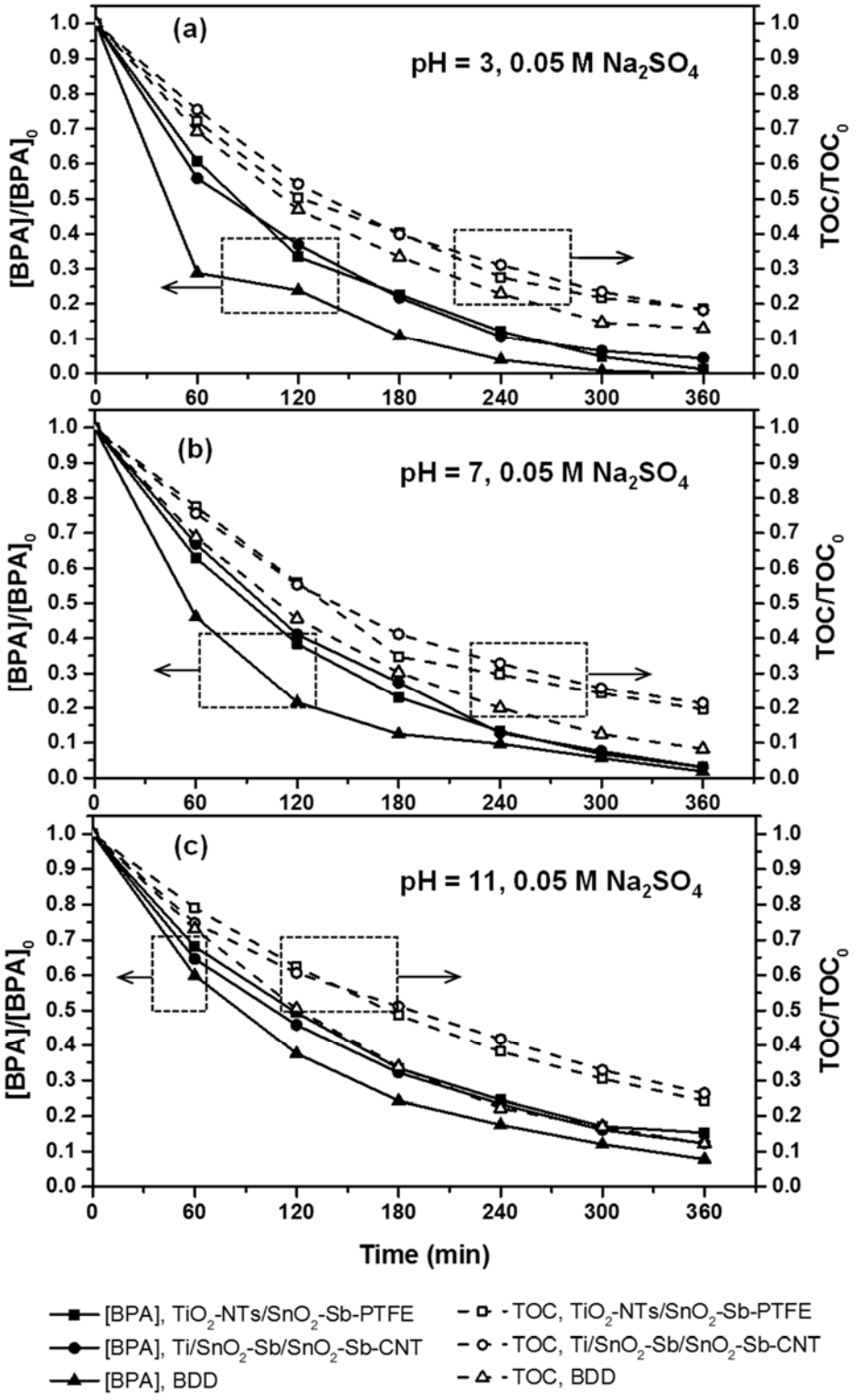

Fig. 5.3 Performance of BPA degradation and TOC removal with modified SnO_2 electrodes and BDD at initial solution pH of (a) 3, (b) 7 and (c) 11 in 0.05 M Na_2SO_4 supporting electrolyte.

The HO• generated on the anode surfaces was quantified by DMSO trapping to help to understand the difference of their electrocatalytic behavior (Fig 5.4). HO• production capabilities of the three anodes follow the descending order: TiO_2-NTs/SnO_2-Sb-PTFE (36.3 μM) > BDD (34.2 μM) > Ti/SnO_2-Sb/SnO_2-Sb-CNT (28.3μM). It is worth noting that the highest OEP of BDD does not result in the highest HO• generation. Similar findings were also reported in other studies (Sires et al. 2008, Zhu et al. 2008b). It suggests that the high electrocataltyic activity of BDD for BPA degradation is not relied on the generation of large amount of HO•, but the higher reactivity of electrogenerated HO• due to the weak BDD- HO• interaction (Kapalka et al. 2008).

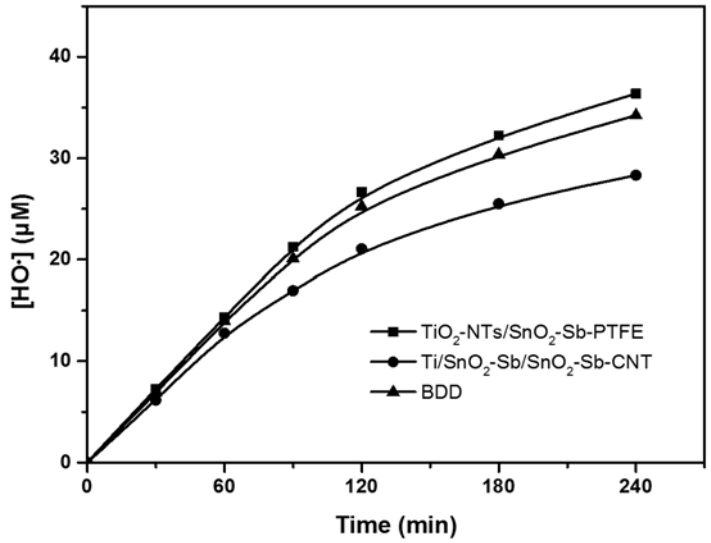

Fig. 5.4 Concentration evolution of hydroxyl radicals on the electrodes in 0.05 M Na_2SO_4.

5.3.2.2 Influence of pH

The effect of solution pH on the electrocatalytic performance of the electrodes was investigated in 0.05 M Na_2SO_4. As can be seen in Fig.5.3, all of the three electrodes show better BPA removal efficiency at acidic solution pH. Complete degradation of BPA could be achieved with TiO_2-NTs/SnO_2-Sb-PTFE and BDD anodes at 6 h and 5 h. Meanwhile, 95.7% BPA was degraded with Ti/SnO_2-Sb/SnO_2-Sb-CNT in pH 3 solution. On the contrary, the electrocatalytic oxidation of BPA seems to be less

effective in pH 11 solutions wherein only 84.2% – 90.2% BPA degradation could be achieved. The solution pH could influence the electrocatalytic activity of the anodes in several aspects. First, the solution pH affects the oxidative power the $HO^{\bullet}$ radicals generated on the anode surfaces, as has been discussed in Section 3.2.2.2. In acidic pH range, $HO^{\bullet}$ exhibits a higher oxidative potential and thus complete degradation of BPA is favorable. Second, CO_2, as a main product of electrochemical oxidation, could be dissolved in alkaline solution and exisits as HCO_3^- and CO_3^{2-} ions. Both anions are strong $HO^{\bullet}$ scavengers and therefore inhibit BPA oxidation by $HO^{\bullet}$.

However, it is interesting that a similar TOC removal efficiency for BPA oxidation in pH 11(87.9%) and pH 3 (87.1%) solutions was observed with BDD anode. It can be related to the ionization of BPA. The dissociation constant (pK_a) of BPA is ranging from 9.6 to 10.2. Thus, in pH 11 solution, deprotonation reaction occurs and BPA will present as bisphenolate anions. The bisphenolate anions could be drawn towards the positively charged anode surface by electric potential as well as being attacked by the electrophilic $HO^{\bullet}$. Such effect gives rise to the improved mass transfer which offsets the effect of lower oxidative power of $HO^{\bullet}$ at alkaline condition. Thus, the TOC removal rate was not decreased with pH.

5.3.2.3 Influence of the type of supporting electrolyte

The type of supporting electrolyte plays an important role in the electrocatalytic oxidation of organic pollutants, since it can result in the generation of different secondary oxidants which are involved in electrocatalytic reactions. Apart from SO_4^{2-}, Cl^- is the other type of most common anions in natural water system or wastewaters. Fig. 5.5 shows the time course of BPA degradation and TOC removal using the three electrodes in 0.1 M NaCl with pH 7. It is surprising that significantly different trends were observed for BPA degradation and TOC removal when using NaCl as the supporting electrolyte. BPA concentration seems to decrease rather rapidly, especially for BDD anode. In fact, the BPA compound could not be detected by HPLC after 1-

h bulk electrolysis with BDD anode. For TiO_2-NTs/SnO_2-Sb-PTFE and Ti/SnO_2-Sb/SnO_2-Sb-CNT, the BPA degrades at a slower rate and the periods for its total degradation is 3 h and 5 h, respectively. However, their BPA degradation rates are still much faster than those in 0.05 M Na_2SO_4, where complete degradation of BPA could not be achieved in pH 7 solution.

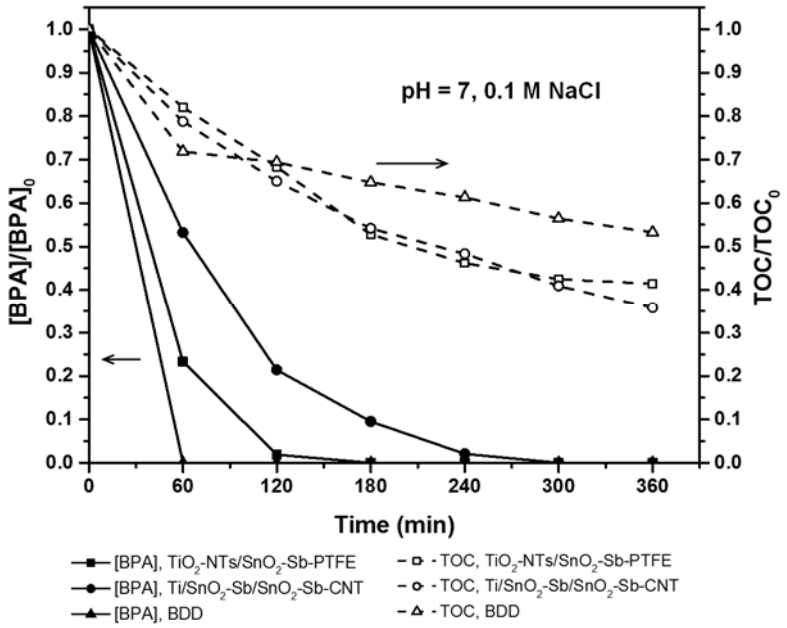

Fig. 5.5 Performance of BPA degradation and TOC removal with modified SnO_2 electrodes and BDD at initial solution pH of 7 in 0.1 M NaCl supporting electrolyte.

On the contrary, the rates of TOC removal are much slower under the same experimental condition, indicating that the BPA is not effectively mineralized to CO_2. Among the three electrodes investigated, the best TOC removal is obtained with Ti/SnO_2-Sb/SnO_2-Sb-CNT (64%), while that of BDD is only 47%. The TOC removal rates are much less than those achieved in 0.05 M Na_2SO_4 (79% and 92%). Murugananthan et al. (2008) reported that in electrocatalytic oxidation of BPA with BDD anode, TOC removal could be inhibited by employing NaCl as supporting electrolyte, but no significant difference were observed with Na_2SO_4 or $NaNO_3$ as supporting electrolyte. However, it is interesting that the TOC degraded at a much faster rate with BDD anode than TiO_2-NTs/SnO_2-Sb-PTFE and Ti/SnO_2-Sb/SnO_2-

Sb-CNT during the first hour. It could be attributed to the production of active chlorine in the presence of Cl^- (Eqn. 3.7 – 3.9). In LSV experiments of the three electrodes in 3 M NaCl, the dramatic increase of current in the potential range of 1.1 V – 1.5 V (vs Ag/AgCl) shows that the active chlorine is produced before the OER (Fig. 5.6). Massive production of active chlorine is responsible for the fast TOC removal during the initial stage of bulk electrolysis of BPA. On the other hand, BPA may undergo dramatic chlorination reactions to produce organochlorine intermediates, which are more recalcitrant for subsequent degradation and more toxic. In fact, accumulation of foam was observed during bulk electrolysis of BPA in 0.1 M NaCl supporting electrolyte with BDD anode, which may be an evidence of the polymerization of the organochlorine intermediates. However, such effect was not observed when using modified SnO_2-Sb anodes, demonstrating that $HO^{\bullet}$ is generated and participates in the electrocatalytic oxidation of BPA in NaCl supporting electrolyte. The slower BPA degradation rate but higher TOC removal with Ti/SnO_2-Sb/SnO_2-Sb-CNT anode indicates that less chlorinated byproducts is generated, which is an important advantage over BDD for electrocatalytic oxidation of BPA in NaCl supporting electrolyte.

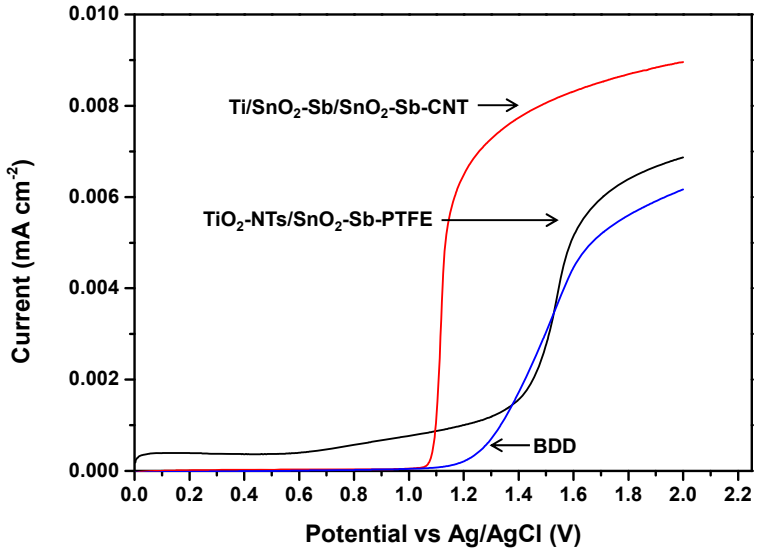

Fig. 5.6 Linear sweep voltammetric curves of TiO_2-NTs/SnO_2-Sb-PTFE, Ti/SnO_2-Sb/SnO_2-Sb-CNT and BDD anodes in 3 M NaCl at a scan rate of 50 mV s^{-1}.

5.3.2.4 Concentration change of chlorine species

Since active chlorine species are expected to play an important role in the electrochemical oxidation of BPA in 0.1 M NaCl, more detailed information could be provided by examining the production of chlorine species. Apart from Cl^- which has been originally presented in the synthetic wastewater, considerable amount of chlorate (ClO_3^-) could also been detected by IC for the treated water. However, other chorine species such as hypochlorite (ClO^-), chlorite (ClO_2^-) and perchlorate (ClO_4^-) could not be detected by IC. The absence of ClO^- and ClO_2^- in water may due to their nature of high reactivity and weak stability in water, which may results in their decomposition to more stable chlorine species or reaction with BPA. ClO^- and ClO_2^- have been reported to decompose spontaneously through the following reactions (Adam and Gordon 1999):

$$3ClO^- \rightarrow ClO_3^- + 2Cl^- \quad (5.1)$$

$$ClO^- + ClO_2^- \rightarrow ClO_3^- + Cl^- \quad (5.2)$$

$$2ClO^- \rightarrow 2Cl^- + O_2 \quad (5.3)$$

Moreover, the generation of ClO_4^- is not favorable since it requires excessive oxidation potential. As a result, Cl^- and ClO_3^- are the dominant chlorine species in treated water.

Fig. 5.7 shows the evolution of the percentages of ClO_3^- and residual Cl^- in synthetic wastewater during the electrochemical oxidation of BPA in 0.1 M NaCl. There are Cl losses in the wastewater with all of the three anodes. For BDD anode, only 94.2% of initial Cl is detected as Cl^- and ClO_3^- after 6-h bulk electrolysis, while the values are 96.2% and 97.9% for TiO_2-NTs/SnO_2-Sb-PTFE and Ti/SnO_2-Sb/SnO_2-Sb-CNT anodes. Cl_2 is produced and they could be released from the synthetic wastewater as gas Cl_2, contributing to the loss of initial Cl. Among the three electrodes, BDD has a relatively high chorine evolution potential of 1.3 V (vs

Ag/AgCl) and the smallest peak current (Fig. 5.6), indicating its less drastic Cl_2 generation. However, the highest level of Cl loss is observed with BDD, demonstrating that more Cl^- has been involved in the generation of organochlorine compounds during BPA oxidation. This is in agreement with its rapid BPA degradation and slow TOC removal (Fig. 5.5). Apart from the Cl loss, BDD and the modified SnO_2 anodes also exhibit significantly different performance for the amount of ClO_3^- produced. For TiO_2-NTs/SnO_2-Sb-PTFE and Ti/SnO_2-Sb/SnO_2-Sb-CNT, the final ClO_3^- only corresponds to 0.36% and 0.24% of the initial Cl in treated water after 6-h bulk electrolysis experiments. Nevertheless, the value is 10.87% for BDD, which increases by a factor greater than 30 comparing with those of modified SnO_2-Sb anodes. In BDD, steady formation of ClO_3^- is observed after 2 h, but the Cl loss seems to slow down. This is probably due to the dramatic formation of organochlorine compounds during the first 2 h, which consumed a large amount of Cl^-. After that, the oxidation power of active chlorine species is not strong enough for further degradation of organochlorine byproducts. Least Cl loss was detected during electrocatalytic oxidation of BPA with Ti/SnO_2-Sb/SnO_2-Sb-CNT anode. Therefore, it exhibits the best performance for BPA oxidation. The SO_4^- concentrations of the treated water were also determined by IC when using Na_2SO_4 as supporting electrolyte. Negligible change of SO_4^- concentration was detected during bulk electrolysis of BPA at various solution pH, demonstrating that Na_2SO_4 was quite stable and did not involve in the electrocatalytic oxidation of BPA.

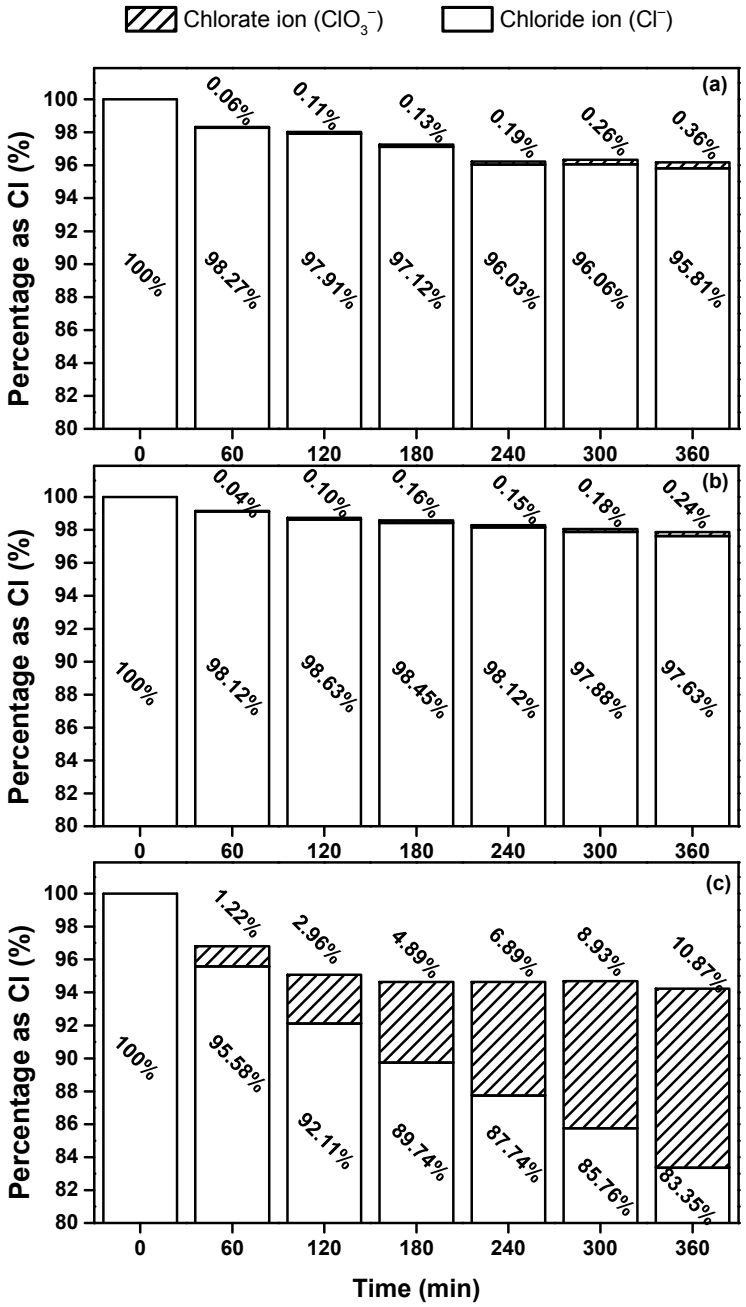

Fig. 5.7 Evolution of percentages of Cl existing as Cl^- and ClO_3^- during electrochemical oxidation of synthetic wastewater consisting of 100 mg L^{-1} BPA and 0.1 M NaCl with (a) TiO_2-NTs/SnO_2-Sb-PTFE, (b) Ti/SnO_2-Sb/SnO_2-Sb-CNT and (c) BDD.

5.3.3 Intermediate products and reaction pathways

5.3.3.1 Aromatic intermediates

Since both BDD and modified SnO_2 anodes are non-active anodes, the non-

selective oxidation of BPA by surface-generated $HO^{\bullet}$ could lead to the generation of various intermediate products via different pathways, including electron transfer, hydrogen abstraction and radical addition (Oppenländer 2007). Among them, aromatic byproducts of BPA are of great concern due to the potential endocrine-disrupting activity and other toxicity. Thus, identification of the aromatic byproducts helps to understand the reaction pathway of BPA degradation as well as the environmental benignity of the electrochemical oxidation process. LC–MS/MS were used to analyze the aromatic intermediates of treated water with initial solution pH of 7. Table 5.1 summarizes the five main compounds that were detected by LC–MS/MS. The product ions at m/Z of 241, 243, 257 and 259 are attributed to the $[M - H]^-$ ions of aromatic intermediates (Fig. 5.8). The $[M - H]^-$ ion of BPA was also detected at m/Z 227. When the bulk electrolysis of BPA was conducted in NaCl supporting electrolyte, none of the peaks associated with the above-mentioned intermediates were detected. However, various peaks with high signal intensity were observed in m/Z range of 400 to 1200, which could be probably due to the polymerization of organochlorine byproducts (Fig. 5.9).

Table 5.1 Compounds detected through LC-MS/MS

Name of compound	Retention time (min)	m/Z	Structure
4-[2-(3,4-dihydroxyphenyl)propan-2-yl]-quinone	4.22	257	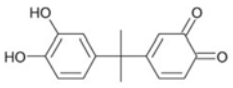
BPA dicatechol	4.23	259	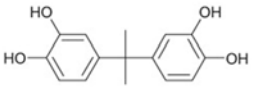
BPA 3,4-quinone	5.18	241	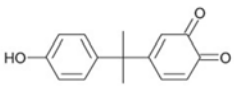
BPA catechol	5.19	243	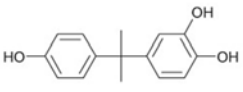
BPA	6.15	227	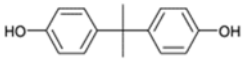

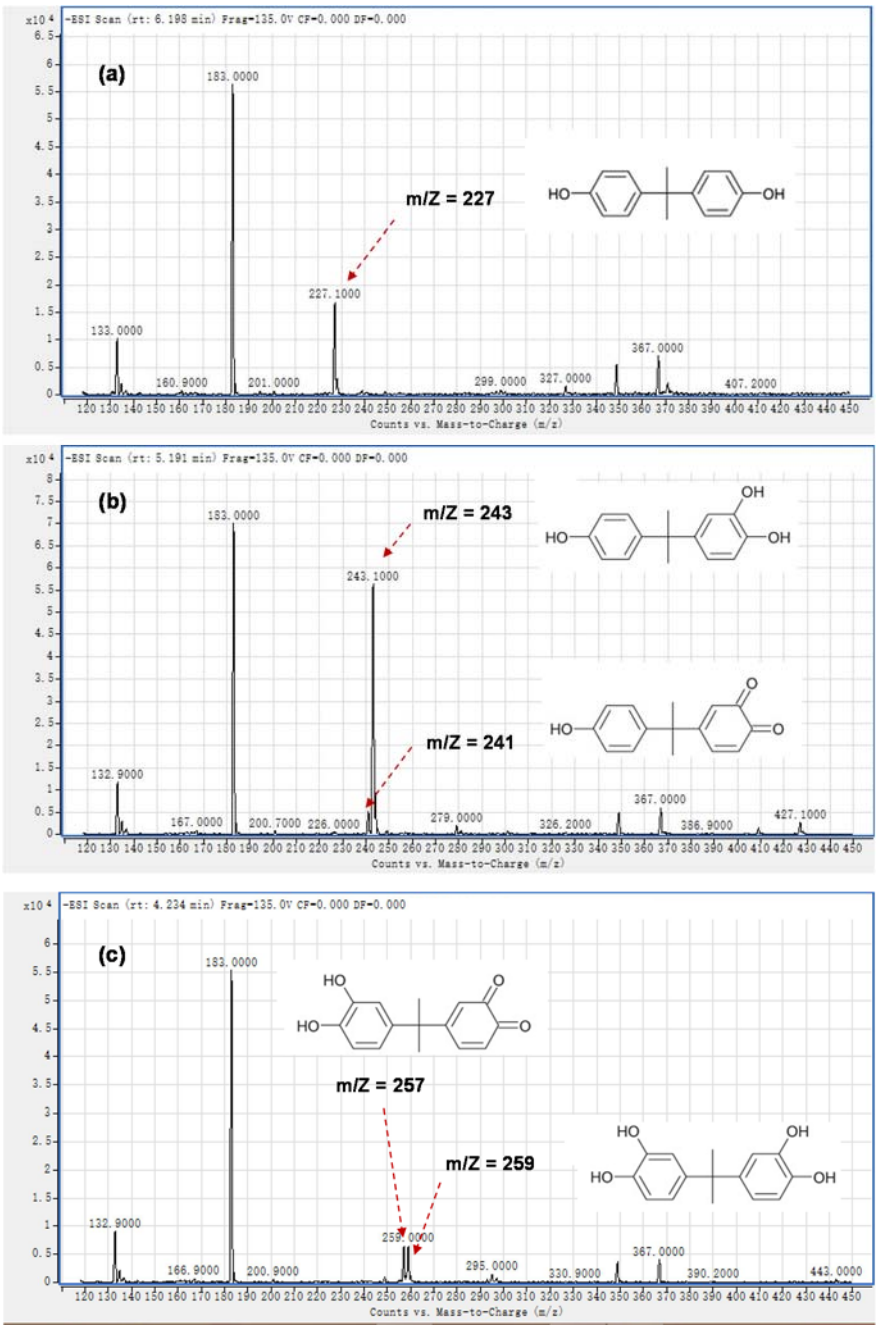

Fig. 5.8 Mass spectra of the main peaks of LC–MS/MS chromatogram. Experimental condition: [BPA] = 100 mg L^{-1}, 0.05 M Na_2SO_4, I = 0.16 A, BDD anode, electrolysis time = 1 h.

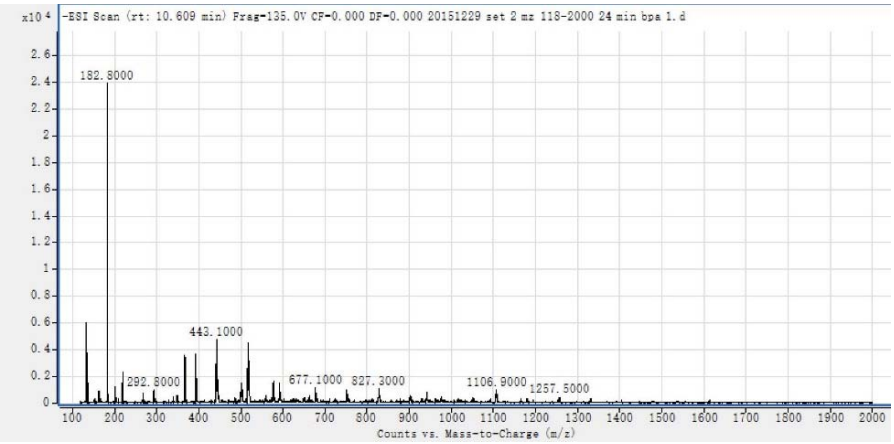

Fig. 5.9 Mass spectra of the main peaks of LC–MS/MS chromatogram at retention time of 10.6 min. Experimental condition: [BPA] = 100 mg L^{-1}, 0.1M NaCl, I = 0.16 A, BDD anode, electrolysis time = 1 h.

5.3.3.2 Aliphatic acid intermediates

Aliphatic acids could be generated after ring-opening reactions of BPA molecules or aromatic intermediates. Various aliphatic acid intermediates for electrocatalytic oxidation of BPA have been reported in literature (Cui et al. 2009b). In this study, several acids including formic acid, acetic acid and oxalate acid were quantified through IC. Fig. 5.10 shows the concentration evolution of the detected aliphatic acids in 0.05 M Na_2SO_4 at different solution pH. The concentrations of the aliphatic acids are expressed as carbon content (mg.C L^{-1}) for ease comparing their contribution to the TOC of wastewater. It is clear that the formation and accumulation of aliphatic acids are influenced by both the anode material and solution pH. Formic acid and oxalic acid are found to be produced in larger amount in pH 3 solution, while the production of acetic acid is favorable at pH 11. Among them, oxalic acid contributes most to the TOC with all the three anodes. Therefore, the production of formic acid and acetic acid intermediates may be pH-dependent. Besides, the concentrations of oxalic acid increase rather fast in the first hour, and start to decay after 1 – 2 hours at pH 7 and pH 11 solutions and 3 hours at pH 3 solution. Although the completely removal of the aliphatic acids is not obtained within the period of bulk

electrolysis, they are environmentally benign compounds which would not cause secondary pollution.

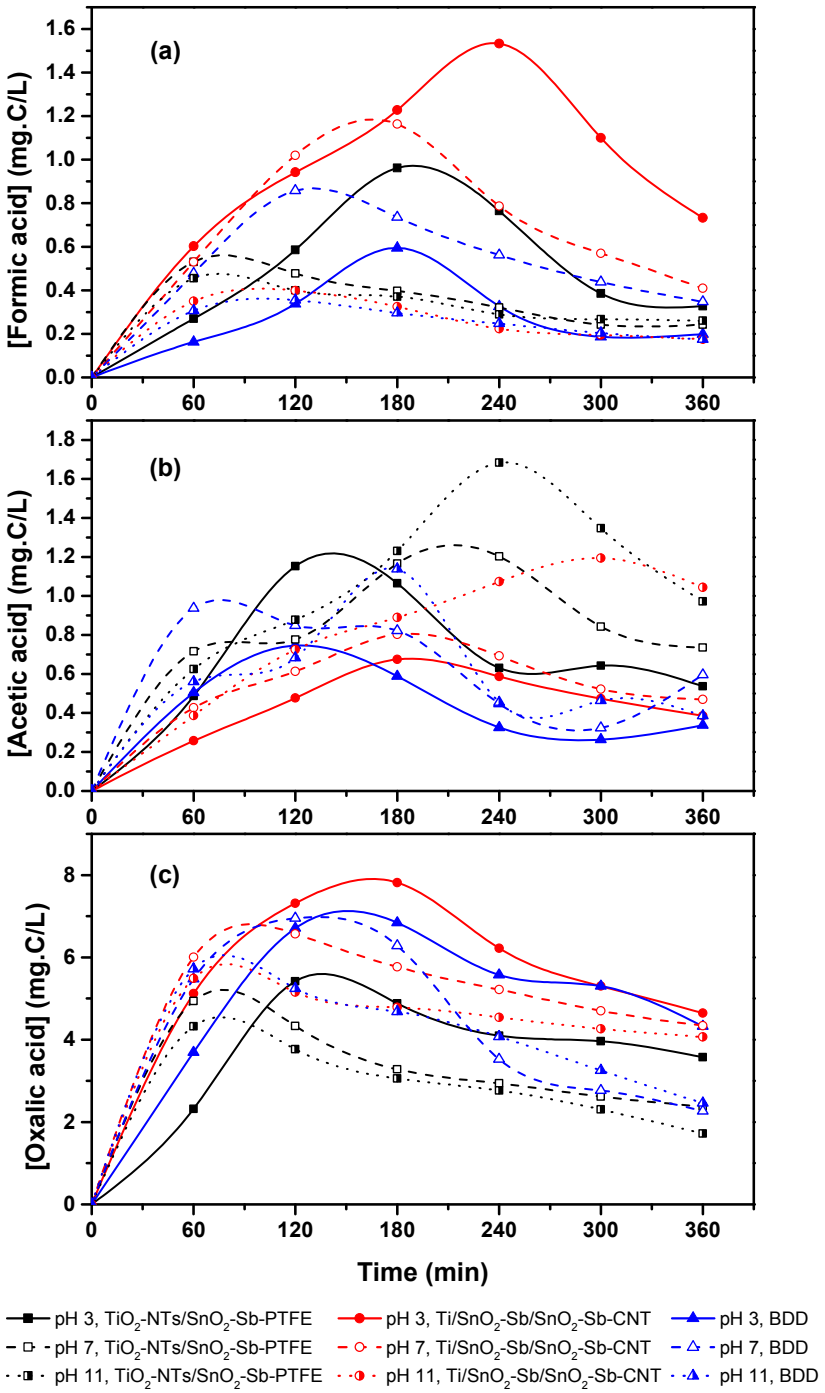

Fig. 5.10 Evolution of (a) formic acid, (b) acetic acid and (c) oxalic acid during the bulk electrolysis of BPA in 0.05M Na_2SO_4 at pH of 3, 7 and 11.

In 0.1 M NaCl, the behavior of aliphatic acid production could be quite different during the bulk electrolysis of BPA (Fig. 5.10). Continuous accumulation of formic acid and acetic acid were observed throughout the bulk electrolysis process, resulting in their much higher concentrations after 6 h. It indicates that the active chlorine species are not effective enough to completely degrade them CO_2 and H_2O. However, oxalic acid accumulates very fast during the first hour, and then degrades steadily after reaching the maximum concentration. The oxidation of oxalic acid may lead to the formation of formic acid and CO_2 (Eqn. 5.4), thus contributing to the reduction of TOC and continuous accumulation of formic acid.

$$C_2H_2O_4 \rightarrow CH_2O_2 + CO_2 \quad (5.4)$$

In order to understand the nature of the treated water in NaCl, the percentage contribution of a combination of formic acid, acetic acid and oxalic acid to the solution TOC are calculated and shown in Fig. 5.11. The detected aliphatic acids account for 8% to 10% of solution TOC after 1-h bulk electrolysis of BPA with the modified SnO_2 anode, smaller than that of BDD (11%). However, after 6-h bulk electrolysis, the values for TiO_2-NTs/SnO_2-Sb-PTFE and Ti/SnO_2-Sb/SnO_2-Sb-CNT are 41% and 44% respectively, which are much larger than that of BDD (19%). Since BPA molecules have been totally removed with BDD anodes after 1 h (Fig. 5.5), the rest of TOC must be originated from the aromatic intermediates and organochlorine intermediates and aliphatic acids. When using BDD anode, the less contribution of aliphatic acids to TOC of the treated water indicates that the aromatic and organochlorine intermediates are not effectively degraded. Since those byproducts are likely to exhibit higher toxicity than aliphatic acids, the use of BDD anode for the treatment of wastewater which contains a large amount of Cl^- must be executed with great caution.

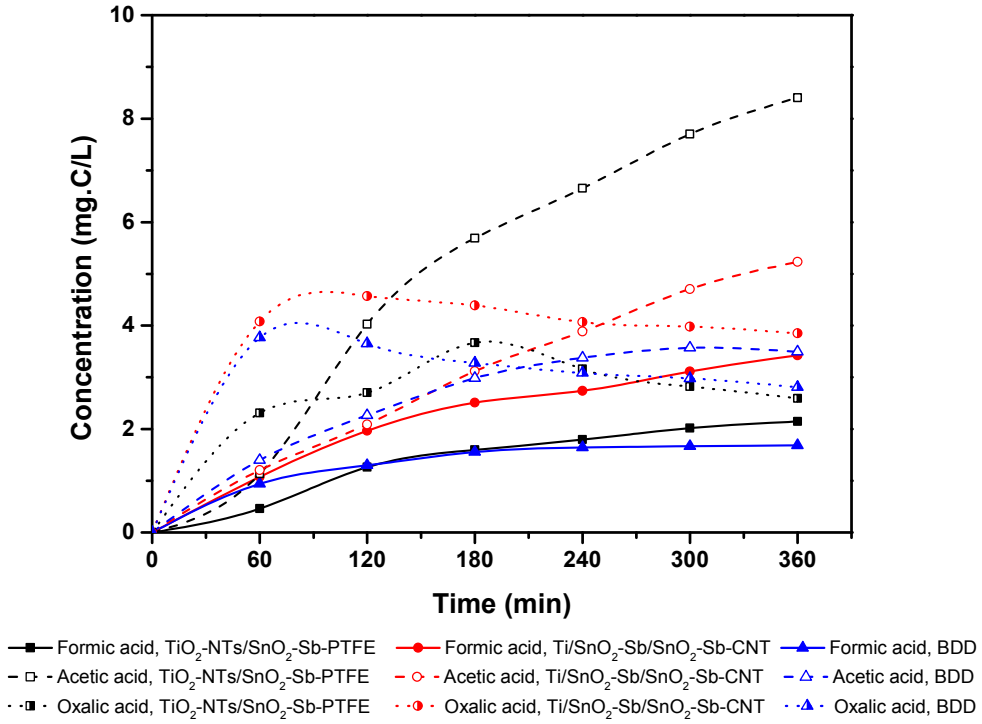

Fig. 5.11 Evolution of (a) formic acid, (b) acetic acid and (c) oxalic acid during the bulk electrolysis of BPA in 0.1 M NaCl at pH 7.

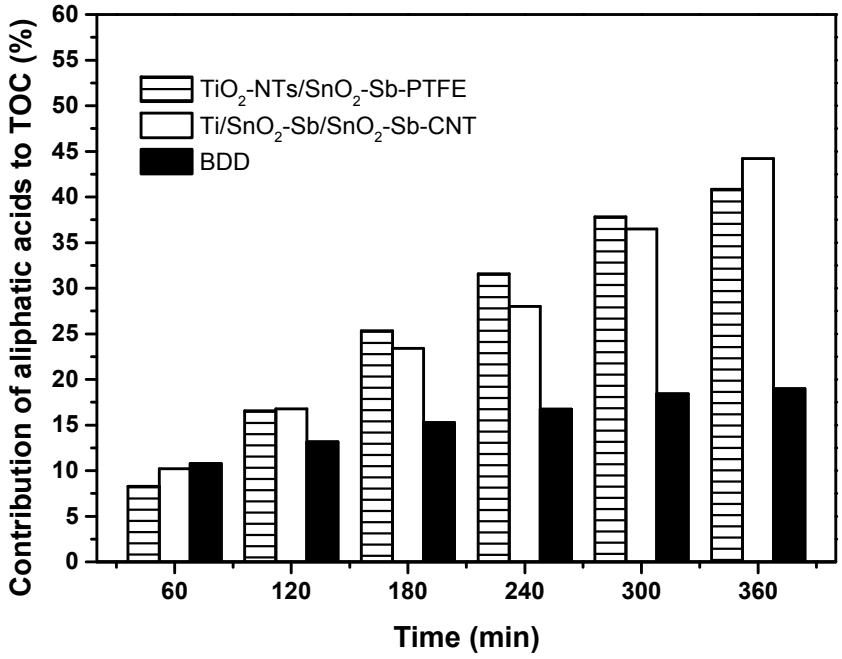

Fig. 5.12 Evolution of the contribution of the aliphatic acids to the TOC during bulk electrolysis of BPA in 0.1 M NaCl at pH 7.

5.3.3.3 Reaction pathway

The possible reaction pathways for electrocatalytic oxidation of BPA are proposed and shown in Fig. 5.12. In Na_2SO_4 supporting electrolyte, $HO^{\bullet}$ seems to firstly attack the aromatic ring of BPA and generate hydroxylated products such as BPA catechol and BPA dicatechol through radical addition. Then the hydroxylated products are subsequently oxidized by $HO^{\bullet}$ through dehydrogenation reaction and form byproducts of 4-[2-(3,4-dihydroxyphenyl)propan-2-yl]-quinone and BPA 3,4-quinone. Kitamura et al. (2005) investigated the estrogenic activity of BPA derivatives and their findings suggested that the estrogenic activity of BPA could be reduced by additional hydroxyl groups on the aromatic ring. Therefore, BPA catechol and BPA dicatechol are supposed to exhibit less endocrine-disrupting activity. However, BPA 3,4-quinone has been reported to cause the oxidative DNA damage of liver and thus it has to be completely removed (Sakuma et al. 2010). LC–MS/MS results indicate that BPA 3,4-quinone has been totally degraded after 4 h, 5 h and 5 h with TiO_2-NTs/SnO_2-Sb-PTFE, Ti/SnO_2-Sb/SnO_2-Sb-CNT and BDD anodes, respectively. In NaCl supporting electrolyte, the generation of active chlorine lead to the formation of organochlorine byproducts by chlorination reactions. They can further undergo polymerization reactions to produce the polymer byproducts, which are more resistant for oxidation. The formation of aliphatic acids demonstrates that the ring-opening reactions of BPA and its aromatic byproducts occurred. Finally, they are completely mineralized to CO_2 and H_2O and the TOC is decreased.

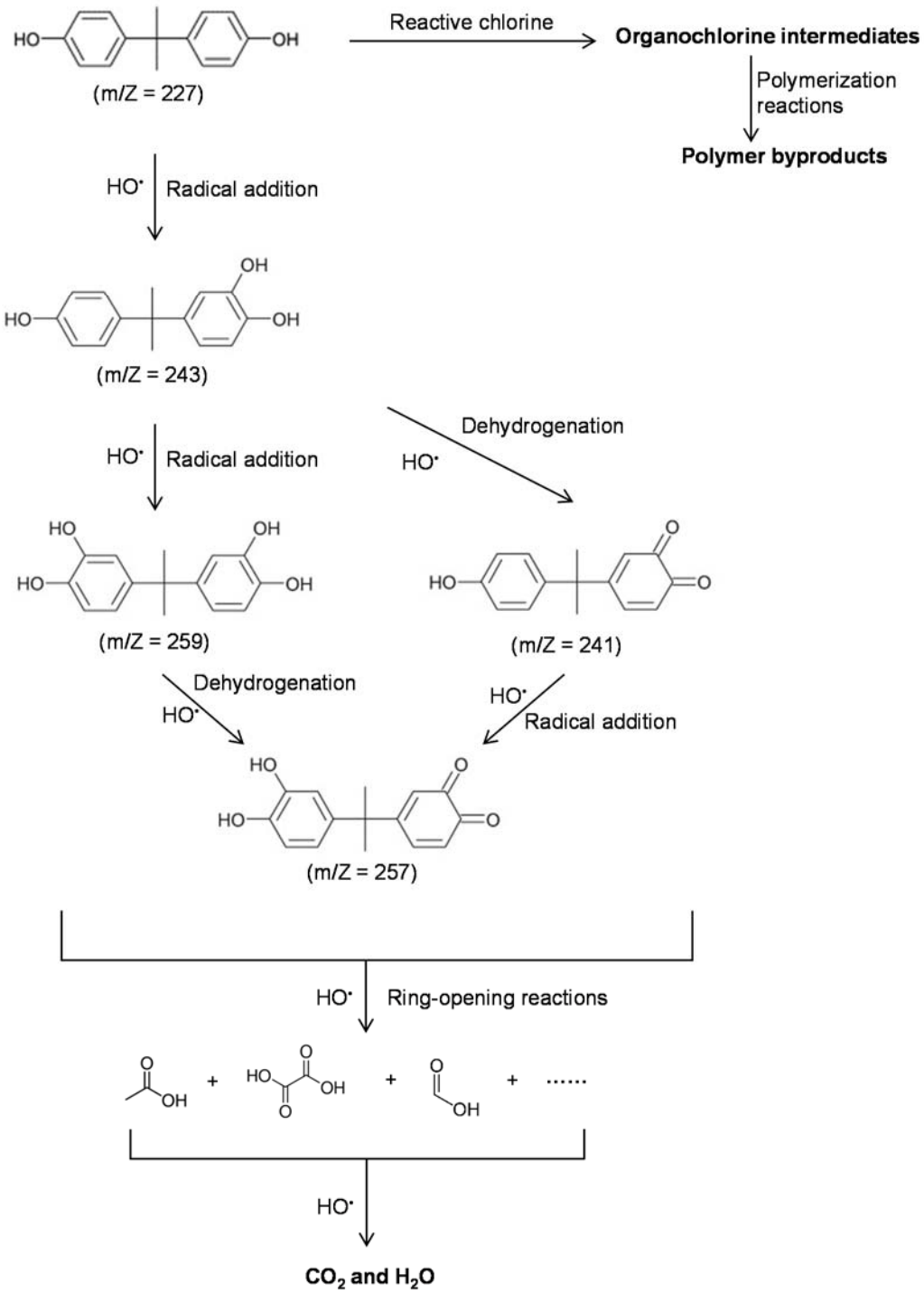

Fig. 5.13 Proposed reaction pathways of electrocatalytic oxidation of BPA by the anodes.

5.4 Conclusions

A comparative study on the eletrochemical oxidation of BPA by TiO_2-NTs/SnO_2-Sb-PTFE, Ti/SnO_2-Sb/SnO_2-Sb-CNT and the commercial BDD anode was conducted. BDD anode exhibits the most superior electrocatalytic activity for BPA oxidation in 0.05 M Na_2SO_4, due to its high OEP and effective utilization of $HO^{\bullet}$. However, Ti/SnO_2-Sb/SnO_2-Sb-CNT shows the best electrocatalytic activity for BPA oxidation in 0.1 M NaCl with the least Cl loss and ClO_3^- generation. While using BDD anode may lead to the dramatic formation of organochlorine intermediates and their resulting polymer byproducts, which may cause toxicity in the treated water. The degradation of BPA occurs through a reaction pathway with four main aromatic intermediates identified by LC–MS/MS and three aliphatic intermediates quantified by IC. Hydroxylation, dehydrogenation and ring-opening reactions are involved in the reaction pathways.

CHAPTER 6 CONCLUSIONS AND RECOMMENDATIONS

6.1 Overall conclusions

In this study, two types of modified SnO_2-Sb electrodes were fabricated through pulse electrodeposition method. Extensive characterization of the resulting electrodes have been carried out including FESEM/EDX, TEM, XRD, XPS, LSV and CV. Their electrocatalytic activities for electrochemical oxidation of phenol were evaluated using a single-compartment batch cell. Influences of operating parameters such as solution pH, type of supporting electrolyte and applied current density on the performance efficiency were studied.

It was found that TiO_2-NTs/SnO_2-Sb-PTFE(4.5), a novel SnO_2-Sb electrode with hydrophobic surface, had a high electrocatalytic activity for phenol oxidation due to its superior ability of $HO^{\bullet}$ generation. TiO_2-NTs/SnO_2-Sb-PTFE(4.5) also exhibited higher OEP (2.4 V vs Ag/AgCl (3 M NaCl)), smaller electrochemical resistance and better electrochemical stability than the conventional Ti/SnO_2-Sb (2.0 V vs Ag/AgCl (3 M NaCl)) fabricated by thermochemical decomposition.

Ti/SnO_2-Sb/SnO_2-Sb-CNT(0.8), a duplex-structured SnO_2-Sb electrode modified by incorporation of SnO_2-Sb-CNT composite, could enable the synergistic adsorption and electrochemical oxidation of phenol. It exhibited good adsorption capacity for phenol, high oxygen evolution potential (2.2 V vs Ag/AgCl (3 M NaCl)), large electroactive surface area and good electrochemical stability. Moreover, it was stable over a wide range of current density and under acidic to neutral condition, making it economically attractive for practical applications.

Finally, the modified SnO_2-Sb electrodes including TiO_2-NTs/SnO_2-Sb-PTFE(4.5)

and Ti/SnO_2-Sb/SnO_2-Sb-CNT(0.8) were compared with the commercial BDD electrode with respect to the electrochemical oxidation of BPA. It was found that the type of supporting electrolyte had the most significant influence on the electrocatalytic performance of the three electrodes. In Na_2SO_4, commercial BDD could degrade BPA most effectively but the results obtained with modified SnO_2-Sb electrodes were comparable with that of BDD. However, in the presence of Cl^-, Ti/SnO_2-Sb/SnO_2-Sb-CNT showed the best electrocatalytic activity for BPA oxidation, and the generation of organochlorine intermediates and polymer byproducts posed a main disadvantage to commercial BDD. Therefore, the versatile performance of the modified SnO_2-Sb electrodes for BPA degradation and showed a great potential as alternative anodes to BDD for practical applications.

6.2 Recommendations for future research

To further extend the potential application of the modified SnO_2-Sb electrode for industrial wastewater treatment, the following recommendations for future research are proposed:

1. Highly active SnO_2-Sb electrode

- Novel fabrication methods should be developed to prepare highly active SnO_2-Sb electrode with further improved electrocatalytic activity and electrochemical stability. It can be achieved through further modification of existing fabrication method or combining existing fabrication method with other techniques.
- Other characterization techniques could be employed to gain more in-depth insights into the relationship between physicochemical properties and the material performance. Such characterization techniques include Fourier transform infrared spectroscopy (FTIR), thermogravimetric analysis (TGA) and atomic force microscopy (AFM).

- Considering that various intermediates can be produced at different stages of electrocatalytic oxidation of recalcitrant organics, the toxicity of the treated water has to be assessed at various stages of electrochemical process.
- The fouling or deactivation mechanism of modified SnO_2-Sb electrode should be further investigated, as well as the regeneration of the used SnO_2-Sb electrode.

2. Electrochemical cell design and operation

- Other design of electrochemical cell such as flow cell or filter press could be applied for long-term electrochemical oxidation tests and large volume of wastewater treated in continuous flow mode.
- Pilot-scale operation is important to investigate the economical performance of electrochemical oxidation for practical applications.
- Electrochemical cell with divided anodic and cathodic chambers separated by ion exchange membrane could be applied. The divided electrochemical cell has the advantages of: (1) the oxidation products at the anode will not become the competitive species for reduction reaction at the cathode, therefore the overall process efficiency could be improved; (2) the determination of the reaction mechanism in the anodic chamber would be more precise by avoiding the above mentioned process which may falsify the primary electrochemical reactions..

3. Electrochemical oxidation coupled with other processes

- For industrial wastewaters containing recalcitrant organic compounds, electrochemical oxidation could be considered as an effective pretreatment method before their toxicity is alleviated to acceptable levels for biological treatment.
- Electrochemical oxidation could also be utilized as post-treatment of reverse osmosis (RO) concentrate or landfill leachates treated with membrane

bioreactor, in order to achieve efficient reduction of COD and color.

- Other techniques such as pressure-driven membrane process, ultrasonic irradiation, photoelectrochemical process and so on could be coupled with electrochemical oxidation to boost the process performance as well as reducing the electrode fouling.

REFERENCES

Adam, L.C. and Gordon, G. (1999), "Hypochlorite ion decomposition: Effects of temperature, ionic strength, and chloride ion", Inorganic Chemistry, Vol. 38, No. 6, pp. 1299-1304.

Adams, B., Tian, M. and Chen, A. (2009), "Design and electrochemical study of SnO_2-based mixed oxide electrodes", Electrochimica Acta, Vol. 54, No. 5, pp. 1491-1498.

Al, S.-Y., Li, J.-Q., Li, L.-P., Peng, H.-Q., Yang, Y. and Jin, L.-T. (2005), "Electrochemical Deposition and Properties of Nanometer-structure Ce-doped Lead Dioxide Film Electrode", Chinese Journal of Chemistry, Vol. 23, No. 1, pp. 71-75.

Alfaro, M.A.Q., Ferro, S., Martinez-Huitle, C.A. and Vong, Y.M. (2006), "Boron doped diamond electrode for the wastewater treatment", Journal of the Brazilian Chemical Society, Vol. 17, No. 2, pp. 227-236.

An, H., Cui, H., Zhang, W., Zhai, J., Qian, Y., Xie, X. and Li, Q. (2012), "Fabrication and electrochemical treatment application of a microstructured TiO_2-NTs/Sb–SnO_2/PbO_2 anode in the degradation of C.I. Reactive Blue 194 (RB 194)", Chemical Engineering Journal, Vol. 209, pp. 86-93.

An, H., Li, Q., Tao, D., Cui, H., Xu, X., Ding, L., Sun, L. and Zhai, J. (2011), "The synthesis and characterization of Ti/SnO_2–Sb_2O_3/PbO_2 electrodes: The influence of morphology caused by different electrochemical deposition time", Applied Surface Science, Vol. 258, No. 1, pp. 218-224.

Andrade, L.S., Rocha-Filho, R.C., Bocchi, N., Biaggio, S.R., Iniesta, J., Garcia-Garcia, V. and Montiel, V. (2008), "Degradation of phenol using Co- and Co,F-doped PbO_2 anodes in electrochemical filter-press cells", Journal of Hazardous

materials, Vol. 153, No. 1-2, pp. 252-260.

Andreozzi, R., Marotta, R. and Paxeus, N. (2003), "Pharmaceuticals in STP effluents and their solar photodegradation in aquatic environment", Chemosphere, Vol. 50, No. 10, pp. 1319-1330.

Anglada, A., Urtiaga, A. and Ortiz, I. (2009), "Contributions of electrochemical oxidation to waste-water treatment: fundamentals and review of applications", Journal of Chemical Technology and Biotechnology, Vol. 84, No. 12, pp. 1747-1755.

Arafat, M.M., Dinan, B., Akbar, S.A. and Haseeb, A.S.M.A. (2012), "Gas Sensors Based on One Dimensional Nanostructured Metal-Oxides: A Review", Sensors, Vol. 12, No. 6, pp. 7207-7258.

Ardizzone, S., Fregonara, G. and Trasatti, S. (1990), "Inner and Outer Active Surface of RuO_2 Electrodes", Electrochimica Acta, Vol. 35, No. 1, pp. 263-267.

Armijo, F., Torres, I., Tapia, R., Molero, L., Antilen, M., del Rio, R., del Valle, M.A. and Ramirez, G. (2010), "Captopril Electrochemical Oxidation on Fluorine-Doped SnO_2 Electrodes and Their Determination in Pharmaceutical Preparations", Electroanalysis, Vol. 22, No. 19, pp. 2269-2276.

Asaithambi, P., Garlanka, L., Anantharaman, N. and Matheswaran, M. (2012), "Influence of Experimental Parameters in the Treatment of Distillery Effluent by Electrochemical Oxidation", Separation Science and Technology, Vol. 47, No. 3, pp. 470-481.

Awad, H.S. and Galwa, N.A. (2005), "Electrochemical degradation of Acid Blue and Basic Brown dyes on Pb/PbO_2 electrode in the presence of different conductive electrolyte and effect of various operating factors", Chemosphere, Vol. 61, No. 9, pp. 1327-1335.

Bagastyo, A.Y., Batstone, D.J., Rabaey, K. and Radjenovic, J. (2013), "Electrochemical oxidation of electrodialysed reverse osmosis concentrate on

Ti/Pt-IrO_2, Ti/SnO_2-Sb and boron-doped diamond electrodes", Water Research, Vol. 47, No. 1, pp. 242-250.

Bagastyo, A.Y., Radjenovic, J., Mu, Y., Rozendal, R.A., Batstone, D.J. and Rabaey, K. (2011), "Electrochemical oxidation of reverse osmosis concentrate on mixed metal oxide (MMO) titanium coated electrodes", Water Research, Vol. 45, No. 16, pp. 4951-4959.

Basha, C.A., Sendhil, J., Selvakumar, K.V., Muniswaran, P.K.A. and Lee, C.W. (2012), "Electrochemical degradation of textile dyeing industry effluent in batch and flow reactor systems", Desalination, Vol. 285, pp. 188-197.

Blanco, S., Carrazan, S.R.G. and Rives, V. (2008), "Oxidative dehydrogenation of propane on Mg-V-Al mixed oxides", Applied Catalysis a-General, Vol. 342, No. 1-2, pp. 93-98.

Bock, C. and MacDougall, B. (1999), "The anodic oxidation of p-benzoquinone and maleic acid", Journal of the Electrochemical Society, Vol. 146, No. 8, pp. 2925-2932.

Borras, C., Berzoy, C., Mostany, J., Herrera, J.C. and Scharifker, B.R. (2007), "A comparison of the electrooxidation kinetics of p-methoxyphenol and p-nitrophenol on Sb-doped SnO_2 surfaces: Concentration and temperature effects", Applied Catalysis B-Environmental, Vol. 72, No. 1-2, pp. 98-104.

Borras, C., Laredo, T. and Scharifker, B.R. (2003), "Competitive electrochemical oxidation of p-chlorophenol and p-nitrophenol on Bi-doped PbO_2", Electrochimica Acta, Vol. 48, No. 19, pp. 2775-2780.

Bouya, H., Errami, M., Salghi, R., Bazzi, L., Zarrouk, A., Al-Deyab, S.S., Hammouti, B., Bazzi, L. and Chakir, A. (2012), "Electrochemical Degradation of Cypermethrin Pesticide on a SnO_2 Anode", International Journal of Electrochemical Science, Vol. 7, No. 4, pp. 3453-3465.

Brillas, E., Sires, I. and Oturan, M.A. (2009), "Electro-Fenton Process and Related

Electrochemical Technologies Based on Fenton's Reaction Chemistry", Chemical Reviews, Vol. 109, No. 12, pp. 6570-6631.

Canevari, T.C., Vinhas, R.C.G., Landers, R. and Gushikem, Y. (2011), "$SiO_2/SnO_2/Sb_2O_5$ microporous ceramic material for immobilization of Meldola's blue: Application as an electrochemical sensor for NADH", Biosensors and Bioelectronics, Vol. 26, No. 5, pp. 2402-2406.

Canizares, P., Paz, R., Lobato, J., Saez, C. and Rodrigo, M.A. (2006), "Electrochemical treatment of the effluent of a fine chemical manufacturing plant", Journal of Hazardous materials, Vol. 138, No. 1, pp. 173-181.

Carlesi Jara, C., Fino, D., Specchia, V., Saracco, G. and Spinelli, P. (2007), "Electrochemical removal of antibiotics from wastewaters", Applied Catalysis B: Environmental, Vol. 70, No. 1-4, pp. 479-487.

Carlesi Jara, C., Salazar-Banda, G.R., Arratia, R.S., Campino, J.S. and Aguilera, M.I. (2011), "Improving the stability of Sb doped Sn oxides electrode thermally synthesized by using an acid ionic liquid as solvent", Chemical Engineering Journal, Vol. 171, No. 3, pp. 1253-1262.

Catanho, M., Malpass, G.R.P. and Motheo, A.J. (2006), "Photoelectrochemical treatment of the dye reactive red 198 using DSA® electrodes", Applied Catalysis B: Environmental, Vol. 62, No. 3-4, pp. 193-200.

Chai, S., Zhao, G., Li, P., Lei, Y., Zhang, Y.-n. and Li, D. (2011), "Novel Sieve-Like SnO_2/TiO_2Nanotubes with Integrated Photoelectrocatalysis: Fabrication and Application for Efficient Toxicity Elimination of Nitrophenol Wastewater", The Journal of Physical Chemistry C, Vol. 115, No. 37, pp. 18261-18269.

Chaiyont, R., Badoe, C., de León, C.P., Nava, J.L., Recio, F.J., Sirés, I., Herrasti, P. and Walsh, F.C. (2013), "Decolorization of Methyl Orange Dye at IrO_2-SnO_2-Sb_2O_5 Coated Titanium Anodes", Chemical Engineering and Technology, Vol. 36, No. 1, pp. 123-129.

Chaplin, B.P. (2014), "Critical review of electrochemical advanced oxidation processes for water treatment applications", Environ Sci Process Impacts, Vol. 16, No. 6, pp. 1182-1203.

Chatzisymeon, E., Xekoukoulotakis, N.P., Coz, A., Kalogerakis, N. and Mantzavinos, D. (2006), "Electrochemical treatment of textile dyes and dyehouse effluents", Journal of Hazardous materials, Vol. 137, No. 2, pp. 998-1007.

Chellammal, S., Kalaiselvi, P., Ganapathy, P. and Subramanian, G. (2012), "Anodic incineration of phthalic anhydride using RuO_2–IrO_2–SnO_2–TiO_2 coated on Ti anode", Arabian Journal of Chemistry.

Chen, F., Yu, S., Dong, X. and Zhang, S. (2012a), "High-efficient treatment of wastewater contained the carcinogen naphthylamine by electrochemical oxidation with gamma-Al_2O_3 supported MnO_2 and Sb-doped SnO_2 catalyst", Journal of Hazardous materials, Vol. 227-228, pp. 474-479.

Chen, I.L., Chen, T.Y., Hu, C.C. and Lee, C.H. (2013), "Thermal-induced growth of RuO_2 nanorods from a binary Ru-Ti oxide composite and alteration in supercapacitive characteristics", Journal of Materials Chemistry A, Vol. 1, No. 6, pp. 2039-2049.

Chen, T.S., Huang, K.L. and Pan, Y.C. (2012b), "Electrochemical versus Ce(IV)-Mediated Electrochemical Oxidation (MEO) Degradation of Acetaminophen in Aqueous Solutions", International Journal of Electrochemical Science, Vol. 7, No. 11, pp. 11191-11205.

Chen, X.M., Gao, F.R. and Chen, G.H. (2005), "Comparison of Ti/BDD and Ti/SnO_2-Sb_2O_5 electrodes for pollutant oxidation", Journal of Applied Electrochemistry, Vol. 35, No. 2, pp. 185-191.

Chen, Y., Dong, L., Jin, Y.S., Xu, B. and Ji, W.J. (1996), "Studies on supported metal oxide-oxide support interactions (An incorporation model)", 11th International Congress on Catalysis - 40th Anniversary, Pts a and B, Vol. 101, pp. 1293-1302.

Chen, Y., Hong, L., Xue, H.M., Han, W.Q., Wang, L.J., Sun, X.Y. and Li, J.S. (2010), "Preparation and characterization of TiO_2-NTs/SnO_2-Sb electrodes by electrodeposition", Journal of Electroanalytical Chemistry, Vol. 648, No. 2, pp. 119-127.

Chen, Y., Li, H.Y., Liu, W.J., Tu, Y., Zhang, Y.H., Han, W.Q. and Wang, L.J. (2014), "Electrochemical degradation of nitrobenzene by anodic oxidation on the constructed TiO_2-NTs/SnO_2-Sb/PbO_2 electrode", Chemosphere, Vol. 113, pp. 48-55.

Cheng, C.Y. and Kelsall, G.H. (2007), "Models of Hypochlorite production in electrochemical reactors with plate and porous anodes", Journal of Applied Electrochemistry, Vol. 37, No. 11, pp. 1203-1217.

Cheng, S.A., Fung, W.K., Chan, K.Y. and Shen, P.K. (2003), "Optimizing electron spin resonance detection of hydroxyl radical in water", Chemosphere, Vol. 52, No. 10, pp. 1797-1805.

Cheng, W., Yang, M., Xie, Y., Fang, Z., Nan, J. and Tsang, P.E. (2013a), "Electrochemical degradation of the antibiotic metronidazole in aqueous solution by the Ti/SnO_2–Sb–Ce anode", Environmental Technology, pp. 1-11.

Cheng, W., Yang, M., Xie, Y., Liang, B., Fang, Z. and Tsang, E.P. (2013b), "Enhancement of mineralization of metronidazole by the electro-Fenton process with a Ce/SnO_2–Sb coated titanium anode", Chemical Engineering Journal, Vol. 220, pp. 214-220.

Chu, Y., Zhang, D., Liu, L., Qian, Y. and Li, L. (2013), "Electrochemical degradation of m-cresol using porous carbon-nanotube-containing cathode and Ti/SnO-SbO-IrO anode: Kinetics, byproducts and biodegradability", Journal of Hazardous materials, Vol. 252-253C, pp. 306-312.

Chu, Y.Y., Qian, Y., Wang, W.J. and Deng, X.L. (2012), "A dual-cathode electro-Fenton oxidation coupled with anodic oxidation system used for 4-nitrophenol

degradation", Journal of Hazardous materials, Vol. 199, pp. 179-185.

Cid, C.C.P., Spada, E.R. and Sartorelli, M.L. (2013), "Effect of the cathodic polarization on structural and morphological proprieties of FTO and ITO thin films", Applied Surface Science, Vol. 273, pp. 603-606.

Ciriaco, L., Santos, D., Pacheco, M.J. and Lopes, A. (2011), "Anodic oxidation of organic pollutants on a Ti/SnO_2-Sb_2O_4 anode", Journal of Applied Electrochemistry, Vol. 41, No. 5, pp. 577-587.

Cohn, C.A., Simon, S.R. and Schoonen, M.A.A. (2008), "Comparison of fluorescence-based techniques for the quantification of particle-induced hydroxyl radicals", Particle and Fibre Toxicology, Vol. 5.

Comninellis, C. (1994), "Electrocatalysis in the Electrochemical Conversion/Combustion of Organic Pollutants for Waste-Water Treatment", Electrochimica Acta, Vol. 39, No. 11-12, pp. 1857-1862.

Comninellis, C. and Nerini, A. (1995), "Anodic-Oxidation of Phenol in the Presence of Nacl for Waste-Water Treatment", Journal of Applied Electrochemistry, Vol. 25, No. 1, pp. 23-28.

CorreaLozano, B., Comninellis, C. and DeBattisti, A. (1997), "Service life of Ti/SnO_2-Sb_2O_5 anodes", Journal of Applied Electrochemistry, Vol. 27, No. 8, pp. 970-974.

Cossu, R., Polcaro, A.M., Lavagnolo, M.C., Mascia, M., Palmas, S. and Renoldi, F. (1998), "Electrochemical treatment of landfill leachate: Oxidation at Ti/PbO_2 and Ti/SnO_2 anodes", Environmental Science & Technology, Vol. 32, No. 22, pp. 3570-3573.

Coteiro, R.D., Teruel, F.S., Ribeiro, J. and de Andrade, A.R. (2006), "Effect of solvent on the preparation and characterization of DSA((R))-type anodes containing RuO_2-TiO_2-SnO_2", Journal of the Brazilian Chemical Society, Vol. 17, No. 4, pp. 771-779.

Cui, Y.-H., Feng, Y.-J. and Liu, Z.-Q. (2009a), "Influence of rare earths doping on the structure and electro-catalytic performance of Ti/Sb–SnO_2 electrodes", Electrochimica Acta, Vol. 54, No. 21, pp. 4903-4909.

Cui, Y.H., Li, X.Y. and Chen, G.H. (2009b), "Electrochemical degradation of bisphenol A on different anodes", Water Research, Vol. 43, No. 7, pp. 1968-1976.

Da Silva, L.M., De Faria, L.A. and Boodts, J.F.C. (2001), "Determination of the morphology factor of oxide layers", Electrochimica Acta, Vol. 47, No. 3, pp. 395-403.

Da Silva, L.M., De Faria, L.A. and Boodts, J.F.C. (2002), "Electrochemical impedance spectroscopic (EIS) investigation of the deactivation mechanism, surface and electrocatalytic properties of Ti/RuO_2(x)+Co_3O_4(1-x) electrodes", Journal of Electroanalytical Chemistry, Vol. 532, No. 1-2, pp. 141-150.

Dai, Q., Shen, H., Xia, Y., Chen, F., Wang, J. and Chen, J. (2013), "The application of a novel Ti/SnO_2–Sb_2O_3/PTFE-La-Ce-β-PbO_2 anode on the degradation of cationic gold yellow X-GL in sono-electrochemical oxidation system", Separation and Purification Technology, Vol. 104, pp. 9-16.

Dai, Q., Xia, Y. and Chen, J. (2016a), "Mechanism of enhanced electrochemical degradation of highly concentrated aspirin wastewater using a rare earth La-Y co-doped PbO_2 electrode", Electrochimica Acta, Vol. 188, pp. 871-881.

Dai, Q., Zhou, J., Meng, X., Feng, D., Wu, C. and Chen, J. (2016b), "Electrochemical oxidation of cinnamic acid with Mo modified PbO_2 electrode: Electrode characterization, kinetics and degradation pathway", Chemical Engineering Journal, Vol. 289, pp. 239-246.

Dai, Q., Zhou, J., Weng, M., Luo, X., Feng, D. and Chen, J. (2016c), "Electrochemical oxidation metronidazole with Co modified PbO_2 electrode: Degradation and mechanism", Separation and Purification Technology, Vol. 166, pp. 109-116.

Datta, M.K., Kadakia, K., Velikokhatnyi, O.I., Jampani, P.H., Chung, S.J., Poston,

J.A., Manivannan, A. and Kumta, P.N. (2013), "High performance robust F-doped tin oxide based oxygen evolution electro-catalysts for PEM based water electrolysis", Journal of Materials Chemistry A, Vol. 1, No. 12, pp. 4026-4037.

de Oliveira, M.C.Q., Tanaka, A.A., los Lanza, M.R.D. and Sotomayor, M.D.T. (2011), "Studies of the Electrochemical Degradation of Acetaminophen Using a Real-Time Biomimetic Sensor", Electroanalysis, Vol. 23, No. 11, pp. 2616-2621.

del Río, A.I., Fernández, J., Molina, J., Bonastre, J. and Cases, F. (2010), "On the behaviour of doped SnO_2 anodes stabilized with platinum in the electrochemical degradation of reactive dyes", Electrochimica Acta, Vol. 55, No. 24, pp. 7282-7289.

Deng, C. (2008), "Monolayer dispersion thresholds and threshold effect displayed by supported catalysts", Frontiers of Chemistry in China, Vol. 3, No. 4, pp. 391-399.

Depauli, C.P. and Trasatti, S. (1995), "Electrochemical Surface Characterization of IrO_2+SnO_2 Mixed-Oxide Electrocatalysts", Journal of Electroanalytical Chemistry, Vol. 396, No. 1-2, pp. 161-168.

Desilvestro, J. and Haas, O. (1990), "Metal Oxide Cathode Materials for Electrochemical Energy Storage: A Review", Journal of the Electrochemical Society, Vol. 137, No. 1, pp. 5C-22C.

Devilliers, D. and Mahé, E. (2010), "Modified titanium electrodes: Application to Ti/TiO_2/PbO_2 dimensionally stable anodes", Electrochimica Acta, Vol. 55, No. 27, pp. 8207-8214.

Diaz-Uribe, C.E., Daza, M.C., Martinez, F., Paez-Mozo, E.A., Guedes, C.L.B. and Di Mauro, E. (2010), "Visible light superoxide radical anion generation by tetra(4-carboxyphenyl)porphyrin/TiO_2: EPR characterization", Journal of Photochemistry and Photobiology a-Chemistry, Vol. 215, No. 2-3, pp. 172-178.

Domashevskaya, E.P., Chuvenkova, O.A., Ryabtsev, S.V., Yurakov, Y.A., Kashkarov, V.M., Shchukarev, A.V. and Turishchev, S.Y. (2013), "Electronic structure of

undoped and doped SnO_x nanolayers", Thin Solid Films.

Dryer, D.J. and Korshin, G.V. (2007), "Investigation of the reduction of lead dioxide by natural organic matter", Environmental Science & Technology, Vol. 41, No. 15, pp. 5510-5514.

Duan, T.G., Chen, Y., Wen, Q. and Duan, Y. (2014), "Enhanced electrocatalytic activity of nano-TiN composited Ti/Sb-SnO_2 electrode fabricated by pulse electrodeposition for methylene blue decolorization", Rsc Advances, Vol. 4, No. 101, pp. 57463-57475.

Duverneuil, P., Maury, F., Pebere, N., Senocq, F. and Vergnes, H. (2002), "Chemical vapor deposition of SnO_2 coatings on Ti plates for the preparation of electrocatalytic anodes", Surface & Coatings Technology, Vol. 151, pp. 9-13.

Erler, C. and Novak, J. (2010), "Bisphenol A Exposure: Human Risk and Health Policy", Journal of Pediatric Nursing-Nursing Care of Children & Families, Vol. 25, No. 5, pp. 400-407.

Espinoza, J.D., Drogui, P., Zolfaghari, M., Dirany, A., Ledesma, M.T., Gortares-Moroyoqui, P. and Buelna, G. (2016), "Performance of electrochemical oxidation process for removal of di (2-ethylhexyl) phthalate", Environ Sci Pollut Res Int, Vol. 23, No. 12, pp. 12164-12173.

Fan, J., Zhao, G., Zhao, H., Chai, S. and Cao, T. (2013), "Fabrication and application of mesoporous Sb-doped SnO_2 electrode with high specific surface in electrochemical degradation of ketoprofen", Electrochimica Acta, Vol. 94, pp. 21-29.

Farmer, J.C., Wang, F.T., Lewis, P.R. and Summers, L.J. (1992), "Destruction of Chlorinated Organics by Cobalt(Iii)-Mediated Electrochemical Oxidation", Journal of the Electrochemical Society, Vol. 139, No. 11, pp. 3025-3029.

Feng, C., Sugiura, N., Shimada, S. and Maekawa, T. (2003), "Development of a high performance electrochemical wastewater treatment system", Journal of

Hazardous materials, Vol. 103, No. 1-2, pp. 65-78.

Feng, Y., Cui, Y.H., Liu, J. and Logan, B.E. (2010a), "Factors affecting the electro-catalytic characteristics of Eu doped SnO_2/Sb electrode", Journal of Hazardous materials, Vol. 178, No. 1-3, pp. 29-34.

Feng, Y., Wang, C., Liu, J. and Zhang, Z. (2010b), "Electrochemical degradation of 17-alpha-ethinylestradiol (EE2) and estrogenic activity changes", Journal of environmental monitoring : JEM, Vol. 12, No. 2, pp. 404-408.

Feng, Y.J., Cui, Y.H., Logan, B. and Liu, Z.Q. (2008), "Performance of Gd-doped Ti-based Sb-SnO_2 anodes for electrochemical destruction of phenol", Chemosphere, Vol. 70, No. 9, pp. 1629-1636.

Feng, Y.J., Liu, J.F., Zhu, L.M. and Wei, J.Z. (2013), "Combined technology for clomazone herbicide wastewater treatment: three-dimensional packed-bed electrochemical oxidation and biological contact degradation", Water Science and Technology, Vol. 68, No. 1, pp. 257-260.

Frolova, L., Lyskov, N. and Dobrovolsky, Y. (2012), "Nanostructured Pt/SnO_2-SbO_x-RuO_2 electrocatalysts for direct alcohol fuel cells", Solid State Ionics, Vol. 225, pp. 92-98.

Gao, G. and Vecitis, C.D. (2011), "Electrochemical carbon nanotube filter oxidative performance as a function of surface chemistry", Environmental Science & Technology, Vol. 45, No. 22, pp. 9726-9734.

Gao, J.X., Zhao, G.H., Liu, M.C. and Li, D.M. (2009), "Mechanism of Enhanced Electrochemical Oxidation of 2,4-dichlorophenoxyacetic Acid with in situ Microwave Activated Boron-doped Diamond and Platinum Anodes", Journal of Physical Chemistry A, Vol. 113, No. 39, pp. 10466-10473.

Gawande, M.B., Pandey, R.K. and Jayaram, R.V. (2012), "Role of mixed metal oxides in catalysis science—versatile applications in organic synthesis", Catalysis Science & Technology, Vol. 2, No. 6, p. 1113.

Gelfond, N.V., Morozova, N.B., Igumenov, I.K., Filatov, E.S., Gromilov, S.A., Shubin, Y.V., Kvon, R.I. and Danilovich, V.S. (2010), "STRUCTURE OF Ir AND Ir-Al_2O_3 COATINGS OBTAINED BY CHEMICAL VAPOR DEPOSITION IN THE PRESENCE OF OXYGEN", Journal of Structural Chemistry, Vol. 51, No. 1, pp. 82-91.

Georgiou, C.D., Papapostolou, I. and Grintzalis, K. (2008), "Superoxide radical detection in cells, tissues, organisms (animals, plants, insects, microorganisms) and soils", Nature Protocols, Vol. 3, No. 11, pp. 1679-1692.

Grebel, J.E., Pignatello, J.J. and Mitch, W.A. (2010), "Effect of Halide Ions and Carbonates on Organic Contaminant Degradation by Hydroxyl Radical-Based Advanced Oxidation Processes in Saline Waters", Environmental Science & Technology, Vol. 44, No. 17, pp. 6822-6828.

Grimm, J., Bessarabov, D., Maier, W., Storck, S. and Sanderson, R.D. (1998), "Sol-gel film-preparation of novel electrodes for the electrocatalytic oxidation of organic pollutants in water", Desalination, Vol. 115, No. 3, pp. 295-302.

Guerrero-Perez, M.O., Martinez-Huerta, M.V., Fierro, J.L.G. and Banares, M.A. (2006), "Ammoxidation of propane over V-Sb and V-Sb-Nb mixed oxides", Applied Catalysis a-General, Vol. 298, pp. 1-7.

Guoting, L., Jinxia, Y., Jing, C., Meiya, Z., Lingfeng, Z. and Xiwang, Z. (2009), "Degradation of Tetracycline by Eletrochemical Oxidation Using Dimensionally Stable Anode", pp. 253-256.

Haber, J., Machej, T., Serwicka, E.M. and Wachs, I.E. (1995), "Mechanism of surface spreading in vanadia-titania system", Catalysis Letters, Vol. 32, No. 1-2, pp. 101-114.

Han, W., Zhong, C., Liang, L., Sun, Y., Guan, Y., Wang, L., Sun, X. and Li, J. (2014), "Electrochemical degradation of triazole fungicides in aqueous solution using TiO_2-NTs/SnO_2-Sb/PbO_2 anode: Experimental and DFT studies",

Electrochimica Acta, Vol. 130, pp. 179-186.

He, C., Zheng, J.W., Wang, K., Lin, H.Q., Wang, J.Y. and Yang, Y.H. (2015), "Sorption enhanced aqueous phase reforming of glycerol for hydrogen production over Pt-Ni supported on multi-walled carbon nanotubes", Applied Catalysis B-Environmental, Vol. 162, pp. 401-411.

He, D.L. and Mho, S.I. (2004), "Electrocatalytic reactions of phenolic compounds at ferric ion co-doped SnO_2 : Sb^{5+} electrodes", Journal of Electroanalytical Chemistry, Vol. 568, No. 1-2, pp. 19-27.

He, Z.Q., Huang, C.X., Wang, Q., Jiang, Z., Chen, J.M. and Song, S. (2011), "Preparation of a Praseodymium Modified Ti/SnO_2-Sb/PbO_2 Electrode and its Application in the Anodic Degradation of the Azo Dye Acid Black 194", International Journal of Electrochemical Science, Vol. 6, No. 9, pp. 4341-4354.

Hong, X.P., Zhang, R., Tong, S.P. and Ma, C.A. (2011), "Preparation of Ti/PTFE-F-PbO2 Electrode with a Long Life from the Sulfamic Acid Bath and Its Application in Organic Degradation", Chinese Journal of Chemical Engineering, Vol. 19, No. 6, pp. 1033-1038.

Hu, F.P., Cui, X.W. and Chen, W.X. (2010), "Pulse Electro-codeposition of Ti/SnO_2-Sb_2O_4-CNT Electrode for Phenol Oxidation", Electrochemical and Solid State Letters, Vol. 13, No. 9, pp. F20-F23.

Hu, F.P., Dong, Z.Q., Cui, X.W. and Chen, W.X. (2011), "Improved SnO_2-Sb_2O_4 based anode modified with Cr_3C_2 and CNT for phenol oxidation", Electrochimica Acta, Vol. 56, No. 3, pp. 1576-1580.

Hu, J.Y., Aizawa, T. and Ookubo, S. (2002), "Products of aqueous chlorination of bisphenol A and their estrogenic activity", Environmental Science & Technology, Vol. 36, No. 9, pp. 1980-1987.

Hua, M., Zhang, S., Pan, B., Zhang, W., Lv, L. and Zhang, Q. (2012), "Heavy metal removal from water/wastewater by nanosized metal oxides: A review", Journal

of Hazardous materials, Vol. 211-212, pp. 317-331.

Hwang, B.J. and Lee, K.L. (1996), "Electrocatalytic oxidation of 2-chlorophenol on a composite PbO_2/polypyrrole electrode in aqueous solution", Journal of Applied Electrochemistry, Vol. 26, No. 2, pp. 153-159.

Ishibashi, K., Fujishima, A., Watanabe, T. and Hashimoto, K. (2000a), "Detection of active oxidative species in TiO_2 photocatalysis using the fluorescence technique", Electrochemistry Communications, Vol. 2, No. 3, pp. 207-210.

Ishibashi, K., Fujishima, A., Watanabe, T. and Hashimoto, K. (2000b), "Quantum yields of active oxidative species formed on TiO_2 photocatalyst", Journal of Photochemistry and Photobiology a-Chemistry, Vol. 134, No. 1-2, pp. 139-142.

Jara, C.C. and Fino, D. (2010), "Cost optimization of the current density for electroxidation wastewater processes", Chemical Engineering Journal, Vol. 160, No. 2, pp. 497-502.

Joseph, L., Zaib, Q., Khan, I.A., Berge, N.D., Park, Y.G., Saleh, N.B. and Yoon, Y. (2011), "Removal of bisphenol A and 17 alpha-ethinyl estradiol from landfill leachate using single-walled carbon nanotubes", Water Research, Vol. 45, No. 13, pp. 4056-4068.

Juttner, K., Galla, U. and Schmieder, H. (2000), "Electrochemical approaches to environmental problems in the process industry", Electrochimica Acta, Vol. 45, No. 15-16, pp. 2575-2594.

Kadakia, K., Datta, M.K., Jampani, P.H., Park, S.K. and Kumta, P.N. (2013), "Novel F-doped IrO_2 oxygen evolution electrocatalyst for PEM based water electrolysis", Journal of Power Sources, Vol. 222, pp. 313-317.

Kapalka, A., Foti, G. and Comninellis, C. (2008), "Kinetic modelling of the electrochemical mineralization of organic pollutants for wastewater treatment", Journal of Applied Electrochemistry, Vol. 38, No. 1, pp. 7-16.

Karuppiah, M.T. and Raju, G.B. (2009), "Anodic Degradation of CI Reactive Blue

221 Using Graphite and $IrO_2/TaO_2/RuO_2$ Coated Titanium Electrodes", Industrial & Engineering Chemistry Research, Vol. 48, No. 4, pp. 2149-2156.

Kim, J., Korshin, G.V. and Velichenko, A.B. (2005), "Comparative study of electrochemical degradation and ozonation of nonylphenol", Water Research, Vol. 39, No. 12, pp. 2527-2534.

Kim, J.H., Oh, K.K., Lee, S.T., Kim, S.W. and Hong, S.I. (2002a), "Biodegradation of phenol and chlorophenols with defined mixed culture in shake-flasks and a packed bed reactor", Process Biochemistry, Vol. 37, No. 12, pp. 1367-1373.

Kim, K.W., Lee, E.H., Kim, J.S., Shin, K.H. and Jung, B.I. (2002b), "A study on performance improvement of Ir oxide-coated titanium electrode for organic destruction", Electrochimica Acta, Vol. 47, No. 15, pp. 2525-2531.

Kitamura, S., Suzuki, T., Sanoh, S., Kohta, R., Jinno, N., Sugihara, K., Yoshihara, S., Fujimoto, N., Watanabe, H. and Ohta, S. (2005), "Comparative study of the endocrine-disrupting activity of bisphenol A and 19 related compounds", Toxicological Sciences, Vol. 84, No. 2, pp. 249-259.

Klamklang, S., Vergnes, H., Senocq, F., Pruksathorn, K., Duverneuil, P. and Damronglerd, S. (2009), "Deposition of tin oxide, iridium and iridium oxide films by metal-organic chemical vapor deposition for electrochemical wastewater treatment", Journal of Applied Electrochemistry, Vol. 40, No. 5, pp. 997-1004.

Kong, H.S., Lu, H.Y., Zhang, W.L., Lin, H.B. and Huang, W.M. (2012), "Performance characterization of Ti substrate lead dioxide electrode with different solid solution interlayers", Journal of Materials Science, Vol. 47, No. 18, pp. 6709-6715.

Kong, J.T., Shi, S.Y., Kong, L.C., Zhu, X.P. and Ni, J.R. (2007), "Preparation and characterization of PbO_2 electrodes doped with different rare earth oxides", Electrochimica Acta, Vol. 53, No. 4, pp. 2048-2054.

Koppenol, W.H. and Liebman, J.F. (1984), "The Oxidizing Nature of the Hydroxyl Radical - a Comparison with the Ferryl Ion (FeO^{2+})", Journal of Physical Chemistry, Vol. 88, No. 1, pp. 99-101.

Kosaka, K., Yamada, H., Matsui, S., Echigo, S. and Shishida, K. (1998), "Comparison among the methods for hydrogen peroxide measurements to evaluate advanced oxidation processes: Application of a spectrophotometric method using copper(II) ion and 2.9 dimethyl-1,10-phenanthroline", Environmental Science & Technology, Vol. 32, No. 23, pp. 3821-3824.

Kraft, A. (2007), "Doped diamond: A compact review on a new, versatile electrode material", International Journal of Electrochemical Science, Vol. 2, No. 5, pp. 355-385.

Lassali, T.A.F., Boodts, J.F.C. and Bulhoes, L.O.S. (2000), "Faradaic impedance investigation of the deactivation mechanism of Ir-based ceramic oxides containing TiO_2 and SnO_2", Journal of Applied Electrochemistry, Vol. 30, No. 5, pp. 625-634.

Lee, Y., Shin, H.-Y., Chun, S.H., Lee, J., Park, W.J., Baik, J.M., Yoon, S. and Kim, M.H. (2012), "Highly Single Crystalline $Ir_xRu_{1-x}O_2$ Mixed Metal Oxide Nanowires", The Journal of Physical Chemistry C, Vol. 116, No. 30, pp. 16300-16304.

Li, G., Wang, Y.-H. and Chen, Q.-Y. (2013a), "Influence of fluoride-doped tin oxide interlayer on Ni–Sb–SnO_2/Ti electrodes", Journal of Solid State Electrochemistry, Vol. 17, No. 5, pp. 1303-1309.

Li, J.J., Wang, J.S., Guo, X., Zhao, J.H., Song, C.Y. and Wang, L.C. (2012a), "Improving the Stability and Ethanol Electro-Oxidation Activity of Pt Catalysts by Selectively Anchoring Pt Particles on Carbon-Nanotubes-Supported-SnO2", Fuel Cells, Vol. 12, No. 5, pp. 898-903.

Li, P.Q., Zhao, G.H., Cui, X., Zhang, Y.G. and Tang, Y.T. (2009), "Constructing Stake

Structured TiO_2-NTs/Sb-Doped SnO_2 Electrode Simultaneously with High Electrocatalytic and Photocatalytic Performance for Complete Mineralization of Refractory Aromatic Acid", Journal of Physical Chemistry C, Vol. 113, No. 6, pp. 2375-2383.

Li, P.Q., Zhao, G.H., Li, M.F., Cao, T.C., Cui, X. and Li, D.M. (2012b), "Design and high efficient photoelectric-synergistic catalytic oxidation activity of 2D macroporous SnO_2/1D TiO_2 nanotubes", Applied Catalysis B-Environmental, Vol. 111, pp. 578-585.

Li, Q., Zhang, Q., Cui, H., Ding, L., Wei, Z. and Zhai, J. (2013b), "Fabrication of cerium-doped lead dioxide anode with improved electrocatalytic activity and its application for removal of Rhodamine B", Chemical Engineering Journal, Vol. 228, pp. 806-814.

Li, S., Wang, F., Xu, M., Wang, Y., Fang, W. and Hu, Y. (2013c), "Fabrication and Characteristics of a Nanostructure PbO_2 Anode and its Application for Degradation of Phenol", Journal of the Electrochemical Society, Vol. 160, No. 4, pp. E44-E48.

Li, X., Xu, H., Yan, W. and Shao, D. (2016), "Electrocatalytic degradation of aniline by Ti/Sb–SnO_2, Ti/Sb–SnO_2/Pb_3O_4 and Ti/Sb–SnO_2/PbO_2 anodes in different electrolytes", Journal of Electroanalytical Chemistry, Vol. 775, pp. 43-51.

Li, X.H., Pletcher, D. and Walsh, F.C. (2011), "Electrodeposited lead dioxide coatings", Chemical Society Reviews, Vol. 40, No. 7, pp. 3879-3894.

Li, X.M., Wang, M., Jiao, Z.K. and Chen, Z.Y. (2001), "Study on electrolytic oxidation for landfill leachate treatment", Zhongguo Jishui Paishui/China Water & Wastewater, Vol. 17, No. 8, p. 14.

Li, X.W., Wei, J.D., Chai, Y.Z. and Zhang, S. (2015a), "Carbon nanotubes/tin oxide nanocomposite-supported Pt catalysts for methanol electro-oxidation", Journal of Colloid and Interface Science, Vol. 450, pp. 74-81.

Li, X.Y., Cui, Y.H., Feng, Y.J., Xie, Z.M. and Gu, J.D. (2005), "Reaction pathways and mechanisms of the electrochemical degradation of phenol on different electrodes", Water Research, Vol. 39, No. 10, pp. 1972-1981.

Li, X.Y., Wang, C.W., Qian, Y., Wang, Y.J. and Zhang, L.W. (2013d), "Simultaneous removal of chemical oxygen demand, turbidity and hardness from biologically treated citric acid wastewater by electrochemical oxidation for reuse", Separation and Purification Technology, Vol. 107, pp. 281-288.

Li, Y.D., Lu, X., Wang, H.K., Xie, C., Yang, G. and Niu, C.M. (2015b), "Growth of Ultrafine SnO_2 Nanoparticles within Multiwall Carbon Nanotube Networks: Non-Solution Synthesis and Excellent Electrochemical Properties as Anodes for Lithium Ion Batteries", Electrochimica Acta, Vol. 178, pp. 778-785.

Lin, D.H. and Xing, B.S. (2008), "Adsorption of phenolic compounds by carbon nanotubes: Role of aromaticity and substitution of hydroxyl groups", Environmental Science & Technology, Vol. 42, No. 19, pp. 7254-7259.

Lin, H., Niu, J., Ding, S. and Zhang, L. (2012), "Electrochemical degradation of perfluorooctanoic acid (PFOA) by Ti/SnO_2-Sb, Ti/SnO_2-Sb/PbO_2 and Ti/SnO_2-Sb/MnO_2 anodes", Water Research, Vol. 46, No. 7, pp. 2281-2289.

Lin, H., Niu, J., Xu, J., Huang, H., Li, D., Yue, Z. and Feng, C. (2013a), "Highly Efficient and Mild Electrochemical Mineralization of Long-Chain Perfluorocarboxylic Acids (C9-C10) by Ti/SnO_2-Sb-Ce, Ti/SnO_2-Sb/Ce-PbO_2, and Ti/BDD Electrodes", Environmental Science & Technology, Vol. 47, No. 22, pp. 13039-13046.

Lin, H., Niu, J., Xu, J., Li, Y. and Pan, Y. (2013b), "Electrochemical mineralization of sulfamethoxazole by Ti/SnO_2-Sb/Ce-PbO_2 anode: Kinetics, reaction pathways, and energy cost evolution", Electrochimica Acta, Vol. 97, pp. 167-174.

Lin, K.H., Wang, C.B. and Chien, S.H. (2013c), "Catalytic performance of steam reforming of ethanol at low temperature over $LaNiO_3$ perovskite", International

Journal of Hydrogen Energy, Vol. 38, No. 8, pp. 3226-3232.

Lin, Y.P. and Valentine, R.L. (2008), "The release of lead from the reduction of lead oxide (PbO_2) by natural organic matter", Environmental Science & Technology, Vol. 42, No. 3, pp. 760-765.

Lin, Y.P. and Valentine, R.L. (2010), "Reductive Dissolution of Lead Dioxide (PbO_2) in Acidic Bromide Solution", Environmental Science & Technology, Vol. 44, No. 10, pp. 3895-3900.

Lin, Y.P., Washburn, M.P. and Valentine, R.L. (2008), "Reduction of lead oxide (PbO_2) by iodide and formation of iodoform in the PbO2/I-/NOM system", Environmental Science & Technology, Vol. 42, No. 8, pp. 2919-2924.

Liu, L., Zhao, G.H., Wu, M.F., Lei, Y.Z. and Geng, R. (2009a), "Electrochemical degradation of chlorobenzene on boron-doped diamond and platinum electrodes", Journal of Hazardous materials, Vol. 168, No. 1, pp. 179-186.

Liu, S., Wang, Z.Y., Zhang, Y., Zhang, C.B. and Zhang, T. (2015), "High performance room temperature NO_2 sensors based on reduced graphene oxide-multiwalled carbon nanotubes-tin oxide nanoparticles hybrids", Sensors and Actuators B-Chemical, Vol. 211, pp. 318-324.

Liu, X.B., Lu, H.Y., Huang, W.M., Kong, H.S., Ren, X.B. and Lin, H.B. (2012a), "Electrochemical Degradation of Nitrobenzene", Current Organic Chemistry, Vol. 16, No. 17, pp. 1967-1971.

Liu, Y., Liu, H., Ma, J. and Li, J. (2011), "Investigation on electrochemical properties of cerium doped lead dioxide anode and application for elimination of nitrophenol", Electrochimica Acta, Vol. 56, No. 3, pp. 1352-1360.

Liu, Y., Liu, H.L., Ma, J. and Li, J.J. (2012b), "Preparation and electrochemical properties of Ce-Ru-SnO_2 ternary oxide anode and electrochemical oxidation of nitrophenols", Journal of Hazardous materials, Vol. 213, pp. 222-229.

Liu, Y., Liu, H.L., Ma, J. and Wang, X. (2009b), "Comparison of degradation

mechanism of electrochemical oxidation of di- and tri-nitrophenols on Bi-doped lead dioxide electrode: Effect of the molecular structure", Applied Catalysis B-Environmental, Vol. 91, No. 1-2, pp. 284-299.

Lo, C.-P., Wang, G., Kumar, A. and Ramani, V. (2013), "TiO_2–RuO_2 electrocatalyst supports exhibit exceptional electrochemical stability", Applied Catalysis B: Environmental, Vol. 140–141, No. 0, pp. 133-140.

Lua, S.K., Oh, W.D., Zhang, L.Z., Yao, L., Lim, T.T. and Dong, Z.L. (2015), "A molybdovanadophosphate-based surfactant encapsulated heteropolyanion with multi-lamellar nano-structure for catalytic wet air oxidation of organic pollutants under ambient conditions", Rsc Advances, Vol. 5, No. 115, pp. 94743-94751.

Ma, Q., Liu, L., Cui, W., Li, R., Song, T. and Cui, Z. (2015), "Electrochemical degradation of perfluorooctanoic acid (PFOA) by Yb-doped Ti/SnO_2-Sb/PbO_2 anodes and determination of the optimal conditions", Rsc Advances, Vol. 5, No. 103, pp. 84856-84864.

Macak, J.M., Gong, B.G., Hueppe, M. and Schmuki, P. (2007), "Filling of TiO_2 nanotubes by self-doping and electrodeposition", Advanced Materials, Vol. 19, No. 19, pp. 3027-+.

Makgae, M.E., Klink, M.J. and Crouch, A.M. (2008), "Performance of sol-gel Titanium Mixed Metal Oxide electrodes for electro-catalytic oxidation of phenol", Applied Catalysis B-Environmental, Vol. 84, No. 3-4, pp. 659-666.

Makgae, M.E., Theron, C.C., Przybylowicz, W.J. and Crouch, A.M. (2005), "Preparation and surface characterization of Ti/SnO_2-RuO_2-IrO_2 thin films as electrode material for the oxidation of phenol", Materials Chemistry and Physics, Vol. 92, No. 2-3, pp. 559-564.

Malpass, G.R., Miwa, D.W., Machado, S.A. and Motheo, A.J. (2010), "SnO_2-based materials for pesticide degradation", Journal of Hazardous materials, Vol. 180, No. 1-3, pp. 145-151.

Malpass, G.R.P., Miwa, D.W., Miwa, A.C.P., Machado, S.A.S. and Motheo, A.J. (2007), "Photo-assisted electrochemical oxidation of atrazine on a commercial $Ti/Ru_{0.3}Ti_{0.7}O_2$ DSA electrode", Environmental Science & Technology, Vol. 41, No. 20, pp. 7120-7125.

Malpass, G.R.P., Miwa, D.W., Miwa, A.C.P., Machado, S.A.S. and Motheo, A.J. (2009), "Study of photo-assisted electrochemical degradation of carbaryl at dimensionally stable anodes (DSA (R))", Journal of Hazardous materials, Vol. 167, No. 1-3, pp. 224-229.

Malpass, G.R.P., Neves, R.S. and Motheo, A.J. (2006), "A comparative study of commercial and laboratory-made $Ti/Ru_{0.3}Ti_{0.7}O_2$ DSA® electrodes: “In situ” and “ex situ” surface characterisation and organic oxidation activity", Electrochimica Acta, Vol. 52, No. 3, pp. 936-944.

Malpass, G.R.P., Salazar-Banda, G.R., Miwa, D.W., Machado, S.A.S. and Motheo, A.J. (2013), "Comparing atrazine and cyanuric acid electro-oxidation on mixed oxide and boron-doped diamond electrodes", Environmental Technology, Vol. 34, No. 8, pp. 1043-1051.

Mao, X.H., Tian, F., Gan, F.X., Lin, A. and Zhang, X.J. (2008), "Comparison of the performances of Ti/SnO_2-Sb, Ti/SnO_2-Sb/PbO_2, and Nb/BDD anodes on electrochemical degradation of azo dye", Russian Journal of Electrochemistry, Vol. 44, No. 7, pp. 802-811.

Marselli, B., Garcia-Gomez, J., Michaud, P.A., Rodrigo, M.A. and Comninellis, C. (2003), "Electrogeneration of hydroxyl radicals on boron-doped diamond electrodes", Journal of the Electrochemical Society, Vol. 150, No. 3, pp. D79-D83.

Martinez-Huitle, C.A. and Andrade, L.S. (2011), "Electrocatalysis in Wastewater Treatment: Recent Mechanism Advances", Quimica Nova, Vol. 34, No. 5, pp. 850-858.

Martinez-Huitle, C.A., De Battisti, A., Ferro, S., Reyna, S., Cerro-Lopez, M. and Quiro, M.A. (2008), "Removal of the pesticide methamidophos from aqueous solutions by electrooxidation using Pb/PbO_2, Ti/SnO_2, and Si/BDD electrodes", Environmental Science & Technology, Vol. 42, No. 18, pp. 6929-6935.

Martinez-Huitle, C.A. and Ferro, S. (2006), "Electrochemical oxidation of organic pollutants for the wastewater treatment: direct and indirect processes", Chemical Society Reviews, Vol. 35, No. 12, pp. 1324-1340.

Martinez-Huitle, C.A., Ferro, S. and De Battisti, A. (2004a), "Electrochemical incineration of oxalic acid - Role of electrode material", Electrochimica Acta, Vol. 49, No. 22-23, pp. 4027-4034.

Martinez-Huitle, C.A., Quiroz, M.A., Comninellis, C., Ferro, S. and De Battisti, A. (2004b), "Electrochemical incineration of chloranilic acid using Ti/IrO_2, Pb/PbO_2 and Si/BDD electrodes", Electrochimica Acta, Vol. 50, No. 4, pp. 949-956.

Meaney, K.L. and Omanovic, S. (2007), "Sn-0.86-Sb-0.03-Mn-0.10-Pt-0.01-oxide/Ti anode for the electro-oxidation of aqueous organic wastes", Materials Chemistry and Physics, Vol. 105, No. 2-3, pp. 143-147.

Mendoza, F., Hernandez, D.M., Makarov, V., Febus, E., Weiner, B.R. and Morell, G. (2014), "Room temperature gas sensor based on tin dioxide-carbon nanotubes composite films", Sensors and Actuators B-Chemical, Vol. 190, pp. 227-233.

Meng, X.Q., Yao, J.Y., Liu, F.L., He, H.C., Zhou, M., Xiao, P. and Zhang, Y.H. (2013), "Preparation of SnO_2@C-doping TiO_2 nanotube arrays and its electrochemical and photoelectrochemical properties", Journal of Alloys and Compounds, Vol. 552, pp. 392-397.

Mohammadi, M.R. and Fray, D.J. (2011), "Synthesis of Nanostructured and Nanoporous TiO_2-AgO Mixed Oxide Derived from a Particulate Sol-Gel Route: Physical and Sensing Characteristics", Metallurgical and Materials Transactions

a-Physical Metallurgy and Materials Science, Vol. 42A, No. 8, pp. 2481-2492.

Montilla, F., Morallon, E., De Battisti, A. and Vazquez, J.L. (2004), "Preparation and characterization of antimony-doped tin dioxide electrodes. Part 1. Electrochemical characterization", Journal of Physical Chemistry B, Vol. 108, No. 16, pp. 5036-5043.

Murugananthan, M., Yoshihara, S., Rakuma, T. and Shirakashi, T. (2008), "Mineralization of bisphenol A (BPA) by anodic oxidation with boron-doped diamond (BDD) electrode", Journal of Hazardous materials, Vol. 154, No. 1-3, pp. 213-220.

Näslund, L.-Å., Sánchez-Sánchez, C.M., Ingason, Á.S., Bäckström, J., Herrero, E., Rosen, J. and Holmin, S. (2013), "The Role of TiO_2 Doping on RuO_2-Coated Electrodes for the Water Oxidation Reaction", The Journal of Physical Chemistry C, Vol. 117, No. 12, pp. 6126-6135.

Neodo, S., Rosestolato, D., Ferro, S. and De Battisti, A. (2012), "On the electrolysis of dilute chloride solutions: Influence of the electrode material on Faradaic efficiency for active chlorine, chlorate and perchlorate", Electrochimica Acta, Vol. 80, pp. 282-291.

Neto, S.A. and De Andrade, A.R. (2009), "Electrochemical degradation of glyphosate formulations at DSA anodes in chloride medium: an AO_X formation study", Journal of Applied Electrochemistry, Vol. 39, No. 10, pp. 1863-1870.

Nguyen, L.N., Hai, F.I., Yang, S.F., Kang, J.G., Leusch, F.D.L., Roddick, F., Price, W.E. and Nghiem, L.D. (2013), "Removal of trace organic contaminants by an MBR comprising a mixed culture of bacteria and white-rot fungi", Bioresource Technology, Vol. 148, pp. 234-241.

Niu, J., Bao, Y., Li, Y. and Chai, Z. (2013a), "Electrochemical mineralization of pentachlorophenol (PCP) by Ti/SnO_2-Sb electrodes", Chemosphere, Vol. 92, No. 11, pp. 1571-1577.

Niu, J., Lin, H., Xu, J., Wu, H. and Li, Y. (2012), "Electrochemical mineralization of perfluorocarboxylic acids (PFCAs) by ce-doped modified porous nanocrystalline PbO_2 film electrode", Environmental Science & Technology, Vol. 46, No. 18, pp. 10191-10198.

Niu, J., Maharana, D., Xu, J., Chai, Z. and Bao, Y. (2013b), "A high activity of Ti/SnO_2-Sb electrode in the electrochemical degradation of 2,4-dichlorophenol in aqueous solution", Journal of Environmental Sciences, Vol. 25, No. 7, pp. 1424-1430.

Nosaka, Y., Nakamura, M. and Hirakawa, T. (2002), "Behavior of superoxide radicals formed on TiO_2 powder photocatalysts studied by a chemiluminescent probe method", Physical Chemistry Chemical Physics, Vol. 4, No. 6, pp. 1088-1092.

Oehlmann, J., Schulte-Oehlmann, U., Kloas, W., Jagnytsch, O., Lutz, I., Kusk, K.O., Wollenberger, L., Santos, E.M., Paull, G.C., Van Look, K.J.W. and Tyler, C.R. (2009), "A critical analysis of the biological impacts of plasticizers on wildlife", Philosophical Transactions of the Royal Society B-Biological Sciences, Vol. 364, No. 1526, pp. 2047-2062.

Oh, W.D., Lua, S.K., Dong, Z.L. and Lim, T.T. (2014), "High surface area DPA-hematite for efficient detoxification of bisphenol A via peroxymonosulfate activation", Journal of Materials Chemistry A, Vol. 2, No. 38, pp. 15836-15845.

Oppenländer, T. (2007) Photochemical Purification of Water and Air, pp. 145-187, Wiley-VCH Verlag GmbH & Co. KGaA.

Pan, J.H., Chai, S.Y., Lee, C., Park, S.E. and Lee, W.I. (2007), "Controlled formation of highly crystallized cubic and hexagonal mesoporous SnO_2 thin films", Journal of Physical Chemistry C, Vol. 111, No. 15, pp. 5582-5587.

Pan, K., Tian, M., Jiang, Z.-H., Kjartanson, B. and Chen, A. (2012), "Electrochemical oxidation of lignin at lead dioxide nanoparticles photoelectrodeposited on TiO_2 nanotube arrays", Electrochimica Acta, Vol. 60, pp. 147-153.

Panakoulias, T., Kalatzis, P., Kalderis, D. and Katsaounis, A. (2010), "Electrochemical degradation of Reactive Red 120 using DSA and BDD anodes", Journal of Applied Electrochemistry, Vol. 40, No. 10, pp. 1759-1765.

Panizza, M. and Cerisola, G. (2004), "Electrochemical oxidation as a final treatment of synthetic tannery wastewater", Environmental Science & Technology, Vol. 38, No. 20, pp. 5470-5475.

Panizza, M. and Cerisola, G. (2009), "Direct And Mediated Anodic Oxidation of Organic Pollutants", Chemical Reviews, Vol. 109, No. 12, pp. 6541-6569.

Park, H., Bak, A., Ahn, Y.Y., Choi, J. and Hoffmannn, M.R. (2012), "Photoelectrochemical performance of multi-layered BiOx-TiO_2/Ti electrodes for degradation of phenol and production of molecular hydrogen in water", Journal of Hazardous materials, Vol. 211, pp. 47-54.

Park, H., Vecitis, C.D. and Hoffmann, M.R. (2009), "Electrochemical Water Splitting Coupled with Organic Compound Oxidation: The Role of Active Chlorine Species", Journal of Physical Chemistry C, Vol. 113, No. 18, pp. 7935-7945.

Pechini, M. (1967), "US Patent# 3.330. 697", US Patent, 3.330. 697.

Pelegrino, R.L., Di Iglia, R.A., Sanches, C.G., Avaca, L.A. and Bertazzoli, R. (2002), "Comparative study of commercial oxide electrodes performance in electrochemical degradation of organics in aqueous solutions", Journal of the Brazilian Chemical Society, Vol. 13, No. 1, pp. 60-65.

Pereira, G.F., Rocha-Filho, R.C., Bocchi, N. and Biaggio, S.R. (2012), "Electrochemical degradation of bisphenol A using a flow reactor with a boron-doped diamond anode", Chemical Engineering Journal, Vol. 198-199, pp. 282-288.

Perez-Alonso, F.J., Melian-Cabrera, I., Granados, M.L., Kapteijn, F. and Fierro, J.L.G. (2006), "Synergy of $Fe_xCe_{1-x}O_2$ mixed oxides for N_2O decomposition", Journal of Catalysis, Vol. 239, No. 2, pp. 340-346.

Perez, G., Fernandez-Alba, A.R., Urtiaga, A.M. and Ortiz, I. (2010), "Electro-oxidation of reverse osmosis concentrates generated in tertiary water treatment", Water Research, Vol. 44, No. 9, pp. 2763-2772.

Rabaaoui, N., Saad, M.E.K., Moussaoui, Y., Allagui, M.S., Bedoui, A. and Elaloui, E. (2013), "Anodic oxidation of o-nitrophenol on BDD electrode: Variable effects and mechanisms of degradation", Journal of Hazardous materials, Vol. 250, pp. 447-453.

Radjenovic, J., Escher, B.I. and Rabaey, K. (2011), "Electrochemical degradation of the beta-blocker metoprolol by Ti/$Ru_{0.7}Ir_{0.3}O_2$ and Ti/SnO_2-Sb electrodes", Water Research, Vol. 45, No. 10, pp. 3205-3214.

Raghu, S., Lee, C.W., Chellammal, S., Palanichamy, S. and Basha, C.A. (2009), "Evaluation of electrochemical oxidation techniques for degradation of dye effluents-A comparative approach", Journal of Hazardous materials, Vol. 171, No. 1-3, pp. 748-754.

Rajkumar, D. and Kim, J.G. (2006), "Oxidation of various reactive dyes with in situ electro-generated active chlorine for textile dyeing industry wastewater treatment", Journal of Hazardous materials, Vol. 136, No. 2, pp. 203-212.

Rajkumar, D., Kim, J.G. and Palanivelu, K. (2005), "Indirect electrochemical oxidation of phenol in the presence of chloride for wastewater treatment", Chemical Engineering & Technology, Vol. 28, No. 1, pp. 98-105.

Rajkumar, D., Song, B.J. and Kim, J.G. (2007), "Electrochemical degradation of Reactive Blue 19 in chloride medium for the treatment of textile dyeing wastewater with identification of intermediate compounds", Dyes and Pigments, Vol. 72, No. 1, pp. 1-7.

Raju, T., Chung, S.J. and Moon, I.S. (2010), "Electrochemical recovery of silver from waste aqueous Ag(I)/Ag(II) redox mediator solution used in mediated electro oxidation process", Korean Journal of Chemical Engineering, Vol. 26, No. 4, pp.

1053-1057.

Ren, X.M., Chen, C.L., Nagatsu, M. and Wang, X.K. (2011), "Carbon nanotubes as adsorbents in environmental pollution management: A review", Chemical Engineering Journal, Vol. 170, No. 2-3, pp. 395-410.

Rodrigo, M.A., Michaud, P.A., Duo, I., Panizza, M., Cerisola, G. and Comninellis, C. (2001), "Oxidation of 4-chlorophenol at boron-doped diamond electrode for wastewater treatment", Journal of the Electrochemical Society, Vol. 148, No. 5, pp. D60-D64.

Rodríguez, F.A., Mateo, M.N., Aceves, J.M., Rivero, E.P. and González, I. (2013), "Electrochemical oxidation of bio-refractory dye in a simulated textile industry effluent using DSA electrodes in a filter-press type FM01-LC reactor", Environmental Technology, Vol. 34, No. 5, pp. 573-583.

Sakalis, A., Mpoulmpasakos, K., Nickel, U., Fytianos, K. and Voulgaropoulos, A. (2005), "Evaluation of a novel electrochemical pilot plant process for azodyes removal from textile wastewater", Chemical Engineering Journal, Vol. 111, No. 1, pp. 63-70.

Sakuma, S., Nakanishi, M., Morinaga, K., Fujitake, M., Wada, S. and Fujimoto, Y. (2010), "Bisphenol A 3,4-quinone induces the conversion of xanthine dehydrogenase into oxidase in vitro", Food and Chemical Toxicology, Vol. 48, No. 8-9, pp. 2217-2222.

Sala, M., Del Río, A.I., Molina, J., Cases, F. and Gutiérrez-Bouzán, M.C. (2012), "Influence of cell design and electrode materials on the decolouration of dyeing effluents", International Journal of Electrochemical Science, Vol. 7, No. 12, pp. 12470-12488.

Samet, Y., Elaoud, S.C., Ammar, S. and Abdelhedi, R. (2006), "Electrochemical degradation of 4-chloroguaiacol for wastewater treatment using PbO_2 anodes", Journal of Hazardous materials, Vol. 138, No. 3, pp. 614-619.

Santos, D., Pacheco, M.J., Gomes, A., Lopes, A. and Ciriaco, L. (2013), "Preparation of Ti/Pt/SnO_2-Sb_2O_4 electrodes for anodic oxidation of pharmaceutical drugs", Journal of Applied Electrochemistry, Vol. 43, No. 4, pp. 407-416.

Santos, M.J.R., Medeiros, M.C., Oliveira, T.M.B.F., Morais, C.C.O., Mazzetto, S.E., Martínez-Huitle, C.A. and Castro, S.S.L. (2016), "Electrooxidation of cardanol on mixed metal oxide (RuO_2-TiO_2 and IrO_2-RuO_2-TiO_2) coated titanium anodes: insights into recalcitrant phenolic compounds", Electrochimica Acta, Vol. 212, pp. 95-101.

Scialdone, O. (2009), "Electrochemical oxidation of organic pollutants in water at metal oxide electrodes: A simple theoretical model including direct and indirect oxidation processes at the anodic surface", Electrochimica Acta, Vol. 54, No. 26, pp. 6140-6147.

Scialdone, O., Galia, A. and Randazzo, S. (2011), "Oxidation of carboxylic acids in water at IrO_2–Ta_2O_5 and boron doped diamond anodes", Chemical Engineering Journal, Vol. 174, No. 1, pp. 266-274.

Scialdone, O., Randazzo, S., Galia, A. and Filardo, G. (2009a), "Electrochemical oxidation of organics at metal oxide electrodes: The incineration of oxalic acid at IrO_2-Ta_2O_5 (DSA-O_2) anode", Electrochimica Acta, Vol. 54, No. 4, pp. 1210-1217.

Scialdone, O., Randazzo, S., Galia, A. and Silvestri, G. (2009b), "Electrochemical oxidation of organics in water: Role of operative parameters in the absence and in the presence of NaCl", Water Research, Vol. 43, No. 8, pp. 2260-2272.

Seker, S., Beyenal, H., Salih, B. and Tanyolac, A. (1997), "Multi-substrate growth kinetics of Pseudomonas putida for phenol removal", Applied Microbiology and Biotechnology, Vol. 47, No. 5, pp. 610-614.

Shao, D., Liang, J.D., Cui, X.M., Xu, H. and Yan, W. (2014a), "Electrochemical oxidation of lignin by two typical electrodes: Ti/Sb-SnO_2 and Ti/PbO_2",

Chemical Engineering Journal, Vol. 244, pp. 288-295.

Shao, D., Yan, W., Li, X.L., Yang, H.H. and Xu, H. (2014b), "A Highly Stable Ti/TiHx/Sb-SnO_2 Anode: Preparation, Characterization and Application", Industrial & Engineering Chemistry Research, Vol. 53, No. 10, pp. 3898-3907.

Shi, Z. and Stone, A.T. (2009), "PbO_2(s, Plattnerite) Reductive Dissolution by Natural Organic Matter: Reductant and Inhibitory Subfractions", Environmental Science & Technology, Vol. 43, No. 10, pp. 3604-3611.

Shiraishi, Y., Miyarnoto, R. and Hirai, T. (2008), "A hemicyanine-conjugated copolymer as a highly sensitive fluorescent thermometer", Langmuir, Vol. 24, No. 8, pp. 4273-4279.

Sires, I., Brillas, E., Cerisola, G. and Panizza, M. (2008), "Comparative depollution of mecoprop aqueous solutions by electrochemical incineration using BDD and PbO_2 as high oxidation power anodes", Journal of Electroanalytical Chemistry, Vol. 613, No. 2, pp. 151-159.

Song, S., Fan, J., He, Z., Zhan, L., Liu, Z., Chen, J. and Xu, X. (2010a), "Electrochemical degradation of azo dye C.I. Reactive Red 195 by anodic oxidation on Ti/SnO_2-Sb/PbO_2 electrodes", Electrochimica Acta, Vol. 55, No. 11, pp. 3606-3613.

Song, S., Zhan, L.Y., He, Z.Q., Lin, L.L., Tu, J.J., Zhang, Z.H., Chen, J.M. and Xu, L.J. (2010b), "Mechanism of the anodic oxidation of 4-chloro-3-methyl phenol in aqueous solution using Ti/SnO_2-Sb/PbO_2 electrodes", Journal of Hazardous materials, Vol. 175, No. 1-3, pp. 614-621.

Souza, F.L., Aquino, J.M., Irikura, K., Miwa, D.W., Rodrigo, M.A. and Motheo, A.J. (2014), "Electrochemical degradation of the dimethyl phthalate ester on a fluoride-doped Ti/beta-PbO2 anode", Chemosphere, Vol. 109, pp. 187-194.

Staples, C.A., Dorn, P.B., Klecka, G.M., O'Block, S.T. and Harris, L.R. (1998), "A review of the environmental fate, effects, and exposures of bisphenol A",

Chemosphere, Vol. 36, No. 10, pp. 2149-2173.

Sun, J.R., Lu, H.Y., Lin, H.B., Du, L.L., Huang, W.M., Li, H.D. and Cui, T. (2012), "Electrochemical oxidation of aqueous phenol at low concentration using Ti/BDD electrode", Separation and Purification Technology, Vol. 88, pp. 116-120.

Szpyrkowicz, L., Cherbanski, R. and Kelsall, G.H. (2005), "Hydrodynamic effects on the performance of an electrochemical reactor for destruction of disperse dyes", Industrial & Engineering Chemistry Research, Vol. 44, No. 7, pp. 2058-2068.

Szpyrkowicz, L., Juzzolino, C., Kaul, S.N., Daniele, S. and De Faveri, M.D. (2000), "Electrochemical oxidation of dyeing baths bearing disperse dyes", Industrial & Engineering Chemistry Research, Vol. 39, No. 9, pp. 3241-3248.

Tahar, N.B., Abdelhedi, R. and Savall, A. (2009), "Electrochemical polymerisation of phenol in aqueous solution on a Ta/PbO_2 anode", Journal of Applied Electrochemistry, Vol. 39, No. 5, pp. 663-669.

Tahar, N.B. and Savall, A. (1999), "A comparison of different lead dioxide coated electrodes for the electrochemical destruction of phenol", Journal of New Materials for Electrochemical Systems, Vol. 2, No. 1, pp. 19-26.

Tahar, N.B. and Savall, A. (2009), "Electrochemical removal of phenol in alkaline solution. Contribution of the anodic polymerization on different electrode materials", Electrochimica Acta, Vol. 54, No. 21, pp. 4809-4816.

Tai, C., Peng, J.F., Liu, J.F., Jiang, G.B. and Zou, H. (2004), "Determination of hydroxyl radicals in advanced oxidation processes with dimethyl sulfoxide trapping and liquid chromatography", Analytica Chimica Acta, Vol. 527, No. 1, pp. 73-80.

Tan, C., Xiang, B., Li, Y., Fang, J. and Huang, M. (2011), "Preparation and characteristics of a nano-PbO_2 anode for organic wastewater treatment",

Chemical Engineering Journal, Vol. 166, No. 1, pp. 15-21.

Tauchert, E., Schneider, S., de Morais, J.L. and Peralta-Zamora, P. (2006), "Photochemically-assisted electrochemical degradation of landfill leachate", Chemosphere, Vol. 64, No. 9, pp. 1458-1463.

Terrier, C., Chatelon, J.P., Berjoan, R. and Roger, J.A. (1995), "Sb-Doped SnO_2 Transparent Conducting Oxide from the Sol-Gel Dip-Coating Technique", Thin Solid Films, Vol. 263, No. 1, pp. 37-41.

Tian, M., Bakovic, L. and Chen, A. (2007), "Kinetics of the electrochemical oxidation of 2-nitrophenol and 4-nitrophenol studied by in situ UV spectroscopy and chemometrics", Electrochimica Acta, Vol. 52, No. 23, pp. 6517-6524.

Tolba, R., Tian, M., Wen, J.L., Jiang, Z.H. and Chen, A.C. (2010), "Electrochemical oxidation of lignin at IrO_2-based oxide electrodes", Journal of Electroanalytical Chemistry, Vol. 649, No. 1-2, pp. 9-15.

Tong, M.P., Zhu, P.T., Jiang, X.J. and Kim, H. (2011), "Influence of natural organic matter on the deposition kinetics of extracellular polymeric substances (EPS) on silica", Colloids and Surfaces B-Biointerfaces, Vol. 87, No. 1, pp. 151-158.

Tong, S.P., Ma, C.A. and Feng, H. (2008), "A novel PbO_2 electrode preparation and its application in organic degradation", Electrochimica Acta, Vol. 53, No. 6, pp. 3002-3006.

Tran, L.H., Drogui, P., Mercier, G. and Blais, J.F. (2009), "Electrolytic Oxidation of Polynuclear Aromatic Hydrocarbons from Creosote Solution Using Ti/IrO_2 and Ti/SnO_2 Circular Mesh Electrodes", Journal of Environmental Engineering-Asce, Vol. 135, No. 10, pp. 1051-1062.

Tsai, W.T., Lai, C.W. and Su, T.Y. (2006), "Adsorption of bisphenol-A from aqueous solution onto minerals and carbon adsorbents", Journal of Hazardous materials, Vol. 134, No. 1-3, pp. 169-175.

Tucker, M.C. (2010), "Progress in metal-supported solid oxide fuel cells: A review",

Journal of Power Sources, Vol. 195, No. 15, pp. 4570-4582.

Turro, E., Giannis, A., Cossu, R., Gidarakos, E., Mantzavinos, D. and Katsaounis, A. (2011), "Electrochemical oxidation of stabilized landfill leachate on DSA electrodes", Journal of Hazardous materials, Vol. 190, No. 1-3, pp. 460-465.

Valdez, H.C.A., Jimenez, G.G., Granados, S.G. and de Leon, C.P. (2012), "Degradation of paracetamol by advance oxidation processes using modified reticulated vitreous carbon electrodes with TiO_2 and $CuO/TiO_2/Al_2O_3$", Chemosphere, Vol. 89, No. 10, pp. 1195-1201.

Vargas, R., Díaz, S., Viele, L., Núñez, O., Borrás, C., Mostany, J. and Scharifker, B.R. (2013), "Electrochemical oxidation of dichlorvos on $SnO_2Sb_2O_5$ electrodes", Applied Catalysis B: Environmental, Vol. 144, No. 1, pp. 107-111.

Vazquez-Gomez, L., de Battisti, A., Ferro, S., Cerro, M., Reyna, S., Martinez-Huitle, C.A. and Quiroz, M.A. (2012), "Anodic Oxidation as Green Alternative for Removing Diethyl Phthalate from Wastewater Using Pb/PbO_2 and Ti/SnO_2 Anodes", Clean-Soil Air Water, Vol. 40, No. 4, pp. 408-415.

Vazquez-Gomez, L., Ferro, S. and De Battisti, A. (2006), "Preparation and characterization of RuO_2-IrO_2-SnO_2 ternary mixtures for advanced electrochemical technology", Applied Catalysis B: Environmental, Vol. 67, No. 1-2, pp. 34-40.

Vinoth, V., Wu, J.J., Asiri, A.M., Lana-Villarreal, T., Bonete, P. and Anandan, S. (2016), "SnO_2-decorated multiwalled carbon nanotubes and Vulcan carbon through a sonochemical approach for supercapacitor applications", Ultrasonics Sonochemistry, Vol. 29, pp. 205-212.

Wachs, I.E. (2005), "Recent conceptual advances in the catalysis science of mixed metal oxide catalytic materials", Catalysis Today, Vol. 100, No. 1-2, pp. 79-94.

Wang, B., Kong, W. and Ma, H. (2007a), "Electrochemical treatment of paper mill wastewater using three-dimensional electrodes with $Ti/Co/SnO_2$-Sb_2O_5 anode",

Journal of Hazardous materials, Vol. 146, No. 1-2, pp. 295-301.

Wang, C.H., Chen, S.W., Wu, J.M., Wei, C.N. and Bor, H.Y. (2011), "Effect of Postdeposition Oxidation and Subsequent Reduction Annealing on Electric and Optical Properties of Amorphous ZnO-SnO_2 Transparent Conducting Films", Electrochemical and Solid State Letters, Vol. 14, No. 3, pp. P5-P8.

Wang, C.H. and Weng, H.S. (1997), "Al_2O_3-supported mixed-metal oxides for destructive oxidation of $(CH_3)_2S_2$", Industrial & Engineering Chemistry Research, Vol. 36, No. 7, pp. 2537-2542.

Wang, F., Li, S., Xu, M., Wang, Y., Fang, W. and Yan, X. (2012a), "Effect of Electrochemical Modification Method on Structures and Properties of Praseodymium Doped Lead Dioxide Anodes", Journal of the Electrochemical Society, Vol. 160, No. 2, pp. D53-D59.

Wang, H., Sun, D.Z. and Bian, Z.Y. (2010a), "Degradation mechanism of diethyl phthalate with electrogenerated hydroxyl radical on a Pd/C gas-diffusion electrode", Journal of Hazardous materials, Vol. 180, No. 1-3, pp. 710-715.

Wang, H. and Wang, J.L. (2008), "The cooperative electrochemical oxidation of chlorophenols in anode-cathode compartments", Journal of Hazardous materials, Vol. 154, No. 1-3, pp. 44-50.

Wang, J.S., Xi, J.Y., Zhang, L., Zhang, J.J., Guo, X., Zhao, J.H., Song, C.Y. and Wang, L.C. (2013a), "Synthesis of highly active SnO2-CNTs supported Pt-on-Au composite catalysts through site-selective electrodeposition for HCOOH electrooxidation", Electrochimica Acta, Vol. 112, pp. 480-485.

Wang, Q., Jin, T., Hu, Z., Zhou, L. and Zhou, M. (2013b), "TiO_2-NTs/SnO_2-Sb anode for efficient electrocatalytic degradation of organic pollutants: Effect of TiO_2-NTs architecture", Separation and Purification Technology, Vol. 102, pp. 180-186.

Wang, X.P. and Lim, T.T. (2011), "Effect of hexamethylenetetramine on the visible-

light photocatalytic activity of C-N codoped TiO_2 for bisphenol A degradation: evaluation of photocatalytic mechanism and solution toxicity", Applied Catalysis a-General, Vol. 399, No. 1-2, pp. 233-241.

Wang, Y., Shen, C., Zhang, M., Zhang, B.-T. and Yu, Y.-G. (2016), "The electrochemical degradation of ciprofloxacin using a SnO_2-Sb/Ti anode: Influencing factors, reaction pathways and energy demand", Chemical Engineering Journal, Vol. 296, pp. 79-89.

Wang, Y., Shen, Z.Y., Li, Y. and Niu, J.F. (2010b), "Electrochemical properties of the erbium-chitosan-fluorine-modified PbO_2 electrode for the degradation of 2,4-dichlorophenol in aqueous solution", Chemosphere, Vol. 79, No. 10, pp. 987-996.

Wang, Y.B., Zhang, Y.N., Zhao, G.H., Tian, H.Y., Shi, H.J. and Zhou, T.C. (2012b), "Design of a Novel Cu_2O/TiO_2/Carbon Aerogel Electrode and Its Efficient Electrosorption-Assisted Visible Light Photocatalytic Degradation of 2,4,6-Trichlorophenol", Acs Applied Materials & Interfaces, Vol. 4, No. 8, pp. 3965-3972.

Wang, Y.D., Brezesinski, T., Antonietti, M. and Smarsly, B. (2009a), "Ordered Mesoporous Sb-, Nb-, and Ta-Doped SnO_2 Thin Films with Adjustable Doping Levels and High Electrical Conductivity", Acs Nano, Vol. 3, No. 6, pp. 1373-1378.

Wang, Y.H., Chan, K.Y., Li, X.Y. and So, S.K. (2006), "Electrochemical degradation of 4-chlorophenol at nickel-antimony doped tin oxide electrode", Chemosphere, Vol. 65, No. 7, pp. 1087-1093.

Wang, Y.Q., Gu, B. and Xu, W.L. (2009b), "Electro-catalytic degradation of phenol on several metal-oxide anodes", Journal of Hazardous materials, Vol. 162, No. 2-3, pp. 1159-1164.

Wang, Y.Q., Gu, B., Xu, W.L. and Lu, L.D. (2007b), "Electrochemical oxidation of phenol on Ti-based PbO_2 electrodes", Rare Metal Materials and Engineering, Vol.

36, No. 5, pp. 874-878.

Wardman, P. (1989), "Reduction Potentials of One-Electron Couples Involving Free Radicals in Aqueous Solution", Journal of Physical and Chemical Reference Data, Vol. 18, No. 4, pp. 1637-1755.

Watts, R.J., Wyeth, M.S., Finn, D.D. and Teel, A.L. (2008), "Optimization of Ti/SnO_2-Sb_2O_5 anode preparation for electrochemical oxidation of organic contaminants in water and wastewater", Journal of Applied Electrochemistry, Vol. 38, No. 1, pp. 31-37.

Weishaar, J.L., Aiken, G.R., Bergamaschi, B.A., Fram, M.S., Fujii, R. and Mopper, K. (2003), "Evaluation of specific ultraviolet absorbance as an indicator of the chemical composition and reactivity of dissolved organic carbon", Environmental Science & Technology, Vol. 37, No. 20, pp. 4702-4708.

Wu, D., Liu, M., Dong, D.M. and Zhou, X.L. (2007), "Effects of some factors during electrochemical degradation of phenol by hydroxyl radicals", Microchemical Journal, Vol. 85, No. 2, pp. 250-256.

Wu, J., Liu, F., Zhang, H., Zhang, J.H. and Li, L. (2012), "Decolorization of CI Reactive Black 8 by electrochemical process with/without ultrasonic irradiation", Desalination and Water Treatment, Vol. 44, No. 1-3, pp. 36-43.

Wu, J.C., Chung, C.S., Ay, C.L. and Wang, I. (1984), "Nonoxidative Dehydrogenation of Ethylbenzene over Tio_2-Zro_2 Catalysts .2. The Effect of Pretreatment on Surface-Properties and Catalytic Activities", Journal of Catalysis, Vol. 87, No. 1, pp. 98-107.

Wu, M.F., Jin, Y.N., Zhao, G.H., Li, M.F. and Li, D.M. (2010), "Electrosorption-promoted Photodegradation of Opaque Wastewater on A Novel TiO_2/Carbon Aerogel Electrode", Environmental Science & Technology, Vol. 44, No. 5, pp. 1780-1785.

Wu, T., Zhao, G.H., Lei, Y.Z. and Li, P.Q. (2011), "Distinctive Tin Dioxide Anode

Fabricated by Pulse Electrodeposition: High Oxygen Evolution Potential and Efficient Electrochemical Degradation of Fluorobenzene", Journal of Physical Chemistry C, Vol. 115, No. 10, pp. 3888-3898.

Wu, W.Y., Huang, Z.H. and Lim, T.T. (2015), "Enhanced electrochemical oxidation of phenol using a hydrophobic TiO_2-NTs/SnO_2-Sb-PTFE electrode prepared by pulse electrodeposition", Rsc Advances, Vol. 5, No. 41, pp. 32245-32255.

Xu, H., Li, A.-P., Qi, Q., Jiang, W. and Sun, Y.-M. (2012), "Electrochemical degradation of phenol on the La and Ru doped Ti/SnO_2-Sb electrodes", Korean Journal of Chemical Engineering, Vol. 29, No. 9, pp. 1178-1186.

Xu, H., Zhang, Q., Yan, W. and Chu, W. (2011), "A Composite Sb-doped SnO_2 Electrode Based on the TiO_2 Nanotubes Prepared by Hydrothermal Synthesis", International Journal of Electrochemical Science, Vol. 6, No. 12, pp. 6639-6652.

Xu, H., Zhang, Q., Yan, W., Chu, W. and Zhang, L.F. (2013a), "Preparation and Characterization of PbO_2 Electrodes Doped with TiO_2 and Its Degradation Effect on Azo Dye Wastewater", International Journal of Electrochemical Science, Vol. 8, No. 4, pp. 5382-5395.

Xu, L., Guo, Z., Du, L. and He, J. (2013b), "Decolourization and degradation of C.I. Acid Red 73 by anodic oxidation and the synergy technology of anodic oxidation coupling nanofiltration", Electrochimica Acta, Vol. 97, pp. 150-159.

Xu, L., Sun, Y., Zhang, L., Zhang, J. and Wang, F. (2015a), "Electrochemical oxidation of C.I. Acid Red 73 wastewater using Ti/SnO_2-Sb electrodes modified by carbon nanotube", Desalination and Water Treatment, Vol. 57, No. 19, pp. 8815-8825.

Xu, M., Wang, Z., Wang, F., Hong, P., Wang, C., Ouyang, X., Zhu, C., Wei, Y., Hun, Y. and Fang, W. (2016), "Fabrication of cerium doped Ti/nanoTiO_2/PbO_2 electrode with improved electrocatalytic activity and its application in organic degradation", Electrochimica Acta, Vol. 201, pp. 240-250.

Xu, X.B., Geng, H.Z., Meng, Y., Ding, E.X., Wang, Y., Zhang, Z.C. and Wang, W.Y. (2015b), "Synthesis and optimization of tin dioxide/functionalized multi-walled carbon nanotube composites as anode in lithium-ion battery", Materials Chemistry and Physics, Vol. 153, pp. 155-160.

Xue, B., Zhang, Y. and Wang, J.Y. (2011), "Electrochemical Oxidation of Bisphenol A on Ti/SnO_2- Sb_2O_5/PbO_2 Anode for Waste Water Treatment", Procedia Environmental Sciences, Vol. 10, pp. 647-652.

Yang, L., Li, Z., Jiang, H., Jiang, W., Su, R., Luo, S. and Luo, Y. (2016), "Photoelectrocatalytic oxidation of bisphenol A over mesh of TiO_2/graphene/Cu_2O", Applied Catalysis B: Environmental, Vol. 183, pp. 75-85.

Yang, S.Y., Choo, Y.S., Kim, S., Lim, S.K., Lee, J. and Park, H. (2012), "Boosting the electrocatalytic activities of SnO_2 electrodes for remediation of aqueous pollutants by doping with various metals", Applied Catalysis B-Environmental, Vol. 111, pp. 317-325.

Yang, X., Zou, R., Huo, F., Cai, D. and Xiao, D. (2009), "Preparation and characterization of Ti/SnO_2-Sb_2O_3-Nb_2O_5/PbO_2 thin film as electrode material for the degradation of phenol", Journal of Hazardous materials, Vol. 164, No. 1, pp. 367-373.

Yao, P. (2011), "Effects of Sb doping level on the properties of Ti/SnO_2-Sb electrodes prepared using ultrasonic spray pyrolysis", Desalination, Vol. 267, No. 2-3, pp. 170-174.

Yao, P., Chen, X. and Shen, Z. (2013), "A novel combined electrochemical-biological method for non-biodegradable pollutants degradation", Desalination and Water Treatment, pp. 1-7.

Yao, Y.W., Zhao, C.M. and Zhu, J. (2012), "Preparation and characterization of PbO_2-ZrO_2 nanocomposite electrodes", Electrochimica Acta, Vol. 69, pp. 146-151.

Yousefpour, M. and shokuhy, A. (2012), "Electrodeposition of TiO_2–RuO_2–IrO_2

coating on titanium substrate", Superlattices and Microstructures, Vol. 51, No. 6, pp. 842-853.

Yu, J., Wang, Y. and Xiao, W. (2013), "Enhanced photoelectrocatalytic performance of SnO_2/TiO_2 rutile composite films", Journal of Materials Chemistry A, Vol. 1, No. 36, p. 10727.

Yu, X.J., Wang, H., Sun, D.Z., Song, L.W. and Wu, L. (2006), "Mechanism study of electrochemical oxidation in the terylene diaphragm cell", Journal of Environmental Sciences-China, Vol. 18, No. 1, pp. 33-39.

Yu, X.M., Zhou, M.H., Hu, Y.S., Serrano, K.G. and Yu, F.K. (2014), "Recent updates on electrochemical degradation of bio-refractory organic pollutants using BDD anode: a mini review", Environmental Science and Pollution Research, Vol. 21, No. 14, pp. 8417-8431.

Zanta, C.L.P.S., Michaud, P.A., Comninellis, C., De Andrade, A.R. and Boodts, J.F.C. (2003), "Electrochemical oxidation of p-chlorophenol on SnO_2-Sb_2O_5 based anodes for wastewater treatment", Journal of Applied Electrochemistry, Vol. 33, No. 12, pp. 1211-1215.

Zhang, J.G., Wei, Y.P., Jin, G.J. and Wei, G. (2010), "Active Stainless Steel/SnO_2-CeO_2 Anodes for Pollutants Oxidation Prepared by Thermal Decomposition", Journal of Materials Science & Technology, Vol. 26, No. 2, pp. 187-192.

Zhang, L., Liu, J., Tang, C., Lv, J., Zhong, H., Zhao, Y. and Wang, X. (2011a), "Palygorskite and SnO_2-TiO_2 for the photodegradation of phenol", Applied Clay Science, Vol. 51, No. 1-2, pp. 68-73.

Zhang, L.C., Xu, L., He, J. and Zhang, J.J. (2014), "Preparation of Ti/SnO_2-Sb electrodes modified by carbon nanotube for anodic oxidation of dye wastewater and combination with nanofiltration", Electrochimica Acta, Vol. 117, pp. 192-201.

Zhang, Q.L., Liu, Y.C., Zeng, D.M., Lin, J.P. and Liu, W. (2011b), "The effect of Ce

doped in Ti/SnO_2-Sb_2O_3/SnO_2-Sb_2O_3-CeO_2 electrode and its electro-catalytic performance in caprolactam wastewater", Water Science and Technology, Vol. 64, No. 10, pp. 2023-2028.

Zhao, G.H., Cui, X., Liu, M.C., Li, P.Q., Zhang, Y.G., Cao, T.C., Li, H.X., Lei, Y.Z., Liu, L. and Li, D.M. (2009), "Electrochemical Degradation of Refractory Pollutant Using a Novel Microstructured TiO_2 Nanotubes/Sb-Doped SnO_2 Electrode", Environmental Science & Technology, Vol. 43, No. 5, pp. 1480-1486.

Zhao, G.H., Zhang, Y.G., Lei, Y.Z., Lv, B.Y., Gao, J.X., Zhang, Y.A. and Li, D.M. (2010a), "Fabrication and Electrochemical Treatment Application of A Novel Lead Dioxide Anode with Superhydrophohic Surfaces, High Oxygen Evolution Potential, and Oxidation Capability", Environmental Science & Technology, Vol. 44, No. 5, pp. 1754-1759.

Zhao, H., Gao, J., Zhao, G., Fan, J., Wang, Y. and Wang, Y. (2013), "Fabrication of novel SnO_2-Sb/carbon aerogel electrode for ultrasonic electrochemical oxidation of perfluorooctanoate with high catalytic efficiency", Applied Catalysis B: Environmental, Vol. 136-137, pp. 278-286.

Zhao, J., Zhu, C.Z., Lu, J., Hu, C.J., Peng, S.C. and Chen, T.H. (2014), "Electro-catalytic degradation of bisphenol A with modified Co_3O_4/beta-PbO_2/Ti electrode", Electrochimica Acta, Vol. 118, pp. 169-175.

Zhao, K., Zhao, G., Li, P., Gao, J., Lv, B. and Li, D. (2010b), "A novel method for photodegradation of high-chroma dye wastewater via electrochemical pre-oxidation", Chemosphere, Vol. 80, No. 4, pp. 410-415.

Zheng, Y., Su, W., Chen, S., Wu, X. and Chen, X. (2011), "Ti/SnO_2-Sb_2O_5-RuO_2/α-PbO_2/β-PbO_2 electrodes for pollutants degradation", Chemical Engineering Journal, Vol. 174, No. 1, pp. 304-309.

Zhou, M.H., Dai, Q.Z. and Lei, L.C. (2005a), "p-nitrophenol degradation by electrochemical oxidation in the presence of NaCl", Proceedings of the 9th

International Conference on Environmental Science and Technology, Vol a - Oral Presentations, Pts a and B, pp. A1704-A1709.

Zhou, M.H., Dai, Q.Z., Lei, L.C., Ma, C. and Wang, D.H. (2005b), "Long life modified lead dioxide anode for organic wastewater treatment: Electrochemical characteristics and degradation mechanism", Environmental Science & Technology, Vol. 39, No. 1, pp. 363-370.

Zhou, M.H., Dai, Q.Z., Lei, L.C., Wu, Z.C., Ma, C.A. and Wang, D.H. (2004), "Electrochemical oxidation for the degradation of organic pollutants on a novel PbO_2 anode", Acta Physico-Chimica Sinica, Vol. 20, No. 8, pp. 871-876.

Zhou, M.H., Liu, L., Jiao, Y.L., Wang, Q. and Tan, Q.Q. (2011a), "Treatment of high-salinity reverse osmosis concentrate by electrochemical oxidation on BDD and DSA electrodes", Desalination, Vol. 277, No. 1-3, pp. 201-206.

Zhou, M.H., Sarkka, H. and Sillanpaa, M. (2011b), "A comparative experimental study on methyl orange degradation by electrochemical oxidation on BDD and MMO electrodes", Separation and Purification Technology, Vol. 78, No. 3, pp. 290-297.

Zhou, M.H., Wu, Z.C., Zhu, J., Ye, Q. and Fu, J. (2002), "p-Nitrophenol degradation by homogeneous photochemical oxidation combined with electrocatalysis", Chinese Journal of Catalysis, Vol. 23, No. 4, pp. 376-380.

Zhu, K., Zhang, W., Wang, H. and Xiao, Z. (2008a), "Electro-Catalytic Degradation of Phenol Organics with SnO_2-Sb_2O_3/Ti Electrodes", CLEAN – Soil, Air, Water, Vol. 36, No. 1, pp. 97-102.

Zhu, X.P., Tong, M.P., Shi, S.Y., Zhao, H.Z. and Ni, J.R. (2008b), "Essential explanation of the strong mineralization performance of boron-doped diamond electrodes", Environmental Science & Technology, Vol. 42, No. 13, pp. 4914-4920.

Zhuo, Q.F., Deng, S.B., Yang, B., Huang, J. and Yu, G. (2011), "Efficient

Electrochemical Oxidation of Perfluorooctanoate Using a Ti/SnO_2-Sb-Bi Anode", Environmental Science & Technology, Vol. 45, No. 7, pp. 2973-2979.